

DOE/CE/40936--T5-Vol. 2

**Black Liquor Combustion
Validated Recovery Boiler Modeling
Final Year Report**

Volume 2
(Appendices I, section 5 & II section 1)

by

T.M. Grace, W.J. Frederick, M. Salcudean, and R.A. Wessel

August 1998

A Summary Report
of the Project

Work Performed Under Contract DE-FG07-90CE40936

Prepared for

The U.S. Department of Energy
Office of Industrial Technologies
Washington, D.C.

Prepared by

The Institute of Paper Science and Technology
Atlanta, GA

Oregon State University
Corvallis, OR

University of British Columbia
Vancouver, BC, Canada

Babcock & Wilcox Company
Alliance, OH

RECEIVED

DEC 23 1998

OSTI

DISTRIBUTION OF THIS DOCUMENT IS UNLIMITED

MASTER

DISCLAIMER

This report was prepared as an account of work sponsored by an agency of the United States Government. Neither the United States Government nor any agency thereof, nor any of their employees, makes any warranty, express or implied, or assumes any legal liability or responsibility for the accuracy, completeness, or usefulness of any information, apparatus, product, or process disclosed, or represents that its use would not infringe privately owned rights. Reference herein to any specific commercial product, process, or service by trade name, trademark, manufacturer, or otherwise does not necessarily constitute or imply its endorsement, recommendation, or favoring by the United States Government or any agency thereof. The views and opinions of authors expressed herein do not necessarily state or reflect those of the United States Government or any agency thereof.

Table of Contents
Volume 2

APPENDIX I (cont'd)

Section 5	1-62
Radiative Heat Transfer in Kraft Recovery Boilers	

APPENDIX II

Black Liquor Chemistry Data

Section 1	1-124
The Effect of Temperature and Residence Time on the Distribution of Carbon, Sulfur, and Nitrogen between Gaseous and Condensed Phase Products from Low Temperature Pyrolysis of Kraft Black Liquor	

RADIATIVE HEAT TRANSFER IN KRAFT RECOVERY BOILERS

P. Sabhapathy

22nd Dec. 1995

Contents

1	Introduction	3
1.1	Mathematical Modelling of Recovery Boilers	3
1.2	Energy Conservation Equation	4
1.3	Outline of the Report	6
2	Radiative Transfer Equation	7
2.1	Spectral Radiation Intensity	7
2.2	Radiative Heat Transfer Relations	9
2.3	Radiative Transfer Equation	10
2.3.1	The Transfer Equation	10
2.3.2	Boundary Condition	11
2.3.3	Scattering Phase Function	12
2.4	Characteristics of the Transfer Equation	12
3	Radiative Properties of Combustion Products	14
3.1	Combustion Gases	15
3.1.1	Edwards Exponential Wide Band Model	19
3.2	Particulate Media	22
3.2.1	Mie Scattering	24
3.2.2	Rayleigh Scattering	26
3.2.3	Effects of Dispersion	27
4	Radiation Models	31
4.1	Monte Carlo Method	31
4.2	Zonal Method	32
4.3	Flux Methods	33
4.4	Hybrid and Other Methods	33
4.5	Discrete Ordinates Method	33
4.5.1	Selection of Discrete Ordinate Directions	36
4.6	Numerical Method	38

4.7	Solution Procedure	39
5	A Brief Description of the Radiation Code	41
6	Hot Flow Simulations for a Generic Boiler	45
6.1	Boiler Geometry	45
6.2	Air Distribution, and Liquor and Spray Characteristics	46
6.3	Results and Discussion	46
7	Conclusions	48

Summary

An reasonably accurate calculation of radiative heat transfer is necessary for the design, and safe operation of kraft recovery boilers. Prediction of radiation in an emitting, absorbing and scattering medium such as the particle laden gas present inside a kraft recovery boiler is extremely complex. In this report, the fundamentals of radiation in a participating medium, the methods to predict the properties of combustion products and, the methods to predict the radiative heat transfer in furnaces are reviewed. In particular, the exponential wide-band model for the prediction of radiative properties of combustion gases, Mie scattering for the prediction of radiative properties of particulates, and the discrete ordinates method and the resulting numerical procedure for the calculation of radiative heat transfer inside a kraft recovery boiler are described in detail. A brief description of the radiation computer code and its interaction with the UBC flow code are also given. Hot flow simulations for a generic boiler are also given.

Chapter 1

Introduction

1.1 Mathematical Modelling of Recovery Boilers

The recovery boiler is the single highest cost item in a kraft pulp mill. The boiler serves two main functions, namely: (i) to recover the inorganic chemicals (sodium hydroxide and sodium sulfide and others) from the black liquor to form fresh cooking liquor, and (ii) to burn the organic constituents of the black liquor to generate steam for the mill [1]. It is most essential that these twin objectives of recovering chemicals and energy to be carried out at optimum levels to improve the overall efficiency of the pulping process and to reduce the pollution from the mill.

The kraft recovery boiler is usually not over-designed and it cannot also be easily modified for higher capacity, and safety factors cannot be compromised. It is often the bottleneck of the mill and, therefore, there is a need to increase the throughput of the boiler [1]. One of the factors that limit the throughput is plugging of the convective sections by carryover of the smelt and fume by the upward gas flow.

The combustion and carryover in a recovery boiler are difficult to measure and quantify. Some evaluation of combustion can be made through real time monitoring

of the emissions. However, carryover can only be indirectly quantified by monitoring the frequency of soot-blowing and water washes. Therefore, a tool which could predict the combustion and carryover in a recovery boiler would be very useful in improving the throughput of the mill.

Mathematical modelling of the combustion process and chemical recovery helps in identification of the optimum operating conditions of the existing boilers and in the design of new boilers. The modelling also helps in identifying the modifications needed for increasing the throughput without sacrificing the efficiency or safety. An adequate treatment of thermal radiation is very important in the development of the mathematical model of the combustion process and chemical recovery in the boiler. Since the chemical kinetics involved in the combustion process, and the deposition of smelt and fume on the tube walls are strongly temperature dependent, fairly accurate calculation of the local gas temperature is needed if the evaluation of the pollutant formation and concentration, and the plugging of the convective sections are to be meaningful. An fairly accurate determination of the local heat flux distribution at the furnace walls and at the boiler tubes is also necessary for safer operating conditions of the boiler.

1.2 Energy Conservation Equation

The physical and chemical processes occurring in a kraft recovery boiler are extremely complex and depend on a number of parameters. The mathematical modelling of these processes requires simultaneous solution of equations governing the fluid flow, chemical reaction and energy transfer. Radiation does not contribute any

term to the conservation equations of mass, momentum and species. However, the classical conservation of energy equation is modified by contributions which account for the radiation heat transfer. In the energy equation, the contribution of radiation to pressure work term can be neglected because the radiation pressure is usually very small compared to the fluid pressure. Since radiation travels at the speed of light, the radiative contribution to the transient term is negligible. With the above assumptions, the general form of the energy equation for a moving compressible fluid, which emits, absorbs and scatters radiation, can be written as,

$$\rho c_p \frac{DT}{Dt} = \nabla \cdot k \nabla T - \nabla \cdot q_r + \dot{q} + \beta_v T \frac{DP}{Dt} + \phi_v \quad (1.1)$$

where $\nabla \cdot q_r$ is the contribution due to radiation; $\rho c_p \frac{DT}{Dt}$ and $\nabla \cdot k \nabla T$ are the convection and diffusion terms, respectively; \dot{q} is the heat generation per unit volume (eg. due to chemical reaction) and time; $\beta_v T \frac{DP}{Dt}$ accounts for the work done by pressure; and, ϕ_v is the heat production by viscous dissipation. The divergence of radiative heat flux appearing in the energy equation represents the net radiative energy per unit time and volume leaving a differential volume and is given by

$$\nabla \cdot q_r = \int_0^\infty \kappa_\lambda \left[4\pi I_{\lambda b}(r) - \int_0^{4\pi} I_\lambda(r, s) d\Omega \right] d\lambda \quad (1.2)$$

where $I_\lambda(r, s)$ is the spectral radiation intensity at location r and direction s , $I_{\lambda b}(r)$ is the monochromatic blackbody radiation intensity at the local temperature of the medium and κ_λ is the absorption coefficient of the medium. The above equation states that the net radiant energy per unit volume leaving an elemental volume inside a participating medium is the emitted radiant energy per unit volume minus the

absorbed radiant energy per unit volume. The spectral radiation intensity, through emission and temperature-dependent properties, depends on the temperature field and, therefore, cannot be decoupled from the overall energy equation. The above equation is an integral equation in temperature. As a result, when radiation effects are important, the overall energy conservation equation is an integro-differential equation for the calculation of temperature field.

1.3 Outline of the Report

Some of the fundamentals of radiation heat transfer in a participating medium and the radiative heat transfer relations are discussed in Chapter 2. The radiative properties of a participating medium, and, in particular, Edwards Exponential Wide Band Model and Mie Scattering are given in Chapter 3. The radiation models and, in particular, the Discrete Ordinates Method and its numerical solution are given in Chapter 4. A brief description of the radiation computer code and its interaction with the UBC flow code are given in Chapter 5. Sample flow and temperature fields in a generic boiler are given in Chapter 6.

Chapter 2

Radiative Transfer Equation

2.1 Spectral Radiation Intensity

Thermal radiation occurs due to the emission and absorption of electromagnetic waves (or photons) by the particles of matter (molecules, atoms, ions, and electrons) as they undergo internal energy state transitions. The radiative energy produced by these transitions is usually in the ultraviolet, visible, and infrared portions of the electromagnetic spectrum. Thermal radiation travels at the speed of light and its transport does not require the presence of any matter.

The fundamental quantity used for describing the radiant energy transport is the *Spectral Radiation Intensity* I_λ and is defined as the radiant power per unit area perpendicular to the direction of travel per unit solid angle and per unit wavelength interval. Referring to Fig. 2.1, if Δq_λ is the radiant power along the direction (θ, ϕ) at the wavelength λ from a small surface of area ΔA then

$$I_\lambda = \frac{\Delta q_\lambda}{\Delta A_n d\Omega d\lambda} \quad (2.1)$$

where $\Delta A_n (= \Delta A \cos\theta)$ is the projected area of ΔA normal to the direction (θ, ϕ) , $d\Omega$

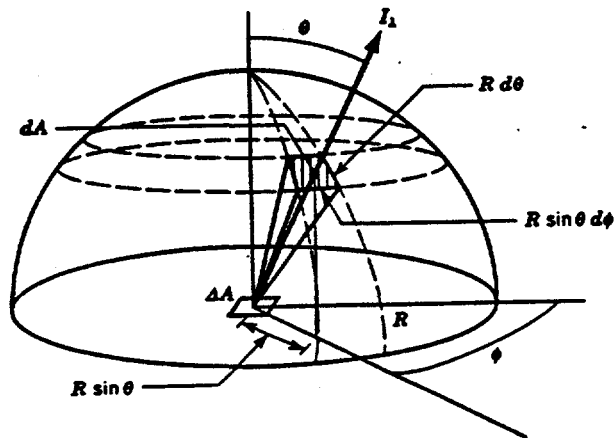


Figure 2.1: Spectral Radiation Intensity

is the solid angle and $d\lambda$ is the wavelength interval. Defined in this way, the intensity is a conserved quantity for radiation propagating in a nonattenuating medium. That is, intensity is constant with distance (s) along any given direction of travel in a nonscattering, nonabsorbing medium. In this case, the calculation of radiation energy transport mainly involves calculation of geometric view factors and is described in detail in many texts on radiation heat transfer, for example in [2,3].

The solid angle is the area on the surface of a sphere of radius R divided by R^2 and has the dimensionless unit of steradians (sr). The area of a differential element, dA_2 on the surface of a hemisphere above ΔA is given by (Fig. 1)

$$dA_2 = R^2 \sin\theta d\theta d\phi \quad (2.2)$$

The solid angle $d\Omega$ subtended by the differential area dA_2 is:

$$d\Omega = \frac{dA_2}{R^2} = \sin\theta d\theta d\phi \quad (2.3)$$

Therefore, the spectral intensity, I_λ , is given by

$$I_\lambda = \frac{\Delta q_\lambda}{\Delta A \cos\theta \sin\theta d\theta d\phi d\lambda} \quad (2.4)$$

The spectral intensity is a function of spatial position (x, y, z) , direction (θ, ϕ) and wavelength, λ .

$$I_\lambda = I_\lambda(x, y, z, \theta, \phi, \lambda) \quad (2.5)$$

When the spectral intensity, I_λ is known, the total intensity, I can be determined by integrating over all wavelengths.

$$I(x, y, z, \theta, \phi) = \int_0^\infty I_\lambda(x, y, z, \theta, \phi, \lambda) d\lambda \quad (2.6)$$

2.2 Radiative Heat Transfer Relations

In heat transfer calculations, heat fluxes are needed for incorporation into thermal energy balance of an element. The equations relating the heat fluxes with radiation intensities are given below.

The spectral heat flux, $\bar{q}_\lambda (= \Delta q_\lambda / \Delta A / d\lambda)$ can be determined by integrating I_λ with respect to direction.

$$\bar{q}_\lambda = \int_0^{2\pi} \int_0^\pi I_\lambda(x, y, z, \theta, \phi, \lambda) \cos\theta \sin\theta d\theta d\phi \quad (2.7)$$

The total heat flux \bar{q} can be obtained by integrating q_λ over all wavelengths

$$\bar{q} = \int_0^\infty q_\lambda d\lambda \quad (2.8)$$

The divergence of the radiative heat flux, $\nabla \cdot q_r$, has already been defined in Chapter 1 (Eq. 1.2).

2.3 Radiative Transfer Equation

2.3.1 The Transfer Equation

The spectral radiation intensity I_λ in a participating medium can be determined as function of the independent variables x, y, z, θ and ϕ from the solution of the *Radiative Transfer Equation* (RTE). The transfer equation is an optical energy balance on a differential volume element along a single line of sight. The RTE forms the basis of quantitative studies of radiation in a participating medium.

Consider a monochromatic pencil of radiation travelling along the direction s in a participating medium, such as the particle laden gas in the recovery boiler. Let us assume that there is negligible multiple scattering and negligible shadowing of particles by one another. The radiation is attenuated due to absorption by gases such as CO_2 and water vapor and by particulates, and due to out-scattering by the particulates. The radiation is augmented by emission from the gases and particulates, and by in-scattering by particulates. Augmentation due to scattering, or "in-scattering" has contribution from all directions and, therefore must be calculated by integration over all solid angles. The radiant energy balance over an elemental solid angle $d\Omega$, in the direction s across an elemental volume as shown in Fig. 2.2 is given by

$$\frac{dI_\lambda(\vec{r}, s)}{ds} = -\beta_\lambda(\vec{r})I_\lambda(\vec{r}, s) + \kappa_\lambda(\vec{r})I_{\lambda b}(\vec{r}) + \frac{\sigma_\lambda(\vec{r})}{4\pi} \int_{4\pi} I_\lambda(\vec{r}, s')\Phi(s', s)d\Omega' \quad (2.9)$$

where β_λ and σ_λ are the extinction and scattering coefficients of the medium, respectively ($\beta_\lambda = \kappa_\lambda + \sigma_\lambda$) and $\Phi(s', s)$, the scattering phase function.

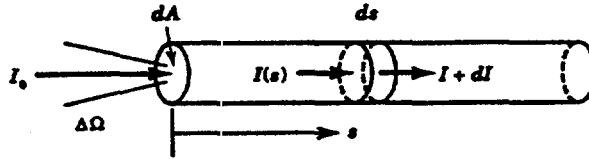


Figure 2.2: Radiation Energy Balance

The first term in the right-hand side of the above equation is the attenuation of radiation through absorption and out-scattering, and, the second and third terms are augmentation due to emission and in-scattering, respectively;

2.3.2 Boundary Condition

For most heat transfer calculations inside enclosures such as that of a kraft recovery boiler, the boundaries can be assumed to be opaque, diffuse surfaces. The radiant energy leaving a opaque, diffuse surface consists of two components, namely, emission due to the temperature of the surface and reflection of incoming intensities. The boundary condition can be expressed mathematically as

$$I_{\lambda}(r_w, s) = \epsilon(r_w)I_{\lambda b}(r_w) + \frac{\rho(r_w)}{\pi} \int_{n \cdot s' < 0} I_{\lambda}(r_w, s') |n \cdot s| d\Omega' \quad (2.10)$$

where $\epsilon(r_w)$ and $\rho(r_w)$ are the emissivity and reflectivity of the wall, respectively, and

n is the unit vector normal to the wall.

2.3.3 Scattering Phase Function

The scattering phase function, $\Phi(s', s)$, occurring in the RTE (Eq. 2.9) is defined as the ratio of energy scattered from s' direction into s direction to the energy scattered into s if scattering were isotropic. The phase function satisfies the following equation:

$$\frac{1}{4\pi} \int_{4\pi} \Phi(s', s) d\Omega' = 1 \quad (2.11)$$

When the radiation is unpolarized and the scattering particles are spherical, the phase function is independent of azimuthal angle, ϕ . For most thermal radiation calculations even the distribution of Φ with respect to the polar angle, θ is often too detailed, and, therefore, some moment of the distribution that describes the relative forward-to-backward ratio, such as the asymmetry parameter is usually used. The asymmetry parameter g is defined as follows:

$$g = \frac{1}{4\pi} \int_{4\pi} \Phi \cos\theta d\Omega \quad (2.12)$$

The value of g ranges from -1 (for maximum backward scattering) to 1 (for maximum forward scattering). When the scattering is isotropic, the scattered energy is equally distributed in all directions. For isotropic scattering, $\Phi=1$ and $g=0$.

2.4 Characteristics of the Transfer Equation

There are no convective terms in RTE indicating that the radiation propagates independently of the local material velocity. This is because the radiation travels at

the speed of light. The RTE is an integro-differential equation. The in-scattering term yields the integral nature of the RTE. If scattering is negligible in the medium, the RTE becomes a linear differential equation. As pointed out earlier, the divergence of the radiative heat flux can be obtained by integrating the RTE over all solid angles and wavelengths. The effects of scattering are not present in the divergence of the radiative heat flux (Eq. 1.2) because scattered energy is conserved. In other words, scattering only redirects the radiant energy and the effects of in-scattering and out-scattering cancel out when integrated over all solid angles and wavelengths. However, scattering does, in general, influence the overall energy transport since I_λ depends on scattering.

The solution of RTE even for a one dimensional, planar, gray medium is quite difficult. Usually the angular dependence of the intensity and the wavelength dependence of properties complicate the problem since all possible directions and wavelengths must be taken into account. Therefore, it is necessary to introduce some simplifying assumptions before attempting to solve the RTE in its general form.

Chapter 3

Radiative Properties of Combustion Products

Calculation of radiative heat transfer in an enclosure with a participating medium such as the kraft recovery boiler involves obtaining a solution of the radiative transfer equation for the prescribed boundary conditions. The calculated radiative intensities depend strongly on the radiative properties, namely, absorption and emission coefficients. The accuracy of radiation heat transfer predictions depends on the accuracy of the radiative properties of combustion products used in the analysis. The products which contribute significantly to radiation in the boiler are combustion gases such as water vapor, CO_2 , CO , SO_2 and NO , and particulate media such as char, fly-ash and black liquor droplets. The wavelength dependence of the radiative properties of these products, and uncertainties about the volume fractions and the size and shape distribution of particles make the task of evaluation of these properties a difficult task. Moreover, the presence of significant quantities of sulfur and sodium, and the associated molecular species whose spectral characteristics are less well known complicate matters tremendously. The level of simplification for the properties should be

consistent with the level of sophistication of the model for the prediction of radiative transfer and the global model for heat transfer.

3.1 Combustion Gases

The gas in the kraft recovery boiler is composed of a number of components such as nitrogen, oxygen, water vapor and carbon-dioxide. The partial pressures of these components depend on the location, the conditions of combustion environment such as the type of fuel, air-fuel ratio, total pressure and temperature. When a photon interacts with a gas atom or molecule, it may be either absorbed or scattered. The scattering of photons by gas molecules is always negligible for heat transfer applications. The gas radiation occurs in bands. Within each band, the absorption or emission occurs over a tiny but finite range of wavenumbers with the maxima at the wavenumber predicted by quantum mechanics.

Gases such as N_2 , H_2 , and O_2 with symmetric diatomic molecules, and monatomic gases such as argon and helium are non-participating except at extremely high temperatures when these gases are ionized. The temperature in the boiler is not high enough for significant ionization to occur, and, therefore, the effects of these gases on furnace radiation are negligible. Gases such as H_2O , CO_2 , CO , SO_2 and NH_3 with non-symmetric molecular structures emit and absorb radiation strongly in certain narrow-wavelength bands associated with their molecular energy levels. The amount of radiation absorbed or emitted by a gas at any wavelength depends on the molecular composition, pressure, temperature and total path length of propagation of the radiation in the gas. Given reasonable estimates of the concentrations of the major species

(H₂O, CO₂, CO, O₂ and N₂), fairly accurate estimates of the radiative properties of the gases can be made.

Emission or absorption of radiation occurs when an atom or molecule of a gas undergoes internal energy transitions from one energy level or state to another. Electronic, vibrational and rotational energy states in a gas atom or molecule are quantized, that is, they occur in discrete, quantum levels. As a result, emission or absorption of radiation in gases occur at distinct frequencies. When a energy transition occurs in a gas molecule or atom, the frequency of the emitted or absorbed photon is the ratio of the energy difference between the two states to Planck's constant ($\nu = \Delta E/h$). No spectral line, however, is truly monochromatic. Several mechanisms such as collision broadening, natural line broadening and Doppler broadening cause broadening of spectral lines. The broadened spectral lines have their maxima at the wavenumber predicted by quantum mechanics.

Electronic states are separated by energy levels of several eV, the vibrational states in the order of 0.1 eV and the rotational states in the order of 0.001 eV. Therefore, the frequency is in the visible and ultraviolet regions for electronic transitions, the infrared for vibrational transitions, and the far infrared and microwave regions for rotational transitions. For gases at moderate temperatures, electronic transitions occur in both atoms and molecules, and rotational transitions and vibrational transitions occur only in molecules. Vibrational transitions are usually accompanied by rotational transitions. For thermal radiation, the most important transitions are the vibration-rotation transitions that involve spectra in the infrared region.

The radiative properties of gases can be described at various levels of complexity,

depending on the scale of the spectral resolution involved. As pointed out earlier, the gas radiation occurs in bands with finite number of discrete spectral lines. The radiant intensity and therefore the emissivity is nonuniform in a spectral line. Moreover the lines often overlap one another. In line-by-line models, the line shape and the intensity variation in each line is prescribed and integrated with respect to wavenumber. The resulting integrated line emissivity is given in terms of effective line width and line overlap parameter. The effective line width is the equivalent width of a black line and the overlap parameter characterizes the extent of line overlapping. Line-by-line parameters for many combustion gases are available in the literature.

At the next level of spectral detail are narrow band models. These models utilize local integration or spectral smoothing over a spectral region, which is narrow with respect to the entire bandwidth but wide with respect to a linewidth. The narrow band models, thus, provide functional variation of the absorption coefficient or emissivity for the band in terms of two parameters, namely, β , the mean line width-to-spacing parameter, and u_n , the smoothed optical depth. At the coarser level are wide band models, which integrate out the gradual spectral variation associated with line intensity and characterize an entire band in terms of an effective bandwidth. The details of various narrow and wide band models can be found in [3]. At a still coarser level is the total emissivity approach, which integrates over all bands and characterizes the gas in terms of a total emissivity. The various descriptions of gas emissivity are shown schematically in Fig. 3.1.

The line-by-line calculations are too detailed, time-consuming, and not practical for radiative heat transfer calculations in a kraft recovery boiler. For example, a typ-

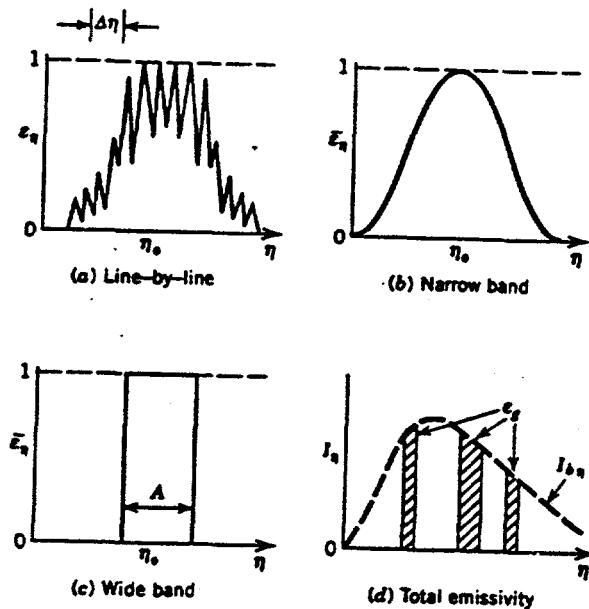


Figure 3.1: Various descriptions of gas emissivity

ical heat transfer calculation might involve 10^5 to 10^6 such lines. Narrow-band model predictions also generally require an extensive and detailed library of input data, and the calculations cannot be performed with reasonable computational effort. Moreover, an accurate calculation of radiative properties with the narrow-band models is not warranted when the concentration distributions of gaseous species are not known accurately due to the approximations in the combustion model. In addition, some of the detailed spectral properties of the combustion gases will be suppressed when they are combined with those of the particles. Therefore, the use of a very accurate model for the prediction of radiative properties of gases may not increase the accuracy of radiative transfer predictions. On the other hand, the combustion gases are anything but gray, and therefore, the assumption of the emissivity to be independent of wavelength as in the total emissivity approach, might predict the radiative heat transfer inaccurately. As a compromise, in this study, the radiative properties of

gaseous species in the kraft recovery boiler are predicted from a wide-band model.

3.1.1 Edwards Exponential Wide Band Model

The wide band models divide the entire wavelength spectrum into a number of bands and assume that the radiation characteristics of each species remain uniform or change smoothly in a given functional form over these bands. These models usually assume that the profile of the band absorption is box or triangular shaped or an exponentially decaying function and integrate over the entire band to obtain an effective bandwidth, defined as,

$$A = \int_{-\infty}^{\infty} \epsilon_{\eta} d(\eta - \eta_0) \quad (3.1)$$

where ϵ_{η} is the smoothed spectral emissivity obtained from a narrow band model, η is the wave number and η_0 is the wavenumber corresponding to the center of the spectral line. The effective bandwidth is the width of an equivalent black rectangle and depends on the integrated optical depth parameter for the band, u , the mean line width-to-spacing or overlap parameter, β , and the bandwidth parameter, ω .

The non-dimensional effective bandwidth is defined as,

$$A^* = \frac{A}{\omega} = A^*(u, \beta) \quad (3.2)$$

The optical depth, u , is defined as

$$u = \frac{X\alpha}{\omega} \quad (3.3)$$

where X is the mass path length ($= \rho_a s$, ρ_a is the density of the gas, and s is the distance) and α is the integrated band intensity. The mean overlap parameter, β ,

can be expressed as a product of a temperature dependent function and a pressure dependent function as follows:

$$\beta = \gamma(T)P_e(P) \quad (3.4)$$

and

$$P_e = \left[\frac{P}{P_0} + \frac{P_a}{P_0}(b-1) \right]^n \quad (3.5)$$

where P is the total pressure, P_a is the partial pressure of the absorbing gas, P_0 is the reference pressure (=1 atm), and b and n are pressure parameters. The model parameters α , ω , and γ are functions of temperature.

The exponential model, first developed by Edwards and his coworkers [4] is by far the most successful of the wide band models. As the name implies, this model assumes that a redistribution of spectral lines results in an exponential profile of mean intensity-to-spacing with the wavenumber. The model provides the dimensionless effective bandwidth, A^* , in the form of an integral containing u and β . Edwards and co-workers [4] have recommended the following curve fit, for A^* :

$$\text{For } \beta < 1 \quad A^* = \left\{ \begin{array}{ll} u & \text{for } 0 < u < \beta \\ 2\sqrt{\beta u} & \text{for } \beta < u < 1/\beta \\ \ln(\beta u) + 2 - \beta & \text{for } u > 1/\beta \end{array} \right\} \quad (3.6)$$

$$\text{For } \beta > 1 \quad A^* = \left\{ \begin{array}{ll} u & \text{for } u < 1 \\ \ln(u) + 1 & \text{for } u > 1 \end{array} \right\} \quad (3.7)$$

The above correlation has two regions, a region of nonoverlapping lines ($\beta < 1$), where line structure influences the effective bandwidth, and a region of overlapping lines ($\beta > 1$), where line structure does not influence the effective bandwidth. Both regions are fitted by a linear relation with optical depth for optically thin conditions and a

logarithmic relation for optically thick conditions. In addition, for nonoverlapping lines there is an intermediate square root region. For the fundamental bands the band intensity parameter α is to a first approximation independent of temperature. Edwards and co-workers have provided the values for the parameters $\omega, \alpha, \gamma, b$ and n for various values of temperature for a number of combustion gases.

The wide band model expresses gas band properties in terms of an effective bandwidth. If the band is assumed to be gray, the spectral transmissivity, τ_η , for the band can be calculated from the dimensionless effective bandwidth as follows [4]:

$$\tau_\eta = \frac{u}{A^*} \frac{dA^*}{du} \quad (3.8)$$

If the transmissivity is greater than 0.9, then it is assigned the value of 0.9. The spectral emissivity can be obtained from the transmissivity ($\epsilon_\eta = 1 - \tau_\eta$). The width of the band, $\Delta\eta$, is determined from

$$\Delta\eta = \frac{A}{1 - \epsilon_\eta} \quad (3.9)$$

If the band center, η_c , is known (e.g. from quantum mechanics), the lower, and upper limits of the band are found from

$$\eta_l = \eta_c - \Delta\eta/2 \quad (3.10)$$

$$\eta_u = \eta_c + \Delta\eta/2 \quad (3.11)$$

The absorption coefficient for the band can be obtained from the emissivity.

The wide band analysis can be carried out for each band of a gas and a table of lower and upper-wave number limits and the associated transmissivity and absorption coefficients can be obtained. In the region where the bands overlap, the band

transmissivity for the overlapped wave number region is taken as the product of the transmissivities for the overlapping bands. The absorption coefficient for the overlapped region is taken as the sum of the absorption coefficients for the overlapping bands. In the region where there are no bands, the absorption coefficient is assumed to be zero.

3.2 Particulate Media

Analysis of heat transfer in the kraft recovery boiler requires accounting of the radiative effects of particulate media, such as fume, soot, fly-ash, char, and fuel droplets. The RTE (Eq. 2.9) indicates that a particulate medium affects radiation by absorption, emission, and scattering. The radiative properties of a particulate medium, namely the monochromatic absorption and scattering coefficients, and the phase function which specifies the angular distribution of the radiation intensity scattered from each particle, can be predicted theoretically.

The theoretical analysis is based on obtaining a solution of Maxwell's equations for a plane, monochromatic wave incident upon a particle of given shape and size. In general, the radiative properties of a cloud of particles such as that encountered in a kraft recovery boiler depend on (i) the shape of the particle, (ii) the optical properties of the particle relative to the surrounding medium, (iii) the size of the particle relative to the wavelength and (iv) the clearance between particles. In a kraft recovery boiler, the particles are either nearly spherical or irregularly shaped, and, therefore, the particles can be assumed to be spherical, for simplicity. For most heat transfer applications including the heat transfer analysis of a recovery boiler, the

scattering can be assumed to be independent, that is, the scattering of one particle is not affected by the presence of surrounding particles. With the above assumption, the radiative properties of a cloud of particles can easily be obtained from those of a single particle because the effects are simply additive.

For independent scattering, the radiative properties of a spherical particle of radius r , are governed by two independent dimensionless parameters, namely, the complex index of refraction, $\tilde{n} = n - ik$ and the size parameter, $x = 2\pi r/\lambda$ where λ is the wavelength of the incident radiation. The imaginary part of the refractive index, k , also known as the absorption index, accounts for the damping or absorption of the radiation as it travels through the medium. The values of optical constants, k and n , generally vary with wavelength, $\tilde{n} = \tilde{n}(\lambda)$. For nonabsorbing materials, $n = c/c_0$ and $k=0$, where c and c_0 are the speed of light in the material and in the vacuum, respectively.

For large size parameters, the radiative properties can be obtained from geometrical optics. For small size parameters ($x \ll 1$), Raleigh theory can be used to predict the radiative properties of the sphere. Mie theory is usually used if the size of the particle is such that it is too large to apply the Raleigh theory but too small to employ geometric optics. In the kraft recovery boiler, the size parameter of fume particles (composed of Na_2SO_4 and Na_2CO_3 and having diameters of less than $1 \mu\text{m}$) fall into the regime of Raleigh scattering, and the size parameters of particles arising from suspension burning of individual black liquor droplets (containing significant amounts of carbon in addition to sodium salts and having diameters from a few to several hundred micrometers) fall into the regime of Mie scattering.

3.2.1 Mie Scattering

Mie theory is based on the solution of Maxwell's equations for a plane, monochromatic wave incident upon a homogeneous sphere in a nonabsorbing medium. The theory and the solution methods are complex and the details can be found in [5].

Mie scattering provides the radiative properties of a spherical particle in terms of absorption, scattering and extinction efficiency factors. They are defined as

$$Q_a = \frac{C_a}{\pi r^2}; \quad (3.12)$$

$$Q_s = \frac{C_s}{\pi r^2}; \quad (3.13)$$

$$Q_e = \frac{C_e}{\pi r^2} \quad (3.14)$$

where C_a , C_s , and C_e refer to the absorption, scattering and extinction cross sections of the particle, and $C_e = C_a + C_s$. The radiative properties of the particle are related to C_a , C_s , and C_e , as will be shown later. The expressions for extinction and scattering efficiencies are:

$$Q_e = \frac{2}{x^2} \sum_{m=1}^{\infty} (2m+1) \operatorname{Re}\{a_m + b_m\} \quad (3.15)$$

$$Q_s = \frac{2}{x^2} \sum_{m=1}^{\infty} (2m+1) (|a_m|^2 + |b_m|^2) \quad (3.16)$$

where

$$a_m = \frac{\psi'_m(\bar{n}x)\psi_m(x) - \bar{n}\psi_m(\bar{n}x)\psi'_m(x)}{\psi'_m(\bar{n}x)\xi_m(x) - \bar{n}\psi_m(\bar{n}x)\xi'_m(x)} \quad (3.17)$$

$$b_m = \frac{\bar{n}\psi'_m(\bar{n}x)\psi_m(x) - \psi_m(\bar{n}x)\psi'_m(x)}{\bar{n}\psi'_m(\bar{n}x)\xi_m(x) - \psi_m(\bar{n}x)\xi'_m(x)} \quad (3.18)$$

The functions ψ_m and ξ_m are Ricatti-Bessel functions, which obey the recursion relation

$$\psi_{m+1}(x) = \frac{2m+1}{x}\psi_m(x) - \psi_{m-1}(x) \quad (3.19)$$

$$\chi_{m+1}(x) = \frac{2m+1}{x}\chi_m(x) - \chi_{m-1}(x) \quad (3.20)$$

where

$$\xi_m = \psi_x - i\chi_m \quad (3.21)$$

$$\psi_{-1}(x) = \cos x \quad \psi_0(x) = \sin x \quad (3.22)$$

$$\chi_{-1}(x) = -\sin x \quad \chi_0(x) = \cos x \quad (3.23)$$

The phase function p for unpolarized incident radiation is

$$\Phi(\theta) = \frac{2(|S_1|^2 + |S_2|^2)}{Q_s x^2} \quad (3.24)$$

where

$$S_1(\theta) = \sum_{m=1}^{\infty} \frac{2m+1}{m(m+1)} (a_m \pi_m + b_m \tau_m) \quad (3.25)$$

$$S_2(\theta) = \sum_{m=1}^{\infty} \frac{2m+1}{m(m+1)} (a_m \tau_m + b_m \pi_m) \quad (3.26)$$

$$\pi_m(\cos\theta) = \frac{1}{\sin\theta} P_m^1(\cos\theta) \quad (3.27)$$

$$\tau_m(\cos\theta) = \frac{d}{d\theta} P_m^1(\cos\theta) \quad (3.28)$$

and P_m^l are associated Legendre polynomials. The asymmetry factor, which is independent of polarization of the incident radiation, can be written in terms of Mie coefficients a_m and b_m as follows:

$$g = \frac{4}{Q_s x^2} \sum_{m=1}^{\infty} \frac{m(m+2)}{m+1} \operatorname{Re}\{a_m a_{m+1}^* + b_m b_{m+1}^*\} + \frac{2m+1}{m(m+1)} \operatorname{Re}\{a_m b_m^*\} \quad (3.29)$$

(superscript * denotes the complex conjugate and Re denotes the real value).

It can be seen that the expressions for obtaining the efficiency factors involves evaluation of an infinite series whose terms contain spherical Riccati-Bessel functions and first and second derivatives of Legendre polynomials. For large size parameters, many terms are needed to evaluate the series accurately and thus involving significant computer time. Often the series can become unstable. Techniques for accurate and efficient evaluation of the efficiency factors for all size parameters are available in the literature [5]. The above analysis indicates that if the particle diameter and its optical constants relative to the medium are known, the radiative properties of the particulate can be obtained.

3.2.2 Rayleigh Scattering

The theory of radiative scattering by spheres that are small compared with wavelength was first proposed by Rayleigh long before the development of Mie's theory [5]. However, Rayleigh scattering can be easily obtained from the limiting case of Mie scattering for the size parameter $x \rightarrow 0$. In that limit, all Mie coefficients except a_1 are zero, and the absorption and scattering efficiencies become:

$$Q_a = -4 \operatorname{Im} \left\{ \frac{\tilde{n}^2 - 1}{\tilde{n}^2 + 2} \right\} x \quad (3.30)$$

$$Q_s = \frac{8}{3} Re \left\{ \frac{\tilde{n}^2 - 1}{\tilde{n}^2 + 2} \right\}^2 x^4 \quad (3.31)$$

For small particles, $x^4 \ll x$ and therefore, scattering can be neglected compared to absorption. As a result, $Q_e \approx Q_a$. The phase function for Rayleigh scattering is

$$\Phi(\theta) = \frac{3}{4}(1 + \cos^2\theta). \quad (3.32)$$

The phase function is symmetric as far as forward and backward scattering is concerned, and does not deviate strongly from isotropic scattering ($g = 1$).

3.2.3 Effects of Dispersion

Mie scattering analysis provides the radiative properties of a single spherical particle. For a cloud of particles such as that encountered in a kraft recovery boiler, the radiative properties can be obtained by simply adding up the effects of all the particles (since the scattering has been assumed to be independent). For homogeneous monodispersion, the scattering and absorption coefficients are:

$$k_\lambda = C_a N_0 \quad (3.33)$$

$$\sigma_\lambda = C_s N_0 \quad (3.34)$$

where N_0 is the total number of particles per unit volume. For monodispersion of spherical particles, the number density, N_0 is related to the particle volume fraction as

$$N_0 = \frac{3f_v}{4\pi r_0^3} \quad (3.35)$$

where r_0 is the radius of the particles.

For a cloud of spherical particles of the same composition but different sizes (homogeneous polydispersion), assuming the size distribution to be a continuous function, the spectral absorption and scattering coefficients can be written as:

$$k_\lambda = \int_0^\infty C_a(r, \lambda) N(r) dr = \pi \int_0^\infty Q_a(r, \lambda) r^2 N(r) dr = \pi N_0 \int_0^\infty Q_a(r, \lambda) r^2 f(r) dr \quad (3.36)$$

$$\sigma_\lambda = \int_0^\infty C_s(r, \lambda) N(r) dr = \pi \int_0^\infty Q_s(r, \lambda) r^2 N(r) dr = \pi N_0 \int_0^\infty Q_s(r, \lambda) r^2 f(r) dr \quad (3.37)$$

where $N(r)dr$ is the number of particles per unit volume with radius between r and $r + dr$. The normalized particle size distribution $f(r)$ is defined as:

$$\int_0^\infty f(r) dr = \frac{1}{N_0} \int_0^\infty N(r) dr \quad (3.38)$$

The total number of particles per unit volume N_0 is

$$N_0 = \int_0^\infty N(r) dr \quad (3.39)$$

and the particle volume fraction is

$$f_v = \frac{4}{3} \pi \int_0^\infty r^3 N(r) dr \quad (3.40)$$

For Rayleigh scattering, the absorption coefficient for a cloud of nonuniform-size particles is:

$$k_\lambda = \pi \int_0^\infty Q_a r^2 N(r) dr = -4 \operatorname{Im} \left\{ \frac{\bar{n}^2 - 1}{\bar{n}^2 + 2} \right\} \int_0^\infty \frac{2\pi r}{\lambda} \pi r^2 N(r) dr \quad (3.41)$$

In other words, the absorption coefficient,

$$k_\lambda = \operatorname{Im} \left\{ \frac{\bar{n}^2 - 1}{\bar{n}^2 + 2} \right\} \frac{6\pi f_v}{\lambda} \quad (3.42)$$

The above equation shows that the absorption coefficient for Rayleigh scattering does not depend on particle size distribution but only on the volume fraction of these particles.

Since there are several type of particles in the kraft recovery boiler, it is more convenient to use particle size groups for calculating the radiative properties of each particle species. The spectral absorption and scattering coefficients of each particle species, m is:

$$k_{\lambda m} = \pi \sum_{m=1}^{N_m} r_m^2 N_m Q_{a,m}(r_m, \lambda) \quad (3.43)$$

$$\sigma_{\lambda m} = \pi \sum_{m=1}^{N_m} r_m^2 N_m Q_{s,m}(r_m, \lambda) \quad (3.44)$$

The number of particles per unit volume is calculated from the mass fraction, the density of the particle-gas mixture and the mass of a single particle. If the particle size distributions and the optical constants are known, the radiative properties can be determined.

Mie theory provides the monochromatic absorption and scattering coefficients as a function of spectral complex index of refraction. Though it is conceptually straight-forward to take into account the dependence of refraction on wavelength, it is computationally time-consuming. Therefore, some spectrally averaged properties need to be used in the heat transfer analysis. One possible method is to divide the entire spectrum into a number of bands as in the case of gases, and obtaining an average value for the band. If a single band encompasses the entire spectrum, then total properties can be found. There is not enough data available at present

for the material properties of particulate media occurring in kraft recovery boiler. To this end, an experimental research project has been undertaken by Wessel [6] to measure the properties of char and black liquor droplets for various furnace conditions. Estimates of these values for char and ash can be obtained from coal combustion (for char $\bar{n} = 2.2 - 1.12i$ and for ash $\bar{n} = 1.5 - 0.02i$).

Chapter 4

Radiation Models

The radiation intensity is a function of space, wavelength and direction. It is not possible to develop a single general solution method for the RTE which would be equally applicable to different systems. Consequently, several different solution methods have been developed over the years. Some of the most widely used methods for prediction of radiative heat transfer in furnaces are (1) Monte Carlo Method, (2) Zonal Method, (3) Flux Methods, and (4) Hybrid Methods.

4.1 Monte Carlo Method

Monte Carlo method [3] is a statistical numerical method of predicting the radiant heat transfer from one location to another and is one of many purely statistical approaches of solving the radiation heat transfer problems. In Monte Carlo method, the solution domain is divided into a number of elemental areas and volumes. Each elemental area or volume is assigned a finite number of photon bundles with a specified energy. The path history of each photon bundle including path direction, spectral characteristics, absorption, reflection, scattering etc. is determined by a probability

analysis based on the physical laws governing the radiation process. By counting the number of bundles absorbed by an elemental volume or area that were emitted by another element, the radiation heat transfer from the one element to another is calculated. Monte Carlo method can be used for complex geometries and spectral effects can be accounted without much difficulty. The method in principle can yield the exact solution to any radiation heat transfer problem if the number of samples are sufficiently high. The primary limitation of this method is the requirement of large computer time to obtain accurate results. This problem becomes acute when the grid size of the Monte Carlo solution has to match the fine grids often required for the computation of momentum and energy equations. Moreover, the method is always subject to statistical errors and lack of convergence.

4.2 Zonal Method

In Zonal Method [3], the surface and volume enclosure is divided into a number of zones, each one is assumed to have a uniform distribution of temperature and radiative properties. Then the direct exchange areas (factors) between the surface and volume elements are evaluated and the total exchange area are determined using matrix inversion techniques. For an absorbing and emitting medium such as the furnace gas in kraft recovery boiler, the calculation of direct exchange areas become complicated as the attenuation of radiation along the path connecting two area (area-volume and volume-volume) elements must be taken into account. The inclusion of scattering of radiation into zonal method is difficult.

4.3 Flux Methods

In flux methods [7], the angular dependence of the radiation intensity is separated from the spatial dependence by certain assumptions in order to simplify the RTE. One method is to assume that the intensity is uniform on a given intervals of the solid angle. The six flux method and the discrete ordinates method are derived in this manner. Another way of avoiding complicated expressions due to the angular dependence of the intensity is to integrate the RTE over the space after multiplying it by certain direction cosines. This procedure yields spherical harmonic method.

4.4 Hybrid and Other Methods

All of the above methods have some flaws. In order to take advantage of the desirable features of the different models, various hybrid models have been developed. These methods have not been tested widely and some are hard to implement in a fluid flow code. The discrete transfer method combines some of the virtues of Monte Carlo, Zonal and Discrete Ordinates Methods. Radiant ray method is another hybrid method. Other methods include finite element method, and the finite volume method of Raithby and Chui [8].

4.5 Discrete Ordinates Method

For a three dimensional enclosure containing an absorbing, emitting and scattering medium such as the kraft recovery furnace, previous studies show that the discrete ordinates method yields more accurate results than the spherical harmonic method

and the six flux method [9,10]. This method can easily be integrated into the control volume method used for the calculation of fluid flow in the furnace.

The discrete ordinates method, also called as "SN method" is a flux method and is based on a discrete representation of the directional variation of the radiation intensity. A solution to the radiation heat transfer is found by solving the RTE for a set of discrete directions spanning the entire solid angle range of 4π . The integrals over solid angles are replaced by numerical quadratures.

The discrete ordinates method is based on a discrete representation of the directional variation of the radiation intensity. A solution to the radiation heat transfer is found by solving the RTE for a set of discrete directions spanning the entire solid angle range of 4π . The integrals over solid angles are replaced by numerical quadratures, that is,

$$\int_{4\pi} f(s) d\Omega = \sum_{i=1}^n w_i f(s_i) \quad (4.1)$$

where $s_i, i = 1, 2, \dots, N$ are the N different directions, and w_i are the corresponding weighting factors.

The equation of transfer can then be written as,

$$s_i \cdot \nabla I_\lambda(\vec{r}, s_i) = -\beta_\lambda(\vec{r}) I_\lambda(\vec{r}, s_i) + \kappa_\lambda(\vec{r}) I_{\lambda b}(\vec{r}) + \frac{\sigma_\lambda(\vec{r})}{4\pi} \sum_{j=1}^N w_j I_\lambda(\vec{r}, s_j) \Phi(s_i, s_j) \quad (4.2)$$

Thus the directional dependence of the RTE has been approximated by a set of N equations.

The boundary conditions can also be similarly approximated. The walls are assumed to be opaque and diffuse with the wall emissivity depending on the temperature alone. When the wall temperature is known,

for $n \cdot s_i > 0$

$$I_\lambda(r_w, s_i) = \epsilon(r_w) I_{\lambda b}(r_w) + \frac{\rho(r_w)}{\pi} \sum_{n \cdot s_j < 0} w_j I_\lambda(r_w, s_j) |n \cdot s_j| \quad (4.3)$$

where $I_{\lambda b}(r_w)$ is the blackbody intensity at the temperature of the wall and (n is the unit vector normal to the wall).

for $n \cdot s_i < 0$

$$I_\lambda(r_w, s_i) = \epsilon(r_w) I_{\lambda b}(r_w) + \frac{\rho(r_w)}{\pi} \sum_{n \cdot s_j > 0} w_j I_\lambda(r_w, s_j) n \cdot s_j \quad (4.4)$$

When the wall heat flux is given:

for $n \cdot s_i > 0$

$$I_\lambda(r_w, s_i) = \frac{q}{\pi} + \frac{1}{\pi} \sum_{n \cdot s_j < 0} w_j I_\lambda(r_w, s_j) |n \cdot s_j| \quad (4.5)$$

where q is the prescribed flux at the boundary.

for $n \cdot s_i < 0$

$$I_\lambda(r_w, s_i) = \frac{q}{\pi} + \frac{1}{\pi} \sum_{n \cdot s_j > 0} w_j I_\lambda(r_w, s_j) n \cdot s_j \quad (4.6)$$

Symmetry conditions and periodic conditions can also be specified. For example, if the b.c. at west wall is a symmetry condition,

$$I_\lambda(r_w, s_i) = I_\lambda(r_w, s_j) \text{ where } |\mu_i| = |\mu_j| \quad (4.7)$$

The above equations constitute a set of N simultaneous, first-order, linear partial differential equations for the unknown $I_\lambda(r, s_i)$. If scattering is present ($\sigma_\lambda \neq 0$), the equations are coupled in such a way that generally an iterative procedure is necessary.

Even in the absence of scattering, the temperature field is usually not known, thus making iterations necessary.

Once the intensities are determined, the radiative heat flux, inside the medium, $q(r)$ or at a surface, $q(r_w)$, can be found from

$$q(r) = \int_0^\infty \left[\int_{4\pi} I(r, s) s d\omega \right] d\lambda = \int_0^\infty \left[\sum_i^N w_i I_i(r) s_i \right] d\lambda \quad (4.8)$$

and

$$q(r_w) = q \cdot n(r_w) = \int_0^\infty \left[\epsilon(r_w) (\pi I_b(r_w) - \sum_{n \cdot s < 0} w_i I_i(r_w) |n \cdot s_i|) \right] d\lambda \quad (4.9)$$

If spectrally averaged properties are used in the analysis, wavelength-by-wavelength calculations of the radiation intensity are not necessary, and this greatly simplifies the prediction of the heat fluxes. The solution of RTE can also be simplified if the scattering is assumed to be either isotropic or linear-anisotropic. For isotropic scattering

$$\Phi(s_i, s_j) = 1 \quad (4.10)$$

while, for linearly anisotropic scattering,

$$\Phi(s_i, s_j) = 1 + g(r) s_i \cdot s_j \quad (4.11)$$

where g is the asymmetry parameter.

4.5.1 Selection of Discrete Ordinate Directions

In the solution of the equation of transfer using Eq. (4.2) with the boundary conditions, namely, Eqs. (4.3) to (4.7), directions, μ_i , η_i and ψ_i , and angular weights

w_i are needed. The set of directions s_i and quadrature weights w_i are chosen such that they are completely symmetric and satisfy the zeroth, first and second moments.

$$\int_{4\pi} d\omega = 4\pi = \sum_{i=1}^N w_i \quad (4.12)$$

$$\int_{4\pi} s d\omega = 0 = \sum_{i=1}^N w_i s_i \quad (4.13)$$

$$\int_{4\pi} s s d\omega = \frac{4\pi}{3} \delta = \sum_{i=1}^N w_i s_i s_i \quad (4.14)$$

where δ is the unit tensor. Different sets of directions and weights satisfying all these criteria are available in the literature. In order to predict the wall heat fluxes accurately and to avoid directional discontinuities in the intensity at the wall, it is essential that the set of directions and the weights also satisfy the first moment over a half range that is,

$$\int_{n \cdot s < 0} |n \cdot s| d\omega = \int_{n \cdot s > 0} n \cdot s d\omega = \pi = \sum_{n_i \cdot s_i > 0} w_i n \cdot s_i \quad (4.15)$$

While it is impossible to satisfy the above equation for arbitrary orientations of the surface normal, they can be satisfied for the three principal directions. Sets of ordinates and weights that satisfy the symmetry requirement, the moment equations and the half-moment equation for three principal directions are available in the literature. For S2, S4 and S6 methods, the number of directions are 8, 24 and 48, respectively.

4.6 Numerical Method

The RTE for an ordinate direction i can be rewritten as (dropping the subscript λ for the sake of convenience),

$$\mu_i \frac{\partial I^i}{\partial x} + \xi_i \frac{\partial I^i}{\partial y} + \eta_i \frac{\partial I^i}{\partial z} = -\beta I^i + \kappa I_b + \frac{\sigma}{4\pi} \sum_j w_j \Phi(i, j) I^j \quad (4.16)$$

where μ_i , ξ_i and η_i denote the direction cosines of the discrete direction, i .

The finite difference form of the RTE can be obtained by integrating over a cubical control volume (same as that used in the flow calculations).

$$\mu_i A(I_e^i - I_w^i) + \xi_i B(I_n^i - I_s^i) + \eta_i C(I_t^i - I_b^i) = -\beta \Delta v I_P^i + \kappa \Delta v I_{bP} + \Delta v \frac{\sigma}{4\pi} \sum_j w_j \Phi_{i,j} I_P^j \quad (4.17)$$

where A , B , C and Δv denote the area of the sides and the volume of the cell surrounding the node P , respectively ($A = \Delta y \cdot \Delta z$, $B = \Delta z \cdot \Delta x$, $C = \Delta x \cdot \Delta y$ and $\Delta v = \Delta x \cdot \Delta y \cdot \Delta z$).

The intensities at the face of the control volume can be related to the cell center intensity, I_P as follows:

$$I_P^i = \alpha I_{le}^i + (1 - \alpha) I_{lr}^i \quad (4.18)$$

where l denotes the coordinate directions x , y and z , and α is an interpolation parameter. The subscripts e and r denote the end- and reference-face values of the control volume.

The value of α depends on the type of spatial differencing scheme. The most commonly used spatial differencing schemes are the step, diamond, positive and variable weights scheme. For step scheme, $\alpha=1$ and for the diamond scheme $\alpha=0.5$. In this

analysis, the step scheme is used. The step scheme ensures the radiation intensity at all locations to be always positive.

For a positive direction cosine μ_i , the end face is east face of the control volume and the reference face is the west face. For a negative direction cosine μ_i , the end face is west face of the control volume and the reference face is the east face. Eliminating the unknown intensities in equation (4.17) from equation (4.18), the resulting equation for the radiation intensity, I_P^i at the center of a control volume is given by

$$I_P^i = \frac{|\mu_i| AI_{zr}^i + |\xi_i| BI_{yr}^i + |\eta_i| CI_{zr}^i + \alpha S \Delta v}{|\mu_i| A + |\xi_i| B + |\eta_i| C + \alpha \beta \Delta v} \quad (4.19)$$

where

$$S_1 = \kappa I_b \quad (4.20)$$

and,

$$S_2 = \frac{\sigma}{4\pi} \sum_j w_j \Phi_{i,j} I_P^j \quad (4.21)$$

4.7 Solution Procedure

The numerical solution to the equation of transfer is iterative because the emission, scattering source terms, and the boundary conditions depend on the intensities. The calculations are started by assuming the boundaries are black, and the in-scattering source terms are zero. The intensities along a particular ordinate direction are computed starting from the node next to the wall and visiting all nodes one after another. The points in the computational domain are visited according to the direction that the radiation beam propagates (for positive μ_i the calculation is carried out from the

west to east and for negative μ_i the calculation is carried out from the east to west and so on). This procedure is repeated for all the ordinate directions, and all possible wavelengths, in the case of spectrally dependent properties. Once all directions (and wavelengths) have been scanned, the wall heat fluxes and the source terms in due to scattering are updated. The radiation intensity at a particular node in the computational domain is calculated for all directions and for all wavelengths, in the case of spectrally dependent properties. Once all nodal points (and wavelengths) have been scanned, the wall heat fluxes and the source terms in due to scattering are updated. The procedure is continued until the desired accuracy in radiation intensity calculation is obtained. The divergence of the radiative heat flux term is obtained, and the gas temperature field is then obtained from the numerical solution of the energy equation with appropriate boundary conditions. The radiative properties such as the emissivities are updated, and the procedure is continued until convergence is obtained for the gas temperature field.

Chapter 5

A Brief Description of the Radiation Code

Radiation does not affect the conservation equations for mass, momentum or species and its contribution is a source term to the conservation equation for energy. The radiation intensity needed in the calculation of this source term is obtained from the solution of radiative transfer equation at all locations and all possible directions. The radiation intensity does not depend on the flow field. It is directly coupled with the temperature field, and is indirectly coupled with the temperature and species concentration fields through the radiative properties.

The computer programs for the flow and heat transfer analysis of kraft recovery boiler has been arranged in such a way that the prediction of flow, temperature and concentration fields, and the prediction of radiation intensities are carried out independently with periodic interaction between them. The two programs have the flexibility to be executed in parallel. The interaction between the two programs occurs through computer files stored in the hard disk of the system. The program for the prediction of radiation transfer reads the temperature and concentration fields from

the flow program, converts these fields to the radiation grid, calculates the radiation properties, and iterates to obtain an improved radiation intensity field. It outputs periodically the radiation source terms needed for the solution of energy equation in the flow program. The flow program reads the radiation sources, calculates an improved flow, temperature and concentration fields, and outputs temperature and concentration fields periodically.

In the discrete ordinate method, the radiation intensity is calculated only along discrete directions. The S2 method with 8 radiation directions does not predict the wall heat fluxes accurately and therefore, S4 or S6 method is needed. The S4 method uses 24 radiation directions. The S6 method uses 48 directions and therefore uses much more CPU. The difference in wall heat fluxes and source terms between S4 and S6 method is small and therefore, in this study, S4 method will be used most of the time. The grids for flow and radiation calculations should be compatible for easy exchange of information between the two parts of the code. The radiation program has been written in such a way that the radiation grid can be chosen either to be the same as the flow grid or to be coarser than that of the flow grid. The degree of coarseness can be specified individually for each segment and direction.

The radiation code has a lot of similarities with the flow code. It has four major parts. The common arrays and variables are in "radcom.f" and "rad.par". "Rad.par" is similar to "geo.par" in flow code. It contains the parameters for the array dimensions. As in the flow code, at the start of the run, the parameters in "rad.par" are given large values. At the end of initial run, the parameters are reset so that correct dimensions of the arrays are used in the program.

The first part of the radiation program initializes the variables and sets the correct dimensions. This is similar to "geo.f" in the flow code. This part has the routines "rstart", "rcoord", "rcont", "rsegr", "rgrcrd" and "rdisc". The routine "rstart" initializes the arrays. As stated previously, the radiation code uses a grid that is compatible with the flow code. The number of flow grid cells that correspond to one radiation grid are user specified in the file "rad.in". The subroutine "rcoord" divides the calculation domain into a number of control volumes for radiation calculations and is similar to "divbl" in "geo.f" of the flow code. The subroutines "rcont", "rsegr" and "rgrcrd" are similar to the subroutines "cont", "segr" and "grcrd" in the flow code and take care of intersegmental continuation of radiation intensities. The subroutine "rdisc" contains the direction cosines and the weighting factors for the discrete directions of the "SN" method.

The second part of the program interacts with the flow and radiation codes, and it consists of the subroutine "temrad" and the input file "temp.in". The subroutine "temrad" reads the temperature field (the periodic output of "trans.f" of flow code), the geometric parameters from "geo.temp" (an output file from "geo.f" of the flow code), and the prescribed temperatures of the void regions (the bed and bull nose) from the file "temp.in". It outputs the temperature field, the types of boundary conditions, the boundary temperatures and other necessary information for use of subroutines that calculate the radiation intensities.

The third part of the program contains the subroutines "radnew" and "rblock". The subroutine "radnew" loads the intensities, geometrical parameters and radiative properties and calls "rblock" where the updated intensities and source terms are

obtained. The subroutine "radnew" also stores the updated intensities in the global arrays and outputs the radiation source term used by the flow program.

In the fourth part of the program, the radiative properties are calculated. It contains the subroutines "rprop", "hottel", and others. "Rprop" reads the scalar values from large one dimensional array "s" of the file "f.dat", a periodic output of the flow program. It calculates the partial pressures of the various constituents of the furnace gas and calls the subroutines "hottel" and others to obtain the radiative properties of the furnace gas.

A separate subroutine "ios3" makes sure that there are no conflicts when the files either read or written out by the radiation and flow programs. This routine is very flexible and it can be called in such a way that one program waits for the other to provide the updated values or to continue running. Each program checks the files periodically to see whether updated values, namely the temperatures and concentrations or radiation sources, are available. While one program is either reading or writing an array, the other waits for the file to be freed.

Chapter 6

Hot Flow Simulations for a Generic Boiler

This section presents the hot flow runs for a generic boiler. A generic boiler design was selected because of obvious implications of the results on the competitive position of actual boiler manufacturers and operators.

6.1 Boiler Geometry

The schematic of the generic boiler is shown in Figs. 6.1. The boiler has 10.0 m square base, and is 40 m high. The bullnose is located at 26.5 m from the floor and the boiler depth at this level is 6.5 m. The boiler features three levels of air: four wall primary (1.2 m above the floor), four wall secondary (3.0 m above the floor) and two wall tertiary (10.0 m above the floor). There are 4 liquor guns, one at center of each wall, 7.0 m above floor. The char bed has the shape of a truncated pyramid with a 8 m square base and 5 m square top. The height of bed is 2.0m.

The primary ports on all four walls are modelled as slots 9.6 m wide and 0.08 m high. There are 5 secondary ports on each wall. Each of these ports has a width of

0.1 m and a height of 0.2 m. There are 7 tertiary ports each on the south and north walls. Each of these ports has a width of 0.1 m and a height of 0.05m.

6.2 Air Distribution, and Liquor and Spray Characteristics

The details of the air system is shown in Fig. 6.2. The boiler operates with a total air input of about 88 kg/s at a temperature of 150 °C. The air input was split 49.4%, 31.2% and 19.4% among the primary, secondary and tertiary levels. This results in a calculated air inputs of 156500, 98750, and 61270 kg/hr through primary, secondary and tertiary ports, respectively. No air leakage is assumed to occur the liquor gun ports.

The black liquor solids flow rate is 18 kg/s with a solids content of 65%. The black liquor has a higher heating value of 15.0 MJ/kg of dry solids. The liquor nozzles are positioned horizontally and are stationary. The liquor spray due to the splash plates is simulated with a log normal distribution for the droplet diameter having a mean of 2.5 mm, and with a horizontal spray angle of 160°.

6.3 Results and Discussion

Figs. 6.3 to 6.8 show the flow and temperature fields at various horizontal planes. At the primary level, the gas flow is upward near the edges of the bed with small regions of downward flow near the walls (Fig. 6.3). The gas temperature is hotter near the bed and cooler near the walls. At the secondary level, the flow is strongly upward in the regions between the jets (Fig. 6.4). Small regions of downward flow occur near the corners. The gas is hotter near the center of the boiler and cooler near

the corners. At the liquor gun level, a strong upward flowing central core exists (Fig. 6.5). Small regions of downward flow are observed near the corners of the boiler. The gas is also hotter in the center and cooler near the corners. At the tertiary level, the central core is more elongated (Fig. 6.6). Small regions of strong upward flow are present near the south wall. In addition, a small region of downward flow occurs near the north-east corner. The gas temperature is higher near the center and cooler near the jets. At locations above the tertiary level, the central core is more elongated as at the tertiary level (Fig. 6.7). Downward flow occurs near the south and north walls. The gas temperature is higher in the regions of upward flow and lower in the regions of downward flow. At the bullnose level, the core is near the tip of the bullnose and is closer to the west wall (Fig. 6.8). The flow is downward near the south (front) wall. The gas is hotter in the regions of upward flow and cooler in the regions of downward flow. Fig. 6.9 shows the flow and temperature field in the vertical central plane parallel to the side walls. Fig. 6.10 shows the flow and temperature field in the vertical central plane perpendicular to the side walls. The central core and the hotter gas temperatures in the center are clearly seen.

The central core occurs due to the interaction of the secondary jets in the center of the boiler. The tertiary jet velocities are not large enough to break up this central core. As a result, it persists up to the bullnose. Because of the presence of a strong central core, the smelt carryover is fairly large (about 5%). Since the liquor gun ports are located fairly above the bed and because of the large primary air input, the unburned carbon on the bed is fairly low (about 60 mg/s).

Chapter 7

Conclusions

The fundamentals of radiation in a participating medium, the methods to predict the properties of combustion products and, the methods to predict the radiative heat transfer in kraft recovery furnaces were reviewed. In particular, the exponential wide-band model for the prediction of radiative properties of combustion gases, Mie scattering for the prediction of radiative properties of particulates, and the discrete ordinates method and the resulting numerical procedure for the calculation of radiative heat transfer inside a kraft recovery boiler were described in detail. A brief description of the radiation computer code and its interaction with the UBC flow code were also given. Hot flow simulations for a generic boiler were also given.

References

1. T. N. Adams and W. J. Frederick, *Kraft Recovery Boiler Physical and Chemical Processes*, American Paper Institute, New York, 1988.
2. S. Chandrasekhar, *Radiative Transfer*, Oxford at Clarendon Press, London, 1950.
3. R. Siegel and J. R. Howell, *Thermal Radiation Heat Transfer*, McGraw-Hill, Toronto, 1981.
4. D. K. Edwards, *Radiative Transfer Notes*, Hemisphere Publishing Co., New York, 1981.
5. C. F. Bohren and D. R. Huffman, *Absorption and Scattering of Light by Small Particles*, John Wiley & Sons, New York, 1983.
6. R. A. Wessel, Personal Communication, 1994.
7. R. G. Siddall and N. Selcuk, "Evaluation of a New Six-Flux Model for Radiative Transfer in Rectangular Enclosures", *Trans IChemE*, Vol. 57, pp. 163-169, 1979.
8. G. D. Raithby and E. H. Chui, "A Finite-Volume Method for Predicting a Radiant Heat Transfer in Enclosures with Participating Media", *ASME J. Heat Transfer*, Vol. 112, pp. 415-423, 1990.
9. W. A. Fiveland, "Discrete-Ordinates Solutions of the Radiative Transport Equation for Rectangular Enclosures", *ASME J. Heat Transfer*, Vol. 106, pp. 699-706, 1984.
10. W. A. Fiveland, "Three-Dimensional Radiative Heat Transfer Solutions by the Discrete-Ordinates Method", *J. Thermophysics and Heat Transfer*, 2: J309-J316 (1988).
11. P. Matys, P. Sabhapathy, P. Nowak, Z. Abdullah and M. Salcudean, "Effects of Air and Liquor Delivery on Carryover in a Kraft Recovery Boiler", *CPPA Pacific Region Technical Conference*, April, 1995.
12. M.E. Salcudean, P. Nowak and Z. Abdullah, "Cold Flow Computational Model of Recovery Boiler" *J. Pulp and Paper Sci*, 19(5):J186-J194 (1993).

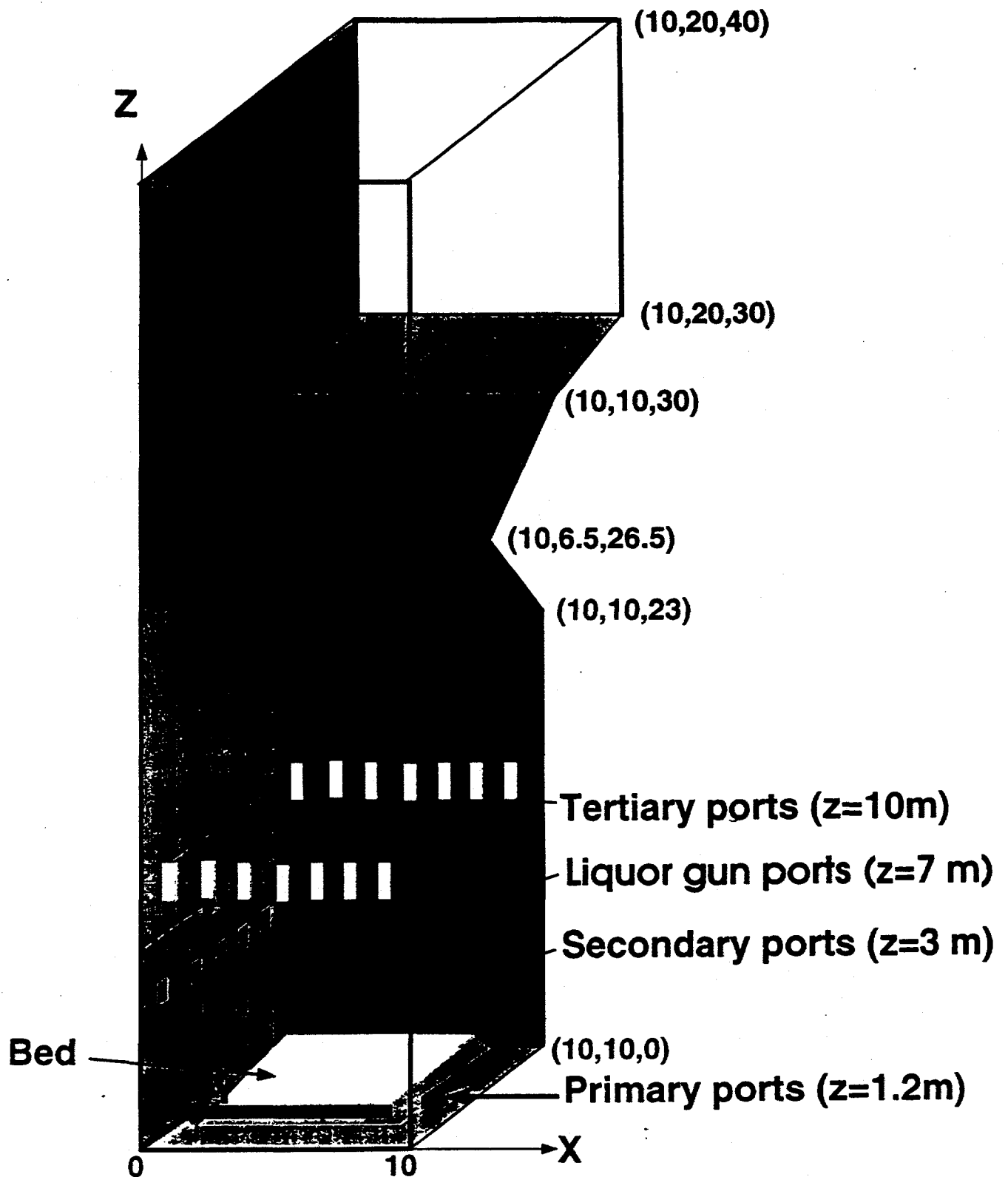
Nomenclature

A	effective bandwidth
A^*	dimensionless effective bandwidth
A, B, C	control volume face areas, m^2
C_a, C_s, C_e	Cross section for absorption, scattering and extinction, respectively
b	pressure parameter
c_p	specific heat at constant pressure, J/kg·K
f	particle distribution function
f_v	volume fraction
g	asymmetry parameter for scattering
I_λ	radiation intensity, $W/m^2 \cdot \mu m \cdot K$
k	thermal conductivity, W/m·K
n	unit normal vector, refractive index
P	pressure, N/m ²
P_a	partial pressure, N/m ²
p	phase function
q	heat flux, W/m ²
q_r	radiative heat flux, W/m ²
Q_a, Q_s, Q_e	efficiency factors for absorption, scattering and extinction, respectively
\dot{q}	local heat generation, W/m ³
S_1, S_2	source terms
S_1, S_2	vectors in Mie scattering
s and s'	radiation intensity directions
T	temperature, K
t	time, s
u	optical depth
x	size parameter
x	x-corodinate, m
y	y-corodinate, m
z	z-corodinate, m
α	interpolation parameter, integrated intensity parameter
β	overlap parameter in the wide band model
β_v	volumetric thermal expansion coefficient, K ⁻¹
β_λ	extinction coefficient = $(\kappa_\lambda + \sigma_\lambda) m^{-1}$
δ	unit tensor
η	wave number = $\frac{1}{\lambda}$
γ	temperature dependent function for β

ϵ	emissivity
κ_λ	absorption coefficient, m^{-1}
σ_λ	scattering coefficient, m^{-1}
λ	wavelength
σ	Stefan-Boltzmann's constant
μ	viscosity (in energy equation), Nm/s^2
μ, ξ, η	direction cosines
ω	bandwidth parameter
Ω	solid angle, steradian
Φ	phase function
ϕ_v	energy dissipation
ρ	fluid density (in energy equation), kg/m^3
$\rho(r_w)$	reflectivity of the wall

Subscripts

b	black body
e, w, n, s, t, b	east, west, north, south, top and bottom faces of the control volume
i, j	directions i and j
x	x-direction
y	y-direction
z	z-direction
λ	wavelength



Generic Kraft Recovery Boiler
Figure 6.1

Figure 6.2

Generic Kraft Recovery Boiler

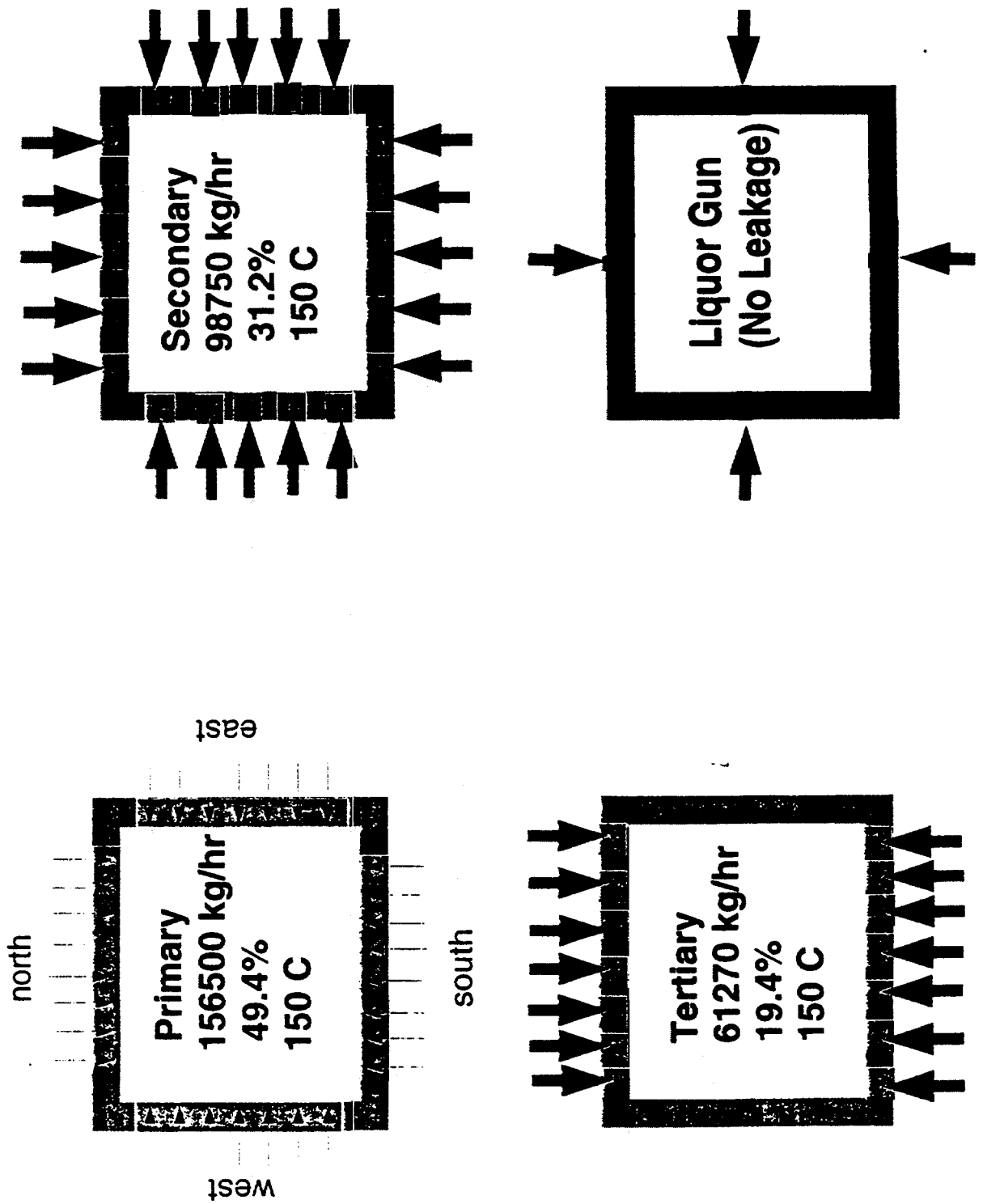


Figure 6.3
Generic Kraft Recovery Boiler
 Flow and Temperature Fields - Horizontal Plane
 Primary Level ($z=1.2$ m)

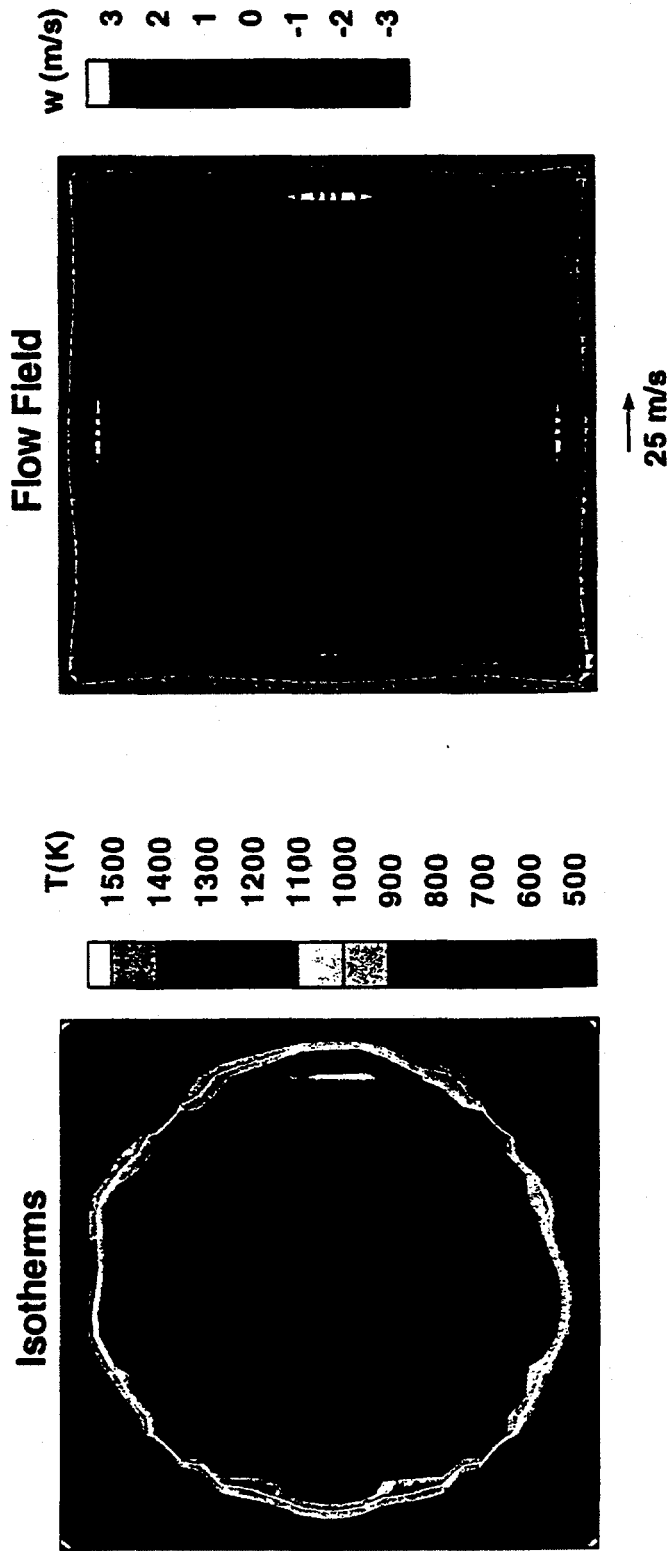


Figure 6.4
Generic Kraft Recovery Boiler
 Flow and Temperature Fields - Horizontal Plane
 Secondary Level ($z=3.0$ m)

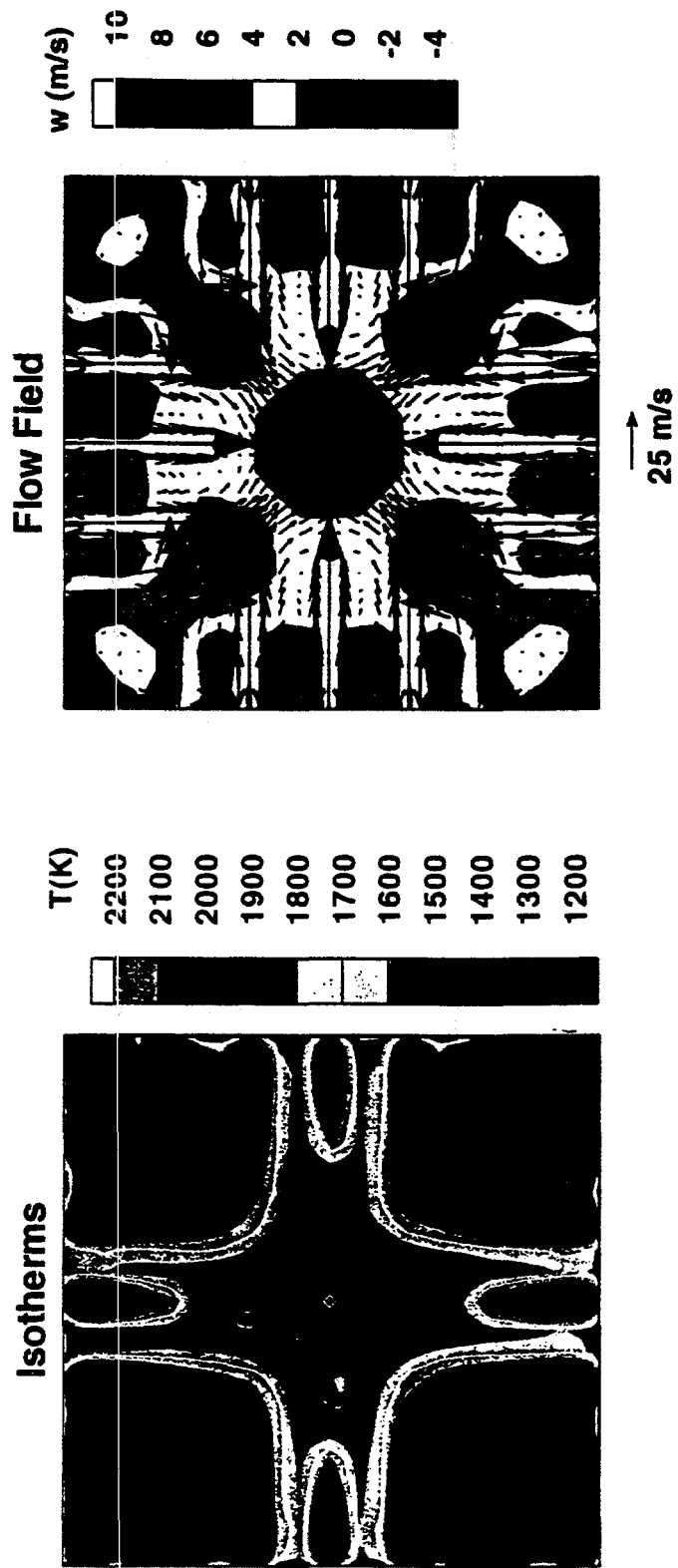


Figure 6.5
Generic Kraft Recovery Boiler
Flow and Temperature Fields - Horizontal Plane
Liquor Gun Level ($z=7.0$ m)

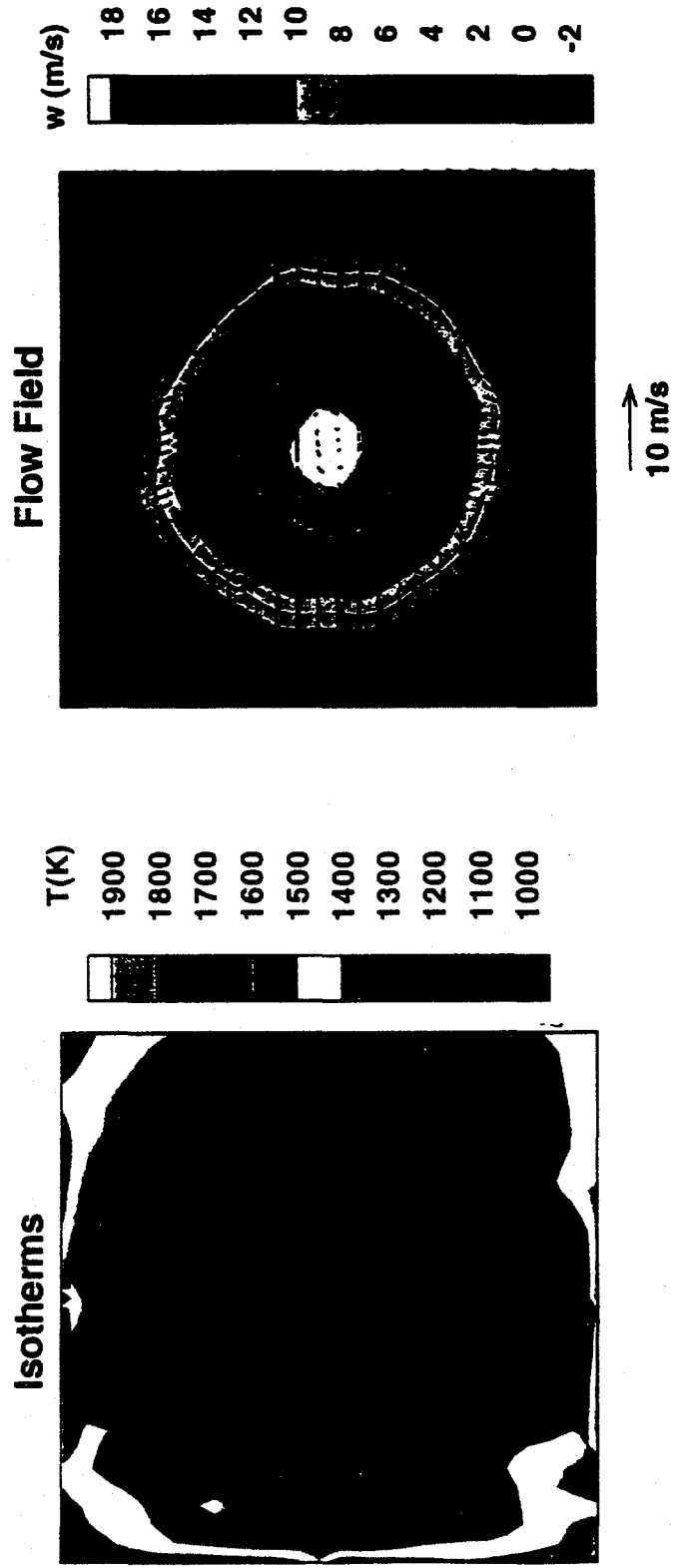


Figure 6.6
Generic Kraft Recovery Boiler
 Flow and Temperature Fields - Horizontal Plane
 Tertiary Level ($z=10.0$ m)

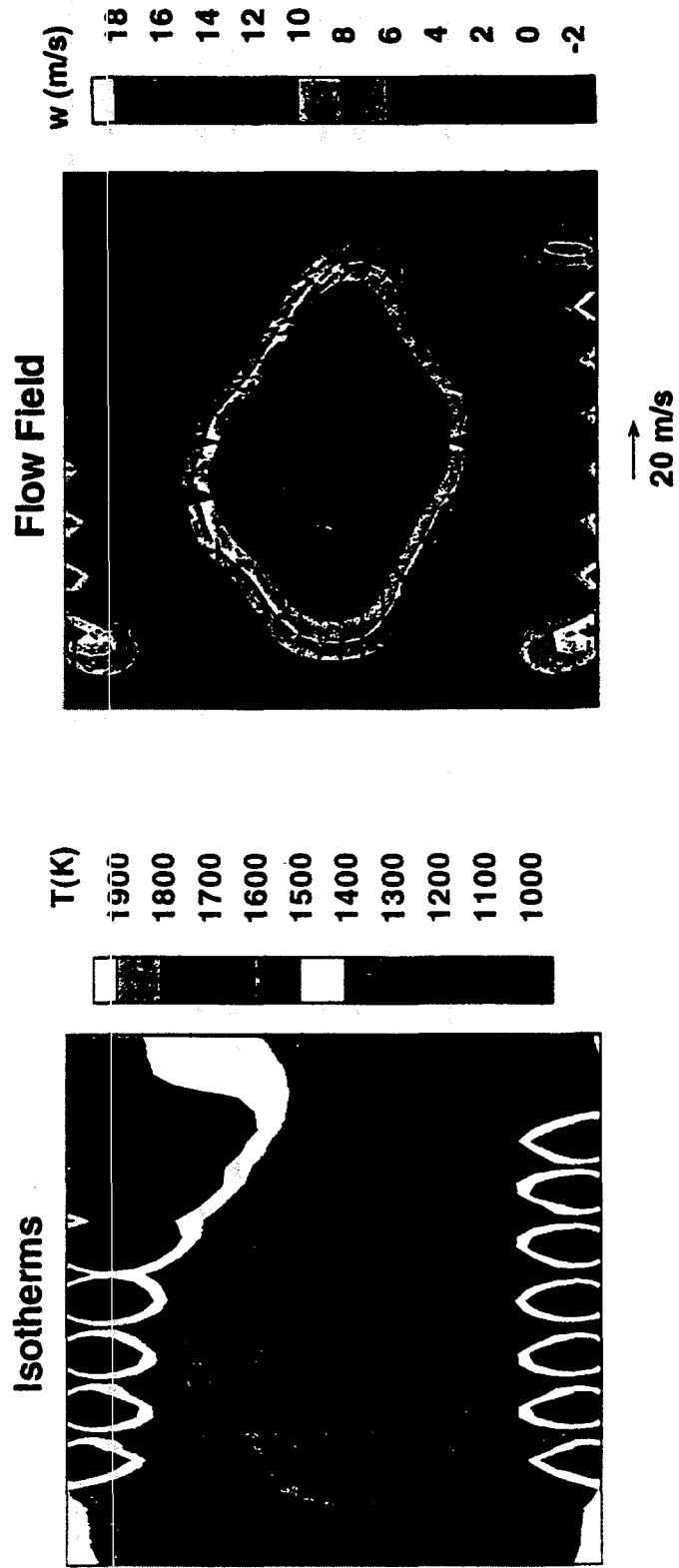


Figure 6.7
Generic Kraft Recovery Boiler
 Flow and Temperature Fields - Horizontal Plane
 Above Tertiary Level (z=15.0 m)

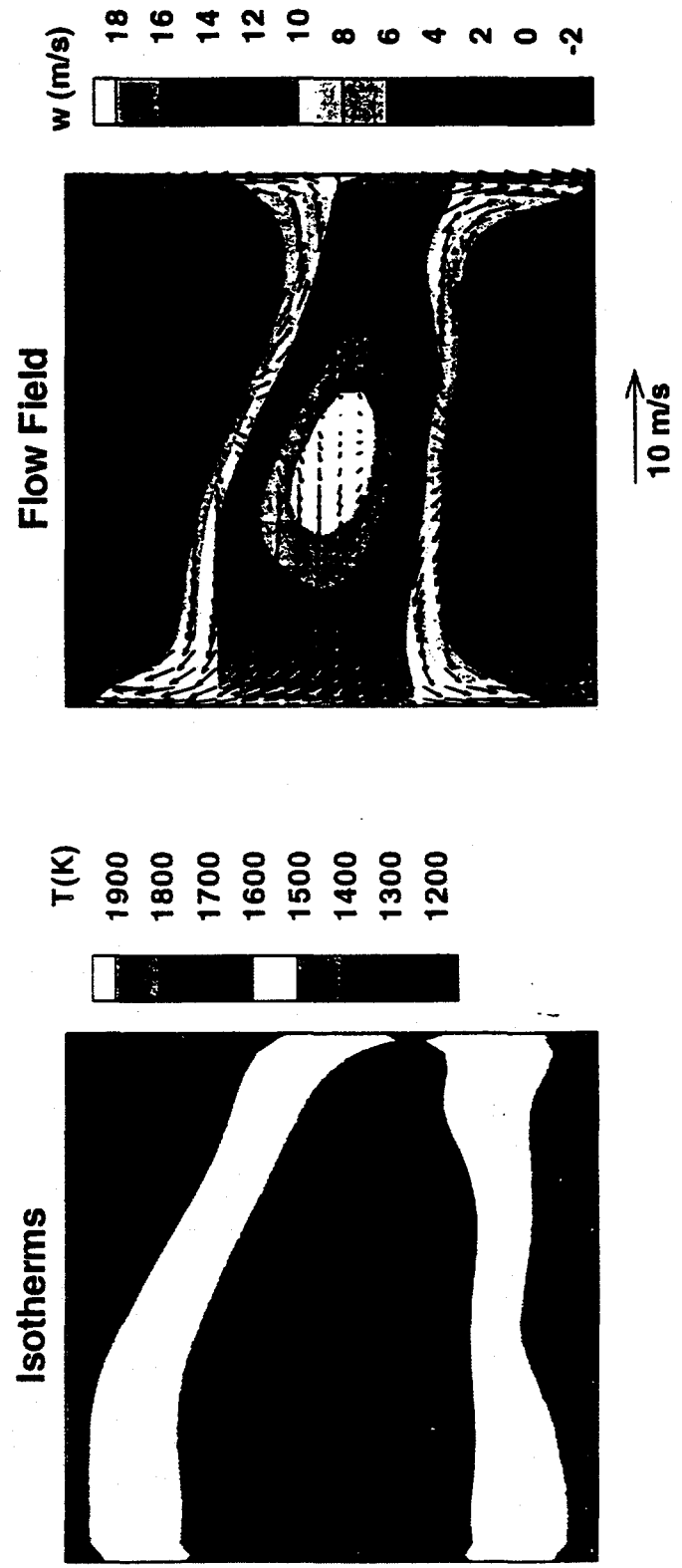


Figure 6.8
Generic Kraft Recovery Boiler
 Flow and Temperature Fields - Horizontal Plane
 Bullnose Level ($z=26.5$ m)

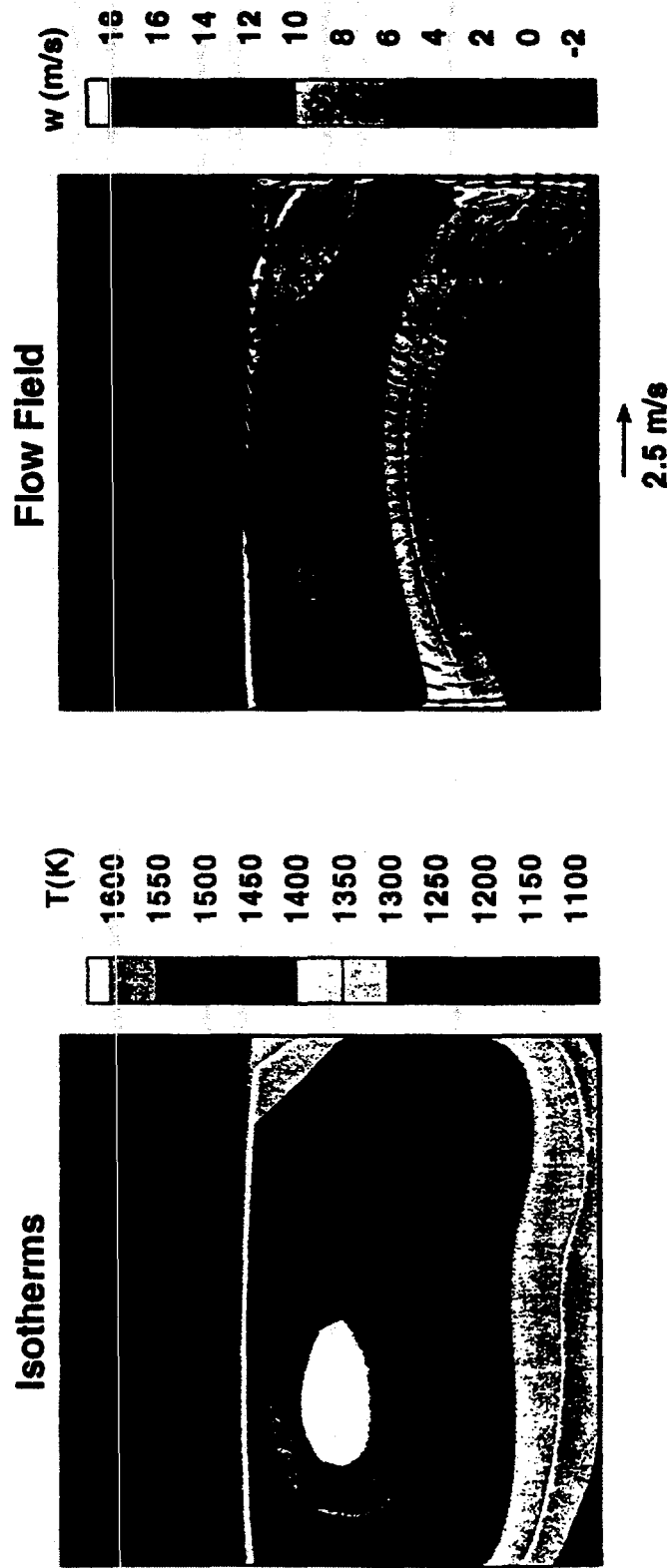


Figure 6.9
Generic Kraft Recovery Boiler
Flow and Temperature Fields in a Vertical Central Plane

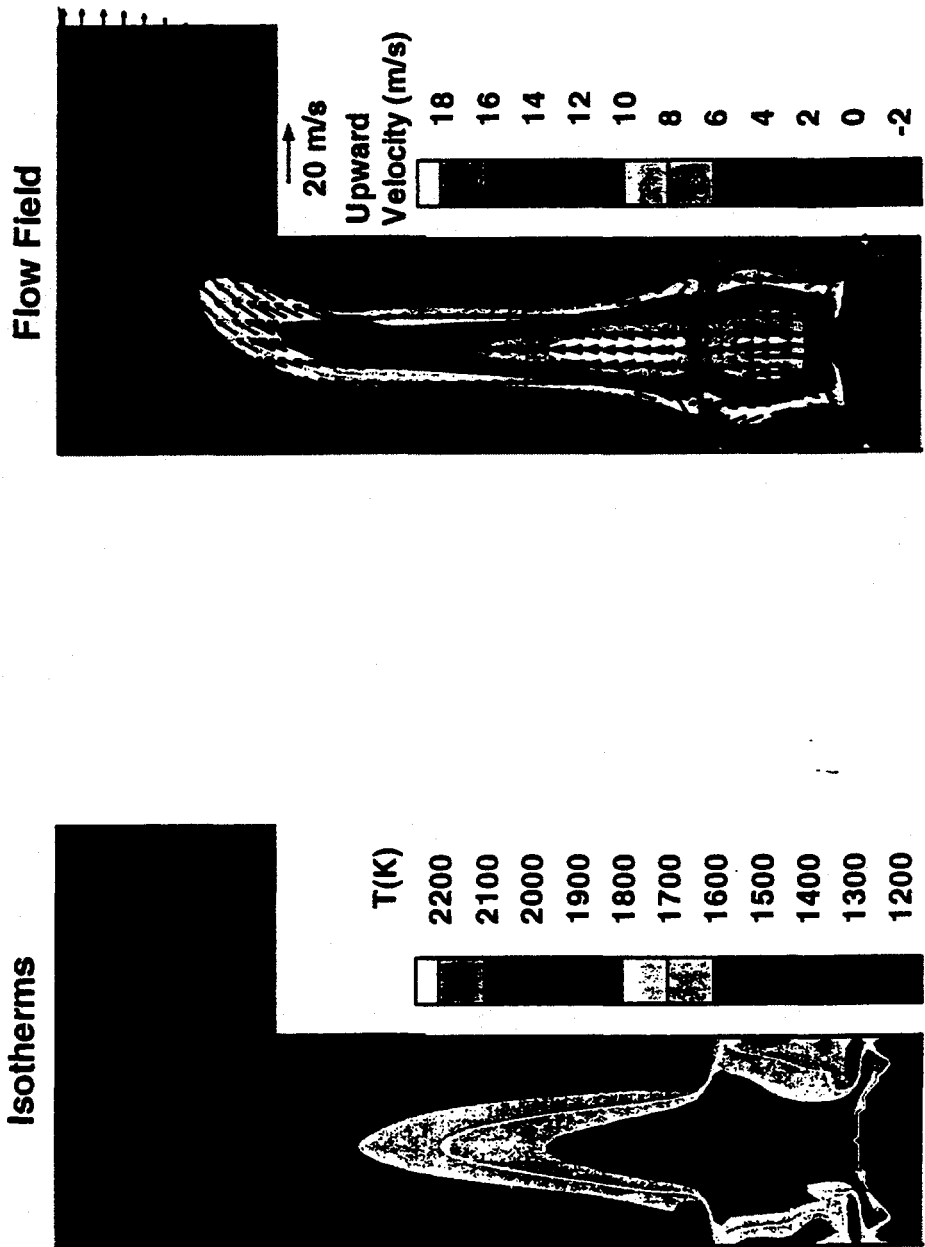
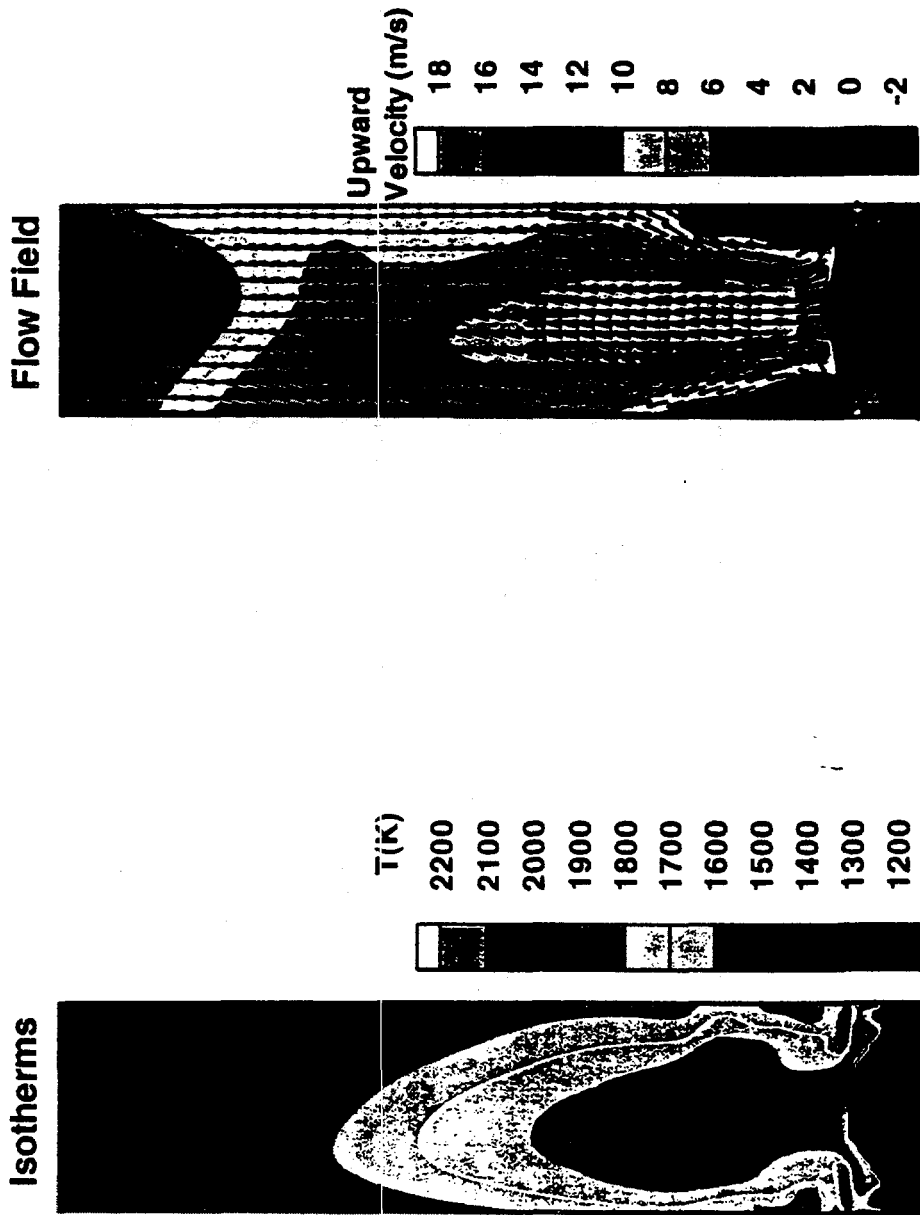


Figure 6.10
Generic Kraft Recovery Boiler
Flow and Temperature Fields in a Vertical Central Plane



APPENDIX II

Black Liquor Chemistry Data

Section 1

The Effect of Temperature and Residence Time on the
Distribution of Carbon, Sulfur, and Nitrogen between
Gaseous and Condensed Phase Products from Low Temperature
Pyrolysis of Kraft Black Liquor

(124 pages)

Section 2

Formation and Destruction of Nitrogen Oxides
In Recovery Boilers

(88 pages)

Section 3

Sintering and Densification of Recovery Boiler
Deposits Laboratory Data and a Rate Model

(34 pages)

**THE EFFECT OF TEMPERATURE AND RESIDENCE TIME
ON THE DISTRIBUTION OF CARBON, SULFUR, AND NITROGEN
BETWEEN GASEOUS AND CONDENSED PHASE PRODUCTS FROM
LOW TEMPERATURE PYROLYSIS OF KRAFT BLACK LIQUOR¹**

By:

Varut Phimolmas

And

W. J. Frederick

INSTITUTE OF PAPER SCIENCE AND TECHNOLOGY

¹ The results reported here are from the M.S. Thesis of Varut Phimolmas (1997).

Contents

Introduction	1
Objectives	3
Literature Review	3
Characteristics and Composition of Black Liquor Solids	3
Black Liquor Droplet Combustion	6
Pyrolysis of Kraft Black Liquor	8
Experimental Procedures and Sample Analysis	20
Experimental Equipment	20
Material	27
Experimental Conditions	28
Experimental Procedure	29
Results and Discussion	32
Carbon Yield from Pyrolysis of Black Liquor Solids	32
Fine Particle Yield from Pyrolysis of Black Liquor Solids	42
Char Residue Yield from Pyrolysis of Black Liquor Solids	45
Carbon Recovered from Pyrolysis of Black Liquor Solids	51
Sulfur Yield in Char Residue from Pyrolysis of Black Liquor Solids	57
Nitrogen Yield in Char Residue from Pyrolysis of Black Liquor Solids	61
Kinetic Model of Conversion of Carbon to Gases During Devolatilization	65

Conclusions

Char Residue Yields from Pyrolysis of Black Liquor Solids	68
Fine Particle Yields from Pyrolysis of Black Liquor Solids	68
Conversion of Carbon to Gases, Fine Particles, and Char	69
Total Carbon Recovered from Pyrolysis of Black Liquor Solids	69
Sulfur Yield in the Char Residue from Pyrolysis of Black Liquor Solids	70
Nitrogen Yield in the Char Residue from Pyrolysis of Black Liquor Solids	70
References	70
Tables	73

INTRODUCTION

The recovery boiler is the main unit operation in the recovery process. Even though recovery boilers have been operated for more than fifty years, the fundamental chemical processes, especially pyrolysis and char combustion, remain not well understood. With the complex chemical composition of black liquor, it is difficult to predict the pyrolysis behavior of black liquor. It is also difficult to relate operational problems to liquor-specific characteristics.

During black liquor burning, the droplets dry and devolatilize. The resulting char burns, and finally homogeneous combustion of volatile gases occurs. Pyrolysis is an important step in which many species are released as volatiles and transformed to different species. Some of the species released cause problems with recovery boiler operation and control and/or the environment. These include alkali metal, sulfur release, nitrogen release, and aromatic hydrocarbon release. These chemical releases are difficult to predict and explain.

Previous studies of black liquor pyrolysis can be divided into two categories, low heating rate measurements (Bhattacharya et al., 1986; Kubes, 1984; Li and van Heiningen, 1991) and single droplet measurements (Gairns et al., 1994; Hupa et al., 1982, 1987; Verrill and Nichols, 1993). Even though these studies provided a great deal of empirical understanding of black liquor burning, the data obtained is of limited value with respect to fundamental burning characteristics. Low heating rate experiments are of limited value because pyrolysis is complete before the particles begin to approach furnace temperatures. This can result in a higher char yield (Niksa et al., 1984) and a distribution of gaseous products that are not representative of those obtained at higher heating rates. Single droplet data are often difficult to interpret because of the steep temperature gradients within the droplets during devolatilization. Due to these limitations, the data obtained is difficult to apply directly to industrial problems. Thus, the other, new experimental methods need to be used to provide data that can be used to understand and model black liquor pyrolysis.

Laminar entrained-flow reactors (LEFR) are commonly used to measure the pyrolysis and combustion characteristics of coal and other solid fuels (Quann et al., 1982; Hurt and Mitchell, 1992).

There are two important features of LEFRs that make it possible to obtain fundamental pyrolysis and combustion data. First, in an LEFR the small particles of black liquor solids that are processed can be heated very rapidly, and temperature differences within the particles are negligible. Another important advantage is that all aspects of pyrolysis and combustion, e.g. carbon volatilization, char formation, sulfur release, sulfate reduction, and volatilization of sodium, potassium, and chloride, and the formation and destruction of nitrogen species, can be studied in a single experiment.

The products from a LEFR pyrolysis experiment with black liquor are char, fine particle, and gas. The procedures used to analyze these products depend on the purpose of study. A Fourier-transform infrared spectrometer can be used to analyze hydrocarbon and organic sulfur species in the LEFR product gas.

Although FTIR can be used to analyze many hydrocarbon species in the LEFR product gas, there are important condensable products that can not be measured. These condensable products may contain aromatic hydrocarbon structure as well as sulfur. In an earlier experimental study of the pyrolysis products from black liquor using a laminar entrained-flow reactor (Sricharoenchaikul, 1994), the major carbon containing species were CO, CO₂, methane, and acetylene. The fraction of carbon converted to CO, CO₂, and methane increased continuously with increasing experimental temperature from 700 to 1000°C. Other carbon species went through a maximum with time at lower temperatures. The distribution of carbon among pyrolysis products (char, fume particles, and gas) was also measured in that study. Carbon not recovered in the gas, char, or fume particles was assumed to have condensed as tar. No experimental data were obtained at lower temperatures (<700°C) where the effect of condensable organic and organic sulfur compounds may be important. Condensable organic compounds have caused problems in low temperature, black liquor gasifiers.

In the work reported here, the objective was to obtain new data on the pyrolysis rate for kraft black liquor solids at temperatures of 6000C and below. The data is to be used to better understand the kinetics of carbon conversion to gases during pyrolysis and to lead to a model for carbon-containing gas evolution during pyrolysis of kraft black liquor.

OBJECTIVES

The objectives of this research were to determine the effects of residence time and temperature on:

1. the distribution of carbon in the char residue, fine particles and gas products from pyrolysis of kraft black liquor solids at 600°C and below,
2. the distribution of nitrogen in the char residue, and
3. the distribution of sulfur as species in the char residue.

LITERATURE REVIEW

Characteristics and Composition of Black Liquor Solids

In the kraft pulping process, black liquor is an important chemical- and energy-containing waste product. It contains most of the original inorganic cooking chemicals (mainly sodium and sulfur compounds), alkali lignin, saccharinic acids, polysaccharides, and other organic matter separated from wood during the pulping process. The initial concentration of weak black liquor is typically about 15% dry solids content, which is not suitable for burning. Thus, evaporation is used to concentrate the weak black liquor to strong black liquor (about 65-70% solid content). An elemental analysis of black liquor solids from a typical black liquor, representative of liquors from pulping of North American or Nordic wood species, is shown in Table 3.1. The range organic species constituting Kraft black liquor is shown in Table 3.2.

From the Table 3.1, carbon and oxygen are major elements in kraft black liquor. This corresponds with the organic species in kraft black liquor, i.e. that alkali lignin and hydroxy acids are the major organic species. In most North American wood-species, lignin comprises 18-25% of hardwoods, and 25-35% of those in softwoods. Lignin is a complex polymer consisting of phenylpropane units, is amorphous, and has a three dimensional structure. Lignin's molecular weight in wood is very high and

not easily measured. Lignin is the adhesive or binder in wood that holds the fibers together. The glass transition temperature of lignin (softening temperature) is approximately 130-150°C (265-300°F).

Table 3.1 Elemental analysis of typical black liquor solids from North American and Nordic wood species (Frederick et al.,1995)

Element	wt.%
Carbon	34 - 39
Hydrogen	3 - 5
Oxygen	33 - 38
Sodium	17 - 25
Sulfur	3 - 7
Potassium	0.1 - 2
Chloride	0.2 - 2
Nitrogen	0.04 - 0.2
Other	0.1 - 0.3

Table 3.2 Organic species in typical black liquor solids from North American and Nordic wood species. (Frederick et al., 1995)

Organic species	wt.%
Alkali lignin	30 - 45
Hydroxy acids	25 - 35
Extractives	3 - 5
Acetic acid	5
Formic acid	3
Methanol	1

The other hydrocarbon-organic species in kraft black liquor are extractives. Extractives are compounds diverse in nature with low to moderately high molecular weights. They are by definition soluble (extractable) in organic solvents or water. Extractives impart color, odor, taste, and, in some cases, decay resistance to wood. There are hundreds of compounds in the extractives of a single wood species. The composition of extractives varies widely from species to species. Typical examples of extractives are terpenes, triglycerides and their component fatty acids, and phenolic compounds.

Terpenes are a broad class of compounds appearing in relatively high quantities in the softwoods. Species such as pines have large amounts of terpenes. Mills pulping highly resinous species with the kraft process collect the terpenes and sell them. Hardwoods have very small amounts of the terpenes. Terpenes are made from phosphated isoprene units in the living wood cells. It is usually very easy to identify the individual isoprene building blocks of a terpene. Isoprene has the empirical formula of C_5H_8 , monoterpenes have the empirical formula of $C_{10}H_{16}$, sesquiterpenes are $C_{15}H_{24}$, and the resin acids are oxygenate diterpenes and have the empirical formula of $C_{20}H_{32}O_2$. Turpentine consists of the volatile oils, especially the monoterpenes such as α - or β -pinene; these are also used in household pine oil cleaners that act as mild disinfectants and have a pleasant aroma. Because turpentine consists of volatile compounds, it is recovered from the vent gases given off while heating the digester.

The triglycerides and their component fatty acids are another important class of extractives. Triglycerides are esters of glycerol (a trifunctional alcohol) and three fatty acids. Most fatty acids exist as triglycerides in the wood; however, triglycerides are saponified during kraft cooking to liberate the free fatty acids. The principal components are the C-18 fatty acids with varying amounts of unsaturation, that is, the presence of carbon-carbon double bonds such as oleic acid, linoleic acid, and linolenic acid.

Phenolic compounds are more common in heartwood than sapwood and are major constituents in the bark of many wood species. Some classes of these compounds are the flavonoids, which have a $C_6C_3C_6$ structure; the tannins, which are water-soluble; polyflavonoids and other polyphenol compounds

that are used to convert animal hides into leather; and the lignans, which have two phenyl propane units ($C_6C_3-C_3C_6$) connected between the β -carbon atoms.

Another interesting aspect of the elemental composition of kraft black liquor is sulfur. Release of sulfur gases is a serious problem. Much of the sulfur released during black liquor burning is in the form of total reduced sulfur (TRS) which results in an odor problem. Also, these TRS gases can further react with oxygen to form sulfur dioxide (SO_2) which contributes to formation and hardening of deposits in heat transfer sections and corrosion of the recovery boiler. The sulfur in black liquor is present mainly in the form of inorganic sulfur such as sodium sulfide (Na_2S), sodium thiosulfate ($Na_2S_2O_3$), sodium sulfate (Na_2SO_4), sodium sulfite (Na_2SO_3), and polysulfide (Na_2S_x). These four inorganic sulfur species constitute 65-75% of the total sulfur in black liquor. Differences in the pulping and recovery processes from one mill to another can affect the distribution of sulfur species in kraft black liquor. For example, sodium sulfide is not found in oxidized black liquor, and the thiosulfate content of oxidized black liquor is higher than that of unoxidized liquors.

Black Liquor Droplet Combustion

There are four major stages that occur during black liquor droplet combustion, similar to those in the combustion of other solid and liquid fuels. Although the stages may overlap, it can be useful to visualize the stages of combustion as being separate and distinct. Figure 3.1 shows qualitatively the characteristic stages: drying, devolatilization, char burning, and smelt reactions. In the first stage, *drying*, water in the droplet is evaporated. The black liquor droplet does not ignite and the other stages can not begin until much of the water has been evaporated. The second stage of burning, *devolatilization*, is marked by the appearance of a flame at the droplet surface. The flame quickly engulfs the droplet, and the droplet swells continuously to several times its original volume while the flame is present. The flame disappears at the point when the droplet reaches its maximum volume. In the devolatilization stage, the organic material in black liquor droplet is degraded irreversibly into

volatile compounds consisting of CO, CO₂, H₂O, light hydrocarbons, tars, H₂S and TRS compounds. These volatile compounds are burned when contacted with oxygen. The residual organic carbon along with inorganic (mostly in form of sodium salts) from the pulping chemicals is known as char.

Devolatilization is the loss of volatile matter from thermal decomposition of the organic fraction of black liquor. It begins when the droplet temperature approaches 200°C. The term devolatilization and pyrolysis are often used synonymously but devolatilization actually refers to the loss of volatile matter on heating while pyrolysis refers to the processes that occur, including devolatilization, when a particle or droplet is heated in an inert environment. Devolatilization continues until a black liquor droplet has been reduced to a char particle, but pyrolysis continues as long as the char particle remains in a hot environment.

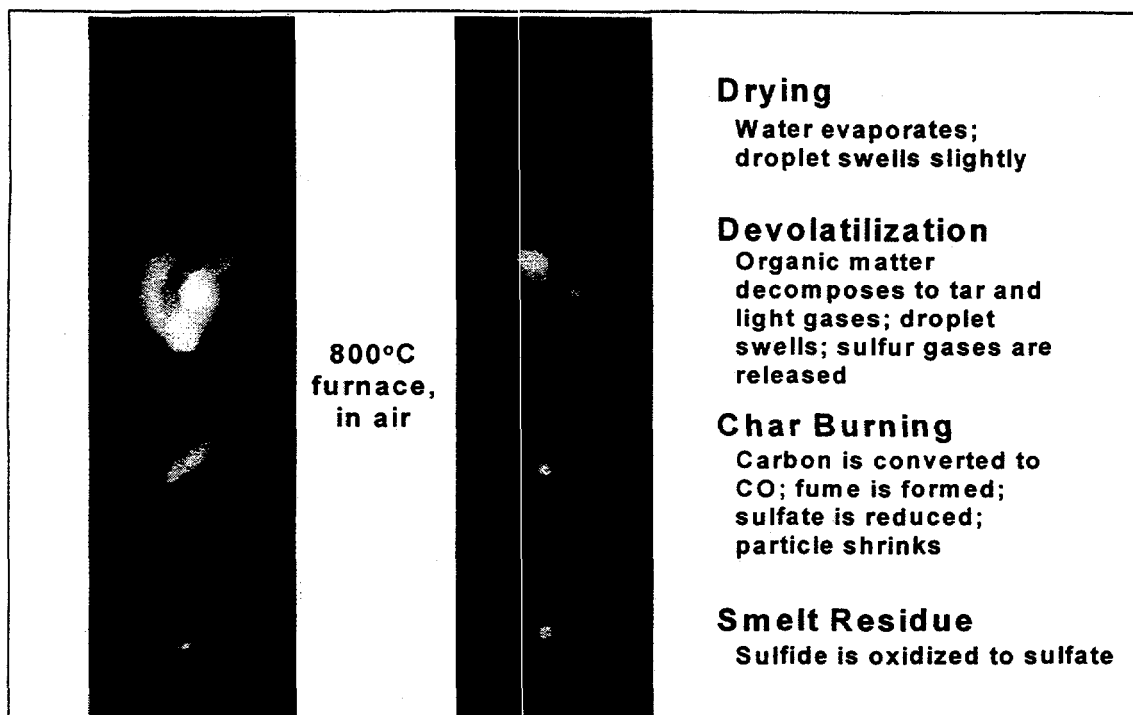


Figure 3.1 Black Liquor Droplet Burning Stages

The third stage, *char burning*, begins when a black liquor particle has reached its largest volume and the flame around the droplet disappears. During the char burning stage, carbon in black liquor is oxidized to form CO and/or CO₂. The black liquor particle shrinks during burning and becomes a smelt droplet at the end. During char burning, carbon in the black liquor particle reacts with oxygen, CO₂, and H₂O vapor at the particle surface to form CO and/or CO₂. In the fourth and final burning stage, known as the *smelt reactions stage*, the smelt reacts with the surrounding gases and Na₂S is oxidized to Na₂SO₄. In this stage, fuming may occur and small particles may be ejected violently from the smelt droplet.

Pyrolysis of Kraft Black Liquor

Pyrolysis is the important part of the process of burning kraft black liquor. Pyrolysis can be often defined as chemical decomposition due to exposure to high temperature (Tromp and Moulijn, 1988) or specifically as thermal decomposition under inert atmospheres. Pyrolysis of organic matter

produces three primary product groups including hydrogen rich gases, hydrogen rich condensable vapors (tar), and a carbon rich residue (char).

During pyrolysis, the least stable bonds in aromatic polymers such as lignin which are the functional group bridges between the aromatic building blocks are the first to break. Bhattacharya et al. (1986) stated that at low temperature, the carbonyl and mercaptan bonds are the weakest in black liquor. Their breaking leads to the production of CO₂ and H₂S. When the least stable bonds in aromatic polymers are broken, free radicals are produced. Then, the volatile free radicals react with other volatile free radicals to form stable volatile compounds. The non-volatile free radicals react, through polymerization and condensation reactions, to form a more aromatic, carbon-rich condensed material. Stable volatiles may further crack to produce lighter hydrocarbons in higher temperature regions. With the bond breaking that occurs, higher temperatures cause dehydration reactions that produce hydrogen and carbon monoxide.

Pyrolysis experiments have traditionally been classified as either slow or rapid (Tromp and Moulijn, 1988). The heating rate of slow pyrolysis experiments is 0.1-1°C/s (Bhattacharya et al., 1986; Kubes, 1984; Li and Van Heiningen, 1991; etc.). The heating rate of rapid or flash pyrolysis experiments is 100-1000°C/s (Forssen et al., 1991; Gairns et al., 1994; Harper, 1989; Hupa et al., 1987).

Studies on the pyrolysis of black liquor solids indicate that pyrolysis begins between 200 and 250°C (Feuerstein et al., 1967; Kubes et al., 1982; Bhattacharya et al., 1986; Li, 1989; Miller, 1986; Söderhjelm et al., 1989; Li and Van Heiningen, 1991; Gairns et al., 1994; Sricharonchaikul et al., 1995). The main gas compounds reported to be produced by black liquor pyrolysis are H₂, CO, CO₂, CH₄, C₂H₆, C₂H₂, (Feuerstein et al, 1967; Bhattacharya et al, 1986) and the other minor gas are water vapor, tars, and light sulfur-containing gases. Devolatilization is essentially complete when the residue temperature reaches 400-500 (Li and van Heiningen, 1991). The char residue contains the fixed carbon, some hydrogen, and most of the inorganic matter.

Char Residue Yields from Pyrolysis of Black Liquor

For most solid fuels, the char residue yields from pyrolysis vary widely depending upon fuel characteristics and process conditions. The char residues from coal and biomass fuels are normally reported on an ash-free basis. Black liquor yields much more ash residue than coal or most other biomass fuels, typically 35-45% of the dry solids mass. Thus, the char residue from pyrolysis of black liquor solids normally refers to the solid residue from pyrolysis including the ash as well as carbon and other elements that remain from the organic fraction. For the inorganic residue from pyrolysis or combustion, there are relatively volatile sodium salts including chloride, sulfate and/or sulfide, and carbonate (Reis et al., 1995).

For pyrolysis of coals at temperatures greater than 600 °C, char residue yields typically range from 35 to 70% on a dry, mineral ash-free basis. Both kinetic and stoichiometric factors determine the distribution of carbon between volatile gases and char residue. During devolatilization, the yield of carbon as volatile gases increases with increasing reaction temperature, and the fixed carbon in the char residue decreases (e.g. Anthony et al., 1975; Kobayashi et al., 1977; Solomon and Colket, 1979; Suuberg et al., 1979). Char residue yield data obtained for pyrolysis to the same final temperature but at different heating rates has at most a minor effect on pyrolysis char yield (Sprouse and Schuman, 1981; Niksa et al., 1985).

For pyrolysis of biomass fuels, char residue yields are much lower than with coals because of the higher oxygen content of biomass. The char residue yield from rapid pyrolysis of cellulose is less than 5% for pyrolysis temperatures above 400 (Hajjallgol et al., 1982; Scott et al., 1988). For pyrolysis of lignocellulosic materials, char residue yields are higher, typically between 10-25% on a mineral free basis for rapid pyrolysis at temperatures above 500°C (i.e. Scott and Piskorz, 1984; Scott et al., 1985; Scott et al., 1988). The char residue yields for the larger particles are greater which indicate that there may be an effect of heating rate on pyrolysis residue yield. There is less data on the effect of heating rate on the split of carbon between volatile products and char residue species.

For pyrolysis of black liquor, data on the distribution of pyrolysis products between volatile matter and char residue is very limited. Bhattacharya et al. (1986) pyrolyzed low-sulfur black liquor solids in ceramic boats to final temperatures of 620-740°C and obtained char residue yields of 48-52%. Gairns et al. (1994) reported char residue yields for 20 mg droplets of kraft black liquor pyrolyzed in N₂ for 60 seconds at temperature from 500 to 900°C. The yield decreased from 70% at 500°C to 65% at 700°C, but then dropped to 41 % at 800°C. Fixed carbon yields were not reported in either of these studies.

Frederick et al. (1994) measured char residue from 2-3 mm droplets of kraft black liquor pyrolyzed for 10 seconds in a nitrogen atmosphere at temperatures from 700 to 1200°C. Their conditions corresponded to heating rates of the order of 100°C/s. Their char residue yields decreased with increasing temperature, from 68% at 700°C to 21% at 1200°C.

In rapid pyrolysis of black liquor using a laminar entrained-flow reactor (LEFR), dry black liquor solids with particle size of 90-125 microns were pyrolyzed at 700-1100°C, and char yields versus residence time between 0.3-2.2 seconds were reported by Carangal, 1994; and Pianpucktr 1995. Carangal reported char residue yields were 35-60% at residence time 0.85 seconds and 30-65% at residence time between 0.6-1.1 seconds.

In the Pianpucktr study, the char yield decreased as residence time increased. At 700°C, the char yield was 82% at 0.3 seconds, and it quickly decreased to 65% at 0.6 seconds. At residence times above 0.6 seconds, the char yield gradually decreased to 53% at 2.2 seconds. This indicates that the black liquor solids were volatilized rapidly until the residence time of 0.6 seconds, after which they were volatilized more gradually.

At 900°C and 1100°C, the char yields decreased during the residence times studied, 0.3-2.2 seconds. At the shortest residence time studied, 0.3 seconds, the char yield was 60% at 900°C and 50% at 1100°C. This implies that substantial amounts of volatile species in the black liquor solids were released at residence times below 0.3 seconds. The lowest char yield in this study was 20% at 1100°C

and 2.2 seconds, i.e. 80% of black liquor solids were released as gas species. This indicates that considerable amounts of inorganic material in addition to C,H, and N, were vaporized.

In the Pianpucktr study, substantial amounts of volatile species in the black liquor solids were released at residence times below 0.3 seconds. The temperature of 100 micron particles at short residence times were estimated using a model developed by Frederick (1990). Results of the Frederick model showed that at all of the furnace temperatures in the Pianpucktr study, the particles are within 1°C of the furnace temperature in less than 0.09 seconds as shown in Table 3.3. Further, the time to complete loss of volatile pyrolysis products was less, approximately 0.02-0.04 seconds. These estimates indicate that at temperature of 700°C and above, the loss of volatile gases produced by pyrolytic decomposition of the organic matter in black liquor is complete before the particles reach their final temperature.

Table 3.3 Time to complete loss of volatile pyrolysis products, time for particles to reach the furnace temperature, and average heating rate during devolatilization versus furnace temperature for dry 100 micron black liquor particles as estimated using the devolatilization model of Frederick (1994).

Furnace temperature °C	Time to complete loss of volatile organic matter (s)	Time for particle to reach within 1°C of the furnace temperature (s)	Average heating rate during loss of volatile organic matter (°C/s)
700	0.041	0.089	15,400
900	0.029	0.075	25,600
1000	0.025	0.069	31,200
1100	0.022	0.064	37,300

Carbon Yield in Char Residue from Pyrolysis of Black Liquor

Frederick et al. (1994) measured the carbon yield in char residue from 2-3 mm droplets of a kraft black liquor pyrolyzed for 10 seconds in a nitrogen atmosphere at temperatures from 700-1200°C. Their

conditions corresponded to heating rates of the order of 100°C/s. The amount of carbon initially in the black liquor that remained as carbon in the char residue decreased from 66% at 700°C to 18% at 1200°C. In similar experiments with six kraft liquors at 800°C, the carbon in the char residue ranged from 26-48% of the carbon originally in the black liquor solids.

Frederick et al. (1995) measured the total carbon in the char residue collected at furnace temperatures between 700-1100°C and residence time between 0.3-1.6 seconds for 100 micron dry black liquor solids in a laminar entrained flow reactor. The total carbon versus time data are similar to the char residue data for the 100 micron - the carbon content of the char residue decreases rapidly during devolatilization ($t < 0.3$ seconds). It continues to decrease but at a slower rate after devolatilization is complete. For temperatures 700-1100°C and a residence time of 0.3 seconds, the total carbon in char residue decreased from 68% at 700°C to 42% at 1100°C. At a residence time of 1.6 seconds, the total carbon in the char residue decreased from 50% at 700°C to 20% at 1100°C.

Frederick et al. (1995) compared the carbon in the char residue from LEFR experiments immediately after devolatilization is completed with data from single droplet pyrolyzed for 60 seconds by Gairns et al. (1994). The trends of the carbon versus time data are similar to those for the char residue yields - the carbon decreases with increasing furnace temperature but more slowly for the 100 micron particles, and seems to approach an asymptotic value near 50% at higher furnace temperatures. The carbon remaining in the larger droplets continued to decrease as temperature increased. The Frederick study showed that using small black liquor particles (100 micron) gave more reliable char residue and char carbon yield data than those using 2-3 mm black liquor droplets. This is because inorganic reactions that occur after devolatilization is complete continue to remove carbon. Sulfate reduction and carbonate reduction both convert carbon to gases, and sodium is volatilized during carbonate reduction (Cameron and Grace, 1985; Li and van Heiningen, 1990; Reis et al., 1995). Shedding of char residue fragments is another possible mechanism of mass loss after devolatilization (Verrill et al., 1992). Frederick's black liquor char residue and char carbon yield data did not decrease significantly with

increasing furnace temperature above 900°C, and that they were not very sensitive to heating rate in the range ~100-10,000°C/s.

3.3.3 Product Gas from Pyrolysis of Black Liquor

The main gaseous products gas from pyrolysis of black liquor are H₂, CO, CO₂, CH₄, C₂H₆, C₂H₂ (Feuerstein et al., 1967; Bhattacharya et al, 1986) and the other minor gas are water vapor, tars and light sulfur-containing gases.

Bhattacharya et al. (1986) studied pyrolysis of black liquor solids in ceramic boats to a final temperature of 620-740°C, they reported the effects of reaction time and temperature on the composition of the major gaseous products for the largest particle size (-30/+60 mesh). The product gas consisted of CO₂, CO, H₂, CH₄, and H₂S. With an increase in the pyrolysis temperature, the concentrations of CO₂, CH₄, and H₂S in the product gas decreased, while the concentrations of CO and H₂ increased. Unaccounted gases decreased with temperature and varied from 8 to 14 mole percent of the gaseous product. These unaccounted gases were most probably CH₃SH, (CH₃)₂S, and possibly SO₂. At a constant temperature, with an increase in reaction time, the concentration of CO₂, H₂S, and unaccounted gases decreased; the concentration of CO and H₂ increased, whereas the CH₄ concentration showed a maximum.

The oxygen in black liquor solids was distributed between the gas, solid residue, and tar. At 590°C, approximately 18 wt% of the oxygen in the black liquor solid left as carbon oxides (CO and CO₂), whereas at 740°C the carbon oxides account for 27 wt-% of the feed oxygen. There was no appreciable effect of feed particle size on the gaseous composition. Since the trends in the composition of the product gases with time and temperature for the other two sizes were found to be similar, graphical plots were not shown for these fractions.

Goheen et al. (1976) studied the indirect pyrolysis of black liquor solids in the temperature range of 350-500°C. A typical analysis reported for the product gases was CH₄ 5%, H₂S 15%, CO 30%, and

CO₂ 30% by volume. Bhattacharya et al. (1986) reported the range for product gases components was CH₄ 1-5%, H₂S 8-20%, CO 25-45%, and CO₂ 30-40% by volume.

Carbon-Containing Products and Carbon Recovered from Pyrolysis of Black Liquor

In experimental measurements of the pyrolysis products from black liquor using a laminar entrained-flow reactor (Sricharoenchaikul, 1994), dry black liquor solids with particle size 90-125 micron were entrained into the reactor at reactor temperatures of 700-1100°C and carbon-containing product and carbon recovered as light gases and char were reported. A large number of carbon-containing species were detected by Fourier-Transform Infrared spectrometer (FTIR) in the pyrolysis products as shown in Table 3.4.

The major carbon containing species were CO, CO₂, methane, and acetylene, while eleven other carbon-containing gases were measured quantitatively in amounts corresponding to less than 1% of the carbon in the black liquor solids fed to the reactor. The fraction of carbon converted to CO and methane increased continuously during the experiments. The fraction converted to CO₂ increased with time for experiments to 1000°C but went through a maximum at 1100°C. Other carbon species went through a maximum with time at lower temperatures.

Table 3.4 Carbon-containing pyrolysis products detected by FTIR, as % of carbon input, for 1.5 seconds residence time (Sricharoenchaikul, 1994)

% of Carbon	Temperature (°C)			
	700	800	900	1000
input as	700	800	900	1000
CO	1.10	4.11	5.88	29.9
CO ₂	1.50	7.41	8.83	10.5
CH ₄	0.45	2.11	2.60	5.90
C ₂ H ₄	0.07	0.53	0.96	2.27
C ₂ H ₂	0.00	0.05	0.19	0.52
CH ₃ OH	0.22	0.44	0.00	0.00
CH ₂ O	0.06	0.13	0.11	0.00
C ₂ H ₄ O	0.31	1.07	0.08	0.00
CH ₃ OCH ₃	0.06	0.52	0.04	0.04
COS	0.00	0.01	0.00	0.00
CS ₂	0.00	0.02	0.04	0.00

For carbon recovery at 1000°C, the fraction of the carbon in black liquor solids that was collected as gas increased with residence time to nearly 50% after 1.7 seconds. The amount of carbon collected as char decreased from 47% to 32% during the experiments. Most of the remaining carbon was probably tar which passed through the cyclone and hot filter - Bhattacharya et al. (1986) and Gairns et al. (1994) have reported tar yields of 7-35% of the black liquor solids input in slower heating rate experiments (~10°C/s and ~100°C/s respectively). At 1000°C, the unaccounted carbon remained fairly constant at about 40% of the carbon input until about 2.5 seconds, and then decreased to 15% of the carbon input. At 1100°C, almost all of the carbon was recovered as gases or char. In general there was a trend of increased carbon recovery as light gases and char with longer residence times and higher reactor temperatures due to decomposition of tar that is formed as primary pyrolysis products. This explanation is supported by measurements of the formation of various other carbon-containing light gases at

residence times beyond 0.5 seconds, presumably as a result of the thermal decomposition of these tars. A small amount of carbon, typically 3-6% of the carbon input, was also collected on the filter.

Nitrogen in Char Residue from Pyrolysis of Black Liquor

Data on the retention of fuel nitrogen in the char residue of black liquor is limited. Aho et al. (1994a,b) reported that 40-80% of the nitrogen in black liquor was converted to char nitrogen during devolatilization. Aho et al. measured the nitrogen retained in char residue for black liquor kept at 400°C for one hour. Forssen et al. (1995) measured the percentage of the fuel nitrogen that was retained in the char residue of single droplets placed in a furnace for 300 seconds. The nitrogen retained decreased from 300 to 500°C, was constant at 20-30% of fuel N from 500-900°C, and was lower at 1000°C.

Carangal (1994) measured nitrogen retained in the char residue after devolatilization at furnace temperature between 700-1100°C and residence time between 0.3-2.2 seconds for 100 micron dry black liquor solids in a laminar entrained flow reactor. At residence times longer than 0.5 second, the char nitrogen yield is essentially the same at 700°C and 900°C. The nitrogen content of the char residue as a percentage of the nitrogen in the black liquor solids was substantially lower at 1100°C.

Table 3.5 Retention of nitrogen and carbon in char residue and the rates of decrease of nitrogen and carbon in the char residue during extended char pyrolysis. (Carangal, 1995)

Temperature (°C)	N and C in char residue at the end of devolatilization, (% of N and C in black liquor solids)		Rate of change of N and C in char residue, (%/s, based on N and C in black liquor solids)	
	Char N, (%)	Char C, (%)	Char N, (%/s)	Char C, (%/s)
700	56.7	71.3	-8.5	-6.1
900	49.6	63.0	-5.7	-6.2
1100	45.7	47.8	-12.9	-7.2

Table 3.5 compares the percentages of nitrogen and carbon retained in the char residue after devolatilization, obtained by extrapolating the data of nitrogen content of the char residue as a percentage of the nitrogen in the black liquor solids back to time zero. The percentage of nitrogen retained in the char residue after devolatilization is less than the carbon retained at 700°C and 900°C, but about the same at 1100°C. Table 3.5 also compares the rates of depletion of nitrogen and carbon from the char residue, expressed as percent of the initial nitrogen or carbon per second. At 700°C, the char nitrogen seems to decrease more rapidly during devolatilization than the char carbon decreased. At longer times, the rate of nitrogen depletion from the char residue at 700°C and 900°C is about the same as the rate of carbon loss when expressed as a percentage of the nitrogen or carbon in the black liquor solids. At 1100°C, nitrogen is depleted more rapidly than carbon on the same basis.

Sulfur Species in Char Residue from Pyrolysis of Black Liquor

Sulfur behaves very differently than carbon or nitrogen during pyrolysis. Forssen et al. (1992) showed that the sulfur retained in the char residue after pyrolysis of black liquor went through a minimum with increasing furnace temperature at 600-700°C. The fraction of the sulfur initially in the black liquors that was retained in the char residue was independent of the sulfur content or the sulfur species distribution in the liquors used, increasing from about 20% at 300°C to 65% at 600°C and then decreasing to 25% at 1050°C. Forssen's analysis was based on data from his own experiments and from three other studies (Brink et al., 1970; Clay et al., 1984, 1987; Cantrell, 1986) involving a total of nine different kraft black liquors. Single droplets, 2-3 mm in diameter, were used in all four studies. Gairns et al. (1994) obtained somewhat different results, with the sulfur retained in the char residue increasing continuously from 33% at 500°C to 57% at 900°C. Clay et al. (1984,1987) reported limited data on the distribution of sulfur species in char residue produced by pyrolysis of 1.5 mm droplets at 900°C. The predominant sulfur species in the char residue were thiosulfate, sulfide, and sulfate.

Frederick et al. (1995) studied sulfur species in char residue from pyrolysis of black liquor solids using laminar entrained flow reactor at furnace temperature between 700-1100°C and residence time

between 0.3-1.6 seconds. Almost all of the thiosulfate initially present in the black liquor solids had disappeared in less than 0.3 seconds. The sulfite content of the char residue increased from zero to a flat maximum between 0.3 and 0.8 seconds, and then decreased to zero. The sulfate content was nearly constant for the first 0.8 seconds but then decreased, nearly disappearing after 1.6 seconds. The sulfide content remains at zero until after 0.7 seconds, and then increases rapidly.

In the Frederick study (1995), the effect of residence time and temperature on total sulfur in char residue was determined. At 900-1000°C, the sulfur content of the char residue has decreased to about 20% of the initial sulfur content of the black liquor solids before beginning to increase. At 700°C, the decrease in char residue sulfur content was slower, but the minimum value, achieved after 1 second particle residence time, was about the same. The sulfur in the char residue then increased with residence time.

A comparison between the Frederick et al. (1995) study of the sulfur content of the char residue after 1.5 seconds and data from other studies (Forssen et al., 1992; Gairns et al., 1994) was made. With the different experimental methods and equipment, Gairns et al. and Forssen et al. used 2-3 mm black liquor droplets, while Frederick et al. used dry, 100 microns particles. The Gairns et al. data agree very well with the Forssen et al. data. However, the Frederick et al. data fell below Forssen's curve. The main difference between Frederick et al. technique and that of Forssen et al. and Gairns et al. was that in Forssen et al. and Gairns et al. experiments, the product gas was removed immediately from the suspended single droplets. The droplets therefore pyrolyze in a nitrogen or helium atmosphere, without water vapor or CO₂ present. By contrast, Frederick et al. experiments were conducted at steady state so that the gases and particles were not separated but flowed together through the reactor. The gases contain water vapor and CO₂ (Sricharoenchaikul, 1995). These can react with Na₂S to produce H₂S and COS, further reducing the sulfur content of the char residue (Li, 1989; Li and van Heiningen, 1991; Wag et al., 1995).

The fact that the sulfur content of the char residue decreased to around 20% at all temperatures was compatible with the sulfur gas versus time data from these experiments (Sricharoenchaikul et al.,

1995). The total sulfur as gases increased rapidly with time, in the same time frame at which the char residue sulfur passes through a minimum. Most of the sulfur in the gas phase was organosulfur compounds.

The Frederick et al. (1995) data reported support a mechanism by which sulfur is first released from black liquor during devolatilization and is then recaptured by the inorganic species in the char residue. The data indicated that sulfur release during devolatilization was the result of decomposition of thiosulfate, sulfide, and organic sulfur to gases. At temperatures of 900°C and above, these were converted to sulfur gases in less than 0.3 seconds for the small particles used in this study. At 700°C, more than 1 second was required to reach the minimum. Sulfur gases are then recaptured by the char residue particles.

EXPERIMENTAL PROCEDURES AND SAMPLE ANALYSIS

Experimental Equipment

The experimental equipment used for pyrolysis of black liquor solids is shown in simplified form in Figure 4.1. The major parts of the experiment are as follows:

- Reactor : Laminar Entrained-Flow Reactor (LEFR)
- Solids Separation Equipment : Cyclone/filter assembly
- Gas Analyzers : CO₂ Gas Analyzer
- Gas Oxidizer : Oxidizer

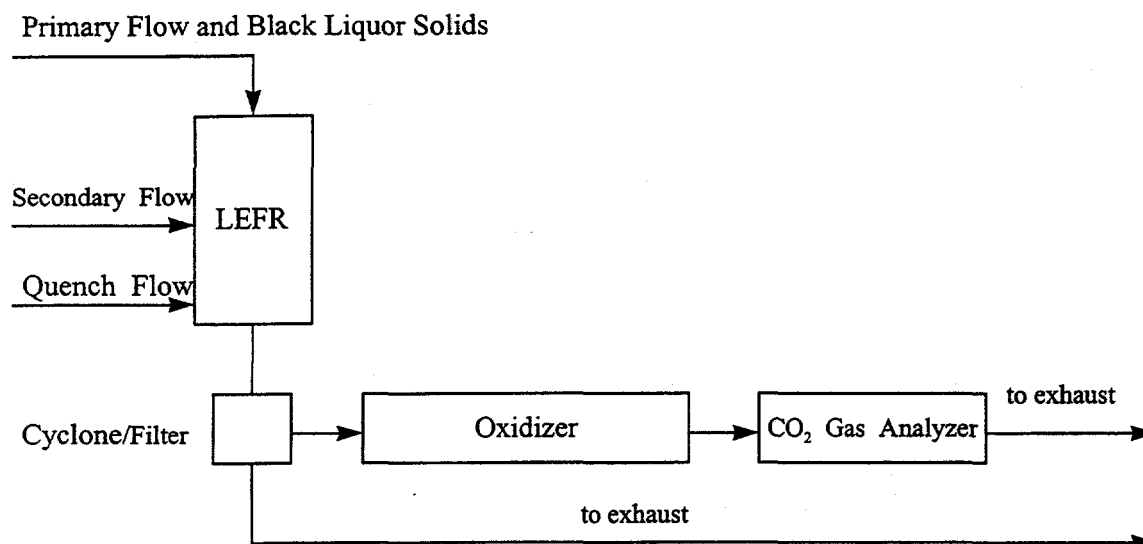


Figure 4.1 Simplified Schematic Diagram of Experimental Equipment

Laminar Entrained Flow Reactor (LEFR)

A simplified schematic diagram of the Laminar Entrained-Flow Reactor is shown in Figure 4.2. The LEFR consists of two major parts, the reactor and the collector. The reactor consists coaxially of two cylindrical mullite tubes inserted in the furnace. The furnace is subdivided into three heating zones controlled by Omega CN76000 Microprocessor Based Temperature and Process Controllers capable of ramping to a set point temperature at a maximum heating rate of 300°C/hr. The downward flowing high temperature gas at laminar conditions include primary and secondary gas streams whose flow rates are controlled by Omega FMA5600 Electronic Mass Flow Meters (MFM).

The black liquor solids are entrained by the primary gas stream from the particle feeder and flow through the injector into the reactor at the center of the inner mullite tube. The particles and primary gas stream are prevented from premature heating while passing through the injector by cooling water flowing through the outer shell of the injector. The secondary gas stream enters the LEFR through the bottom and is preheated to the furnace temperature as it flows upward through the annular space between the mullite tubes. It then flows downward into the reactor through a flow straightener located at the top of

the inner mullite tube. The flow straightener is used to obtain a uniform velocity profile for the secondary gas. The primary and secondary gas streams merge together to form a single laminar flow entering the reaction zone. The particles rapidly heat and react while exposed to the high temperature of the secondary gas stream and radiation from the reactor walls. The particles are heated rapidly at about 10^4C/sec .

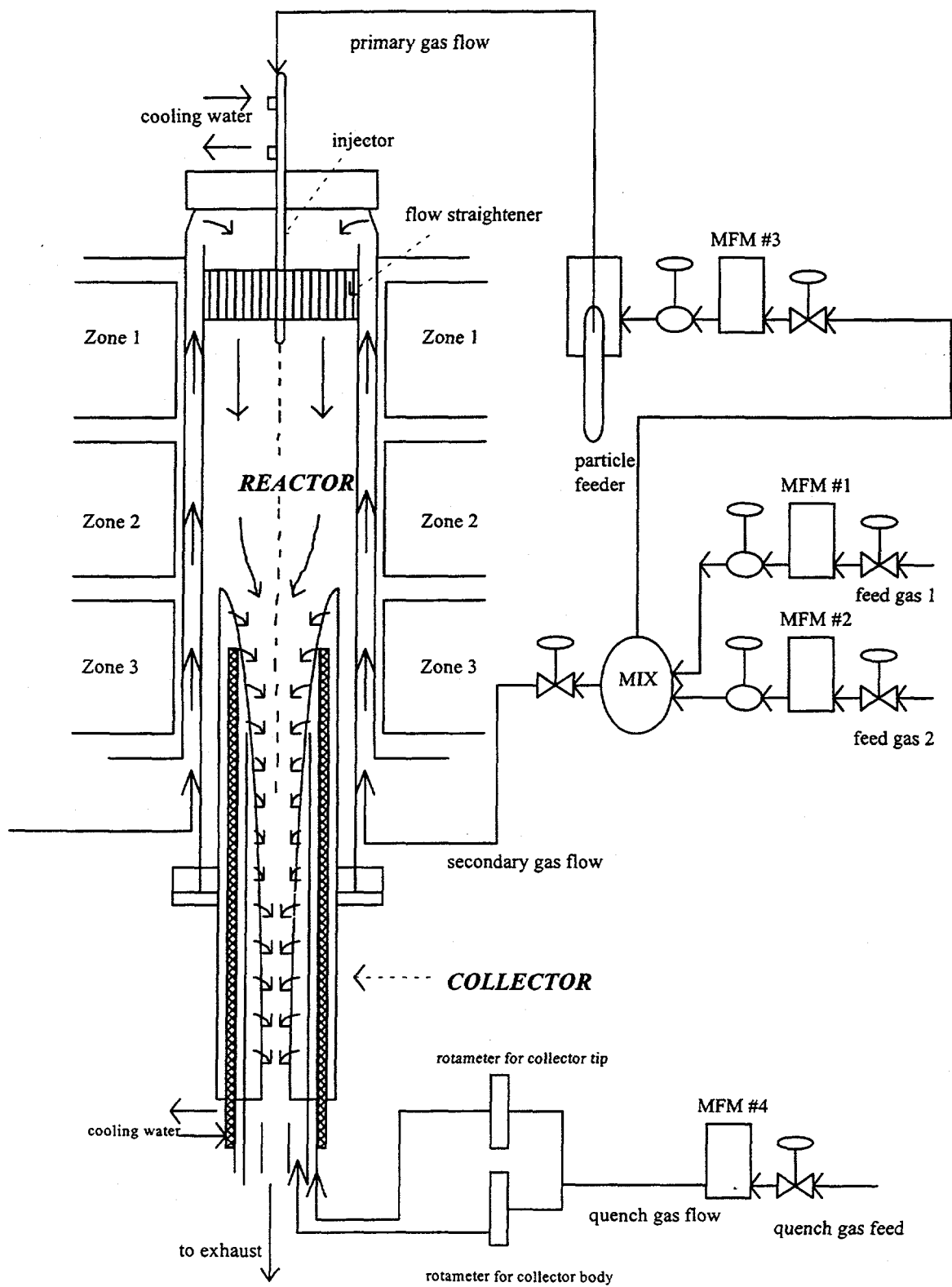


Figure 4.2 Laminar Entrained Flow Reactor

The residence time of the particles is controlled by adjusting the position of a movable collector and/or adjusting the flow rates of the primary and secondary gas streams. The residence time of the particles is calculated with a predictive model based on Flaxman's computational fluid dynamic algorithm (Flaxman and Hallett, 1987) and depends mainly on the furnace temperature, gas flow rate, and reaction path length. The particles are reacted for the required residence time, and then are cooled by a quench gas stream to stop any further chemical reactions as they enter the collector.

The collector can be moved inside the reactor to vary the reaction path length to adjust the required residence time. The outer part of the collector is a mullite tube insulated inside with a layer of mullite fiber to minimize heating from the reactor walls. The inner wall of the collector is porous to allow distribution of the quench gas along the length of the collector. The porous wall is enclosed by a segmented shell of stainless steel, with two passes for cooling water to prevent the heating of the quench gas, and one for flowed path of quench gas stream. The porous wall has two sections of different permeabilities. The first is a very permeable section, approximately 2 cm in length located near the tip of the collector. About half of the quench gas enters through this section to decrease rapidly the gas and particle temperature. The second is a much less permeable wall section that comprises the rest of the porous wall. It allows quench gas to flow through the wall fast enough to prevent fine particles from depositing on the walls of the collector by thermophoresis.

Cyclone/Filter Assembly

The combined reactor effluent and quench gas stream flow from the collector into a cyclone and filter assembly. The illustration of the cyclone/filter assembly is shown in Figure 4.3.

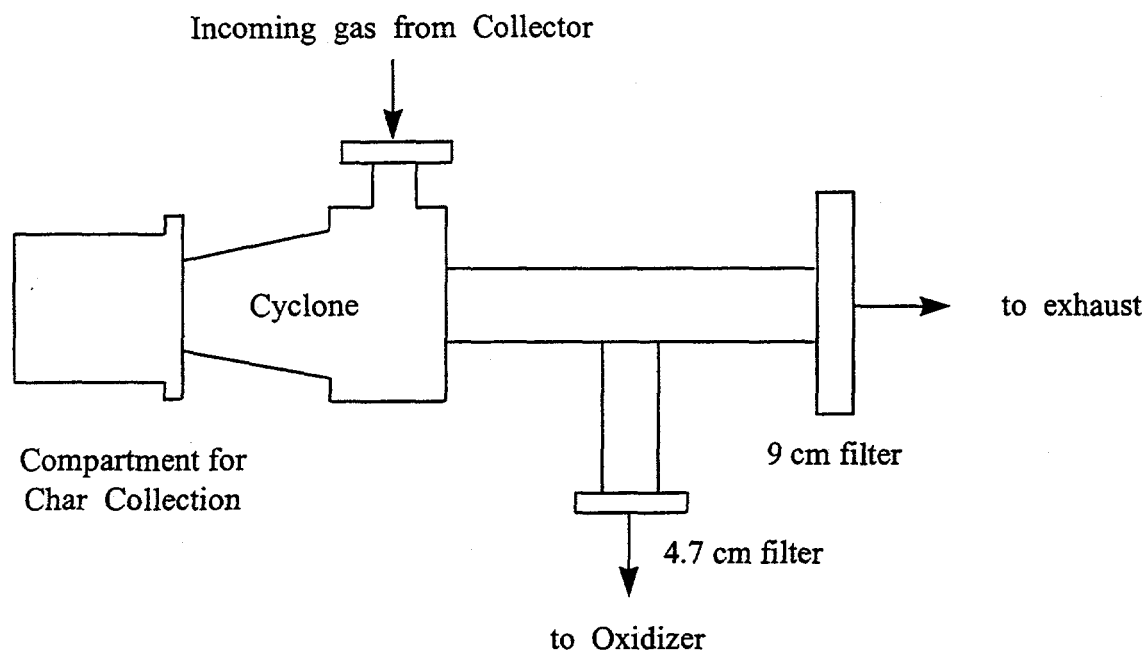


Figure 4.3 Cyclone/Filter Assembly

The particles are separated from the effluent gas by the cyclone with a nominal cut-off size of 3 μm . The particles collected in the cyclone are referred to as char. The effluent gas exiting the cyclone is filtered to obtain fine particles by means of two glass fiber filters with 0.8 μm pore size. Filters with this pore size are effective in collecting particles as small as 0.1 μm . The first filter, 9 cm in diameter, is located directly downstream of the cyclone as shown in Figure 4.3. Gases passing through this filter go directly to the exhaust. The second filter, 4.7 cm in diameter is located perpendicular to the cyclone axis. Gases passing through this filter go directly to the oxidizer.

Oxidizer

In order to determine the carbon balance in pyrolysis of black liquor, the total carbon in the LEFR product gas needed to be measured. An oxidizer was connected to the LEFR by 5 feet of unheated tubing. It was used to convert all oxidizable carbon-containing components in the LEFR effluent gas to carbon dioxide.

A simplified schematic diagram of the cylindrical gas oxidizer is shown in Figure 4.4. The reaction chamber is a mullite tube inserted horizontally in the furnace. The furnace heating zone were controlled by an Omega CN76000 microprocessor-based temperature and process controller set at 900°C.

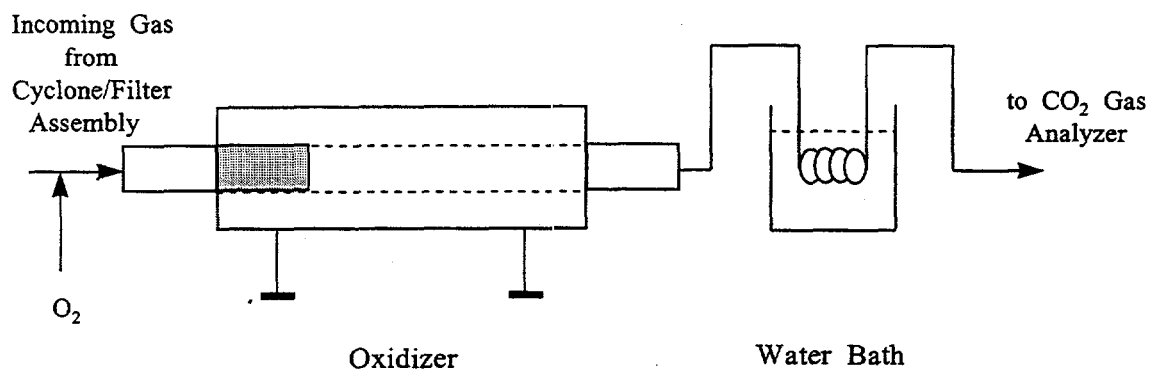


Figure 4.4 A Simplified Schematic Diagram of the Oxidizer

The LEFR effluent gas is mixed with air before flowing through the reaction chamber of the oxidizer. A flow straightener is used to obtain a uniform velocity profile. In the high-temperature (900°C) reaction chamber, all oxidizable components are combusted to their stable oxides. Thus all carbon in the carbon-containing species in the LEFR effluent gas is converted to carbon dioxide. The effluent gas from the oxidizer is cooled to 25°C by a cooling coil immersed in a water bath before it enters the CO₂ gas analyzer. This is done to prevent temperature fluctuations that effect accuracy of the CO₂ concentration reading, and also to prevent damage of the analyzer sampling line.

CO₂ Gas Analyzer

The CO₂ Gas Analyzer used in the experiments is a Riken Infrared Analyzer Model RI-550. The effluent gas from the gas oxidizer is drawn into the CO₂ gas analyzer through sampling line by means of an internal vacuum pump. The effluent gas passes through an optical system and the concentration of the constituent to be measured is read out directly on a meter.

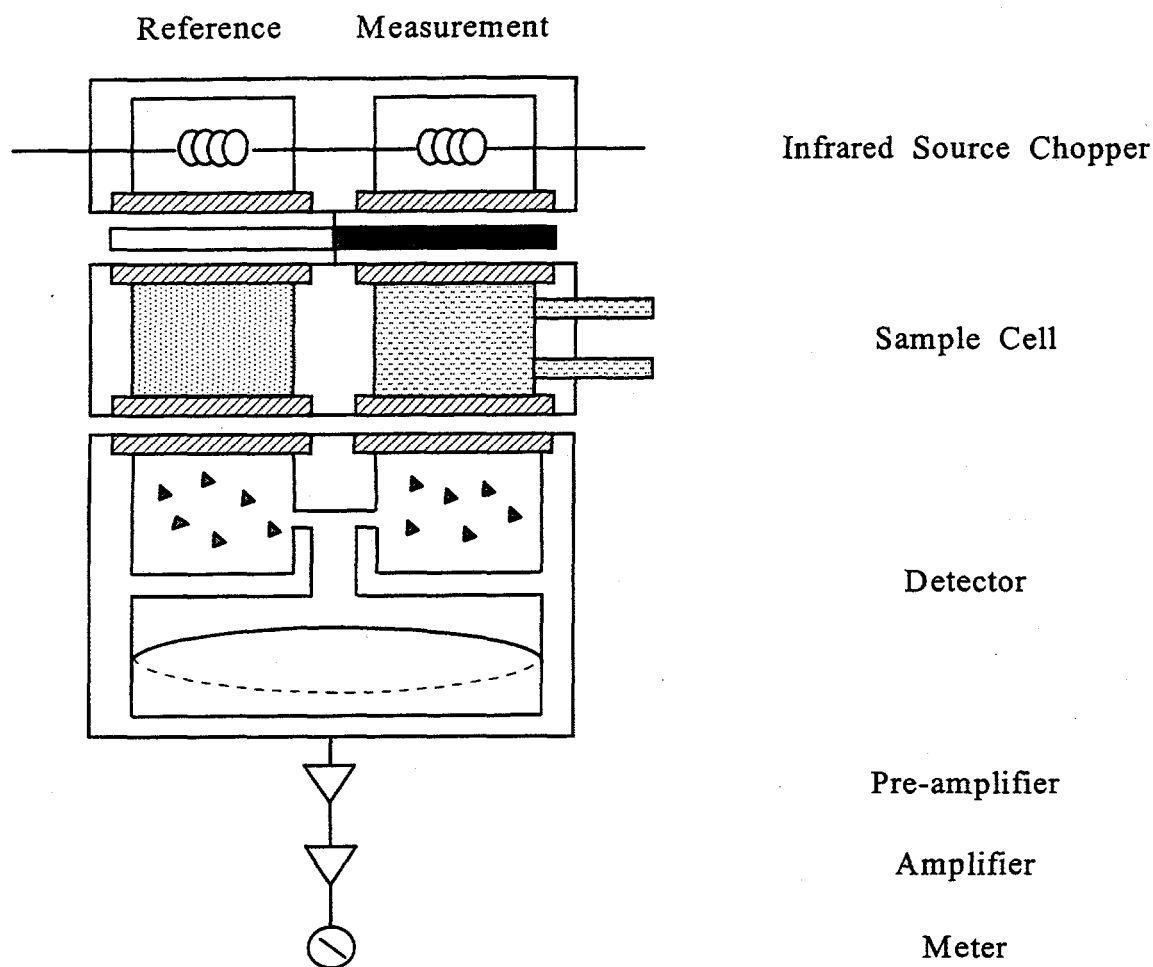


Figure 4.5 The Optical Schematic of CO₂ Gas Analyzer

Material

The dry black liquor solids used in this study were prepared from an oxidized southern pine kraft black liquor. The 2.5-gallon black liquor container was shaken well to ensure a uniform concentration before pouring the liquor into a stainless steel drying pan. The black liquor level in the pan was kept at 2 cm in order to prevent non-uniform deposition of inorganic solids during drying. The black liquor was dried in an oven at 80-100°C for 24 hours. The dry black liquor solids were then carefully scraped from the pan and stored in a vacuum oven at 50°C for 48 hours to remove any remaining water without loss of any remaining volatile matter in the black liquor. The dried black liquor solids were then ground into powder with a coffee grinder. The black liquor powder was again stored in the vacuum oven at 50°C for

24 hours to remove moisture adsorbed during the grinding process. Then, the completely dried black liquor powder was sieved to provide black liquor solids in the 90-125 micron particle size range used in the LEFR experiments. All black liquor solids were kept in desiccator to avoid absorption of moisture. The elemental composition of the black liquor solids is shown in Table 4.1

Table 4.1 Elemental composition of the Black Liquor Solids

Element	wt. %
Carbon	34.8
Oxygen	35.3
Sodium	22.6
Hydrogen	3.0
Sulfur	2.9
Potassium	0.62
Chloride	0.67
Nitrogen	0.08

Experimental Conditions

For pyrolysis of black liquor solids, the effect of residence time at different temperatures was studied. The residence time was varied from 0.3 to 2.0 seconds and temperature was varied from 400°C to 600°C. The particle residence times were calculated by Flaxman's computational fluid dynamic and heat transfer model of particles in a laminar entrained flow reactor. The model had been modified to accounts for the swelling and mass loss behavior of kraft black liquor, and it accounts for momentum transport, gas-particle slip, and convective and radiative heat transfer between the gas, reactor wall, and particles. The residence time that can be achieved by the LEFR is limited by the reactor path length and maximum input gas flow rate. The experimental conditions in this study are shown in Table 4.2.

Experimental Conditions

Residences time (sec)	Temperature (°C)		
	400	500	600
0.3	X	X	X
0.5	X	X	X
0.7	X	X	X
0.9	X	X	X
1.1	X	X	X
1.3	X	X	X
1.5	X	X	X
1.7	X	X	X
2.0	X	X	X

Experimental Procedure

Pre-run preparation

Laminar Entrained-Flow Reactor (LEFR)

- At room temperature, move the collector to the desired position and set the alignment of the collector to be center.
- Turn on water cooling system (The cooling system must be on all the time, even though the furnace is shut off. The cooling system can be off whenever the temperature of the reactor has come down to room temperature)
- Set the temperature controller to the desired set point. (maximum ramping rate is 200°C/hr)

Cyclone/Filter

- All filters are stored in an oven at 105°C to remove moisture.
- Cyclone and all connection parts must be cleaned and dried.
- Weight filter and place in the cyclone/filter system

Oxidizer

- Fill the water bath.
- Connect oxygen line to the oxidizer.
- Set the temperature controller to 900°C.

CO₂ Gas Analyzer

- With all power off, adjust mechanical zero on the meter with a small screwdriver, if necessary.
- Lift out the dust filter/drain separator and fill with absorbent cotton.
- Reset the dust filter/drain separator in previous position.
- Connect sampling line from cylindrical gas oxidizer to CO₂ gas analyzer.
- Turn on gas analyzer and allow 3 minutes for stabilization or 30 minutes for greatest accuracy.
- Turn switch to 'MEAS' (sampling pump is activated).
- Turn Zero adjusting knob and set indicating pointer on meter to zero.
- Check span adjustment using gas or test filter.

Feeding System

- Feeding tube and feeding connection must be clean and dry.
- Fill dry black liquor solid into feeding tube and weigh.
- Install the feeding tube in the feeding system.

Pyrolysis Runs

- Open quench & total gas flows and adjust until achieving the desired set point while the pressure is set at 25 psi.
- Open the primary flow until achieving the desired set point.
- Open excess oxygen flow to cylindrical gas oxidizer.

- Turn on the feeding motor and set to low speed allowing black liquor solids to be entrained to LEFR by the primary gas flow.
- Turn off the feeding motor immediately after particles start exiting the reactor while all gases are left flowing into the reactor and the collector.
- Attach cyclone/filter assembly to the bottom of the collector and connect sampling line from cyclone/filter assembly to cylindrical gas oxidizer.
- Turn on the feeding motor to start pyrolysis and run about 10 minutes for steady state condition.
- At the end of the experiment, turn off the primary flow and turn the feeding motor in reverse while total gas flow and quench flow are kept flowing around 2 more minutes until the CO₂ level, as display in CO₂ meter, is down to zero.
- Shut off all gas flow.
- Weigh char and filter (collected fume) before placing in sample container.
- Reattach cyclone/filter assembly and then flush all the remaining particle in feeding line and LEFR by using maximum primary gas flow rate for approximately 1 minute.
- Weigh flushed char and flushed filter, then discard.
- Clean all necessary equipment and prepare for next run.

Sample Analysis

There are two kinds of solid samples as follows

1. Char collected by the cyclone
2. Fine particles collected by both the large and small filters

Char and Fume samples are analyzed for total carbon, nitrogen and sulfur by a Carbon, Nitrogen and Sulfur Analyzer at the Crop Science Laboratory, Oregon State University.

RESULTS AND DISCUSSION

In this section, the results from the experiments are divided into different subsections according to the objectives of the study. In each subsection, the experimental results are shown and compared with the data from previous studies, and data trends are examined.

Carbon Yield from Pyrolysis of Black Liquor Solids

Carbon Yield in Gas from Pyrolysis of Black Liquor Solids

In this study, all oxidizable product gases and tar from the LEFR that passed the fine particle filter were converted to carbon dioxide in an oxidizer. The CO₂ content of the gas exiting the oxidizer was measured, and the total carbon content in the gas at each experimental condition was calculated based on the carbon dioxide concentration of product gas.

Figure 5.1 shows the carbon yield in the gas versus residence time from pyrolysis of black liquor solids at 600°C. *The carbon yield in the gas increased as residence time increased.* The reproducibility obtained in replicate runs was an average $\pm 1.0\%$ of the carbon in the black liquor solids input to the LEFR. At a residence time of 0.3 seconds, the carbon yield in the gas was 8% and it rapidly increased to 20% at residence time 1.1 seconds. It gradually increased to 23% at residence time 2.0 seconds.

Figure 5.2 and Figure 5.3 show the carbon yield in the gas phase versus residence time from pyrolysis of black liquor solids at 500°C and 400°C respectively. *The carbon yield in the gas phase increased as residence time increased.* The reproducibility in replicate runs at 500°C was an average $\pm 0.8\%$, and at 400°C was $\pm 1.4\%$ of the carbon in the black liquor solids. For 500°C, at a residence time of 0.3 seconds, the carbon yield in the gas was 7%. It increased linearly as residence time increased to 23% at a residence time of 2.0 seconds. For 400°C, at residence times from 0.3 to 0.5 seconds, the carbon yield in the gas phase increased slowly to about 2%. At residence times from 0.5 to 1.5 seconds,

the carbon yield in the gas phase increased more rapidly from 2% to 17%. At residence times above 1.5 seconds, the carbon yield in the gas phase gradually increased to 20% at residence time of 2.0 seconds.

Figure 5.4 compares the carbon yield in the gas phase versus residence time from pyrolysis of black liquor solids at temperature of 600°C, 500°C, and 400°C. *The higher the temperature, the higher the carbon yield as gases phase at each residence time.*

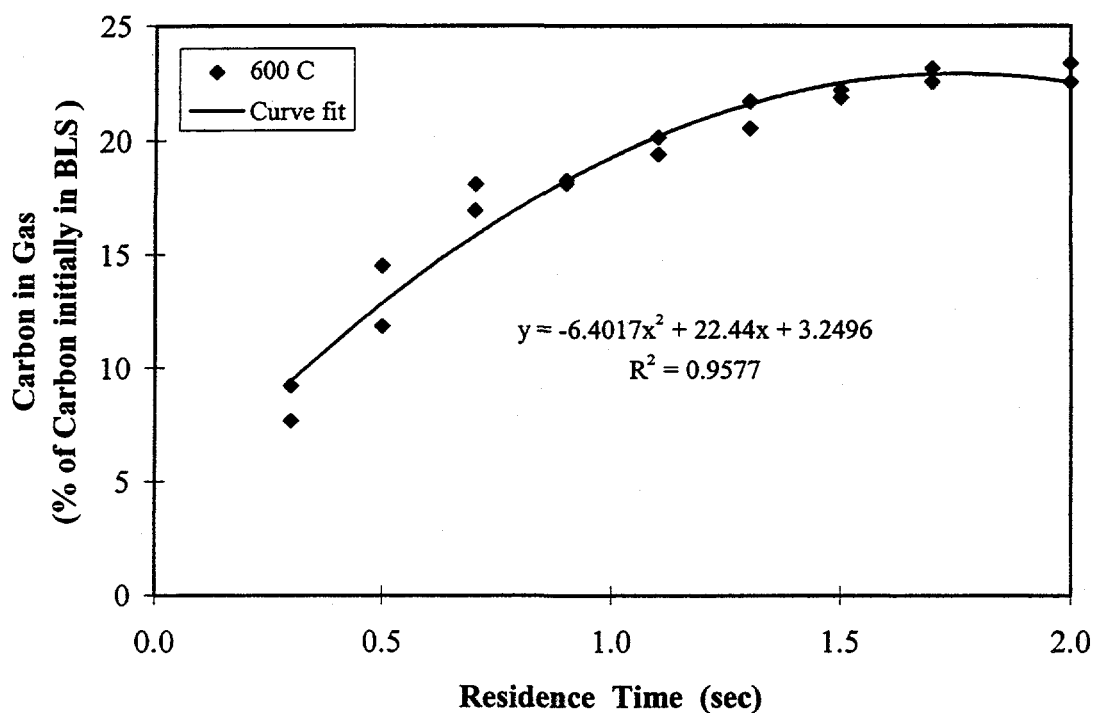


Figure 5.1 Carbon Yield in Gas from Pyrolysis of Black Liquor Solids at 600°C

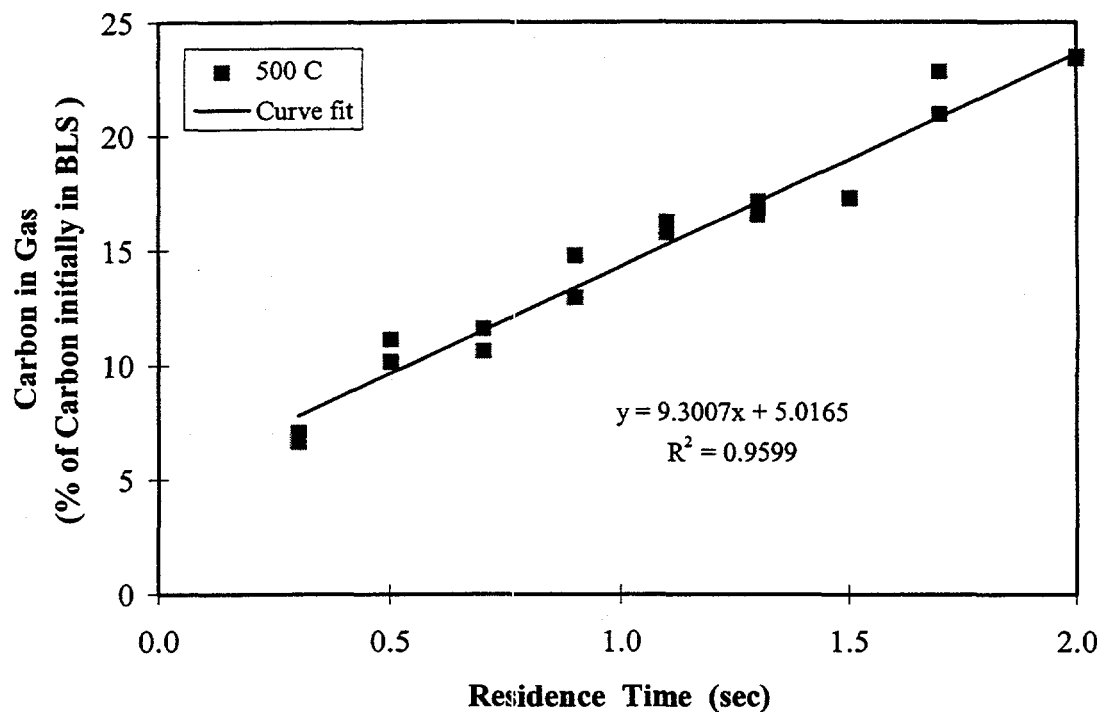


Figure 5.2 Carbon Yield in Gas from Pyrolysis of Black Liquor Solids at 500°C

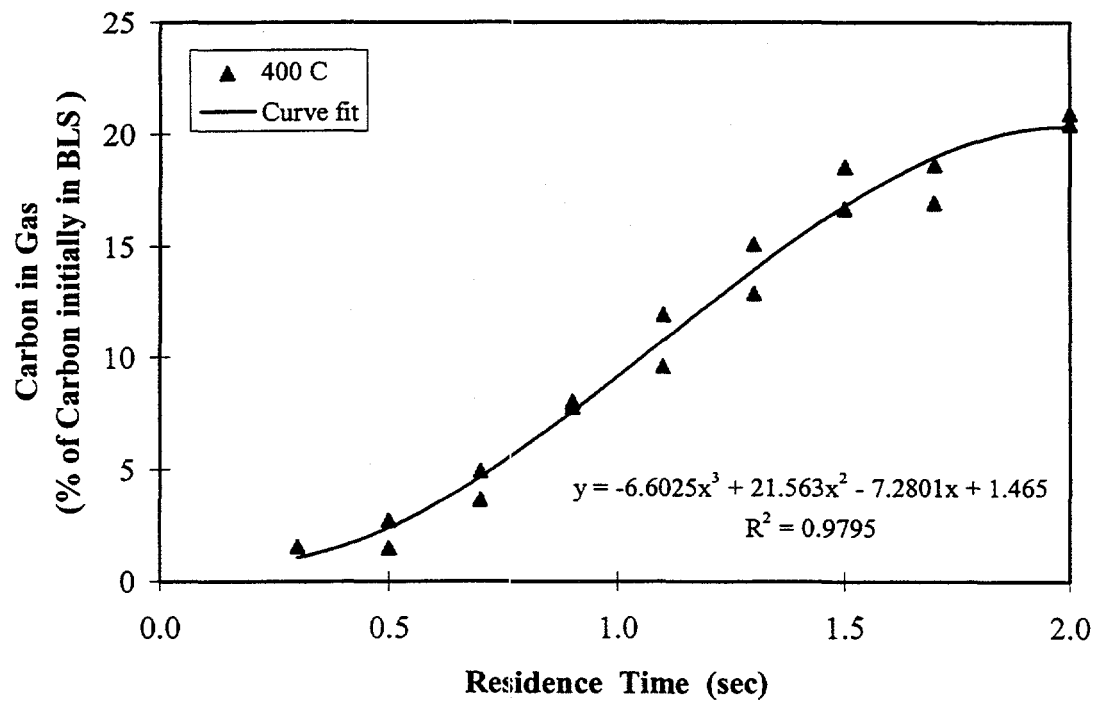


Figure 5.3 Carbon Yield in Gas from Pyrolysis of Black Liquor Solids at 400°C

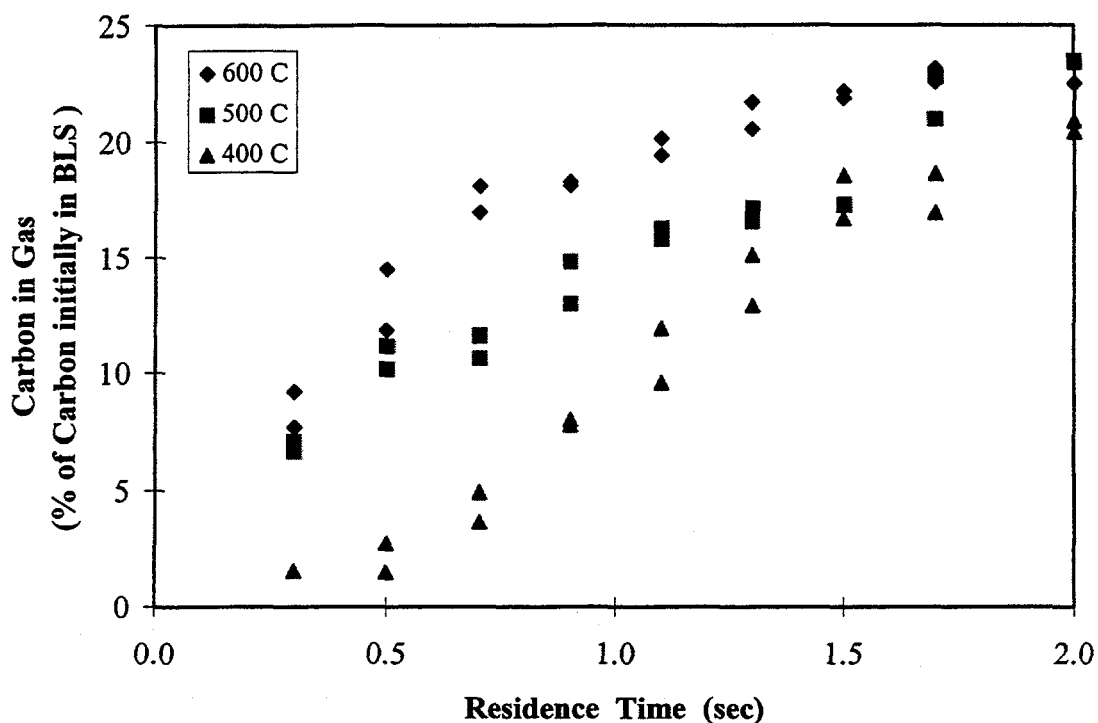


Figure 5.4 Carbon Yield in Gas from Pyrolysis of Black Liquor Solids at 400-600°C

Carbon Yield in the Fine Particles from Pyrolysis of Black Liquor Solids

In this study, *fine particles* refers to the particles that passed through the 3 μm cutoff cyclone and were collected on the filter down stream, they consisted mainly of tar and small char particles. The experimental temperatures were from 400 to 600°C which is too low for significant volatilization of sodium and potassium salts to occur. Thus, the fine particles are different from the inorganic condensation aerosols that are produced during pyrolysis of black liquor at much higher temperature (fume).

Figure 5.5 shows the carbon yield in the fine particles versus residence time from pyrolysis of black liquor solids at 600°C. Overall, the carbon yield in the fine particles increased as residence time increased. The reproducibility obtained in replicate runs was ± 0.1 of the carbon input as black liquor solids. At residence times of 0.3-1.1 seconds, the carbon yield in the fine particle was constant 0.5%. At

residence times above 1.1 seconds, the carbon yield in the fine particle increased rapidly to 2.5% at a residence time of 2.0 seconds.

Figure 5.6 and Figure 5.7 show the carbon yield in the fine particles versus residence time from pyrolysis of black liquor solids at 500°C and 400°C respectively. The carbon yield in the fine particles increased at 500°C. At 400°C, it was nearly constant until 1.5 seconds and then increased slowly. The reproducibility obtained in replicate runs at 500°C and at 400°C were an average $\pm 0.1\%$ of the carbon in the black liquor solids input. At the shortest residence time, 0.3 seconds, the carbon yield in the fine particles was 0.27% at 500°C and 0.31% at 400°C. At the longest residence time, 2.0 seconds, the carbon yield in the fine particles was an average 1.8% at 500°C and 1.0% at 400°C.

Figure 5.8 compares the carbon yields in the fine particles versus residence time from pyrolysis of black liquor solids at temperature of 600°C, 500°C, and 400°C. The carbon yields in the fine particles differ very little with temperature at residence time below 1.1 seconds. At higher temperatures, the carbon yield in the fine particles is about the same at 500°C and 600°C, but lower at 400°C.

Carbon Yield in the Char Residue from Pyrolysis of Black Liquor Solids

Figures 5.9, 5.10, and 5.11 show the carbon yields in the char residue versus residence time from pyrolysis of black liquor solids at 600°C, 500°C, and 400°C respectively. *The carbon yield in the char residue decreased as residence time increased.* The reproducibility obtained in replicate runs was an average $\pm 3.2\%$ at 600°C, $\pm 1.8\%$ at 500°C, and $\pm 2.2\%$ at 400°C, all as percentage of carbon input as black liquor solids.

At 600°C, the carbon yield in the char residue decreased rapidly from 90% at a residence time of 0.3 seconds to 76% at residence time 1.1 seconds, and then gradually decreased to 70% at residence time 2.0 seconds. At 500°C, the carbon yield in the char residue decreased from 87% at a residence time of 0.3 seconds to 60% at residence time 2.0 seconds. At 400°C, the carbon yield in the char residue was constant at about 95% at residence times of 0.3-0.5 seconds. At residence times between 0.5-1.5 seconds,

the carbon yield in the char residue rapidly decreased to 78%, and then decreased gradually to 75% at a residence time of 2.0 seconds.

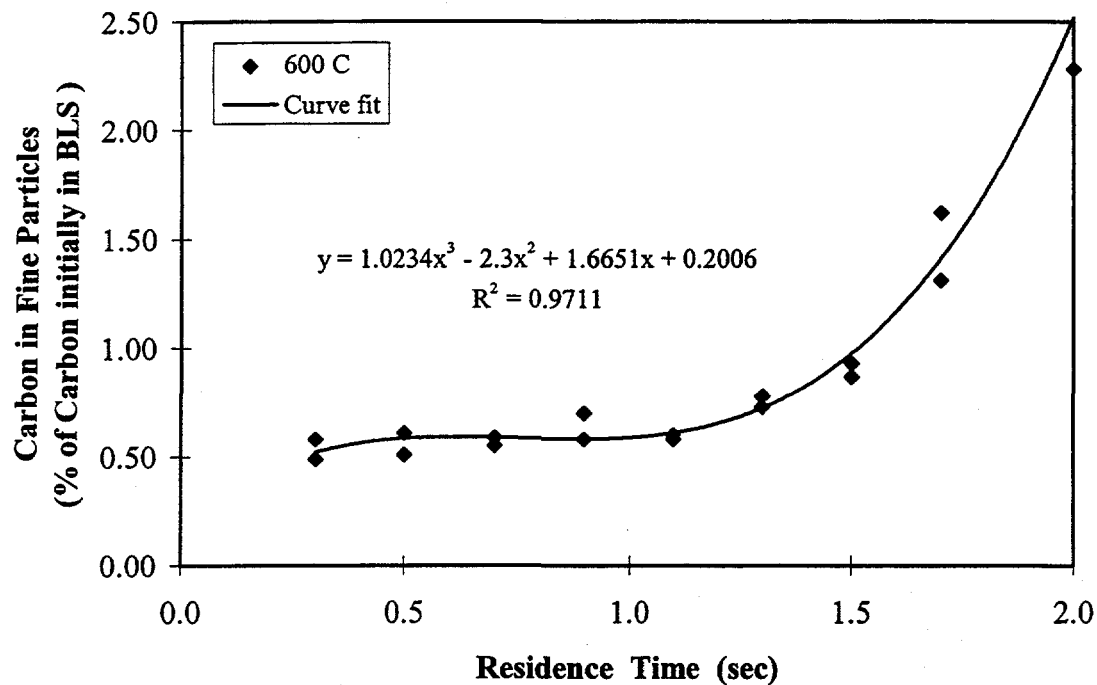


Figure 5.5 Carbon Yield in the Fine Particles from Pyrolysis of Black Liquor Solids at 600°C

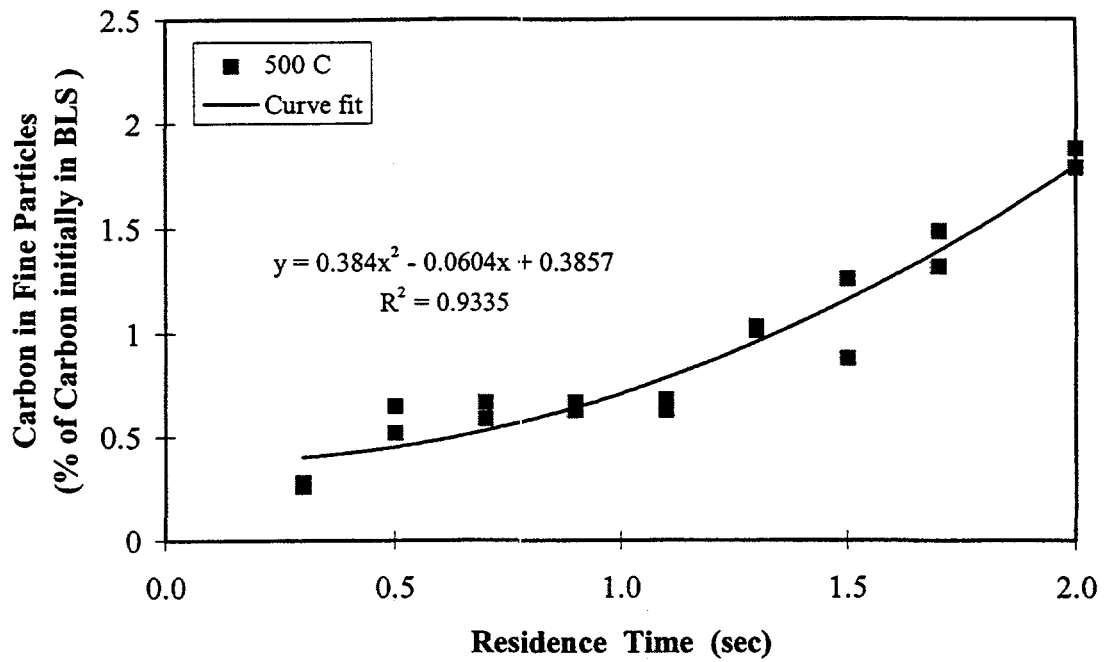


Figure 5.6 Carbon Yield in the Fine Particles from Pyrolysis of Black Liquor Solids at 500°C

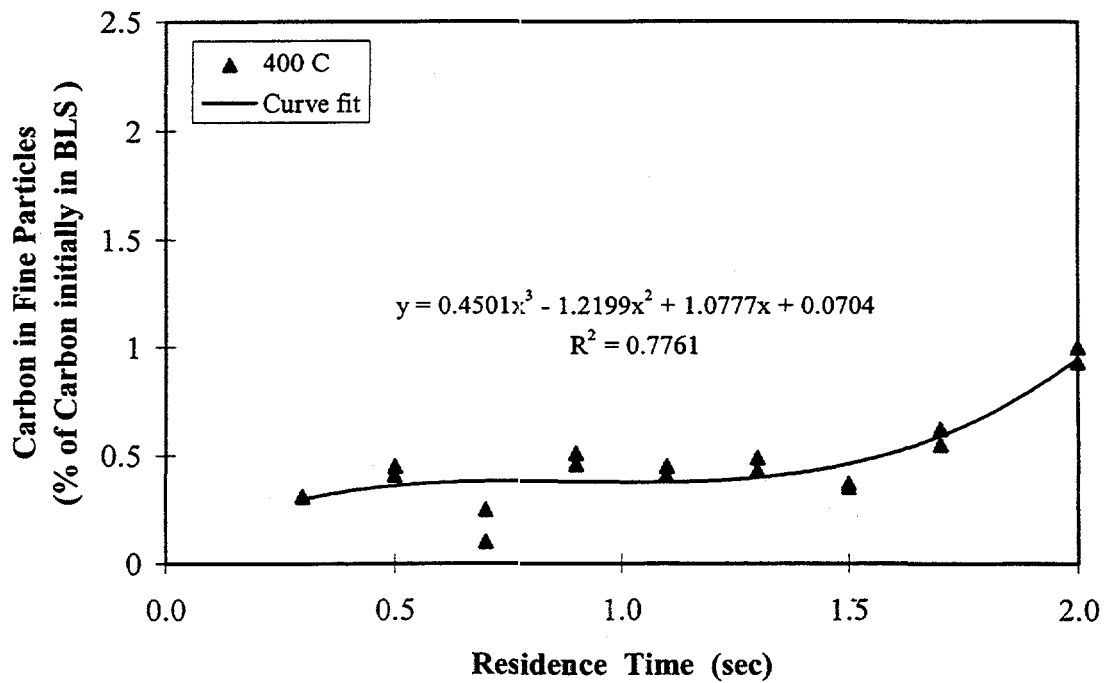


Figure 5.7 Carbon Yield in the Fine Particles from Pyrolysis of Black Liquor Solids at 400°C

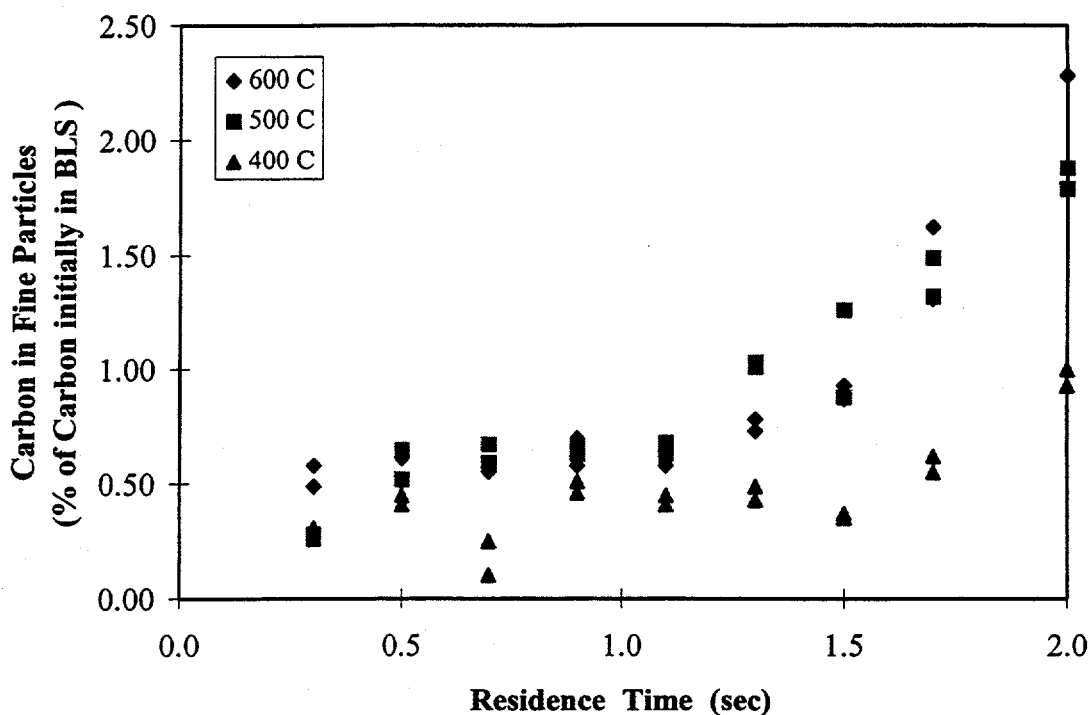


Figure 5.8 Carbon Yield in the Fine Particles from Pyrolysis of Black Liquor Solids at 400-600°C

Figure 5.12 compares the carbon yield in the char residue versus residence time from pyrolysis of black liquor solids at temperature of 600°C, 500°C, and 400°C. The carbon yields in the char residue at 400°C higher than those of 600°C. This is in accordance with the finding of Frederick et al., 1994; Frederick et al., 1995. Frederick et al. (1995) measured the total carbon in the char residue collected at furnace temperature between 700-1000°C and residence time between 0.3-1.6 seconds for 100 micron dry black liquor solids pyrolyzed in similar LEFR experiments. They reported that the carbon content of the char residue decreased rapidly during devolatilization ($t < 0.3$ seconds) and continued to decrease but at a slower rate after devolatilization. Frederick (1995) reported that at a residence time of 0.3 seconds, the total carbon in the char residue decreased from 68% at 700°C to 42% at 1100°C. At a residence time of 1.6 seconds, the total carbon in char residue decreased from 50% at 700°C to 20% at 1100°C. In this study, the temperature range was lower than that used by Frederick et al. (1995), but the trends of the total carbon in char residue versus furnace temperature agree with Frederick's (1995) study.

For a temperature of 500°C and residence time above 1.1 seconds in this study, the carbon yield in char residue was a little lower than at a temperature of 600°C. This is the effect of the lower char residue yield at 500°C and residence time above 1.1 seconds.

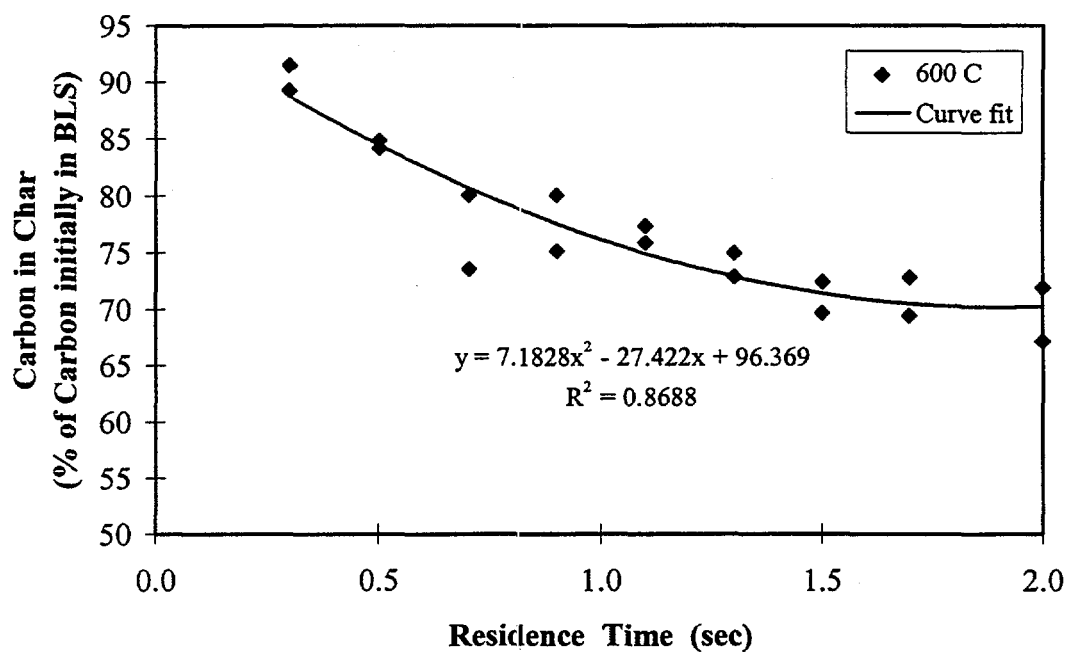


Figure 5.9 Carbon Yield in the Char Residue from Pyrolysis of Black Liquor Solids at 600°C

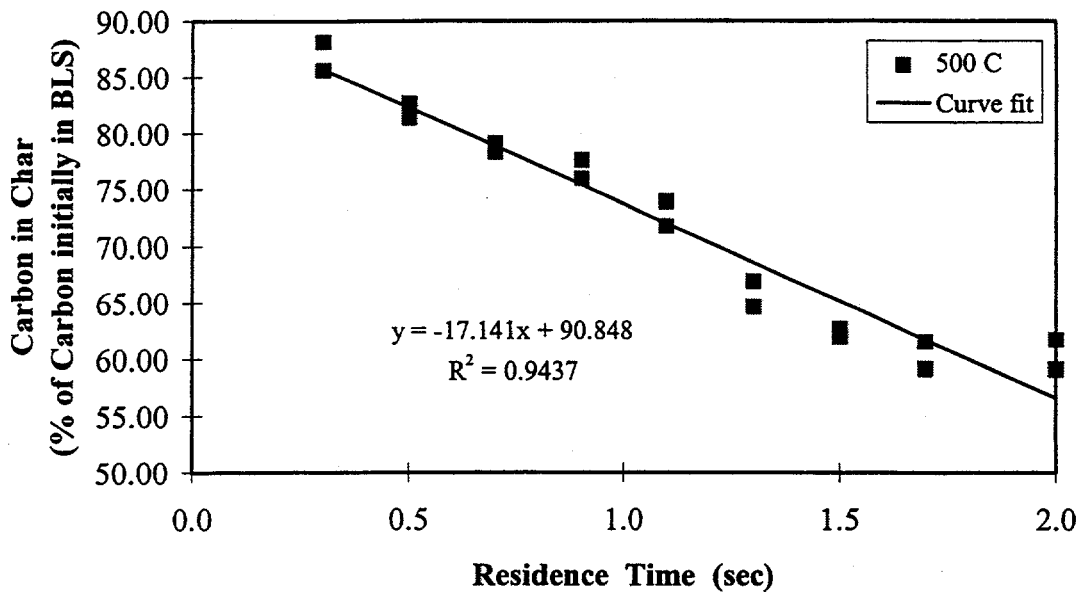


Figure 5.10 Carbon Yield in the Char Residue from Pyrolysis of Black Liquor Solids at 500°C

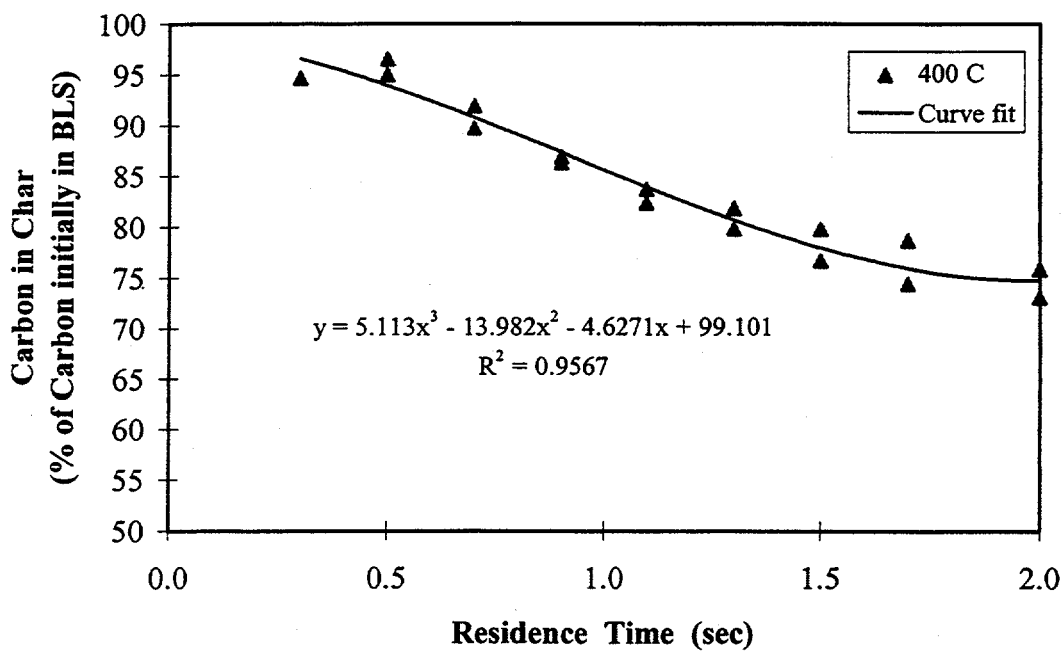


Figure 5.11 Carbon Yield in the Char Residue from Pyrolysis of Black Liquor Solids at 400°C

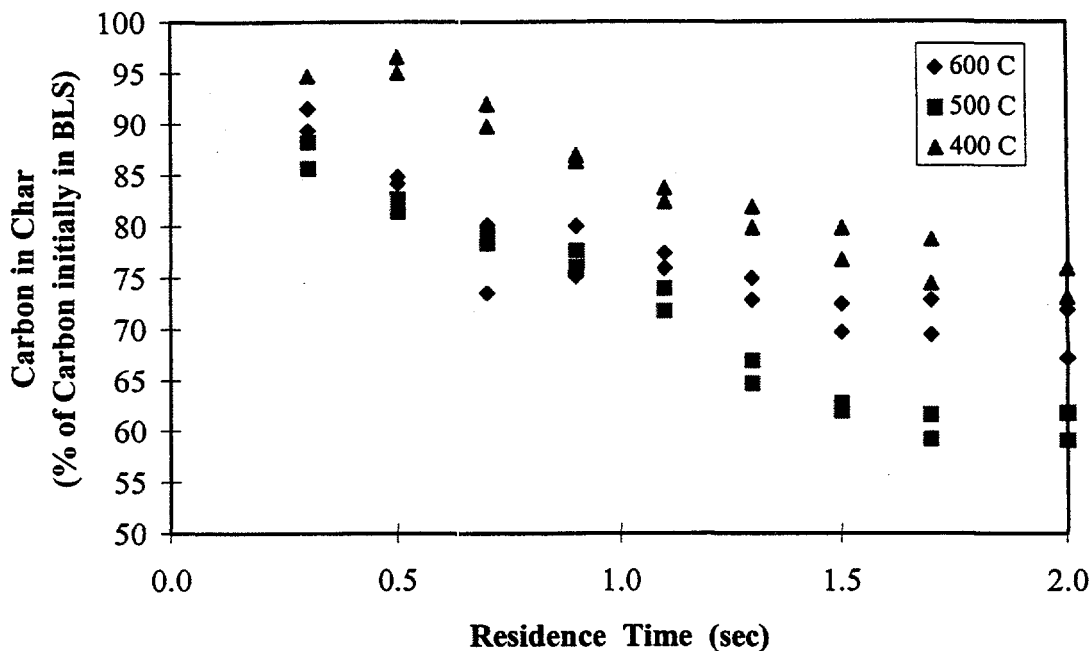


Figure 5.12 Carbon Yield in the Char Residue from Pyrolysis of Black Liquor Solids at 400-600°C

Fine Particle Yield from Pyrolysis of Black Liquor Solids

Figure 5.13 shows the fine particle yield versus residence time from pyrolysis of black liquor solids at 600°C. *The fine particle yield was very low, no greater than 1% of BLS, and overall increased as residence time increased.* The reproducibility obtained in replicate runs was an average $\pm 0.1\%$ of the carbon in the black liquor solids input. At residence time 0.3 seconds, the fine particle yield is 0.58% and decreased to 0.44% at residence time 0.5 seconds and constant until residence time 1.1 seconds. At residence time above 1.1 seconds, fine particle yield increased as residence time increased to 1.00% at residence time 2.0 seconds.

Figure 5.14 and Figure 5.15 show the fine particle yield versus residence time from pyrolysis of black liquor solids at 500°C and 400°C respectively. The results were qualitatively similar to those of 600°C, the fine particle yield increased as residence time increased from 500°C and 400°C. The reproducibility obtained in replicate runs was an average ± 0.1 of the black liquor solids input at 500°C, and at 400°C. At 500°C, the fine particle yield increased from 0.29% at residence time 0.3 seconds to

0.81% at residence time 2.0 seconds. At 400°C, the fine particle yield was essentially constant over the entire range of residence times.

Figure 5.16 shows the comparison of the fine particle yield versus residence time from pyrolysis of black liquor solids between 600°C, 500°C, and 400°C. At residence times above 1.1 seconds, the fine particle yield increased more rapidly at higher temperatures but not at the lower temperature.

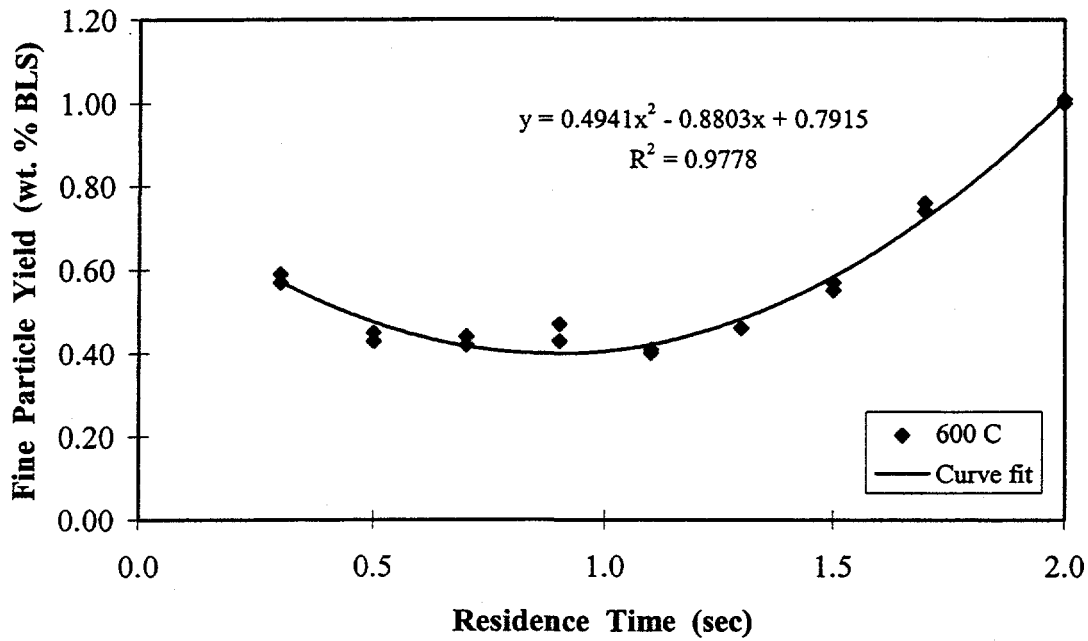


Figure 5.13 Fine Particle Yield from Pyrolysis of Black Liquor Solids at 600°C

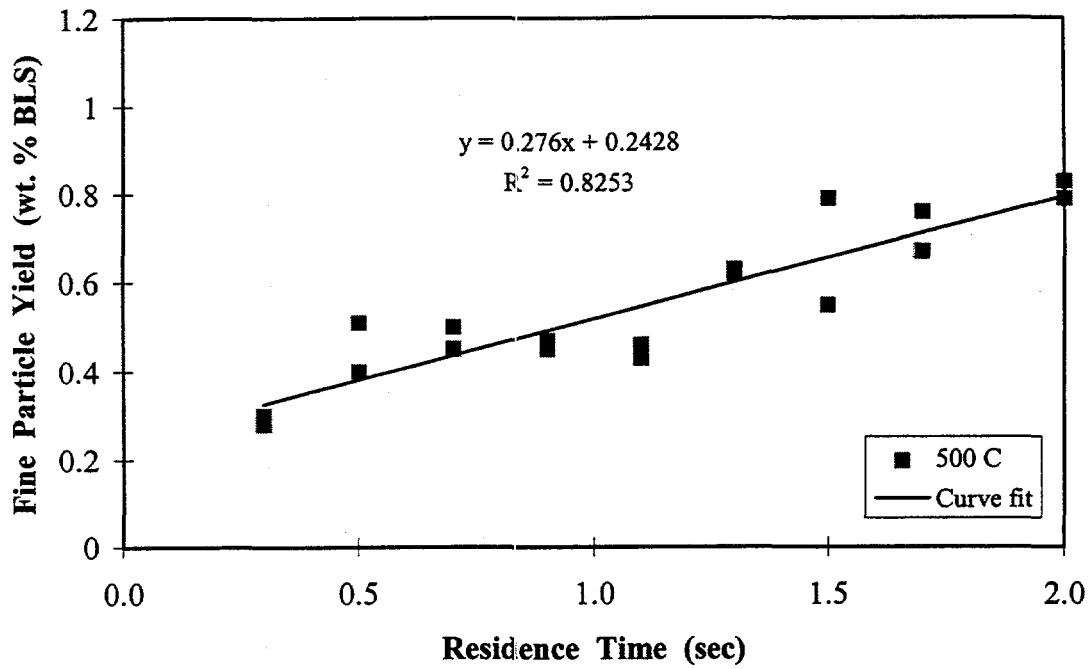


Figure 5.14 Fine Particle Yield from Pyrolysis of Black Liquor Solids at 500°C

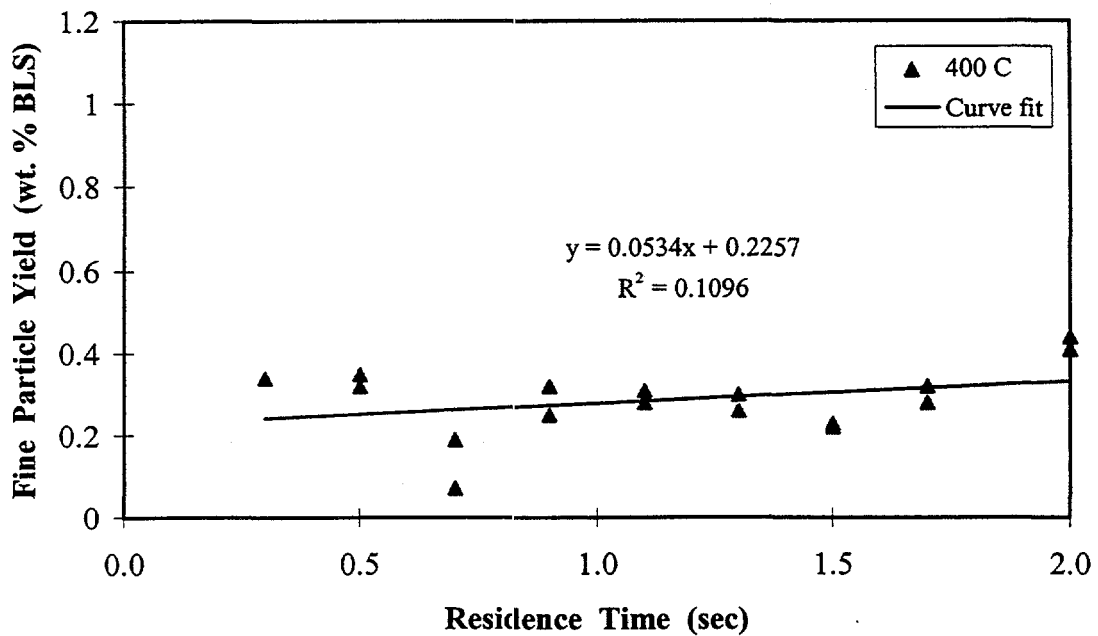


Figure 5.15 Fine Particle Yield from Pyrolysis of Black Liquor Solids at 400°C

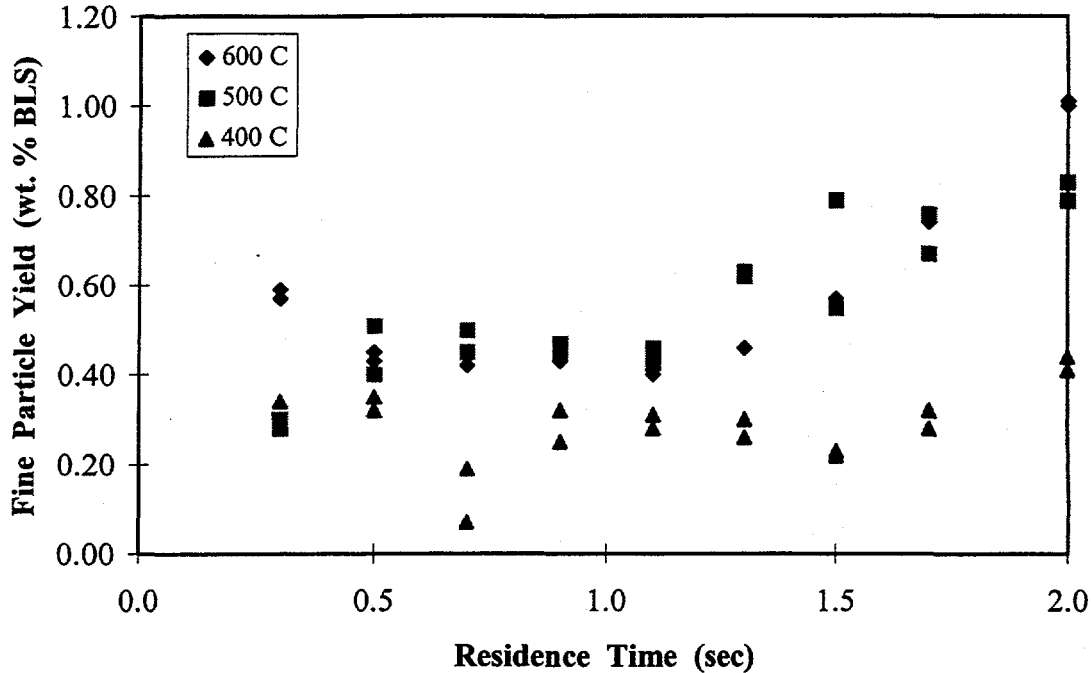


Figure 5.16 Fine Particle Yield from Pyrolysis of Black Liquor Solids at 400-600°C

Char Residue Yield from Pyrolysis of Black Liquor Solids

In this study, *char residue* refers to the solid residue from pyrolysis including the ash as well as carbon and other elements that remain from the organic matter in black liquor. The mineral ash free char residue is referred to as *char*. During pyrolysis, the char residue yields trend in the opposite direction of the volatile gas yield.

The char residue yield was used as a preliminary indicator of whether good closure of the carbon mass balance will be obtained. Incomplete collection of the char residue was formed to be the main problem in the LEFR runs. This was due mainly to collection of char particles on the tip of the collector. As an example, in some replicate runs the char yield varied from e.g. 91% to 93%. Reproducibility runs show that, when char losses are very minor, the char yield is reproducible within about $\pm 2\%$. By comparing the char residue yield with previous char residue yield data, it can quickly be determined whether complete char collection was obtained. Experimental data is accepted or rejected, without a

more detailed analysis. When runs are rejected for poor char recovery, additional runs at the same experimental conditions can be made.

Figure 5.17 shows the char residue yield versus residence time from pyrolysis of black liquor solids at 600°C. *The char residue yield decreased as residence time increased.* The reproducibility obtained in replicate runs was $\pm 2\%$. At a residence time of 0.3 seconds, the char residue yield was 92% and it quickly decreased to 85% at a residence time of 0.5 seconds. At residence times above 0.5 seconds, the char residue yield gradually decreased to 75% at a residence time of 2.0 seconds. This indicates that the black liquor solids were volatilized rapidly until a residence time of 0.7 seconds. After that they were volatilized more gradually. This is in accordance with the finding of Carangal, 1994; and Pianpucktr, 1995. Pianpucktr (1995), for example, reported that at 700°C char residue yield was 82% at 0.3 seconds and it quickly decreased to 65% at 0.6 seconds. At residence times above 0.6 seconds, the char residue yield gradually decreased to 53% at 2.2 seconds.

Figure 5.18 and Figure 5.19 show the char residue yields versus residence time from pyrolysis of black liquor solids at 500°C and 400°C respectively. The results were qualitatively the same as those at 600°C: the char residue yield decreased as residence time increased. The reproducibility obtained in replicate runs was $\pm 1.9\%$ at 500°C, and $\pm 2.3\%$ at 400°C. At the shortest residence time, 0.3 seconds, the char residue yield was 92% at 500°C and 99% at 400°C. This indicates that at 400°C nearly all of the volatile species remained as black liquor solids at residence time 0.3 seconds, i.e. that the black liquor had barely begin to pyrolyze. At residence times above 0.3 seconds, the char residue yield gradually decreased until the longest residence time, 2.0 seconds. At 2.0 seconds the char residue yield was 65% at 500°C and 77% at 400°C.

Figure 5.20 shows the comparison of the char residue yield versus residence time from pyrolysis of black liquor solids between 600°C, 500°C, and 400°C. At residence time between 0.3-1.1 seconds, the char residue yield was about the same at 500°C and 600°C, but higher at 400°C. At residence time above 1.1 seconds, the experimental data from 600°C and 400°C agree well with the result of previous studies,

but the experimental data at 500°C show that the char residue yield was lower than those of previous typical char residue yield data. Carangal (1994) reported char residue yield as a function of temperature at residence time 2.0 seconds and the char residue yield at 500°C was 73.16%. Table 5.1 shows the comparison of char residue yield from pyrolysis of black liquor solids at residence time 2.0 seconds between Carangal's (1994) extrapolated data and this experimental data.

Table 5.1 The comparison of char residue yield from pyrolysis of black liquor solids at residence time 2.0 seconds between Carangal's (1994) extrapolated data and this experimental data for runs made with dry black liquor solids from the same kraft black liquor

Temperature (°C)	Char Residue Yield (wt% BLS)	
	Carangal's (1994) calculation	Experimental data
600	67.6 ± 7.0	75 ± 2.0
500	73.2 ± 3.0	65 ± 1.9
400	78.8 ± 3.0	77 ± 2.3

From Table 5.1, at 600°C, the char residue yield from our experimental data was higher than that of Carangal's extrapolated data. At 500°C, the char residue yield from our experimental data was lower than that of Carangal's extrapolated data. At 400°C, the char residue yield from our experimental data agrees well with Carangal's extrapolated data.

From Carangal's experimental data at 600°C and 2.0 seconds residence time, the char residue yield varied from 60-73%. By comparison in our experimental data the yield varied from 73-75%. There is some overlap between Carangal's experimental char residue data and our experimental data. Since the greatest problem in these experiments is loss of char, we conclude the char residue yield result at 600°C, 2.0 seconds residence time is about 73-75%.

From the Carangal's experimental data at 500°C and 2.0 seconds residence time, the char residue yield was around 70%, compared to our experimental data where it was 63-65%. Also, the char residue

yields at 500°C for residence times above 1.1 seconds, shown in Figure 5.20, are lower than the yields at 600°C.

During devolatilization, black liquor droplets swell rapidly and continuously to a maximum volume at the end of devolatilization. In the experiments, the diameters of the swollen char particle at 500°C were bigger than those of char particles produced at 400°C or 600°C (Phimolmas, 1997). This is similar to the results reported by Miller (1986). Miller studied the effect of gas temperature, heating rate, initial solids content of the particle, and particle size on the maximum swollen volume of black liquor particles during evaporation and pyrolysis using single particle reactor. The gas temperature was varied from 300-900°C. Miller reported that the maximum swollen volume occurred at approximately 500°C. The pyrolyzing black liquor appeared to be most fluid at 500°C. The larger swollen char residue particle at 500°C accumulated at the top of collector and partially blocked the collector entrance. This prevented other char residue particles from entering the collector, and thus caused the lower char residue yield.

At 400°C, the effect of furnace temperature on the maximum swollen volume of black liquor was minor which is in accordance with the experimental results reported here. The char residue yield gradually decreased as the residence time increased and the char residue yield at the longest residence time of study (2.0 seconds) was in agreement with Carangal's (1994) extrapolated data.

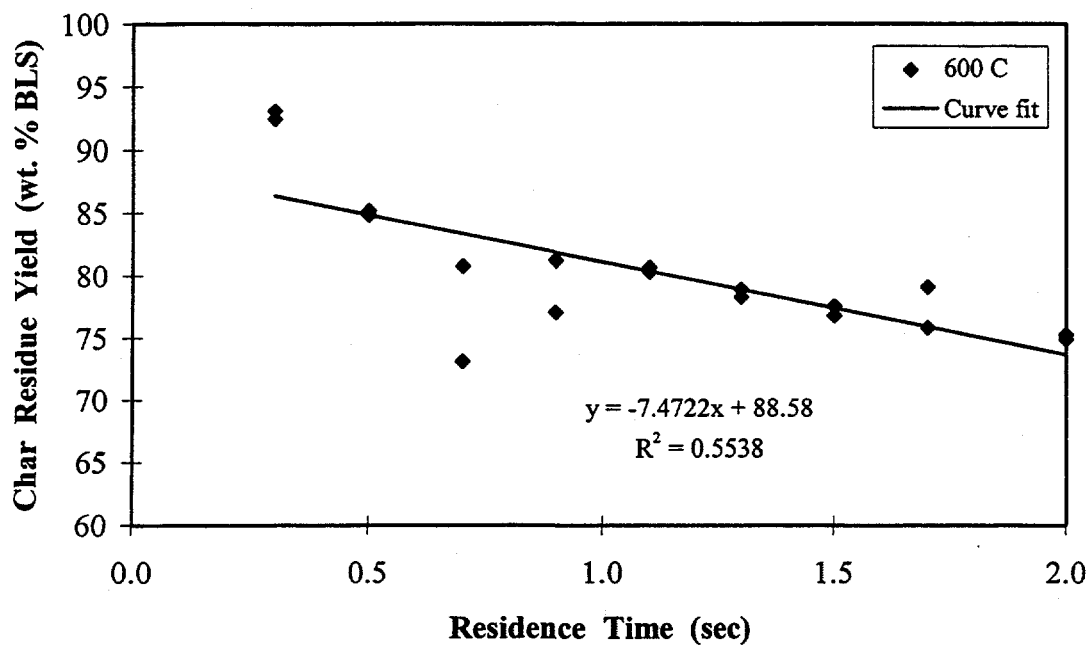


Figure 5.17 Char Residue Yield from Pyrolysis of Black Liquor Solids at 600°C

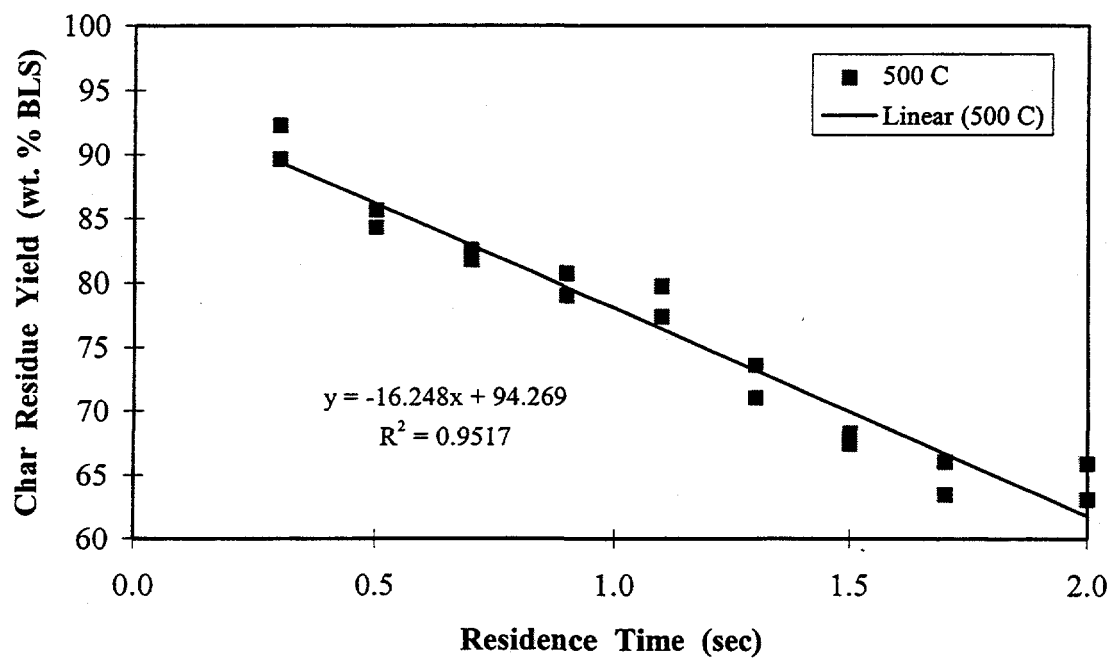


Figure 5.18 Char Residue Yield from Pyrolysis of Black Liquor Solids at 500°C

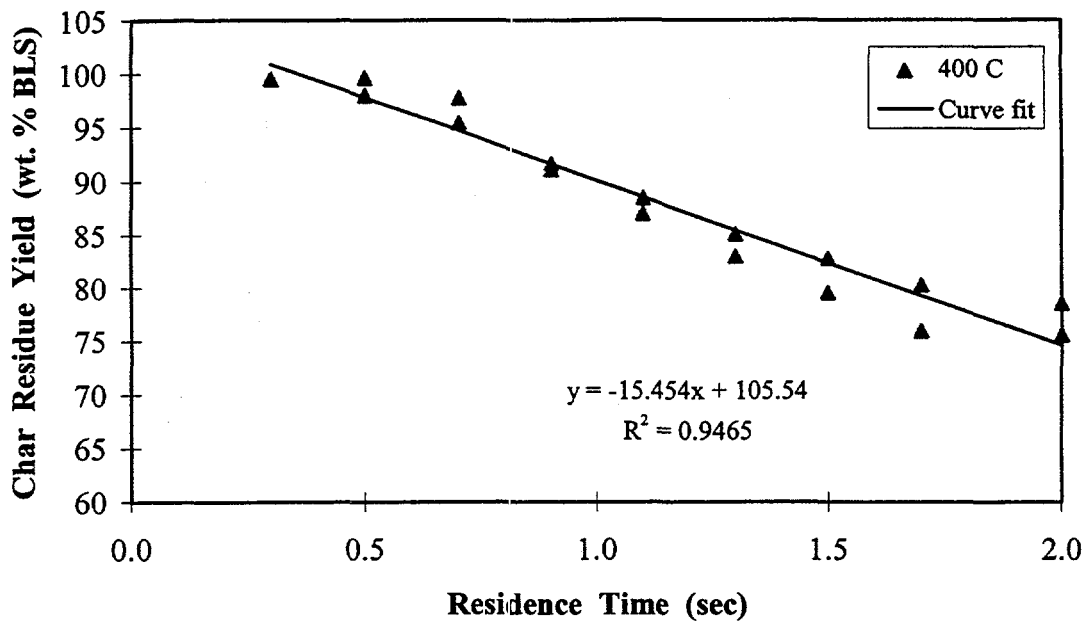


Figure 5.19 Char Residue Yield from Pyrolysis of Black Liquor Solids at 400°C

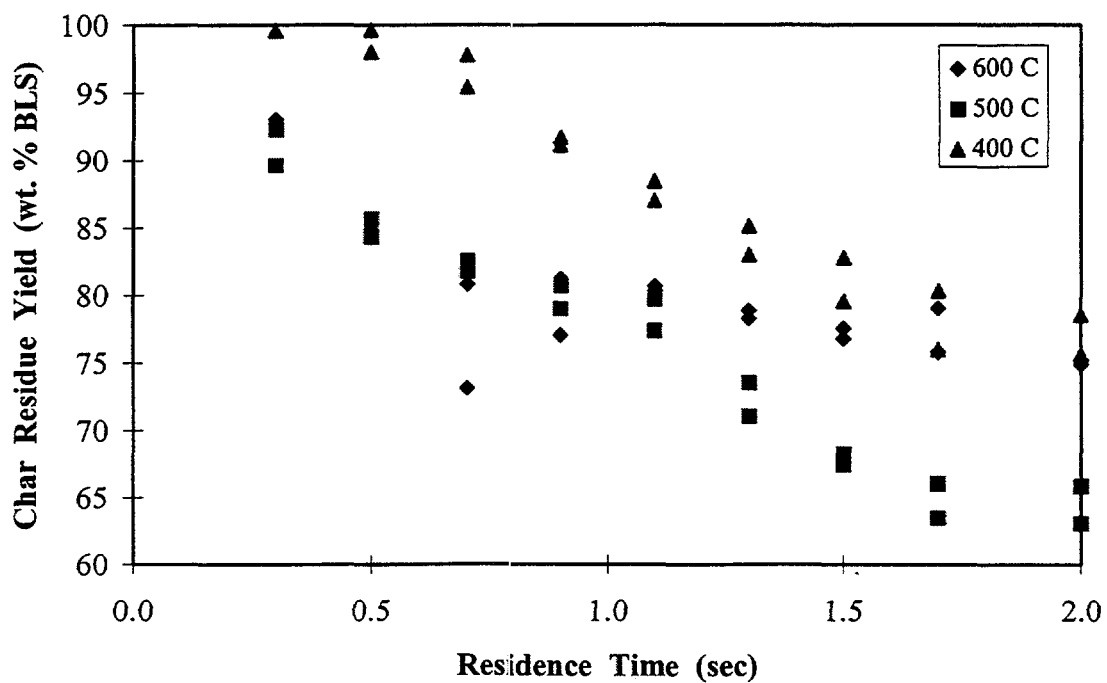


Figure 5.20 Char Residue Yield from Pyrolysis of Black Liquor Solids at 400-600°C

Carbon Recovered from Pyrolysis of Black Liquor Solids

Carbon recovered as gases, fine particles, and char residue from pyrolysis of black liquor solids provided mass balances for carbon at each experimental condition.

Carbon recovery in this study was calculated based on the carbon input as black liquor (100%) and carbon outputs including carbon in char, fine particle, and gas. Details of the calculations are shown in Addendum A of this appendix. The average of carbon recovered from carbon yield in char, carbon yield in fume, and carbon yield in gas are as follows:

1. At temperature 600°C, average carbon recovery 96.2% (range 91.0-99.7%)
2. At temperature 500°C, average carbon recovery 88.1% (range 80.5-95.5%)
3. At temperature 400°C, average carbon recovery 95.7% (range 93.6-99.7%)

At temperatures of 600°C and 400°C, the average carbon recovery was very good. At temperature 500°C, the average carbon recovery was somewhat lower. As discussed in Section 5.3, at 500°C, the char residue yield was lower than expected based on the 400°C and 600°C data, and on Carangal's (1994) data, due to accumulation of the highly swollen char particle on the top of the collector in the LEFR. This reduced the average carbon recovery at 500°C.

These carbon recovery results show that the data on distribution of carbon between char and gases can be considered reliable, especially at 400°C and 600°C. We now examine the data at 500°C where carbon recovery was poorer.

According to the discussion in section 5.2.2, the fine particles should consist mainly of tar or char fines. This can be confirmed by Figure 5.27, Figure 5.28, and Figure 5.29, which show that non-carbon matter in the char residue and in the fine particles at 600°C, 500°C, and 400°C respectively. The non-carbon matter (inorganic matter) in the fine particle decreased as residence time increased. The non-carbon matter in the char residue remained constant as residence time increased. At residence time of 0.3 seconds, the non-carbon matter in the char and in the fine particles was the same, which indicates that

the fine particles are very likely the same material as the char residue. At residence times above 0.3 seconds, the non-carbon matter in the fine particle decreased as residence time increased which indicates that the carbon content of the fine particles increase as residence time increases.

As discussed earlier, the main reason for the poorer carbon recovery at 500°C was the loss of char particles on the tip of the collector. The fraction of carbon input that was recovered as gas and fine particles at 500°C were consistent with the 400°C and 600°C data. The char residue and char carbon yield were therefore adjusted upward, base on the carbon recovered as gas and as fine particles, to give a carbon balance closure of 96%, the average for 400°C and 600°C runs. Details of the calculations are shown in Addendum A of this appendix. The adjusted carbon yield in the char residue is shown in Figure 5.30. The curve of carbon yield in the char residue at 500°C has been shifted up and located between the curves of 400°C and 600°C. The char residue yield at 500°C was also adjusted and shown in the Figure 5.31. The curve of the char residue yield at 500°C is shifted up and located between the curve of 400°C and 600°C. Figure 5.32, Figure 5.33, and Figure 5.34 compares the carbon yield in the char residue, in the fine particles, and in the gas phase at 600°, adjusted-data of 500°C, and 400°C respectively.

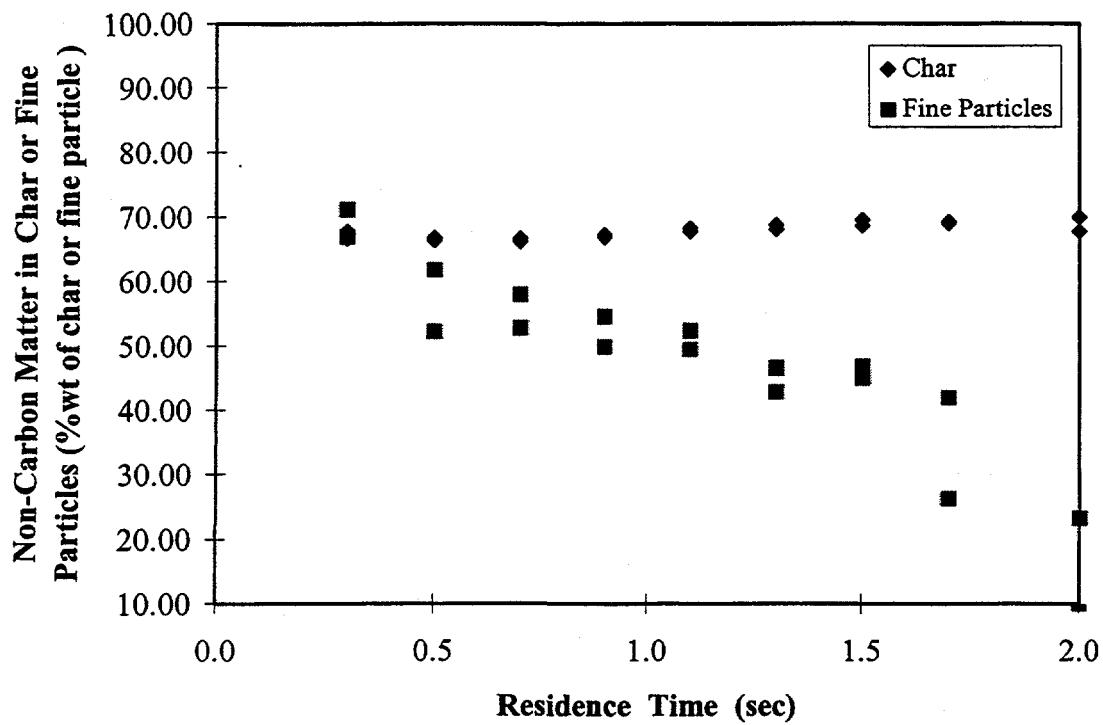


Figure 5.27 Non-Carbon Matter in Char or Fine Particles at 600°C

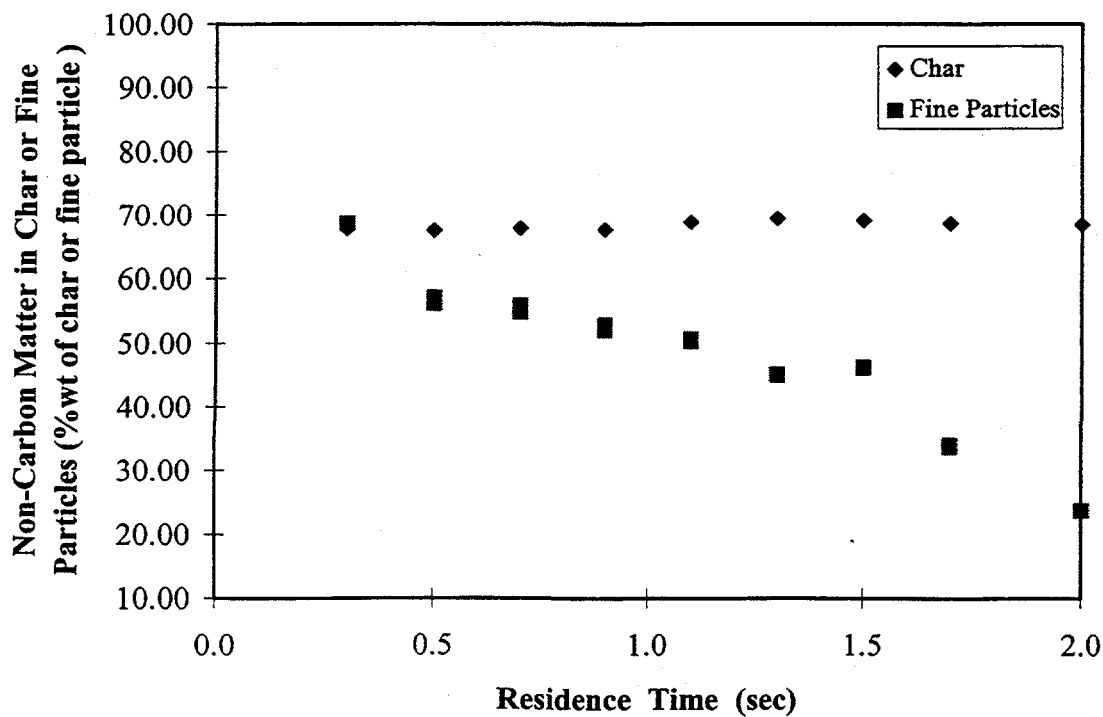


Figure 5.28 Non-Carbon Matter in Char or Fine Particles at 500°C

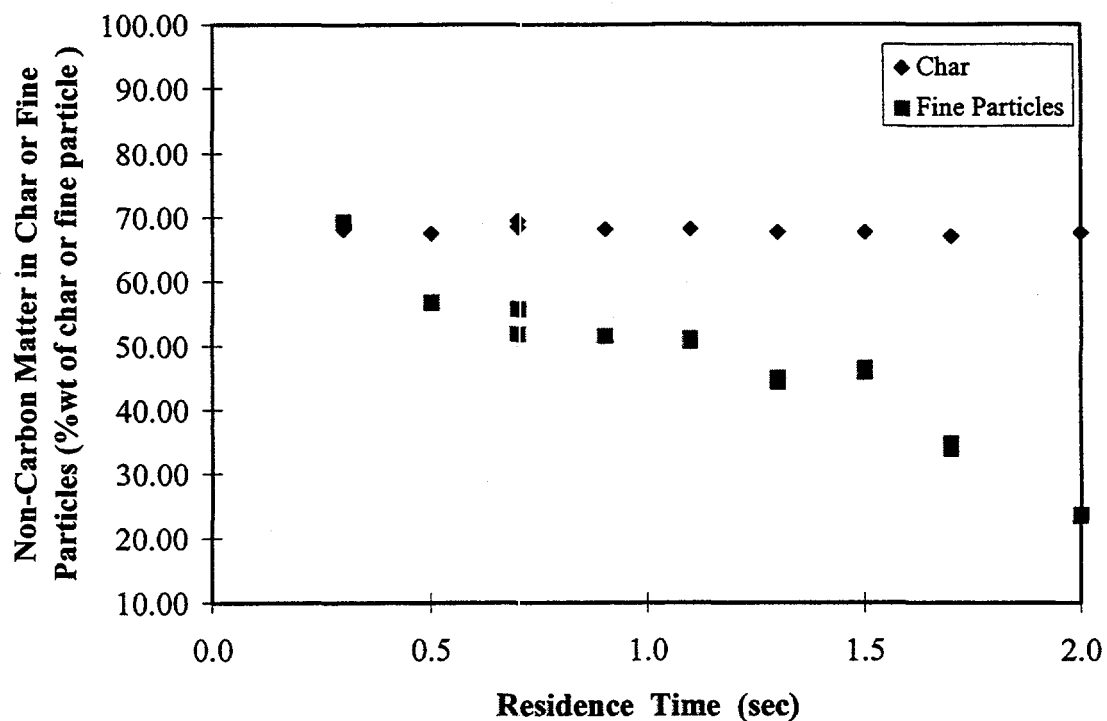


Figure 5.29 Non-Carbon Matter in Char or Fine Particles at 400°C

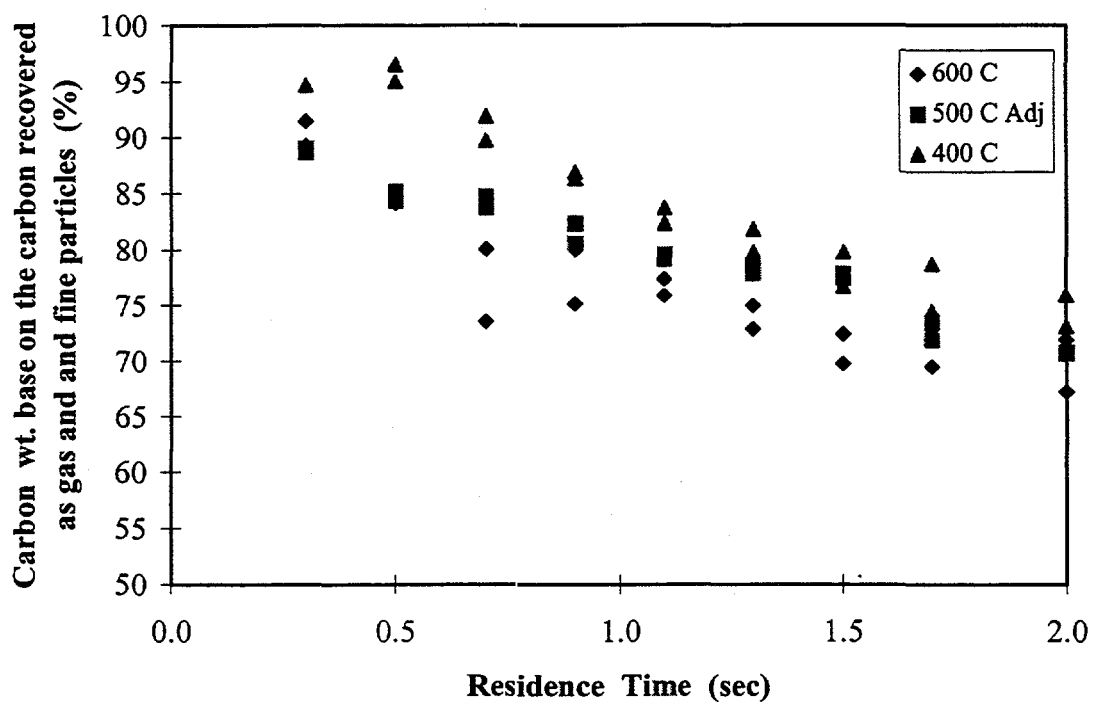


Figure 5.30 Carbon Yield in the Char Residue: Base on the Carbon Recovered as gas and as fine Particles

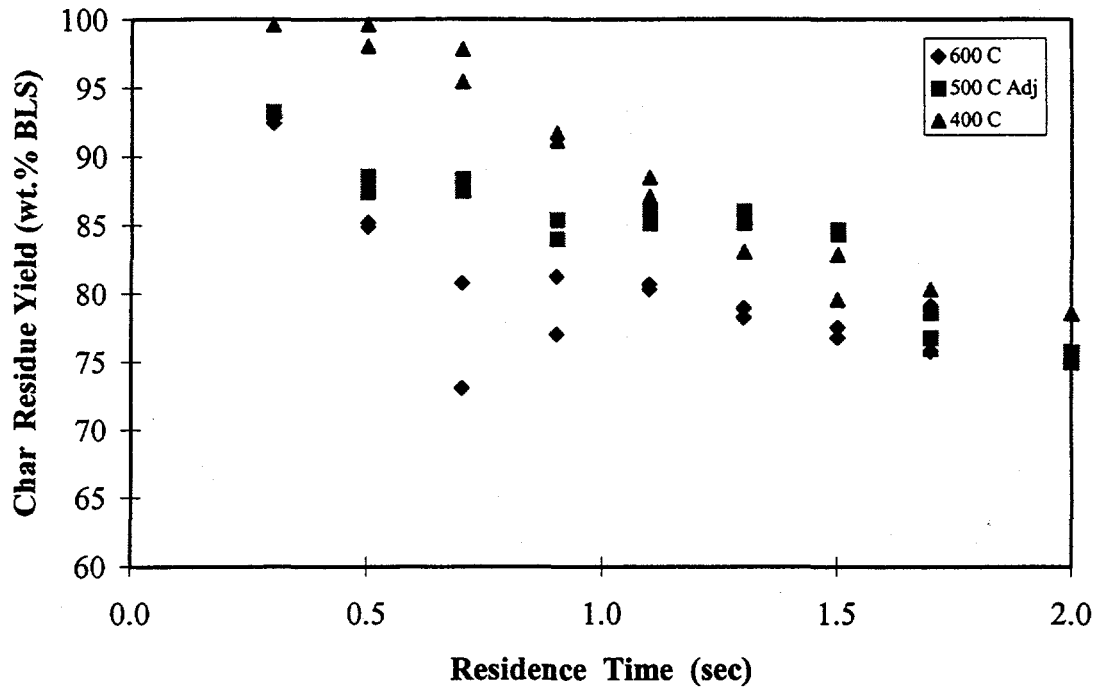


Figure 5.31 Adjusted Char Residue Yield from Pyrolysis of Black Liquor Solids

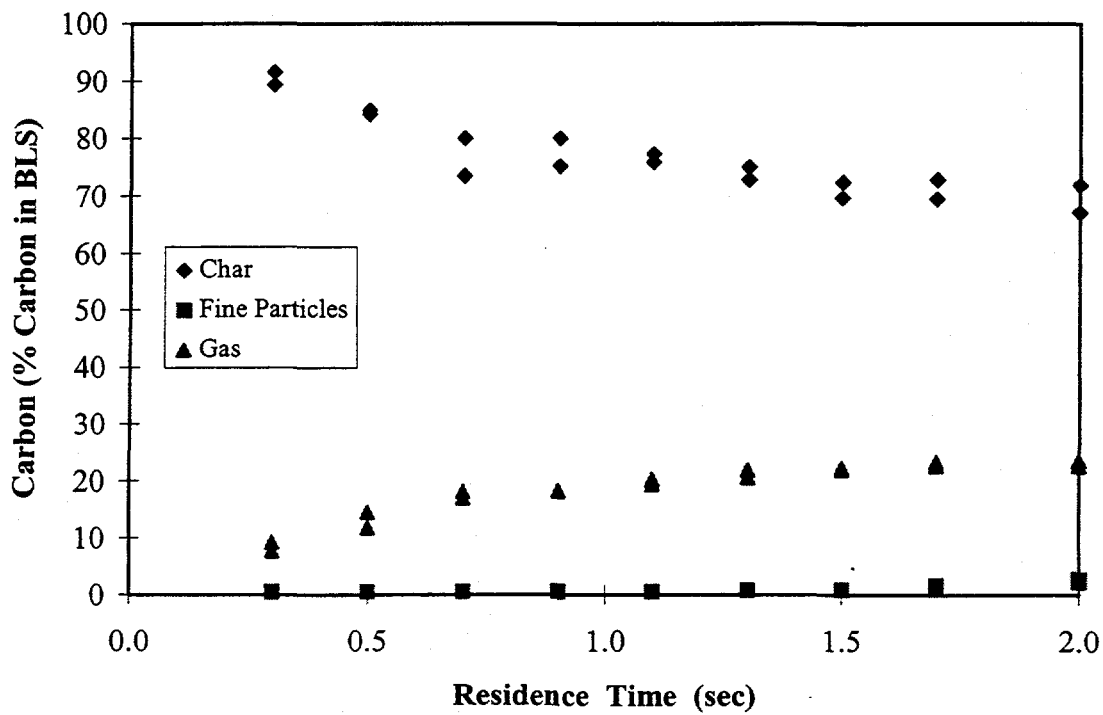


Figure 5.32 Carbon Yield in the Char Residue, Fine Particles, and Gas at 600°C

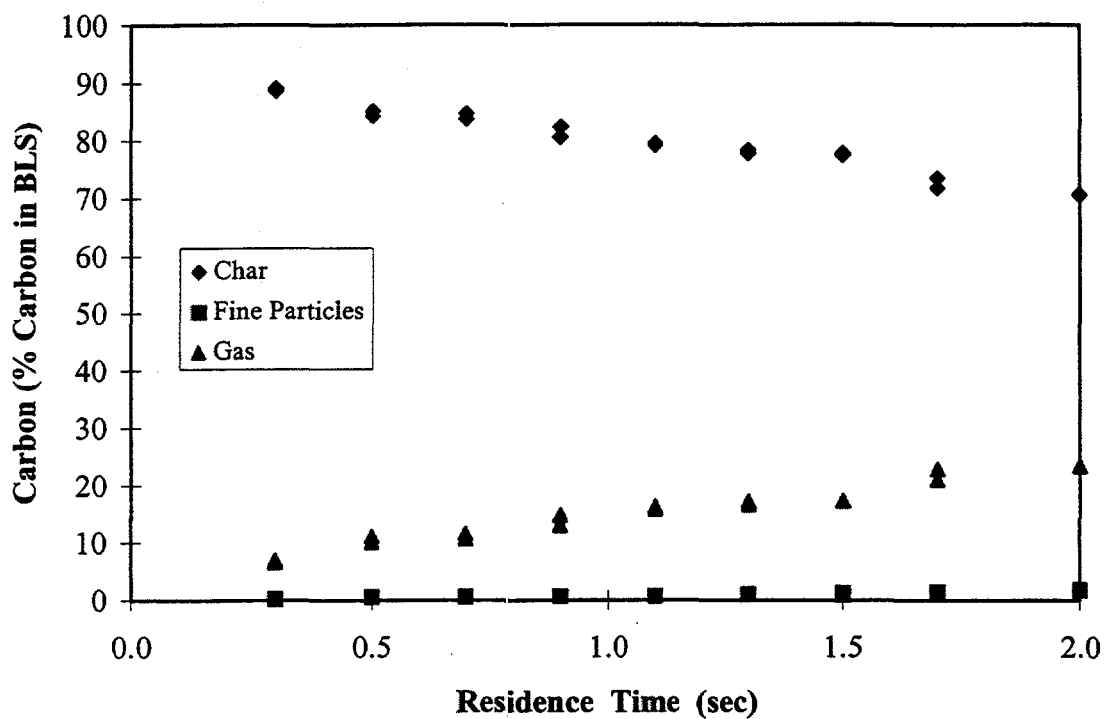


Figure 5.33 Carbon Yield in the Char Residue, Fine Particle, and Gas at 500°C

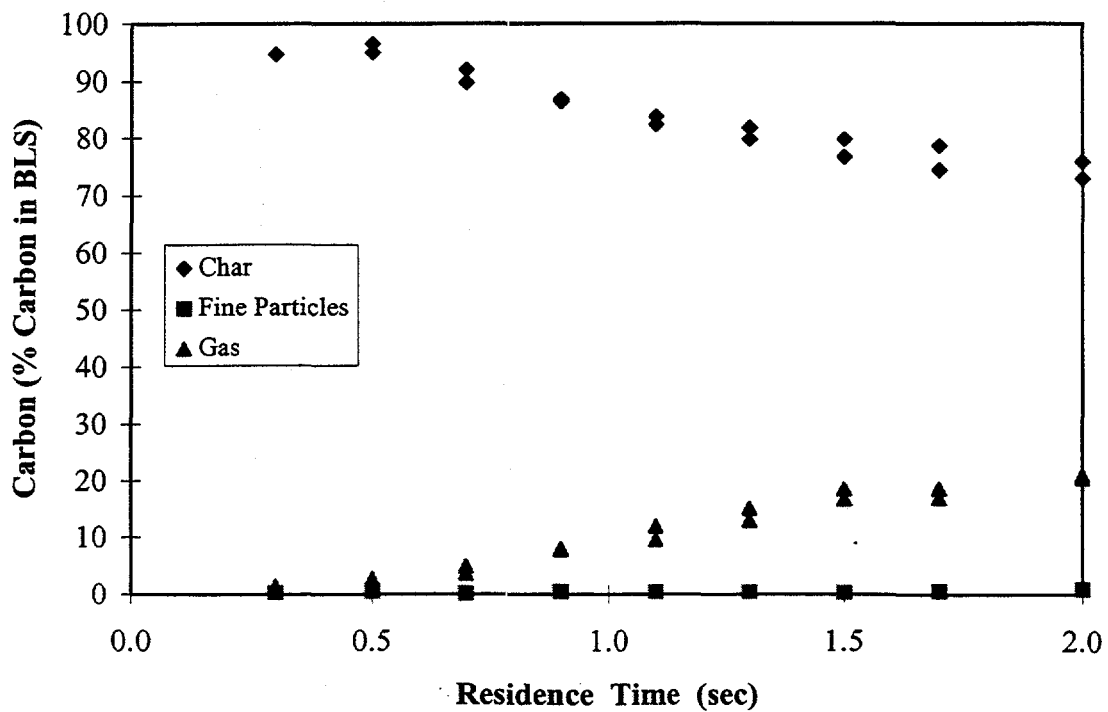


Figure 5.34 Carbon Yield in the Char Residue, Fine Particles, and gas at 400°C

Sulfur Yield in Char Residue from Pyrolysis of Black Liquor Solids

Figure 5.35, Figure 5.36, and Figure 5.37 show sulfur yields in the char residue versus residence time from pyrolysis of black liquor solids at 600°C, 500°C, and 400°C respectively. *The sulfur yield in the char residue decreased as residence time increased.* The reproducibility obtained in replicate runs was an average $\pm 2.8\%$ at 600°C, $\pm 1.5\%$ at 500°C, and $\pm 1.9\%$ at 400°C, all based on the sulfur in the black liquor input. At 600°C and a residence time of 0.3 seconds, the sulfur yield was 88%. It decreased rapidly until a residence time of 1.1 seconds, and then gradually decreased to 38% at a residence time of 2.0 seconds.

At 500°C and a residence time of 0.3 seconds, the sulfur yield was 90% and decreased with decreasing rate to 41% at a residence time of 2.0 seconds. At 400°C and a residence time of 0.3 seconds, the sulfur yield was 97% and gradually decreased to 56% at a residence time of 2.0 seconds.

Figure 5.38 compares the sulfur yield in the char residue versus residence time from pyrolysis of black liquor solids at temperature of 600°C, 500°C, and 400°C. *The higher the temperature, the lower the fraction of sulfur input that was recovered in the char residue.* The sulfur content of the char residue at residence time 2.0 seconds was 56% at 400°C, 41% at 500°C, and 38% at 600°C. This is in accordance with the finding of Forssen et al. (1992) stated that the sulfur retained in the char residue after pyrolysis of black liquor went through a minimum with increasing furnace temperature at 600-700°C. Forssen et al. studied pyrolysis of single droplet, 2-3 mm in diameter. The regression curve of Forssen et al.'s data showed that the sulfur content of the char residue at residence time after 1.5 seconds was 54% at 400°C, 40% at 500°C, and 35% at 600°C. Also the data of, Gairns et al. (1994)'s study agree very well with the Forssen et al. curve. These results are in very good agreement with our experimental data. The data reported by Forssen et al. were for 9 different kraft black liquors. Their results indicate that there is relatively little difference in sulfur release during pyrolysis in their temperature range either between different kraft liquor or between different experimental methods.

Figure 5.39 compares the sulfur yield in the char residue from pyrolysis of black liquor solids at 400°C, 500°C, and 600°C, using the adjusted char yields at 500°C. The curve of sulfur yield at 500°C is shifted up and located between the curve of 400°C and 600°C.

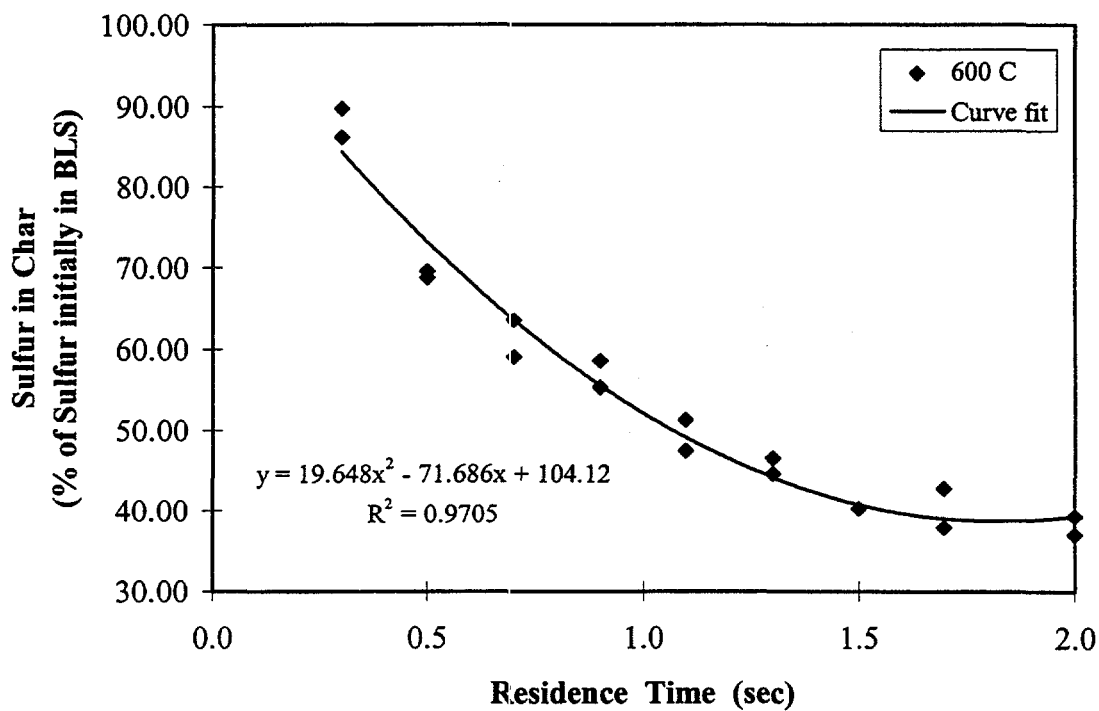


Figure 5.35 Sulfur Yield in the Char Residue from Pyrolysis of Black Liquor Solids at 600°C

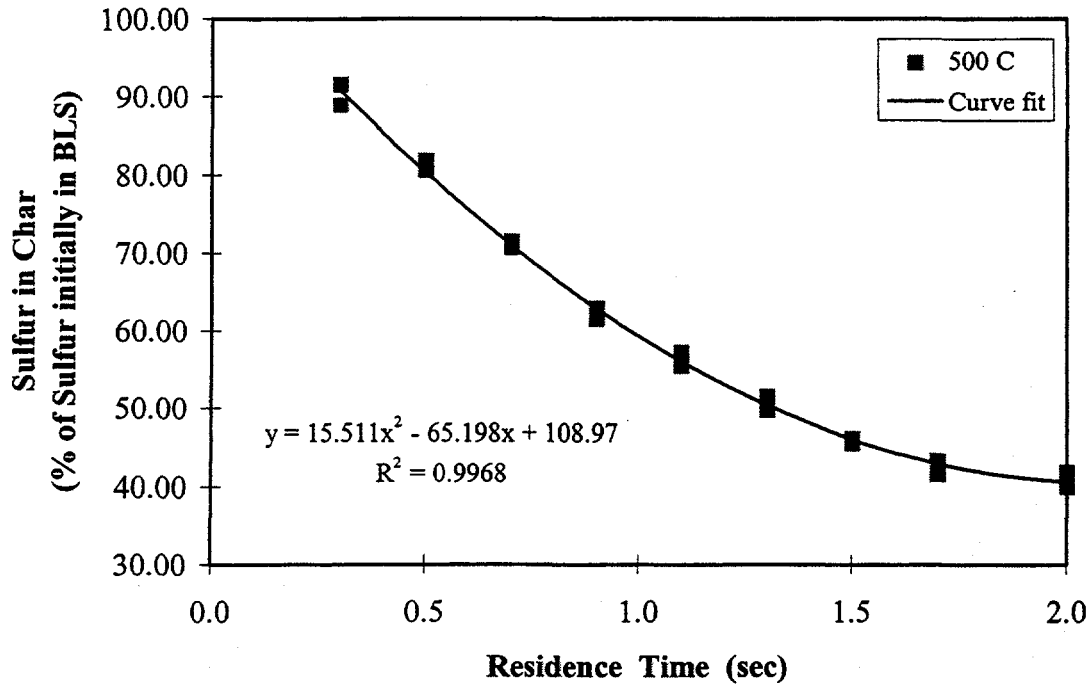


Figure 5.36 Sulfur Yield in the Char Residue from Pyrolysis of Black Liquor Solids at 500°C

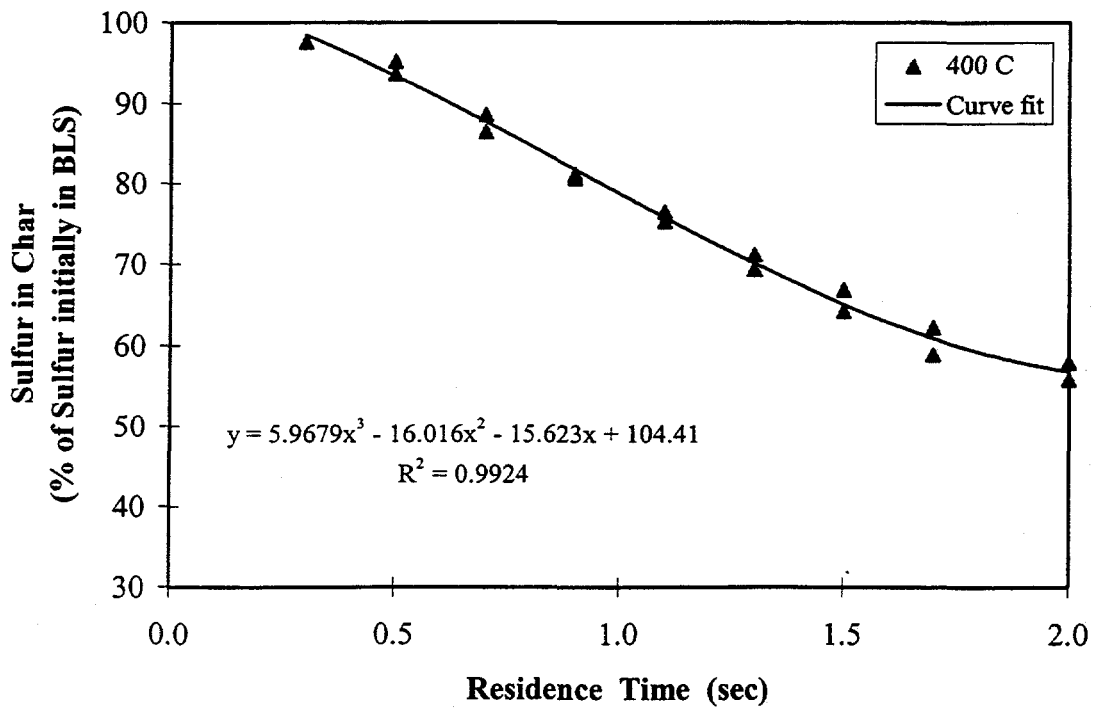


Figure 5.37 Sulfur Yield in the Char Residue from Pyrolysis of Black Liquor Solids at 400°C

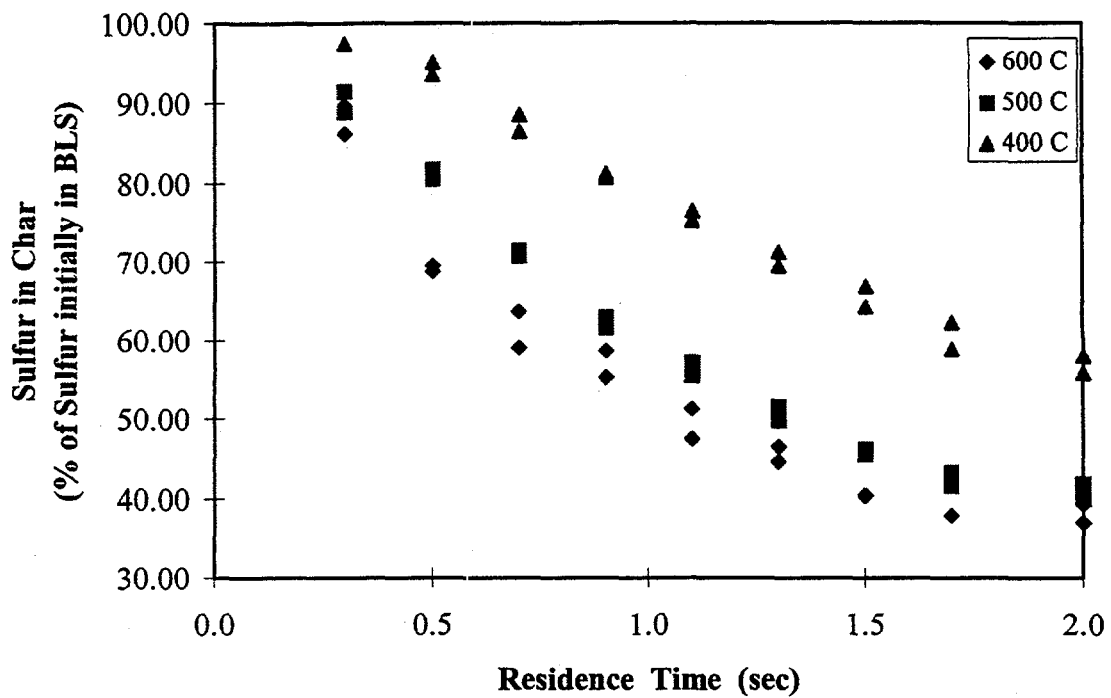


Figure 5.38 Sulfur Yield in the Char Residue from Pyrolysis of Black Liquor Solids at 400-600°C

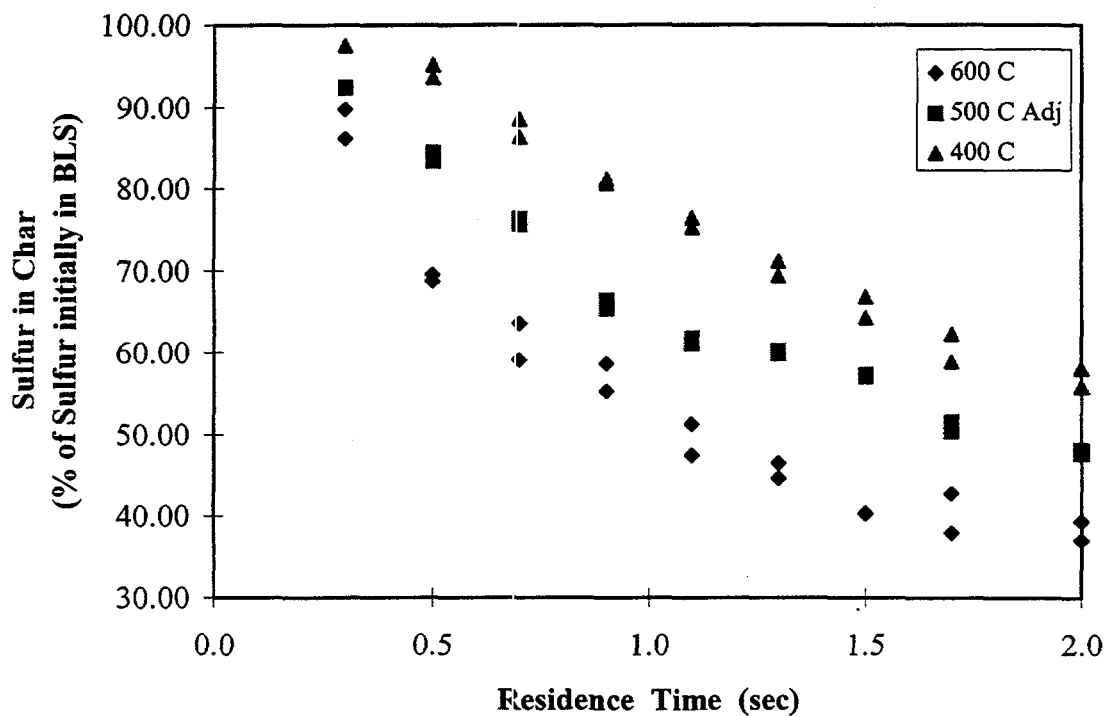


Figure 5.39 Adjusted Sulfur Yield in the Char Residue

Nitrogen Yield in Char Residue from Pyrolysis of Black Liquor Solids

Figure 5.40, Figure 5.41, and Figure 5.42 show the nitrogen yield in the char residue versus residence time from pyrolysis of black liquor solids at 600°C, 500°C, and 400°C respectively. *The nitrogen yield in the char residue decreased as residence time increased.* The reproducibility obtained in replicate runs was an average $\pm 1.0\%$ at 600°C, and $\pm 2.0\%$ at 500°C and 400°C, all as percentage of nitrogen in the black liquor solids input. At a residence time of 0.3 seconds, the nitrogen yield in the char residue was 86% at 600°C, 91% at 500°C, and 98% at 400°C. For all temperatures range, the nitrogen yield in the char residue decreased rapidly at the beginning and then gradually decreased until the longest residence time (2.0 seconds). At a residence time of 2.0 seconds, the nitrogen in the char residue was 59% at 600°C, 60% at 500°C, and 66% at 400°C. This is in accordance with the finding of Carangal (1995), who measured the nitrogen retained in the char residue after devolatilization at furnace temperatures between 700-1100°C and residence times between 0.3-2.2 seconds using the LEFR. Carangal reported that the nitrogen content in the char residue decreased rapidly at the beginning (residence time 0.3 seconds) and then decreased gradually at residence times longer than 0.5 seconds. The percentage of nitrogen retained in the char residue after devolatilization was 56% at 700°C, 49.6% at 900°C, and 45.7% at 1100°C.

Figure 5.43 compares the nitrogen in the char residue versus residence time from pyrolysis of black liquor solids at temperature of 600°C, 500°C, and 400°C. The data at 500°C is based on the uncorrected char yields. The nitrogen yield in the char residue at 600°C and 500°C data are about the same and lower than 400°C. At residence times longer than 0.5 seconds, the nitrogen content in the char residue was nearly the same at 600°C and 500°C, and essentially the same in some experimental condition. And also, this is in accordance with the finding of Frederick et al.(1995). With the lower temperature condition in this study (400-600°C) compared to those of Frederick et al. study (700-1100°C), the nitrogen contents in char residue after devolatilization in this study (59-66%) were higher than those of Frederick study (45.7-56.7%).

Figure 5.44 compares the nitrogen yield in the char residue from pyrolysis of black liquor solids at 400°C, 500°C, and 600°C using the adjusted char yields at 500°C. The curve of nitrogen yield at 500°C is shifted up and located between the curve of 400°C and 600°C at residence times of 0.3-0.8 seconds, but at residence times above 0.8 seconds the adjusted-curve higher than that at 400°C. It is not clear why the nitrogen data at 500°C is inconsistent with the sulfur and carbon data.

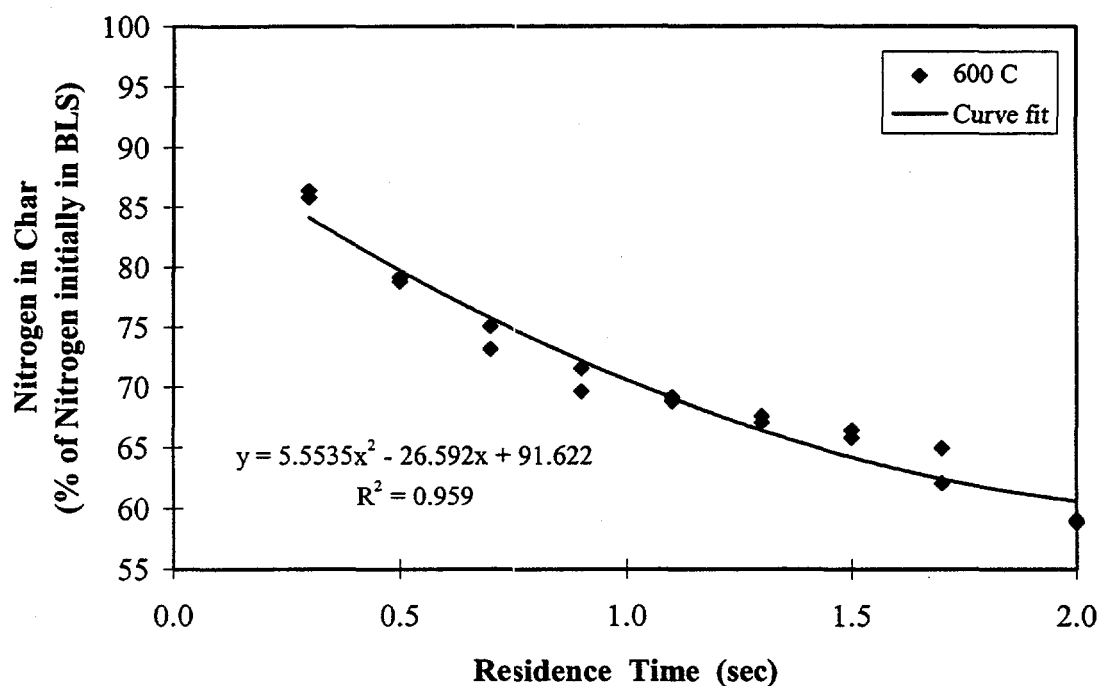


Figure 5.40 Nitrogen Yield in Char Residue from Pyrolysis of Black Liquor Solids at 600°C

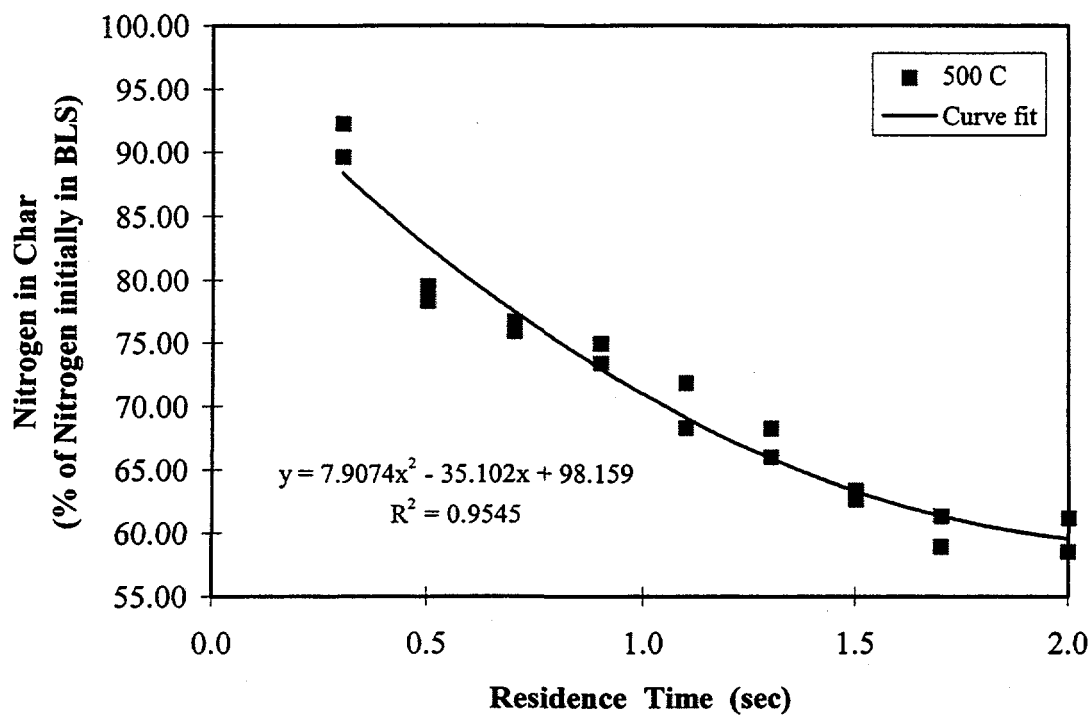


Figure 5.41 Nitrogen Yield in Char Residue from Pyrolysis of Black Liquor Solids at 500°C

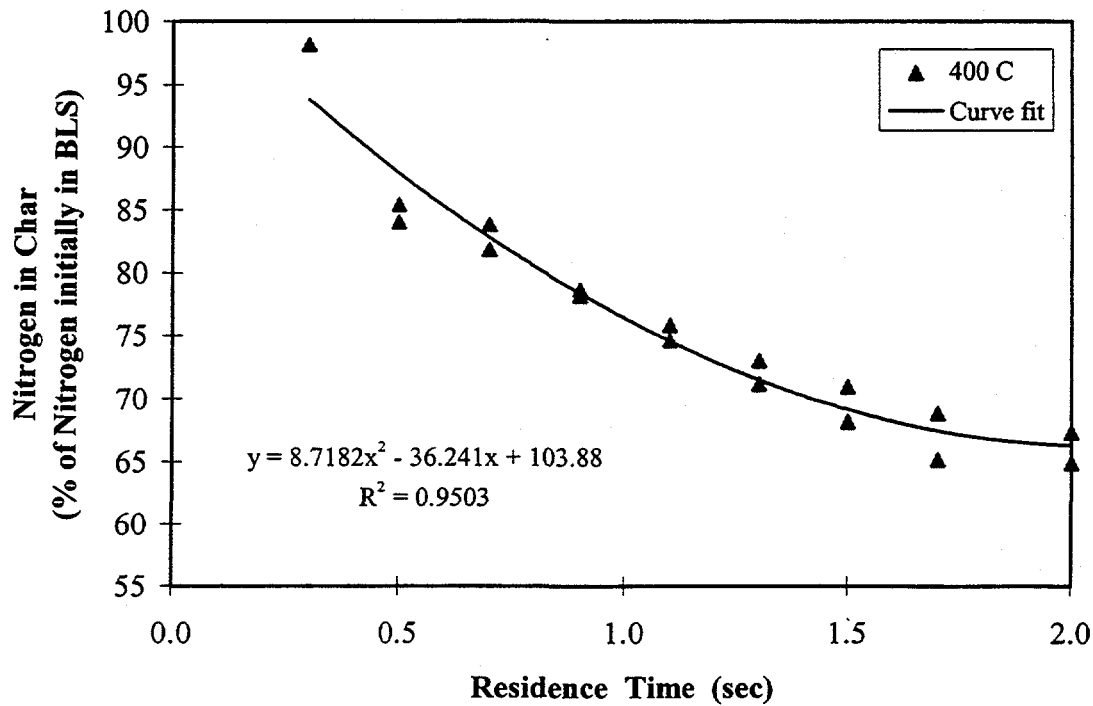


Figure 5.42 Nitrogen Yield in Char Residue from Pyrolysis of Black Liquor Solids at 400°C

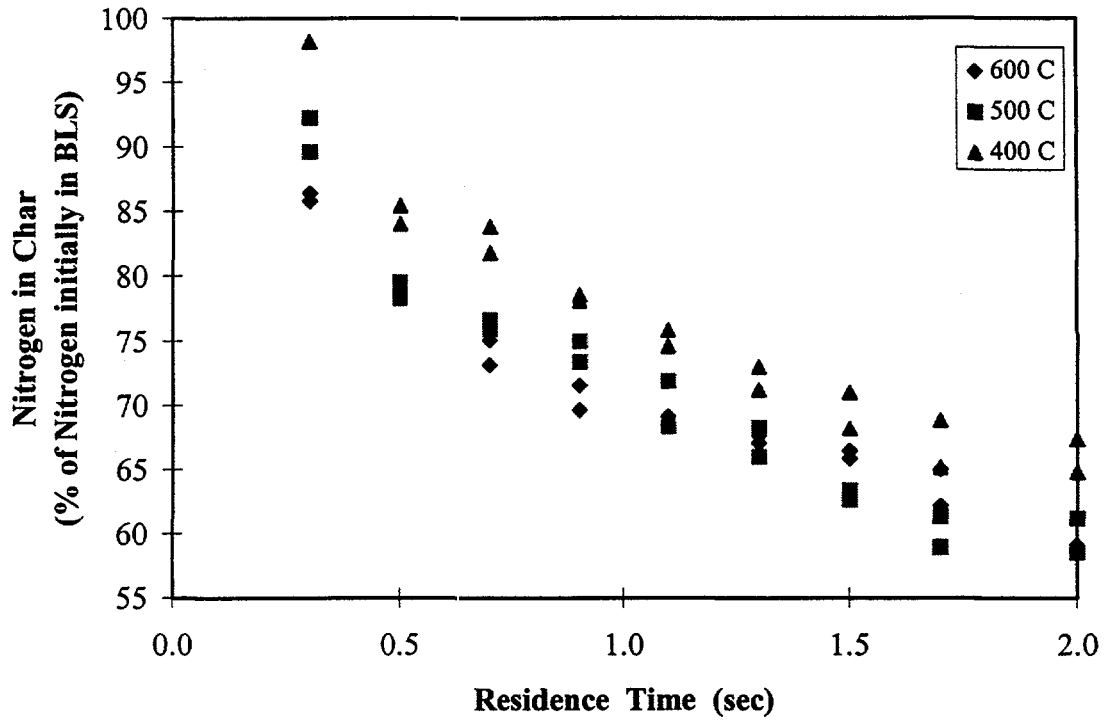


Figure 5.43 Nitrogen Yield in Char Residue from Pyrolysis of Black Liquor Solids at 400-600°C

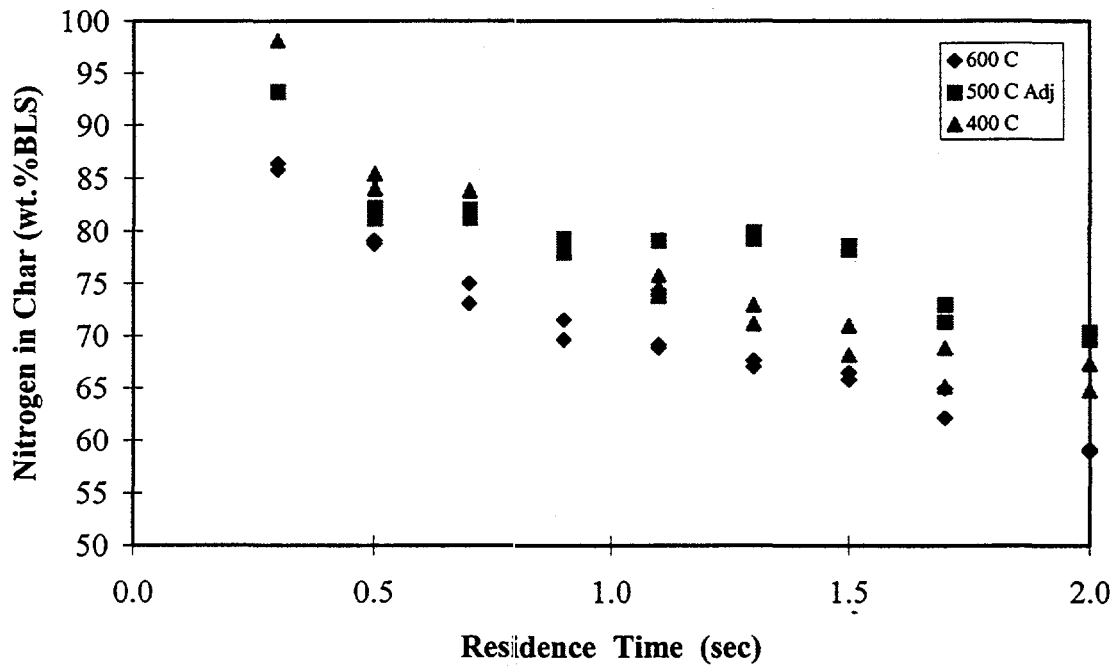


Figure 5.44 Adjusted Nitrogen Yield in the Char Residue

Kinetic Model of Conversion of Carbon to Gases During Devolatilization

Rate constants for a Kobayashi-type model for devolatilization of kraft black liquor were extracted from the data obtained by Sricharoenchaikul (1995) and the data reported here. The data base included 24 data points for temperatures 400-600°C, and one data point each at 700, 900, 1000, and 1100°C.

The form of the model is as described by Bartok and Sarofim (1991). It treats the conversion of organic matter (M) to either fixed carbon (C_f) or gases (V) by parallel paths with different activation energies.

$$M \Rightarrow (1 - \alpha_1)C_{f,1} + \alpha_1V_1 \quad (1)$$

$$M \Rightarrow (1 - \alpha_2)C_{f,2} + \alpha_2V_2 \quad (2)$$

In equations 1 and 2, α_1 and α_2 are the fractions of M reacting by each path that go to V_1 and V_2 , respectively. The rate equations are

$$\frac{dM}{dt} = -(k_1 + k_2)M \quad (3)$$

$$\frac{dV}{dt} = \frac{dV_1 + dV_2}{dt} = (\alpha_1k_1 + \alpha_2k_2)M \quad (4)$$

$$\frac{dC_f}{dt} = \frac{dC_{f,1} + dC_{f,2}}{dt} = [(1 - \alpha_1)k_1 + (1 - \alpha_2)k_2]M \quad (5)$$

The model assumes that part of the organic matter originally present remains unconverted, and the amount of this unconverted organic matter decreases with time as fixed carbon and gases are formed. While this does not describe devolatilization mechanistically, it does provide an engineering model that gives a fixed carbon yield that is particle temperature history dependent.

The model parameters presented here are for only the "non-carbonate" carbon. The non-carbonate carbon is defined as that carbon remaining after the carbon requirement for Na_2CO_3 in the smelt produced as a result of complete combustion of the black liquor has been subtracted from the total carbon initially in the black liquor.

The main limitations of the constants obtained for black liquor is that

1. there were is that there were only single data points available at each temperature from 700 - 1100°C,
2. these data points were obtained at 0.3 secnds, well beyond the end of devolatilization for the 100 micron particles at 900°C and above, and probably 700°C as well, and
3. the times at the end of devolatilization were therefore estimated based on heating rate data and a criterion based on the temperature at which devolatilization was complete for 2 mm droplets (see Figure 2-5, p. 284, DOE Black Liquor Combustion Validated Recovery Boiler Modeling Five-Year Report, DOE/CE/50936-T3).

The temperature versus time profiles for the particles in 700-1100°C environments were obtained by approximating the time-temperature data of Verrill and Wessel (1995 ICRC, p. B96, Figure 13) for 100 micron particles as straight lines to obtain temperature rise rates. For the data at 400-600oC, I used only those points at times at which the particle temperature had reached the furnace temperature. The carbon conversions and estimated times at the end of devolatilization for 700-1100°C used in obtaining

the Kobayashi model parameters for conversion of organic carbon to fixed carbon and carbon in gases are given in Table 1.

Table 1. Carbon conversions and estimated time to end of devolatilization for the LEFR data at 700°C and above.

LEFR Temperature °C	Estimated time to end of devolatilization, s	Conversion of organic carbon to fixed carbon, %
700	0.30	68
900	0.15	58
1000	0.10	45
1100	0.05	43

The model parameters obtained are included in Table 2. All except α_2 were obtained by a regression fit of the model to the data. α_2 was assumed to be 1 minus the mass fraction of carbon remaining at 1100°C the highest experimental temperature. This assumption is based on the fact that the fixed carbon yield at the end of devolatilization appears to level off at about 0.43 at temperatures above 1000°C (see Fig. 2-9, p. 289, DOE Black Liquor Combustion Validated Recovery Boiler Modeling Five-Year Report, DOE/CE/50936-T3, subtract 4.5% carbon for carbonate, and normalize to 100% to get the “non-carbonate” carbon on a 100% basis).

Table 2. Model parameters obtained by fitting the Kobayashi model to LEFR carbon yield data from LEFR runs with a kraft black liquor at 400-1100°C.

$A_1 =$	3.03 s ⁻¹
$E_{a1}/R =$	0
$\alpha_1 =$	0.172
$A_2 =$	1.23x10 ⁵ s ⁻¹
$E_{a2}/R =$	10,561 K
$\alpha_2 =$	0.570

Remaining Work

Data is needed at 700-1100°C if we are to obtain a truly reliable model in the temperature range of interest in recovery boilers. This will require experimental data for much shorter residence times, with a resolution of 0.02 seconds or less.

CONCLUSIONS

Char Residue Yields from Pyrolysis of Black Liquor Solids

The char residue yield decreased as residence time increased. However, the char residue yields at the end of devolatilization decreased only slightly (from 77% to 75%) over the temperature range from 400-600°C. The measured char yields at 500°C were lower than expected based on the 400°C and 600°C data and previous data. This is due to collection of large, highly swollen char particles at the tip of the collector at this temperature. A correction was made to the data, based on a carbon balance closure, to estimate char yields at 500°C.

Fine Particle Yields from Pyrolysis of Black Liquor Solids

The fine particle yield was very low, no greater than 1% of BLS at all conditions investigated, and increased as residence time increased. At 500°C and 600°C, the yields of fine particles were constant until 1 second, at about 0.5% of black liquor solids input. At longer particle residence times, the yields of fine particles increased to 0.8% and 1.0% at these two temperatures. At 400°C, the yield of fine particles was essentially constant, at 0.4% of black liquor solids input, over the entire range of residence times. If these fine particle yields are the result of physical ejection or shedding of char fragments, then these processes are not very important, at least for 100 micron particles.

Conversion of Carbon to Gases, Fine Particles, and Char

The carbon in the gas phase, as percentage of carbon input, increased as residence time increased. The yield carbon as gaseous products increased with residence time during the experiments, leveling off by approximately 2 seconds residence time. The amount of carbon converted to gases by the end of devolatilization increased only slightly with temperature, from 20% at 400°C to 23% at 600°C. These results show that conversion of the carbon in black liquor to gases is not strongly temperature dependent in this temperature range.

The carbon yield in the fine particles differed very little with temperature at residence times below 1.1 seconds. At longer residence times, the fixed carbon in the fine particles increased with increasing reactor temperature, from 1% of carbon input at 400°C to 2.5% at 600°C. These data are for 2.0 seconds particle residence times.

The carbon yield in the char residue decreased as residence time increased. The carbon yield in the char residue decreased slightly with increasing temperature, from 75% at 400°C to 70% at 600°C. . These data are for 2.0 seconds particle residence times. These results support the earlier conclusion that conversion of the carbon in black liquor to gases is not strongly temperature dependent in this temperature range.

Total Carbon Recovered from Pyrolysis of Black Liquor Solids

The average of carbon recovered as char, fine particles, and gas combined are as follows: 96.2% at 600°C, 88.1% at 500°C (corrected to 96%), and 95.7% at 400°C.

Sulfur Yield in the Char Residue from Pyrolysis of Black Liquor Solids

The sulfur retained in the char residue, as a percentage of sulfur input as black liquor solids, decreased as residence time increased at all three temperatures. At 600°C, the sulfur retained in the char residue had leveled off to a constant value (38%) by a particle residence time of 2 seconds. At the lower temperatures, however, it was 56% at 400°C and 42% at 500°C, and was still decreasing with increasing particle residence time after 2 seconds.

Nitrogen Yield in the Char Residue from Pyrolysis of Black Liquor Solids

The nitrogen in the char residue, as a percentage of nitrogen input as black liquor solids, decreased as residence time increased. At 400°C, 66% of the nitrogen input remained in the char after a residence time of two seconds. At 600°C, the value at 2 seconds was 59%.

REFERENCES

- Aho, K., Vakkilainen, E., Hupa, M., 1994a, Fuel nitrogen release during black liquor pyrolysis. Part 1: Laboratory measurements at different conditions. *Tappi J.*, 77(5):107-111.
- Aho, K., Nikkanen, S., Hupa, M., 1994b, Fuel nitrogen release during black liquor pyrolysis. Part 2: Comparisons between different liquors. *Tappi J.*, 77(8):182-188.
- Anthony, D.B., Howard, J.B., Hottel, H.C., and Meissner, H.P., *Proc. Fifteenth Shmp. On Combustion*, p. 1303, Combustion Institute, Pittsburgh (1975).
- Bartok, W., Sarofim, A.F., *Fossil Fuel Combustion*, John Wiley & Sons, New York (1991).
- Bhattacharya, P., Vidyasekara, P., Kunzru, D., "Pyrolysis of Black Liquor Solids", *Ind. Eng. Chem. Proc. Des. Dev.* 25:420-6 (1986).
- Brink, D.L., Thomas, J.F., Jones, K.J., *Tappi J.*, 53(5):837-843 (1970).
- Cameron, J.H. and Grace, T.M., *I&EC Fundamentals*, 1985, 24(4): 443.
- Cantrell, J.G., Clay, D.T., and Hsieh, J.S., "Sulfur release and retention during combustion of kraft black liquor", in *chemical Engineering Technology in Forest Products Processing*, B. Crowell, editor. AIChE For. Prod. Div., Vol. 2 (1986), p. 31-40.
- Carangal, A.B., "The release of NO During Black Liquor Pyrolysis", MS Thesis., Department of Chemical Engineering, Oregon State University, September 6, 1994.
- Clay, D.T., Grace, T.M., Kapheim, R.J., Semerjian, H.G., Macek, A., Charagundla, S.R., "Fundamental study of black liquor combustion. Report No. 1-Phase 1", US DOE report DOE/CE/40637-T1 (DE85013773), Jan 1985.

- Clay, D.T., Grace, T.M., Kapheim, R.J., Semerjian, H.G., Macek, A., Charagundla, S.R., "Fundamental study of black liquor combustion", Report No. 1-Phase 1, "US DOE DEACO2-83CE40637, Jan. 1987.
- Feuerstein, D.L., J.F. Thomas, and D.L. Brink, *Tappi*, Vol. 50 (1967), No. 6: 258-262.
- Flaxman, R.J., and Hallett, L.H. (1987) "Flow and Particle Heating in an Entrained Flow Reactor", *Fuel* 66:607.
- Forsen, M., Frederick, W.J., and Hupa, M., "Sulfur Release During Pyrolysis of Single Black Liquor Droplets", prepared for presentation at the AIChE Annual Meeting, November 17-22, 1991.
- Forsen, M., Frederick, W.J., Hupa, M., and Hyoty, P., "Sulfur release during pyrolysis from single black liquor droplets", AIChE 1991 Forest Products Symposium Proceedings, TAPPI Press, Atlanta, p. 11-22 (1992).
- Forsen, M., Hupa, M., Hellstrom, P., 1995, Liquor-to-liquor differences in combustion and gasification : Nitrogen oxide formation tendency. Proc. 1995 TAPPI Engineering Conf., TAPPI Press, Atlanta, p. 825-832.
- Frederick, W.J., Adams, T.N., "Kraft Recovery Boiler Physical and Chemical Processes", American Paper Institute, New York, 1988.
- Frederick, W.J., and Hupa, M., Combustion Properties of Kraft Black Liquors, US DOE Report DOE/CE/40936-T1 (DE94007502), April 1993.
- Frederick, W.J., Combustion processes in black liquor recovery: analysis and interpretation of combustion rate data and an engineering design model. US DOE Report DOE/CE/40637-T8(DE90012712), March, 1990.
- Frederick, W.J., Hupa, M., Uusikartano, T., Volatiles And Char Carbon Yields During Black Liquor Pyrolysis. *Bioresource Technology* 48 (1994) 59-64.
- Frederick, W.J., Sricharoenchaikul, V., Wag, K.J., Carangal, A.C., Pianpucktr, R., Iisa, K., "Char Residue Yields and Chemical Species Distributions from Rapid Pyrolysis of Kraft Black Liquor", Paper 253g, AIChE Annual Meeting, Miami Beach, Noverber 12-17, 1995.
- Gairns, S.A., Kubes, G.J., van Heiningen, A.R.P. "New insights in to TRS gas formation during pyrolysis of black liquor", Paper 104d, Spring 1994 AIChE National Meeting, Atlanta, April 17-21.
- Goheen, D.W., Orle, J.V., Wither, R.P. in "Thermal Uses and Properties of Carbohydrates and Lignins", Shafizadeh, F., Ed., Academic Press: New York, 1976, p.227-244.
- Hajallgol, M.R., Howard, J.B., Longwell, J.P., Peters, W.A., 1982, *Ind. Eng. Chem. Process Des. Dev.*, v. 21, p. 457-465.
- Harper, F.D., "Sulfur release during the pyrolysis of kraft black liquor", Ph.D. Thesis, The Institute of Paper Chemistry, June, 1989.
- Hupa, M., Backman, R., Hyoty, P., "Investigation of fireside deposition and corrosion in sulphate and sodium bases sulphite recovery boilers", *Proc. Black Liquor Recovery Boiler Symposium 1982*, Finnish Recovery Boiler Committee, Helsinki (August 31-September1, 1982), p. D1-1D1-11.
- Hupa, M., Solin, P., Hyoty, P., "Combustion Behavior of Black Liquor Droplets", *JPPS*, 13(2):J67-72(1987).
- Hurt, R.H., Mitchell, R.E., On the combustion kinetics of heterogeneous char particle populations, Twenty-fourth Symp. (Intl.) on Combustion/The Combustion Institute, 1992, pp. 1233-1241.
- Kobayashi, H., Howard, J.B., Sarofim, A.F., *16th Symp. (Intl.) on Combustion*, The Combustion Institute, Pittsburgh, PA (1977), p. 411-425.

- Kubes, G.J. and Fleming, B.I., MacLeod, J.M., and Bolker, H. I., *J. Wood Chem. Techn.* 2(3):279(1982).
- Kubes, G.J., *J. Pulp Pap. Sci.* 10(3):J63(1984).
- Li, J., "Rate processes during gasification and reduction of black liquor char", Ph.D. Thesis, McGill University, October, 1989.
- Li, J., van Heiningen, A.R.P., "Sulfur emission during slow pyrolysis of kraft black liquor", *Tappi Jl.*, 74(3):237-239 (1991).
- Li, J., van Heiningen, A.R.P., *Ind. Eng. Chem. Res.*, 1990, 29(9), 1776-85.
- Miller, P.T., Ph.D. Thesis, The Institute of Paper Chemistry, Appleton, 1986.
- Niksa, S., Heyd, L.E., Russel, W.B., and Saville, D.A., 20th *Symp. (Intl.) on Combustion*, The Combustion Institute (1984), p. 1445-1453.
- Phimolmas, V., "The Effect of Temperature and Residence Time on the Distribution of Carbon, Sulfur, and Nitrogen Between Gaseous and Condensed Phase Products from Low Temperature Pyrolysis of Kraft Black Liquor," M.S. Thesis, Oregon State University (1997).
- Pianpucktr, R., "Formation of NO During Pyrolysis and Combustion of Kraft Black Liquor", MS Thesis., Department of Chemical Engineering, Oregon State University, September 21, 1995.
- Quann R.J., Neville, M., Janghorbani, M., Mims, C.A., Sarofim, A.F., "Mineral matter and trace-element vaporization in a laboratory-pulverized coal combustion system", *Environ. Sci. Technol.* 1982, 16, 776-781.
- Reis, V. V., Frederick, W. J., Wåg, K. J., Iisa, K., and Sinquefield, S. A., "The Effects of Temperature and Oxygen Concentration on Potassium and Chloride Enrichment During Black Liquor Combustion," *Tappi Jl.*, 78(12):67-76 (1995).
- Scott, D.S., Piskorz, J., 1984, *Can. J. Chem Eng.*, v. 62, p. 404-412.
- Scott, D.S., Piskorz, J., Radlein, D., "Liquid Products from the Continuous Pyrolysis of Biomass," *In. Eng. Chem. Process Des. Dev.*, 24,581-588 (1985).
- Scott, D.S., Piskorz, J., Bergougnou, M.A., Graham, R., Overend, R.P., 1988, *Ind. Eng. Chem. Res.*, v.27, p. 8-15.
- Söderhjelm, L., Hupa, M., and Noopila, T., *J. Pulp and Paper Science* 15(4):J117-J122(1989).
- Solomon, P.R., Colket, M.B., Coal Devolatilization. 17th *Symp. (Intl.) on Combustion*, The Combustion Institute, (1979), p. 131-143.
- Sprouse, K.M., Schuman, M.D., "Prediction lignite devolatilization with the multiple parallel and two-competing reaction models. *Combust. Flame* 43, 265 (1981).
- Sricharoenchaikul, V., "Sulfur Species Transformations and Sulfate Reduction during Pyrolysis of Kraft Black Liquor", MS Thesis., Department of Chemical Engineering, Oregon State University, February 24, 1995.
- Sricharoenchaikul, V., Frederick, W.J., Kumalainen, M., Grace, T.M., "Sulfur Species Transformations and Sulfate Reduction During Pyrolysis of Kraft Black Liquor", Proc. 1995 TAPPE-CPPA International Chemical Recovery Conference, Toronto, April 23-27, p. A227-A235.
- Sricharoenchaikul, V., Reis, V.V., Carangal, A., Sinquefield, S.A., Iisa, K., Frederick W.J., "Experimental Measurements of the Pyrolysis Products from Black Liquor Using a Laminar Entrained-flow Reactor", Paper 253c, 1994 AIChE Annual Meeting, San Francisco, November 13-18.

MATERIAL BALANCE					
DATA ACQUISITION FILE	FVJL601	FVJL602	FVJL603	FVJL604	FVJL605
Date	7/6/96	7/6/96	7/7/96	7/7/96	7/7/96
Raw Material	Valdosta	Valdosta	Valdosta	Valdosta	Valdosta
Particle Size (micron)	90-125	90-125	90-125	90-125	90-125
Reactor Path Length (inch)	28.75	28.75	28.75	28.75	28.75
Residence Time (sec)	2.0	2.0	1.7	1.7	1.5
Temperature (c)	600	600	600	600	600
GAS FLOW					
Primary Flow	0.15	0.15	0.15	0.15	0.15
Total Flow (l/min)	8.00	8.00	11.00	11.00	13.80
N2 (l/min) : (100 %)	8.00	8.00	11.00	11.00	13.80
CO2 (l/min) : (0 %)	0.00	0.00	0.00	0.00	0.00
O2 (l/min) : (0 %)	0.00	0.00	0.00	0.00	0.00
Gas Sample Flow (l/min)	7.24	7.38	7.51	6.55	6.69
Total Running Time (min)	10.00	10.00	10.00	10.00	10.00
WEIGHT DATA					
Input					
1. BL Before (g)	20.0859	21.7559	20.8422	20.6563	20.7995
BL After (g)	14.6564	17.2948	16.2831	14.9224	15.2436
Input black liquor wt.(g)	<i>5.4295</i>	<i>4.4611</i>	<i>4.5591</i>	<i>5.7339</i>	<i>5.5559</i>
2. Flush Char wt. (g)	<i>0.0401</i>	<i>0.0456</i>	<i>0.0511</i>	<i>0.0425</i>	<i>0.0332</i>
3. Flush Filter Before (g)	0.4644	0.4694	0.5257	0.5233	0.5503
Flush Filter After (g)	0.4693	0.4761	0.5315	0.5325	0.5556
Flush Fume wt.(g)	<i>0.0049</i>	<i>0.0067</i>	<i>0.0058</i>	<i>0.0092</i>	<i>0.0053</i>
Total Input black liquor wt. (g)	5.3845	4.4088	4.5022	5.6822	5.5174
Output					
1. Fume Filter Before (g)	0.0874	0.0869	0.0868	0.0861	0.0865
Fume Filter After (g)	0.1023	0.0996	0.0954	0.0952	0.0925
Collected Fume wt. (g)	<i>0.0149</i>	<i>0.0127</i>	<i>0.0086</i>	<i>0.0091</i>	<i>0.006</i>
2. Fume Filter Before (gas outlet) (g)	0.4661	0.4666	0.4685	0.4687	0.4672
Fume Filter After (gas outlet) (g)	0.5053	0.4985	0.4931	0.5028	0.4928
Fume wt. (gas outlet) (g)	<i>0.0392</i>	<i>0.0319</i>	<i>0.0246</i>	<i>0.0341</i>	<i>0.0256</i>
Total Fume wt. in system (g)	<i>0.0541</i>	<i>0.0446</i>	<i>0.0332</i>	<i>0.0432</i>	<i>0.0316</i>
3. Char wt. (g)	<i>4.0334</i>	<i>3.3161</i>	<i>3.5597</i>	<i>4.3071</i>	<i>4.2375</i>
Total wt. output (g)	4.0875	3.3607	3.5929	4.3503	4.2691
Percentage of Total Output wt (%)	75.91	76.23	79.80	76.56	77.38
Percentage of Collected Fume (%)	1.00	1.01	0.74	0.76	0.57
Percentage of Collected Char (%)	74.91	75.22	79.07	75.80	76.80

MATERIAL BALANCE					
DATA ACQUISITION FILE	FVJL606	FVJL607	FVJL608	FVJL609	FVJL610
Date	7/7/96	7/8/96	7/8/96	7/8/96	7/8/96
Raw Material	Valdosta	Valdosta	Valdosta	Valdosta	Valdosta
Particle Size (micron)	90-125	90-125	90-125	90-125	90-125
Reactor Path Length (inch)	28.75	28.75	28.75	28.75	28.75
Residence Time (sec)	1.5	1.3	1.3	1.1	1.1
Temperature (c)	600	600	600	600	600
GAS FLOW					
Primary Flow	0.15	0.15	0.15	0.22	0.22
Total Flow (l/min)	13.80	18.20	18.20	21.80	21.80
N2 (l/min) : (100 %)	13.80	18.20	18.20	21.80	21.80
CO2 (l/min) : (0 %)	0.00	0.00	0.00	0.00	0.00
O2 (l/min) : (0 %)	0.00	0.00	0.00	0.00	0.00
Gas Sample Flow (l/min)	6.71	7.41	8.05	7.78	7.84
Total Running Time (min)	10.00	10.00	10.00	10.00	10.00
WEIGHT DATA					
Input					
1. BL Before (g)	21.1191	21.5675	21.6221	20.9153	21.5366
BL After (g)	15.1868	16.6559	17.0753	15.9681	16.7768
Input black liquor wt.(g)	5.9323	4.9116	4.5468	4.9472	4.7598
2. Flush Char wt. (g)	0.0272	0.0175	0.0155	0.0265	0.0197
3. Flush Filter Before (g)	0.5300	0.5557	0.5339	0.5201	0.5271
Flush Filter After (g)	0.5427	0.5649	0.5441	0.5294	0.5327
Flush Fume wt.(g)	0.0127	0.0092	0.0102	0.0093	0.0056
Total Input black liquor wt. (g)	5.8924	4.8849	4.5211	4.9114	4.7345
Output					
1. Fume Filter Before (g)	0.0861	0.0869	0.0871	0.0868	0.0879
Fume Filter After (g)	0.0918	0.0907	0.0921	0.0899	0.0908
Collected Fume wt. (g)	0.0057	0.0038	0.0050	0.0031	0.0029
2. Fume Filter Before (gas outlet) (g)	0.4637	0.4696	0.4677	0.4705	0.4658
Fume Filter After (gas outlet) (g)	0.4906	0.4882	0.4835	0.4874	0.4818
Fume wt. (gas outlet) (g)	0.0269	0.0186	0.0158	0.0169	0.0160
Total Fume wt. in system (g)	0.0326	0.0224	0.0208	0.0200	0.0189
3. Char wt. (g)	4.5686	3.8534	3.5371	3.9616	3.8025
Total wt. output (g)	4.6012	3.8758	3.5579	3.9816	3.8214
Percentage of Total Output wt (%)	78.09	79.34	78.70	81.07	80.71
Percentage of Collected Fume (%)	0.55	0.46	0.46	0.41	0.40
Percentage of Collected Char (%)	77.53	78.88	78.24	80.66	80.31

MATERIAL BALANCE					
DATA ACQUISITION FILE	FVJL611	FVJL612	FVJL613	FVJL614	FVJL615
Date	7/8/96	7/8/96	7/9/96	7/9/96	7/9/96
Raw Material	Valdosta	Valdosta	Valdosta	Valdosta	Valdosta
Particle Size (micron)	90-125	90-125	90-125	90-125	90-125
Reactor Path Length (inch)	25.75	25.75	19.75	19.75	13.75
Residence Time (sec)	0.9	0.9	0.7	0.7	0.5
Temperature (c)	600	600	600	600	600
GAS FLOW					
Primary Flow	0.30	0.30	0.30	0.30	0.28
Total Flow (l/min)	22.60	22.60	22.30	22.30	22.00
N2 (l/min) : (100 %)	22.60	22.60	22.30	22.30	22.00
CO2 (l/min) : (0 %)	0.00	0.00	0.00	0.00	0.00
O2 (l/min) : (0 %)	0.00	0.00	0.00	0.00	0.00
Gas Sample Flow (l/min)	8.08	7.83	8.00	8.05	8.04
Total Running Time (min)	10.00	10.00	10.00	10.00	10.00
WEIGHT DATA					
Input					
1. BL Before (g)	21.7261	21.2555	21.5593	21.5444	21.7606
BL After (g)	16.242	16.7153	17.0117	16.7092	17.2403
Input black liquor wt.(g)	5.4841	4.5402	4.5476	4.8352	4.5203
2. Flush Char wt. (g)	0.0243	0.0235	0.0415	0.0296	0.0845
3. Flush Filter Before (g)	0.5183	0.5535	0.5203	0.5476	0.5228
Flush Filter After (g)	0.5245	0.5615	0.5324	0.5549	0.5342
Flush Fume wt.(g)	0.0062	0.0080	0.0121	0.0073	0.0114
Total Input black liquor wt. (g)	5.4536	4.5087	4.4940	4.7983	4.4244
Output					
1. Fume Filter Before (g)	0.0861	0.0876	0.0876	0.0866	0.0868
Fume Filter After (g)	0.0901	0.0907	0.0913	0.0908	0.0905
Collected Fume wt. (g)	0.0040	0.0031	0.0037	0.0042	0.0037
2. Fume Filter Before (gas outlet) (g)	0.4656	0.4672	0.4791	0.4739	0.4731
Fume Filter After (gas outlet) (g)	0.4852	0.4851	0.4943	0.4906	0.4885
Fume wt. (gas outlet) (g)	0.0196	0.0179	0.0152	0.0167	0.0154
Total Fume wt. in system (g)	0.0236	0.0210	0.0189	0.0209	0.0191
3. Char wt. (g)	4.2010	3.6627	3.6304	3.5083	3.7689
Total wt. output (g)	4.2246	3.6837	3.6493	3.5292	3.7880
Percentage of Total Output wt (%)	77.46	81.70	81.20	73.55	85.62
Percentage of Collected Fume (%)	0.43	0.47	0.42	0.44	0.43
Percentage of Collected Char (%)	77.03	81.24	80.78	73.12	85.18

MATERIAL BALANCE					
DATA ACQUISITION FILE	FVJL606	FVJL607	FVJL608	FVJL609	FVJL610
Date	7/7/96	7/8/96	7/8/96	7/8/96	7/8/96
Raw Material	Valdosta	Valdosta	Valdosta	Valdosta	Valdosta
Particle Size (micron)	90-125	90-125	90-125	90-125	90-125
Reactor Path Length (inch)	28.75	28.75	28.75	28.75	28.75
Residence Time (sec)	1.5	1.3	1.3	1.1	1.1
Temperature (c)	600	600	600	600	600
GAS FLOW					
Primary Flow	0.15	0.15	0.15	0.22	0.22
Total Flow (l/min)	13.80	18.20	18.20	21.80	21.80
N2 (l/min) : (100 %)	13.80	18.20	18.20	21.80	21.80
CO2 (l/min) : (0 %)	0.00	0.00	0.00	0.00	0.00
O2 (l/min) : (0 %)	0.00	0.00	0.00	0.00	0.00
Gas Sample Flow (l/min)	6.71	7.41	8.05	7.78	7.84
Total Running Time (min)	10.00	10.00	10.00	10.00	10.00
WEIGHT DATA					
Input					
1. BL Before (g)	21.1191	21.5675	21.6221	20.9153	21.5366
BL After (g)	15.1868	16.6559	17.0753	15.9681	16.7768
Input black liquor wt.(g)	5.9323	4.9116	4.5468	4.9472	4.7598
2. Flush Char wt. (g)	0.0272	0.0175	0.0155	0.0265	0.0197
3. Flush Filter Before (g)	0.5300	0.5557	0.5339	0.5201	0.5271
Flush Filter After (g)	0.5427	0.5649	0.5441	0.5294	0.5327
Flush Fume wt.(g)	0.0127	0.0092	0.0102	0.0093	0.0056
Total Input black liquor wt. (g)	5.8924	4.8849	4.5211	4.9114	4.7345
Output					
1. Fume Filter Before (g)	0.0861	0.0869	0.0871	0.0868	0.0879
Fume Filter After (g)	0.0918	0.0907	0.0921	0.0899	0.0908
Collected Fume wt. (g)	0.0057	0.0038	0.0050	0.0031	0.0029
2. Fume Filter Before (gas outlet) (g)	0.4637	0.4696	0.4677	0.4705	0.4658
Fume Filter After (gas outlet) (g)	0.4906	0.4882	0.4835	0.4874	0.4818
Fume wt. (gas outlet) (g)	0.0269	0.0186	0.0158	0.0169	0.0160
Total Fume wt. in system (g)	0.0326	0.0224	0.0208	0.0200	0.0189
3. Char wt. (g)	4.5686	3.8534	3.5371	3.9616	3.8025
Total wt. output (g)	4.6012	3.8758	3.5579	3.9816	3.8214
Percentage of Total Output wt (%)	78.09	79.34	78.70	81.07	80.71
Percentage of Collected Fume (%)	0.55	0.46	0.46	0.41	0.40
Percentage of Collected Char (%)	77.53	78.88	78.24	80.66	80.31

MATERIAL BALANCE			
DATA ACQUISITION FILE	FVJL616	FVJL617	FVJL618
Date	7/9/96	7/9/96	7/9/96
Raw Material	Valdosta	Valdosta	Valdosta
Particle Size (micron)	90-125	90-125	90-125
Reactor Path Length (inch)	13.75	9.75	9.75
Residence Time (sec)	0.5	0.3	0.3
Temperature (c)	600	600	600
GAS FLOW			
Primary Flow	0.28	0.38	0.38
Total Flow (l/min)	22.00	29.00	29.00
N2 (l/min) : (100 %)	22.00	29.00	29.00
CO2 (l/min) : (0 %)	0.00	0.00	0.00
O2 (l/min) : (0 %)	0.00	0.00	0.00
Gas Sample Flow (l/min)	8.00	8.08	8.12
Total Running Time (min)	10.00	10.00	10.00
WEIGHT DATA			
Input			
1. BL Before (g)	21.4458	20.7797	21.4915
BL After (g)	15.9914	16.0875	15.9531
Input black liquor wt.(g)	<i>5.4544</i>	<i>4.6922</i>	<i>5.5384</i>
2. Flush Char wt. (g)	<i>0.0185</i>	<i>0.0861</i>	<i>0.0179</i>
3. Flush Filter Before (g)	0.5206	0.5409	0.5232
Flush Filter After (g)	0.5353	0.5569	0.5381
Flush Fume wt.(g)	<i>0.0147</i>	<i>0.0160</i>	<i>0.0149</i>
Total Input black liquor wt. (g)	5.4212	4.5901	5.5056
Output			
1. Fume Filter Before (g)	0.0864	0.0869	0.0861
Fume Filter After (g)	0.0904	0.0912	0.0914
Collected Fume wt. (g)	<i>0.0040</i>	<i>0.0043</i>	<i>0.0053</i>
2. Fume Filter Before (gas outlet) (g)	0.4796	0.4681	0.4697
Fume Filter After (gas outlet) (g)	0.5001	0.4909	0.4958
Fume wt. (gas outlet) (g)	<i>0.0205</i>	<i>0.0228</i>	<i>0.0261</i>
Total Fume wt. in system (g)	<i>0.0245</i>	<i>0.0271</i>	<i>0.0314</i>
3. Char wt. (g)	<i>4.5995</i>	<i>4.2696</i>	<i>5.0851</i>
Total wt. output (g)	4.6240	4.2967	5.1165
Percentage of Total Output wt (%)	85.29	93.61	92.93
Percentage of Collected Fume (%)	0.45	0.59	0.57
Percentage of Collected Char (%)	84.84	93.02	92.36

MATERIAL BALANCE					
DATA ACQUISITION FILE	FVAG601	FVAG602	FVAG603	FVAG604	FVAG605
Date	8/7/96	8/7/96	8/8/96	8/8/96	8/8/96
Raw Material	Valdosta	Valdosta	Valdosta	Valdosta	Valdosta
Particle Size (micron)	90-125	90-125	90-125	90-125	90-125
Reactor Path Length (inch)	28.75	28.75	28.75	28.75	28.75
Residence Time (sec)	2.0	2.0	1.7	1.7	1.5
Temperature (c)	500	500	500	500	500
GAS FLOW					
Primary Flow	0.15	0.15	0.15	0.15	0.15
Total Flow (l/min)	8.60	8.60	12.20	12.20	15.70
N2 (l/min) : (100 %)	8.60	8.60	12.20	12.20	15.70
CO2 (l/min) : (0 %)	0.00	0.00	0.00	0.00	0.00
O2 (l/min) : (0 %)	0.00	0.00	0.00	0.00	0.00
Gas Sample Flow (l/min)	7.46	7.54	7.84	7.98	7.72
Total Running Time (min)	10.00	10.00	10.00	10.00	9.00
WEIGHT DATA					
Input					
1. BL Before (g)	20.8591	20.5032	20.6908	20.8184	20.3886
BL After (g)	15.7574	15.9561	16.4436	17.6973	17.3975
Input black liquor wt.(g)	5.1017	4.5471	4.2472	3.1211	2.9911
2. Flush Char wt. (g)	0.0000	0.0000	0.0000	0.0000	0.0000
3. Flush Filter Before (g)	0.5122	0.5285	0.5349	0.5611	0.5491
Flush Filter After (g)	0.5302	0.5452	0.5443	0.5696	0.5624
Flush Fume wt.(g)	0.0180	0.0167	0.0094	0.0085	0.0133
Total Input black liquor wt. (g)	5.0837	4.5304	4.2378	3.1126	2.9778
Output					
1. Fume Filter Before (g)	0.0874	0.0881	0.0876	0.0869	0.0878
Fume Filter After (g)	0.1003	0.0996	0.0961	0.0916	0.0926
Collected Fume wt. (g)	0.0129	0.0115	0.0085	0.0047	0.0048
2. Fume Filter Before (gas outlet) (g)	0.4709	0.4662	0.4685	0.4694	0.4745
Fume Filter After (gas outlet) (g)	0.4981	0.4923	0.4921	0.4856	0.4932
Fume wt. (gas outlet) (g)	0.0272	0.0261	0.0236	0.0162	0.0187
Total Fume wt. in system (g)	0.0401	0.0376	0.0321	0.0209	0.0235
3. Char wt. (g)	3.3487	2.8562	2.7995	1.9759	2.0084
Total wt. output (g)	3.3888	2.8938	2.8316	1.9968	2.0319
Percentage of Total Output wt (%)	66.66	63.88	66.82	64.15	68.23
Percentage of Collected Fume (%)	0.79	0.83	0.76	0.67	0.79
Percentage of Collected Char (%)	65.87	63.05	66.06	63.48	67.45

MATERIAL BALANCE					
DATA ACQUISITION FILE	FVAG606	FVAG607	FVAG608	FVAG609	FVAG610
Date	8/8/96	8/8/96	8/8/96	8/13/96	8/13/96
Raw Material	Valdosta	Valdosta	Valdosta	Valdosta	Valdosta
Particle Size (micron)	90-125	90-125	90-125	90-125	90-125
Reactor Path Length (inch)	28.75	28.75	28.75	28.75	28.75
Residence Time (sec)	1.5	1.3	1.3	1.1	1.1
Temperature (c)	500	500	500	500	500
GAS FLOW					
Primary Flow	0.15	0.15	0.15	0.25	0.25
Total Flow (l/min)	15.70	20.60	20.60	23.80	23.80
N2 (l/min) : (100 %)	15.70	20.60	20.60	23.80	23.80
CO2 (l/min) : (0 %)	0.00	0.00	0.00	0.00	0.00
O2 (l/min) : (0 %)	0.00	0.00	0.00	0.00	0.00
Gas Sample Flow (l/min)	8.18	8.27	8.26	6.82	6.76
Total Running Time (min)	9.00	6.00	8.00	10.00	10.00
WEIGHT DATA					
Input					
1. BL Before (g)	20.2547	21.6434	21.4339	20.6165	20.7138
BL After (g)	16.6628	19.4576	20.0207	16.3334	16.3048
Input black liquor wt.(g)	3.5919	2.1858	1.4132	4.2831	4.4090
2. Flush Char wt. (g)	0.0000	0.0000	0.0000	0.0000	0.0000
3. Flush Filter Before (g)	0.5256	0.5354	0.5345	0.5533	0.5265
Flush Filter After (g)	0.5398	0.5461	0.5465	0.5701	0.5426
Flush Fume wt.(g)	0.0142	0.0107	0.0120	0.0168	0.0161
Total Input black liquor wt. (g)	3.5777	2.1751	1.4012	4.2663	4.3929
Output					
1. Fume Filter Before (g)	0.0883	0.0881	0.0873	0.0857	0.0861
Fume Filter After (g)	0.0928	0.0906	0.0893	0.0882	0.0889
Collected Fume wt. (g)	0.0045	0.0025	0.0020	0.0025	0.0028
2. Fume Filter Before (gas outlet) (g)	0.4687	0.4707	0.4727	0.4722	0.4663
Fume Filter After (gas outlet) (g)	0.4838	0.4816	0.4795	0.4882	0.4839
Fume wt. (gas outlet) (g)	0.0151	0.0109	0.0068	0.0160	0.0176
Total Fume wt. in system (g)	0.0196	0.0134	0.0088	0.0185	0.0204
3. Char wt. (g)	2.4421	1.5456	1.0306	3.3014	3.5031
Total wt. output (g)	2.4617	1.5590	1.0394	3.3199	3.5235
Percentage of Total Output wt (%)	68.81	71.67	74.18	77.82	80.21
Percentage of Collected Fume (%)	0.55	0.62	0.63	0.43	0.46
Percentage of Collected Char (%)	68.26	71.06	73.55	77.38	79.74

MATERIAL BALANCE					
DATA ACQUISITION FILE	FVAG611	FVAG612	FVAG613	FVAG614	FVAG615
Date	8/13/96	8/13/96	8/14/96	8/14/96	8/14/96
Raw Material	Valdosta	Valdosta	Valdosta	Valdosta	Valdosta
Particle Size (micron)	90-125	90-125	90-125	90-125	90-125
Reactor Path Length (inch)	23.75	23.75	17.75	17.75	12.75
Residence Time (sec)	0.9	0.9	0.7	0.7	0.5
Temperature (c)	500	500	500	500	500
GAS FLOW					
Primary Flow	0.30	0.30	0.29	0.29	0.29
Total Flow (l/min)	22.00	22.00	20.00	20.00	20.10
N2 (l/min) : (100 %)	22.00	22.00	20.00	20.00	20.10
CO2 (l/min) : (0 %)	0.00	0.00	0.00	0.00	0.00
O2 (l/min) : (0 %)	0.00	0.00	0.00	0.00	0.00
Gas Sample Flow (l/min)	6.63	6.75	6.85	6.84	6.80
Total Running Time (min)	10.00	10.00	10.00	10.00	10.00
WEIGHT DATA					
Input					
1. BL Before (g)	21.2234	21.4586	20.6886	21.3525	20.0361
BL After (g)	15.7966	16.5101	16.9143	15.8638	15.7151
Input black liquor wt.(g)	5.4268	4.9485	3.7743	5.4887	4.3210
2. Flush Char wt. (g)	0.0000	0.0000	0.0000	0.0000	0.0000
3. Flush Filter Before (g)	0.5234	0.5247	0.5271	0.5301	0.0000
Flush Filter After (g)	0.5352	0.5352	0.5388	0.5457	0.0000
Flush Fume wt.(g)	0.0118	0.0105	0.0117	0.0156	0.0000
Total Input black liquor wt. (g)	5.4150	4.9380	3.7626	5.4731	4.3210
Output					
1. Fume Filter Before (g)	0.0865	0.0872	0.0871	0.0867	0.0858
Fume Filter After (g)	0.0906	0.0901	0.0892	0.0904	0.0888
Collected Fume wt. (g)	0.0041	0.0029	0.0021	0.0037	0.0030
2. Fume Filter Before (gas outlet) (g)	0.4702	0.4706	0.4693	0.4701	0.4711
Fume Filter After (gas outlet) (g)	0.4902	0.4909	0.4861	0.4909	0.4901
Fume wt. (gas outlet) (g)	0.0200	0.0203	0.0168	0.0208	0.0190
Total Fume wt. in system (g)	0.0241	0.0232	0.0189	0.0245	0.0220
3. Char wt. (g)	4.3718	3.9025	3.0763	4.5202	3.6438
Total wt. output (g)	4.3959	3.9257	3.0952	4.5447	3.6658
Percentage of Total Output wt (%)	81.18	79.50	82.26	83.04	84.84
Percentage of Collected Fume (%)	0.45	0.47	0.50	0.45	0.51
Percentage of Collected Char (%)	80.73	79.03	81.76	82.59	84.33

MATERIAL BALANCE					
DATA ACQUISITION FILE	FVAG616	FVAG617	FVAG618	FVAG619	FVAG620
Date	8/14/96	8/14/96	8/14/96	8/15/96	8/15/96
Raw Material	Valdosta	Valdosta	Valdosta	Valdosta	Valdosta
Particle Size (micron)	90-125	90-125	90-125	90-125	90-125
Reactor Path Length (inch)	12.75	9.75	9.75	28.75	28.75
Residence Time (sec)	0.5	0.3	0.3	2.0	2.0
Temperature (c)	500	500	500	400	400
GAS FLOW					
Primary Flow	0.29	0.42	0.42	0.15	0.15
Total Flow (l/min)	20.10	29.40	29.40	9.90	9.90
N2 (l/min) : (100 %)	20.10	29.40	29.40	9.90	9.90
CO2 (l/min) : (0 %)	0.00	0.00	0.00	0.00	0.00
O2 (l/min) : (0 %)	0.00	0.00	0.00	0.00	0.00
Gas Sample Flow (l/min)	6.81	6.92	6.92	6.73	6.74
Total Running Time (min)	10.00	10.00	9.00	7.00	7.00
WEIGHT DATA					
Input					
1. BL Before (g)	21.5842	21.3222	21.2576	21.1412	21.1032
BL After (g)	16.0378	15.8861	16.8503	19.2061	18.2734
Input black liquor wt.(g)	5.5464	5.4361	4.4073	1.9351	2.8298
2. Flush Char wt. (g)	0.0000	0.0000	0.0000	0.0000	0.0000
3. Flush Filter Before (g)	0.0000	0.0000	0.0000	0.0000	0.0000
Flush Filter After (g)	0.0000	0.0000	0.0000	0.0000	0.0000
Flush Fume wt.(g)	0.0000	0.0000	0.0000	0.0000	0.0000
Total Input black liquor wt. (g)	5.5464	5.4361	4.4073	1.9351	2.8298
Output					
1. Fume Filter Before (g)	0.0869	0.0867	0.0864	0.0866	0.0872
Fume Filter After (g)	0.0898	0.0884	0.0881	0.0883	0.0902
Collected Fume wt. (g)	0.0029	0.0017	0.0017	0.0017	0.0030
2. Fume Filter Before (gas outlet) (g)	0.4716	0.4663	0.4733	0.4703	0.4713
Fume Filter After (gas outlet) (g)	0.4911	0.4811	0.4841	0.4765	0.4808
Fume wt. (gas outlet) (g)	0.0195	0.0148	0.0108	0.0062	0.0095
Total Fume wt. in system (g)	0.0224	0.0165	0.0125	0.0079	0.0125
3. Char wt. (g)	4.7505	4.8722	4.0662	1.5201	2.1397
Total wt. output (g)	4.7729	4.8887	4.0787	1.5280	2.1522
Percentage of Total Output wt (%)	86.05	89.93	92.54	78.96	76.05
Percentage of Collected Fume (%)	0.40	0.30	0.28	0.41	0.44
Percentage of Collected Char (%)	85.65	89.63	92.26	78.55	75.61

MATERIAL BALANCE					
DATA ACQUISITION FILE	FVAG621	FVAG622	FVAG623	FVAG624	FVAG625
Date	8/15/96	8/15/96	8/15/96	8/15/96	8/16/96
Raw Material	Valdosta	Valdosta	Valdosta	Valdosta	Valdosta
Particle Size (micron)	90-125	90-125	90-125	90-125	90-125
Reactor Path Length (inch)	28.75	28.75	28.75	28.75	28.75
Residence Time (sec)	1.7	1.7	1.5	1.5	1.3
Temperature (c)	400	400	400	400	400
GAS FLOW					
Primary Flow	0.15	0.15	0.15	0.15	0.25
Total Flow (l/min)	14.60	14.60	19.20	19.20	20.00
N2 (l/min) : (100 %)	14.60	14.60	19.20	19.20	20.00
CO2 (l/min) : (0 %)	0.00	0.00	0.00	0.00	0.00
O2 (l/min) : (0 %)	0.00	0.00	0.00	0.00	0.00
Gas Sample Flow (l/min)	6.77	6.87	6.83	7.05	6.85
Total Running Time (min)	8.00	8.00	9.00	10.00	7.00
WEIGHT DATA					
Input					
1. BL Before (g)	20.9799	21.4593	21.4381	21.2487	20.8757
BL After (g)	16.8671	17.4396	16.7426	17.4777	18.5586
Input black liquor wt.(g)	4.1128	4.0197	4.6955	3.771	2.3171
2. Flush Char wt. (g)	0.0000	0.0000	0.0000	0.0000	0.0000
3. Flush Filter Before (g)	0.0000	0.0000	0.0000	0.0000	0.0000
Flush Filter After (g)	0.0000	0.0000	0.0000	0.0000	0.0000
Flush Fume wt.(g)	0.0000	0.0000	0.0000	0.0000	0.0000
Total Input black liquor wt. (g)	4.1128	4.0197	4.6955	3.7710	2.3171
Output					
1. Fume Filter Before (g)	0.0854	0.0854	0.0864	0.0878	0.0861
Fume Filter After (g)	0.0874	0.0876	0.0878	0.0891	0.0871
Collected Fume wt. (g)	0.0020	0.0022	0.0014	0.0013	0.0010
2. Fume Filter Before (gas outlet) (g)	0.4702	0.4656	0.4732	0.4709	0.4692
Fume Filter After (gas outlet) (g)	0.4798	0.4761	0.4821	0.4784	0.4751
Fume wt. (gas outlet) (g)	0.0096	0.0105	0.0089	0.0075	0.0059
Total Fume wt. in system (g)	0.0116	0.0127	0.0103	0.0088	0.0069
3. Char wt. (g)	3.1248	3.2285	3.7358	3.1228	1.9236
Total wt. output (g)	3.1364	3.2412	3.7461	3.1316	1.9305
Percentage of Total Output wt (%)	76.26	80.63	79.78	83.04	83.32
Percentage of Collected Fume (%)	0.28	0.32	0.22	0.23	0.30
Percentage of Collected Char (%)	75.98	80.32	79.56	82.81	83.02

MATERIAL BALANCE					
DATA ACQUISITION FILE	FVAG626	FVAG627	FVAG628	FVAG629	FVAG630
Date	8/16/96	8/16/96	8/16/96	8/16/96	8/16/96
Raw Material	Valdosta	Valdosta	Valdosta	Valdosta	Valdosta
Particle Size (micron)	90-125	90-125	90-125	90-125	90-125
Reactor Path Length (inch)	28.75	28.75	28.75	21.75	21.75
Residence Time (sec)	1.3	1.1	1.1	0.9	0.9
Temperature (c)	400	400	400	400	400
GAS FLOW					
Primary Flow	0.25	0.40	0.40	0.30	0.30
Total Flow (l/min)	20.00	20.20	20.20	21.20	21.20
N2 (l/min) : (100 %)	20.00	20.20	20.20	21.20	21.20
CO2 (l/min) : (0 %)	0.00	0.00	0.00	0.00	0.00
O2 (l/min) : (0 %)	0.00	0.00	0.00	0.00	0.00
Gas Sample Flow (l/min)	6.81	6.81	6.81	6.76	6.74
Total Running Time (min)	10.00	10.00	9.00	10.00	8.00
WEIGHT DATA					
Input					
1. BL Before (g)	21.0514	21.3485	21.4198	21.7911	21.6795
BL After (g)	16.5389	16.4113	17.2829	17.8243	18.5944
Input black liquor wt.(g)	4.5125	4.9372	4.1369	3.9668	3.0851
2. Flush Char wt. (g)	0.0000	0.0000	0.0000	0.0000	0.0000
3. Flush Filter Before (g)	0.0000	0.0000	0.0000	0.0000	0.0000
Flush Filter After (g)	0.0000	0.0000	0.0000	0.0000	0.0000
Flush Fume wt.(g)	0.0000	0.0000	0.0000	0.0000	0.0000
Total Input black liquor wt. (g)	4.5125	4.9372	4.1369	3.9668	3.0851
Output					
1. Fume Filter Before (g)	0.0861	0.0862	0.0867	0.0859	0.0862
Fume Filter After (g)	0.0877	0.0885	0.0884	0.0874	0.0872
Collected Fume wt. (g)	0.0016	0.0023	0.0017	0.0015	0.001
2. Fume Filter Before (gas outlet) (g)	0.4711	0.4706	0.4741	0.4751	0.4721
Fume Filter After (gas outlet) (g)	0.4813	0.4834	0.4841	0.4864	0.4789
Fume wt. (gas outlet) (g)	0.0102	0.0128	0.0100	0.0113	0.0068
Total Fume wt. in system (g)	0.0118	0.0151	0.0117	0.0128	0.0078
3. Char wt. (g)	3.8421	4.2969	3.6589	3.6146	2.8285
Total wt. output (g)	3.8539	4.3120	3.6706	3.6274	2.8363
Percentage of Total Output wt (%)	85.40	87.34	88.73	91.44	91.94
Percentage of Collected Fume (%)	0.26	0.31	0.28	0.32	0.25
Percentage of Collected Char (%)	85.14	87.03	88.45	91.12	91.68

MATERIAL BALANCE					
DATA ACQUISITION FILE	FVAG631	FVAG632	FVAG633	FVAG634	FVAG635
Date	8/18/96	8/18/96	8/18/96	8/18/96	8/18/96
Raw Material	Valdosta	Valdosta	Valdosta	Valdosta	Valdosta
Particle Size (micron)	90-125	90-125	90-125	90-125	90-125
Reactor Path Length (inch)	15.75	15.75	11.75	11.75	9.75
Residence Time (sec)	0.7	0.7	0.5	0.5	0.3
Temperature (c)	400	400	400	400	400
GAS FLOW					
Primary Flow	0.30	0.30	0.30	0.30	0.50
Total Flow (l/min)	14.80	14.80	17.30	17.30	21.00
N2 (l/min) : (100 %)	14.80	14.80	17.30	17.30	21.00
CO2 (l/min) : (0 %)	0.00	0.00	0.00	0.00	0.00
O2 (l/min) : (0 %)	0.00	0.00	0.00	0.00	0.00
Gas Sample Flow (l/min)	6.72	6.75	6.75	6.74	6.75
Total Running Time (min)	6.00	10.00	10.00	10.00	10.00
WEIGHT DATA					
Input					
1. BL Before (g)	21.4672	21.3816	21.4917	21.8221	21.3802
BL After (g)	17.9179	16.9926	16.8844	17.7278	16.4422
Input black liquor wt.(g)	3.5493	4.3890	4.6073	4.0943	4.9380
2. Flush Char wt. (g)	0.0000	0.0000	0.0000	0.0000	0.0000
3. Flush Filter Before (g)	0.0000	0.0000	0.0000	0.0000	0.0000
Flush Filter After (g)	0.0000	0.0000	0.0000	0.0000	0.0000
Flush Fume wt.(g)	0.0000	0.0000	0.0000	0.0000	0.0000
Total Input black liquor wt. (g)	3.5493	4.3890	4.6073	4.0943	4.9380
Output					
1. Fume Filter Before (g)	0.0879	0.0852	0.0867	0.0852	0.0865
Fume Filter After (g)	0.0881	0.0871	0.0889	0.0872	0.0889
Collected Fume wt. (g)	0.0002	0.0019	0.0022	0.0020	0.0024
2. Fume Filter Before (gas outlet) (g)	0.4709	0.4724	0.4731	0.4766	0.4762
Fume Filter After (gas outlet) (g)	0.4733	0.4789	0.4858	0.4889	0.4908
Fume wt. (gas outlet) (g)	0.0024	0.0065	0.0127	0.0123	0.0146
Total Fume wt. in system (g)	0.0026	0.0084	0.0149	0.0143	0.0170
3. Char wt. (g)	3.4712	4.1884	4.5907	4.0140	4.9162
Total wt. output (g)	3.4738	4.1968	4.6056	4.0283	4.9332
Percentage of Total Output wt (%)	97.87	95.62	99.96	98.39	99.90
Percentage of Collected Fume (%)	0.07	0.19	0.32	0.35	0.34
Percentage of Collected Char (%)	97.80	95.43	99.64	98.04	99.56

Carbon Yield in Fume, Char, and Gas at 600 ° C					
DATA ACQUISITION FILE	FVJL601	FVJL602	FVJL603	FVJL604	FVJL605
Reactor Path Length (inch)	28.75	28.75	28.75	28.75	28.75
Residence Time (sec)	2.0	2.0	1.7	1.7	1.5
Temperature (c)	600	600	600	600	600
Mass of Carbon in Gas :					
1st and 2nd Flow of N ₂ (l/min)	8.00	8.00	11.00	11.00	13.80
Quench Flow (l/min)	12.80	12.80	16.50	16.50	20.70
Total gas Flow at Outlet (l/min)	20.80	20.80	27.50	27.50	34.50
Total Running Time (min)	10.00	10.00	10.00	10.00	10.00
Percentage of CO ₂ at Outlet (%)	0.40	0.34	0.26	0.32	0.24
Volumatic Flow of CO ₂ (l/min)	0.0832	0.07072	0.0715	0.0880	0.0828
Total Volume of CO ₂ (l)	0.8320	0.7072	0.7150	0.8800	0.8280
Mass of CO ₂ (g)	1.4968	1.2723	1.2863	1.5831	1.4896
Mol of CO ₂ (mol)	0.0340	0.0289	0.0292	0.0360	0.0339
Mol of C (mol)	0.0340	0.0289	0.0292	0.0360	0.0339
Total Mass of Carbon in Gas (g)	0.4082	0.3470	0.3508	0.4318	0.4062
Carbon Balance :					
Input :					
Total Input Black Liquor wt. (g)	5.3845	4.4088	4.5022	5.6822	5.5174
Carbon wt % in Black Liquor	33.66	33.66	33.66	33.66	33.66
Carbon wt in Black Liquor (g)	1.8124	1.4840	1.5154	1.9126	1.8572
Output :					
1.Total Fume wt. (g)	0.0541	0.0446	0.0332	0.0432	0.0316
Carbon wt % in Fume (%)	76.29	91.09	74.12	57.89	54.86
Carbon wt in Fume (g)	0.0413	0.0406	0.0246	0.0250	0.0173
2.Char wt. (g)	4.0334	3.3161	3.5597	4.3071	4.2375
Carbon wt % in Char (%)	32.29	30.05	30.99	30.83	30.54
Carbon wt in Char (g)	1.3024	0.9965	1.1032	1.3279	1.2941
3.Total Mass of Carbon in Gas (g)	0.4082	0.3470	0.3508	0.4318	0.4062
Total Carbon wt. of Output (g)	1.7519	1.3841	1.4786	1.7846	1.7177
Carbon Yield in Fume (%)	2.28	2.74	1.62	1.31	0.93
Carbon Yield in Char (%)	71.86	67.15	72.79	69.43	69.68
Carbon Yield in Gas (%)	22.52	23.38	23.15	22.57	21.87
Total Carbon Yield of Output (%)	96.66	93.27	97.57	93.31	92.49

Carbon Yield in Fume, Char, and Gas at 600 ° C					
DATA ACQUISITION FILE	FVJL606	FVJL607	FVJL608	FVJL609	FVJL610
Reactor Path Length (inch)	28.75	28.75	28.75	28.75	28.75
Residence Time (sec)	1.5	1.3	1.3	1.1	1.1
Temperature (c)	600	600	600	600	600
Mass of Carbon in Gas :					
1st and 2nd Flow of N ₂ (l/min)	13.80	18.20	18.20	21.80	21.80
Quench Flow (l/min)	20.70	27.30	27.30	32.70	32.70
Total gas Flow at Outlet (l/min)	34.50	45.50	45.50	54.50	54.50
Total Running Time (min)	10.00	10.00	10.00	10.00	10.00
Percentage of CO ₂ at Outlet (%)	0.26	0.16	0.14	0.12	0.12
Volumatic Flow of CO ₂ (l/min)	0.0897	0.0728	0.0637	0.0654	0.0654
Total Volume of CO ₂ (l)	0.8970	0.7280	0.6370	0.6540	0.6540
Mass of CO ₂ (g)	1.6137	1.3097	1.1460	1.1765	1.1765
Mol of CO ₂ (mol)	0.0367	0.0298	0.0260	0.0267	0.0267
Mol of C (mol)	0.0367	0.0298	0.0260	0.0267	0.0267
Total Mass of Carbon in Gas (g)	0.4401	0.3572	0.3125	0.3209	0.3209
Carbon Balance :					
Input :					
Total Input Black Liquor wt. (g)	5.8924	4.8849	4.5211	4.9114	4.7345
Carbon wt % in Black Liquor	33.66	33.66	33.66	33.66	33.66
Carbon wt in Black Liquor (g)	1.9834	1.6443	1.5218	1.6532	1.5936
Output :					
1.Total Fume wt. (g)	0.0326	0.0224	0.0208	0.0200	0.0189
Carbon wt % in Fume (%)	52.91	53.53	57.31	47.95	50.32
Carbon wt in Fume (g)	0.0172	0.0120	0.0119	0.0096	0.0095
2.Char wt. (g)	4.5689	3.8534	3.5371	3.9616	3.8025
Carbon wt % in Char (%)	31.43	31.98	31.33	32.26	31.79
Carbon wt in Char (g)	1.4360	1.2323	1.1082	1.2780	1.2088
3.Total Mass of Carbon in Gas (g)	0.4401	0.3572	0.3125	0.3209	0.3209
Total Carbon wt. of Output (g)	1.8934	1.6015	1.4326	1.6085	1.5392
Carbon Yield in Fume (%)	0.87	0.73	0.78	0.58	0.60
Carbon Yield in Char (%)	72.40	74.95	72.82	77.31	75.85
Carbon Yield in Gas (%)	22.19	21.72	20.54	19.41	20.13
Total Carbon Yield of Output (%)	95.46	97.40	94.14	97.30	96.58

Carbon Yield in Fume, Char, and Gas at 600 °C					
DATA ACQUISITION FILE	FVJL611	FVJL612	FVJL613	FVJL614	FVJL615
Reactor Path Length (inch)	25.75	25.75	19.75	19.75	13.75
Residence Time (sec)	0.9	0.9	0.7	0.7	0.5
Temperature (c)	600	600	600	600	600
Mass of Carbon in Gas :					
1st and 2nd Flow of N ₂ (l/min)	22.60	22.60	22.30	22.30	22.00
Quench Flow (l/min)	33.90	33.90	33.50	33.50	33.00
Total gas Flow at Outlet (l/min)	56.50	56.50	55.80	55.80	55.00
Total Running Time (min)	10.00	10.00	10.00	10.00	10.00
Percentage of CO ₂ at Outlet (%)	0.12	0.10	0.10	0.10	0.08
Volumatic Flow of CO ₂ (l/min)	0.0678	0.0565	0.0558	0.0558	0.0440
Total Volume of CO ₂ (l)	0.6780	0.5650	0.5580	0.5580	0.4400
Mass of CO ₂ (g)	1.2197	1.0164	1.0038	1.0038	0.7916
Mol of CO ₂ (mol)	0.0277	0.0231	0.0228	0.0228	0.0180
Mol of C (mol)	0.0277	0.0231	0.0228	0.0228	0.0180
Total Mass of Carbon in Gas (g)	0.3327	0.2772	0.2738	0.2738	0.2159
Carbon Balance :					
Input :					
Total Input Black Liquor wt. (g)	5.4536	4.5087	4.4940	4.7983	4.4244
Carbon wt % in Black Liquor	33.66	33.66	33.66	33.66	33.66
Carbon wt in Black Liquor (g)	1.8357	1.5176	1.5127	1.6151	1.4893
Output :					
1.Total Fume wt. (g)	0.0236	0.0210	0.0189	0.0209	0.0191
Carbon wt % in Fume (%)	44.88	50.48	47.13	42.31	47.93
Carbon wt in Fume (g)	0.0106	0.0106	0.0089	0.0088	0.0092
2.Char wt. (g)	4.2010	3.6627	3.6304	3.5083	3.7689
Carbon wt % in Char (%)	32.83	33.16	33.36	33.84	33.26
Carbon wt in Char (g)	1.3792	1.2146	1.2111	1.1872	1.2535
3.Total Mass of Carbon in Gas (g)	0.3327	0.2772	0.2738	0.2738	0.2159
Total Carbon wt. of Output (g)	1.7224	1.5024	1.4938	1.4698	1.4786
Carbon Yield in Fume (%)	0.58	0.70	0.59	0.55	0.61
Carbon Yield in Char (%)	75.13	80.03	80.06	73.51	84.17
Carbon Yield in Gas (%)	18.12	18.27	18.10	16.95	14.50
Total Carbon Yield of Output (%)	93.83	98.99	98.75	91.00	99.28

Carbon Yield in Fume, Char, and Gas at 600 °C			
DATA ACQUISITION FILE	FVJL616	FVJL617	FVJL618
Reactor Path Length (inch)	13.75	9.75	9.75
Residence Time (sec)	0.5	0.3	0.3
Temperature (c)	600	600	600
Mass of Carbon in Gas :			
1st and 2nd Flow of N ₂ (l/min)	22.00	29.00	29.00
Quench Flow (l/min)	33.00	43.50	43.50
Total gas Flow at Outlet (l/min)	55.00	72.50	72.50
Total Running Time (min)	10.00	10.00	10.00
Percentage of CO ₂ at Outlet (%)	0.08	0.04	0.04
Volumatic Flow of CO ₂ (l/min)	0.0440	0.0290	0.0290
Total Volume of CO ₂ (l)	0.4400	0.2900	0.2900
Mass of CO ₂ (g)	0.7916	0.5217	0.5217
Mol of CO ₂ (mol)	0.0180	0.0119	0.0119
Mol of C (mol)	0.0180	0.0119	0.0119
Total Mass of Carbon in Gas (g)	0.2159	0.1423	0.1423
Carbon Balance :			
Input :			
Total Input Black Liquor wt. (g)	5.4212	4.5901	5.5056
Carbon wt % in Black Liquor	33.66	33.66	33.66
Carbon wt in Black Liquor (g)	1.8248	1.5450	1.8532
Output :			
1.Total Fume wt. (g)	0.0245	0.0271	0.0314
Carbon wt % in Fume (%)	38.11	32.89	28.64
Carbon wt in Fume (g)	0.0093	0.0089	0.0090
2.Char wt. (g)	4.5995	4.2696	5.0851
Carbon wt % in Char (%)	33.66	32.30	33.34
Carbon wt in Char (g)	1.5482	1.3791	1.6954
3.Total Mass of Carbon in Gas (g)	0.2159	0.1423	0.1423
Total Carbon wt. of Output (g)	1.7734	1.5303	1.8466
Carbon Yield in Fume (%)	0.51	0.58	0.49
Carbon Yield in Char (%)	84.84	89.26	91.48
Carbon Yield in Gas (%)	11.83	9.21	7.68
Total Carbon Yield of Output (%)	97.19	99.05	99.65

Carbon Yield in Fume, Char, and Gas at 500 °C					
DATA ACQUISITION FILE	FVAG601	FVAG602	FVAG603	FVAG604	FVAG605
Reactor Path Length (inch)	28.75	28.75	28.75	28.75	28.75
Residence Time (sec)	2.0	2.0	1.7	1.7	1.5
Temperature (c)	500	500	500	500	500
Mass of Carbon in Gas :					
1st and 2nd Flow of N ₂ (l/min)	8.60	8.60	12.20	12.20	15.70
Quench Flow (l/min)	12.90	12.90	18.30	18.30	23.60
Total gas Flow at Outlet (l/min)	21.50	21.50	30.50	30.50	39.30
Total Running Time (min)	10.00	10.00	10.00	10.00	9.00
Percentage of CO ₂ at Outlet (%)	0.38	0.34	0.20	0.16	0.10
Volumatic Flow of CO ₂ (l/min)	0.0817	0.0731	0.0610	0.0488	0.0393
Total Volume of CO ₂ (l)	0.8170	0.7310	0.6100	0.4880	0.3537
Mass of CO ₂ (g)	1.4698	1.3151	1.0974	0.8779	0.6363
Mol of CO ₂ (mol)	0.0334	0.0299	0.0249	0.0200	0.0145
Mol of C (mol)	0.0334	0.0299	0.0249	0.0200	0.0145
Total Mass of Carbon in Gas (g)	0.4008	0.3587	0.2993	0.2394	0.1735
Carbon Balance :					
Input :					
Total Input Black Liquor wt. (g)	5.0837	4.5304	4.2378	3.1126	2.9778
Carbon wt % in Black Liquor	33.66	33.66	33.66	33.66	33.66
Carbon wt in Black Liquor (g)	1.7112	1.5249	1.4264	1.0477	1.0023
Output :					
1. Total Fume wt. (g)	0.0401	0.0376	0.0321	0.0209	0.0235
Carbon wt % in Fume (%)	76.29	76.29	66.01	66.01	53.89
Carbon wt in Fume (g)	0.0306	0.0287	0.0212	0.0138	0.0127
2. Char wt. (g)	3.3487	2.8562	2.7995	1.9759	2.0084
Carbon wt % in Char (%)	31.56	31.56	31.38	31.38	30.92
Carbon wt in Char (g)	1.0568	0.9014	0.8785	0.6200	0.6210
3. Total Mass of Carbon in Gas (g)	0.4008	0.3587	0.2993	0.2394	0.1735
Total Carbon wt. of Output (g)	1.4883	1.2888	1.1990	0.8733	0.8072
Carbon Yield in Fume (%)	1.79	1.88	1.49	1.32	1.26
Carbon Yield in Char (%)	61.76	59.11	61.59	59.18	61.96
Carbon Yield in Gas (%)	23.43	23.52	20.98	22.85	17.31
Total Carbon Yield of Output (%)	86.97	84.51	84.05	83.35	80.53

Carbon Yield in Fume, Char, and Gas at 500 °C					
DATA ACQUISITION FILE	FVAG606	FVAG607	FVAG608	FVAG609	FVAG610
Reactor Path Length (inch)	28.75	28.75	28.75	28.75	28.75
Residence Time (sec)	1.5	1.3	1.3	1.1	1.1
Temperature (c)	500	500	500	500	500
Mass of Carbon in Gas :					
1st and 2nd Flow of N ₂ (l/min)	15.70	20.60	20.60	23.80	23.80
Quench Flow (l/min)	23.60	30.90	30.90	35.70	35.70
Total gas Flow at Outlet (l/min)	39.30	51.50	51.50	59.50	59.50
Total Running Time (min)	9.00	6.00	8.00	10.00	10.00
Percentage of CO ₂ at Outlet (%)	0.12	0.08	0.04	0.08	0.08
Volumatic Flow of CO ₂ (l/min)	0.0472	0.0412	0.0206	0.0476	0.0476
Total Volume of CO ₂ (l)	0.4244	0.2472	0.1648	0.4760	0.4760
Mass of CO ₂ (g)	0.7636	0.4447	0.2965	0.8563	0.8563
Mol of CO ₂ (mol)	0.0174	0.0101	0.0067	0.0195	0.0195
Mol of C (mol)	0.0174	0.0101	0.0067	0.0195	0.0195
Total Mass of Carbon in Gas (g)	0.2082	0.1213	0.0809	0.2335	0.2335
Carbon Balance :					
Input :					
Total Input Black Liquor wt. (g)	3.5777	2.1751	1.4012	4.2663	4.3929
Carbon wt % in Black Liquor	33.66	33.66	33.66	33.66	33.66
Carbon wt in Black Liquor (g)	1.2043	0.7321	0.4716	1.4360	1.4787
Output :					
1.Total Fume wt. (g)	0.0196	0.0134	0.0088	0.0185	0.0204
Carbon wt % in Fume (%)	53.89	55.42	55.42	49.14	49.14
Carbon wt in Fume (g)	0.0106	0.0074	0.0049	0.0091	0.0100
2.Char wt. (g)	2.4421	1.5456	1.0306	3.3014	3.5031
Carbon wt % in Char (%)	30.92	30.63	30.63	31.22	31.22
Carbon wt in Char (g)	0.7551	0.4734	0.3157	1.0307	1.0937
3.Total Mass of Carbon in Gas (g)	0.2082	0.1213	0.0809	0.2335	0.2335
Total Carbon wt. of Output (g)	0.9739	0.6021	0.4014	1.2733	1.3372
Carbon Yield in Fume (%)	0.88	1.01	1.03	0.63	0.68
Carbon Yield in Char (%)	62.70	64.66	66.93	71.77	73.96
Carbon Yield in Gas (%)	17.29	16.57	17.14	16.26	15.79
Total Carbon Yield of Output (%)	80.87	82.24	85.11	88.67	90.44

Carbon Yield in Fume, Char, and Gas at 500 ° C					
DATA ACQUISITION FILE	FVAG611	FVAG612	FVAG613	FVAG614	FVAG615
Reactor Path Length (inch)	23.75	23.75	17.75	17.75	12.75
Residence Time (sec)	0.9	0.9	0.7	0.7	0.5
Temperature (c)	500	500	500	500	500
Mass of Carbon in Gas :					
1st and 2nd Flow of N ₂ (l/min)	22.00	22.00	20.00	20.00	20.10
Quench Flow (l/min)	33.00	33.00	30.00	30.00	30.20
Total gas Flow at Outlet (l/min)	55.00	55.00	50.00	50.00	50.30
Total Running Time (min)	10.00	10.00	10.00	10.00	10.00
Percentage of CO ₂ at Outlet (%)	0.10	0.08	0.06	0.08	0.06
Volumatic Flow of CO ₂ (l/min)	0.0550	0.044	0.0300	0.0400	0.0302
Total Volume of CO ₂ (l)	0.5500	0.4400	0.3000	0.4000	0.3018
Mass of CO ₂ (g)	0.9895	0.7916	0.5397	0.7196	0.5429
Mol of CO ₂ (mol)	0.0225	0.0180	0.0123	0.0164	0.0123
Mol of C (mol)	0.0225	0.0180	0.0123	0.0164	0.0123
Total Mass of Carbon in Gas (g)	0.2699	0.2159	0.1472	0.1963	0.1481
Carbon Balance :					
Input :					
Total Input Black Liquor wt. (g)	5.4150	4.9380	3.7626	5.4731	4.3210
Carbon wt % in Black Liquor	33.66	33.66	33.66	33.66	33.66
Carbon wt in Black Liquor (g)	1.8227	1.6621	1.2665	1.8422	1.4544
Output :					
1.Total Fume wt. (g)	0.0241	0.0232	0.0189	0.0245	0.0220
Carbon wt % in Fume (%)	47.68	47.68	44.72	44.72	43.02
Carbon wt in Fume (g)	0.0115	0.0111	0.0085	0.0110	0.0095
2.Char wt. (g)	4.3718	3.9025	3.0763	4.5202	3.6438
Carbon wt % in Char (%)	32.36	32.36	32.23	32.23	32.49
Carbon wt in Char (g)	1.4147	1.2628	0.9915	1.4569	1.1839
3.Total Mass of Carbon in Gas (g)	0.2699	0.2159	0.1472	0.1963	0.1481
Total Carbon wt. of Output (g)	1.6961	1.4898	1.1471	1.6641	1.3414
Carbon Yield in Fume (%)	0.63	0.67	0.67	0.59	0.65
Carbon Yield in Char (%)	77.62	75.98	78.29	79.08	81.40
Carbon Yield in Gas (%)	14.81	12.99	11.62	10.65	10.18
Total Carbon Yield of Output (%)	93.05	89.63	90.58	90.33	92.23

Carbon Yield in Fume, Char, and Gas at 500 ° C			
DATA ACQUISITION FILE	FVAG616	FVAG617	FVAG618
Reactor Path Length (inch)	12.75	9.75	9.75
Residence Time (sec)	0.5	0.3	0.3
Temperature (c)	500	500	500
Mass of Carbon in Gas :			
1st and 2nd Flow of N ₂ (l/min)	20.10	29.40	29.40
Quench Flow (l/min)	33.00	33.00	30.00
Total gas Flow at Outlet (l/min)	53.10	62.40	59.40
Total Running Time (min)	10.00	10.00	9.00
Percentage of CO ₂ at Outlet (%)	0.08	0.04	0.04
Volumatic Flow of CO ₂ (l/min)	0.0425	0.02496	0.0238
Total Volume of CO ₂ (l)	0.4248	0.2496	0.2138
Mass of CO ₂ (g)	0.7642	0.4490	0.3847
Mol of CO ₂ (mol)	0.0174	0.0102	0.0087
Mol of C (mol)	0.0174	0.0102	0.0087
Total Mass of Carbon in Gas (g)	0.2084	0.1225	0.1049
Carbon Balance :			
Input :			
Total Input Black Liquor wt. (g)	5.5464	5.4361	4.4073
Carbon wt % in Black Liquor	33.66	33.66	33.66
Carbon wt in Black Liquor (g)	1.8669	1.8298	1.4835
Output :			
1.Total Fume wt. (g)	0.0224	0.0165	0.0125
Carbon wt % in Fume (%)	43.02	30.77	30.77
Carbon wt in Fume (g)	0.0096	0.0051	0.0038
2.Char wt. (g)	4.7505	4.8722	4.0662
Carbon wt % in Char (%)	32.49	32.16	32.16
Carbon wt in Char (g)	1.5434	1.5669	1.3077
3.Total Mass of Carbon in Gas (g)	0.2084	0.1225	0.1049
Total Carbon wt. of Output (g)	1.7615	1.6944	1.4165
Carbon Yield in Fume (%)	0.52	0.28	0.26
Carbon Yield in Char (%)	82.67	85.63	88.15
Carbon Yield in Gas (%)	11.16	6.69	7.07
Total Carbon Yield of Output (%)	94.35	92.60	95.48

Carbon Yield in Fume, Char, and Gas at 400 °C					
DATA ACQUISITION FILE	FVAG619	FVAG620	FVAG621	FVAG622	FVAG623
Reactor Path Length (inch)	28.75	28.75	28.75	28.75	28.75
Residence Time (sec)	2.0	2.0	1.7	1.7	1.5
Temperature (c)	400	400	400	400	400
Mass of Carbon in Gas :					
1st and 2nd Flow of N ₂ (l/min)	9.90	9.90	14.60	14.60	19.20
Quench Flow (l/min)	14.90	14.90	21.90	21.90	28.80
Total gas Flow at Outlet (l/min)	24.80	24.80	36.50	36.50	48.00
Total Running Time (min)	7.00	8.00	9.00	8.00	8.00
Percentage of CO ₂ at Outlet (%)	0.16	0.20	0.16	0.16	0.14
Volumatic Flow of CO ₂ (l/min)	0.0397	0.0496	0.0584	0.0584	0.0672
Total Volume of CO ₂ (l)	0.2778	0.3968	0.5256	0.4672	0.5376
Mass of CO ₂ (g)	0.4997	0.7138	0.9456	0.8405	0.9671
Mol of CO ₂ (mol)	0.0114	0.0162	0.0215	0.0191	0.0220
Mol of C (mol)	0.0114	0.0162	0.0215	0.0191	0.0220
Total Mass of Carbon in Gas (g)	0.1363	0.1947	0.2579	0.2292	0.2638
Carbon Balance :					
Input :					
Total Input Black Liquor wt. (g)	1.9351	2.8298	4.1128	4.0197	4.6955
Carbon wt % in Black Liquor	33.66	33.66	33.66	33.66	33.66
Carbon wt in Black Liquor (g)	0.6514	0.9525	1.3844	1.3530	1.5805
Output :					
1.Total Fume wt. (g)	0.0079	0.0125	0.0116	0.0127	0.0103
Carbon wt % in Fume (%)	76.29	76.29	66.01	66.01	53.89
Carbon wt in Fume (g)	0.0060	0.0095	0.0077	0.0084	0.0056
2.Char wt. (g)	1.5201	2.1397	3.1248	3.2285	3.7358
Carbon wt % in Char (%)	32.52	32.52	32.98	32.98	32.44
Carbon wt in Char (g)	0.4943	0.6958	1.0306	1.0648	1.2119
3.Total Mass of Carbon in Gas (g)	0.1363	0.1947	0.2579	0.2292	0.2638
Total Carbon wt. of Output (g)	0.6366	0.9001	1.2961	1.3024	1.4812
Carbon Yield in Fume (%)	0.93	1.00	0.55	0.62	0.35
Carbon Yield in Char (%)	75.89	73.05	74.44	78.69	76.68
Carbon Yield in Gas (%)	20.92	20.44	18.63	16.94	16.69
Total Carbon Yield of Output (%)	97.74	94.49	93.62	96.26	93.72

Carbon Yield in Fume, Char, and Gas at 400 °C					
DATA ACQUISITION FILE	FVAG624	FVAG625	FVAG626	FVAG627	FVAG628
Reactor Path Length (inch)	28.75	28.75	28.75	28.75	28.75
Residence Time (sec)	1.5	1.3	1.3	1.1	1.1
Temperature (c)	400	400	400	400	400
Mass of Carbon in Gas :					
1st and 2nd Flow of N ₂ (l/min)	19.20	20.00	20.00	20.20	20.20
Quench Flow (l/min)	28.80	30.00	30.00	30.30	30.30
Total gas Flow at Outlet (l/min)	48.00	50.00	50.00	50.50	50.50
Total Running Time (min)	10.00	8.00	10.00	10.00	9.00
Percentage of CO ₂ at Outlet (%)	0.10	0.06	0.08	0.08	0.06
Volumatic Flow of CO ₂ (l/min)	0.0480	0.0300	0.0400	0.0404	0.0303
Total Volume of CO ₂ (l)	0.4800	0.2400	0.4000	0.4040	0.2727
Mass of CO ₂ (g)	0.8635	0.4318	0.7196	0.7268	0.4906
Mol of CO ₂ (mol)	0.0196	0.0098	0.0164	0.0165	0.0111
Mol of C (mol)	0.0196	0.0098	0.0164	0.0165	0.0111
Total Mass of Carbon in Gas (g)	0.2355	0.1178	0.1963	0.1982	0.1338
Carbon Balance :					
Input :					
Total Input Black Liquor wt. (g)	3.7710	2.3171	4.5125	4.9372	4.1369
Carbon wt % in Black Liquor	33.66	33.66	33.66	33.66	33.66
Carbon wt in Black Liquor (g)	1.2693	0.7799	1.5189	1.6619	1.3925
Output :					
1.Total Fume wt. (g)	0.0088	0.0069	0.0118	0.0151	0.0117
Carbon wt % in Fume (%)	53.89	55.42	55.42	49.14	49.14
Carbon wt in Fume (g)	0.0047	0.0038	0.0065	0.0074	0.0057
2.Char wt. (g)	3.1228	1.9236	3.8421	4.2969	3.6589
Carbon wt % in Char (%)	32.44	32.36	32.36	31.85	31.85
Carbon wt in Char (g)	1.0130	0.6225	1.2433	1.3686	1.1654
3.Total Mass of Carbon in Gas (g)	0.2355	0.1178	0.1963	0.1982	0.1338
Total Carbon wt. of Output (g)	1.2533	0.7441	1.4461	1.5742	1.3049
Carbon Yield in Fume (%)	0.37	0.49	0.43	0.45	0.41
Carbon Yield in Char (%)	79.81	79.81	81.86	82.35	83.69
Carbon Yield in Gas (%)	18.55	15.10	12.92	11.93	9.61
Total Carbon Yield of Output (%)	98.74	95.40	95.21	94.73	93.71

Carbon Yield in Fume, Char, and Gas at 400 ° C					
DATA ACQUISITION FILE	FVAG629	FVAG630	FVAG631	FVAG632	FVAG633
Reactor Path Length (inch)	21.75	21.75	15.75	15.75	11.75
Residence Time (sec)	0.9	0.9	0.7	0.7	0.5
Temperature (c)	400	400	400	400	400
Mass of Carbon in Gas :					
1st and 2nd Flow of N ₂ (l/min)	21.20	21.20	14.80	14.80	17.30
Quench Flow (l/min)	31.80	31.80	22.20	22.20	26.00
Total gas Flow at Outlet (l/min)	53.00	53.00	37.00	37.00	43.30
Total Running Time (min)	10.00	8.00	6.00	10.00	10.00
Percentage of CO ₂ at Outlet (%)	0.04	0.04	0.04	0.04	0.02
Volumatic Flow of CO ₂ (l/min)	0.0212	0.0212	0.0148	0.0148	0.0087
Total Volume of CO ₂ (l)	0.2120	0.1696	0.0888	0.1480	0.0866
Mass of CO ₂ (g)	0.3814	0.3051	0.1598	0.2663	0.1558
Mol of CO ₂ (mol)	0.0087	0.0069	0.0036	0.0061	0.0035
Mol of C (mol)	0.0087	0.0069	0.0036	0.0061	0.0035
Total Mass of Carbon in Gas (g)	0.1040	0.0832	0.0436	0.0726	0.0425
Carbon Balance :					
Input :					
Total Input Black Liquor wt. (g)	3.9668	3.0851	3.5493	4.3890	4.6073
Carbon wt % in Black Liquor	33.66	33.66	33.66	33.66	33.66
Carbon wt in Black Liquor (g)	1.3352	1.0384	1.1947	1.4773	1.5508
Output :					
1.Total Fume wt. (g)	0.0128	0.0078	0.0026	0.0084	0.0149
Carbon wt % in Fume (%)	47.68	67.68	44.72	44.72	43.02
Carbon wt in Fume (g)	0.0061	0.0053	0.0012	0.0038	0.0064
2.Char wt. (g)	3.6146	2.8285	3.4712	4.1884	4.5907
Carbon wt % in Char (%)	31.90	31.90	31.64	31.64	32.61
Carbon wt in Char (g)	1.1531	0.9023	1.0983	1.3252	1.4970
3.Total Mass of Carbon in Gas (g)	0.1040	0.0832	0.0436	0.0726	0.0425
Total Carbon wt. of Output (g)	1.2632	0.9908	1.1430	1.4016	1.5459
Carbon Yield in Fume (%)	0.46	0.51	0.10	0.25	0.41
Carbon Yield in Char (%)	86.36	86.89	91.93	89.70	96.53
Carbon Yield in Gas (%)	7.79	8.01	3.65	4.92	2.74
Total Carbon Yield of Output (%)	94.60	95.41	95.67	94.87	99.68

Carbon Yield in Fume, Char, and Gas at 400 °C		
DATA ACQUISITION FILE	FVAG634	FVAG635
Reactor Path Length (inch)	11.75	9.75
Residence Time (sec)	0.5	0.3
Temperature (c)	400	400
Mass of Carbon in Gas :		
1st and 2nd Flow of N ₂ (l/min)	17.30	21.00
Quench Flow (l/min)	26.00	31.50
Total gas Flow at Outlet (l/min)	20.80	52.50
Total Running Time (min)	10.00	10.00
Percentage of CO ₂ at Outlet (%)	0.02	0.01
Volumatic Flow of CO ₂ (l/min)	0.0042	0.0053
Total Volume of CO ₂ (l)	0.0416	0.0525
Mass of CO ₂ (g)	0.0748	0.0944
Mol of CO ₂ (mol)	0.0017	0.0021
Mol of C (mol)	0.0017	0.0021
Total Mass of Carbon in Gas (g)	0.0204	0.0258
Carbon Balance :		
Input :		
Total Input Black Liquor wt. (g)	4.0943	4.9380
Carbon wt % in Black Liquor	33.66	33.66
Carbon wt in Black Liquor (g)	1.3781	1.6621
Output :		
1.Total Fume wt. (g)	0.0143	0.0170
Carbon wt % in Fume (%)	43.02	30.77
Carbon wt in Fume (g)	0.0062	0.0052
2.Char wt. (g)	4.0140	4.9162
Carbon wt % in Char (%)	32.61	32.00
Carbon wt in Char (g)	1.3090	1.5732
3.Total Mass of Carbon in Gas (g)	0.0204	0.0258
Total Carbon wt. of Output (g)	1.3355	1.6042
Carbon Yield in Fume (%)	0.45	0.31
Carbon Yield in Char (%)	94.98	94.65
Carbon Yield in Gas (%)	1.48	1.55
Total Carbon Yield of Output (%)	96.91	96.51

Nitrogen Yield in Fume, and Char at 600 °C					
DATA ACQUISITION FILE	FVJL601	FVJL602	FVJL603	FVJL604	FVJL605
Date	7/6/96	7/6/96	7/7/96	7/7/96	7/7/96
Raw Material	Valdosta	Valdosta	Valdosta	Valdosta	Valdosta
Particle Size (micron)	90-125	90-125	90-125	90-125	90-125
Reactor Path Length (inch)	28.75	28.75	28.75	28.75	28.75
Residence Time (sec)	2.0	2.0	1.7	1.7	1.5
Temperature (c)	600	600	600	600	600
Nitrogen wt.% in Fume :					
1. Fume Filter Before (g)	0.0874	0.0869	0.0868	0.0861	0.0865
Fume Filter After (g)	0.1023	0.0996	0.0954	0.0952	0.0925
Collected Fume wt. (g)	0.0149	0.0127	0.0086	0.0091	0.006
2. Fume Filter Before (gas outlet) (g)	0.4661	0.4666	0.4685	0.4687	0.4672
Fume Filter After (gas outlet) (g)	0.5053	0.4985	0.4931	0.5028	0.4928
Fume wt. (gas outlet) (g)	0.0392	0.0319	0.0246	0.0341	0.0256
Total Fume wt. in system (g)	0.0541	0.0446	0.0332	0.0432	0.0316
Total Paper weight (g)	0.5535	0.5535	0.5553	0.5548	0.5537
Percentage of Nitrogen (P+F) (%)	0.04	0.04	0.03	0.03	0.01
Percentage of Nitrogen in Paper(%)	0.00	0.00	0.00	0.00	0.00
Nitrogen wt. in Paper+fume (g)	0.0002	0.0002	0.0002	0.0002	0.0001
Nitrogen wt. in Paper (g)	0.00000	0.00000	0.00000	0.00000	0.00000
Nitrogen wt. in Fume (g)	0.0002	0.0002	0.0002	0.0002	0.0001
Nitrogen wt.% in Fume	0.45	0.54	0.53	0.42	0.19
Nitrogen Balance :					
Input :					
Total Input Black Liquor wt. (g)	5.3845	4.4088	4.5022	5.6822	5.5174
Nitrogen wt. % in Black Liquor (%)	0.07	0.07	0.07	0.07	0.07
Nitrogen wt. in Black Liquor (g)	0.003769	0.003086	0.003152	0.003978	0.003862
Output :					
1. Total Fume wt. (g)	0.0541	0.0446	0.0332	0.0432	0.0316
Nitrogen wt. % in Fume (%)	0.45	0.54	0.53	0.42	0.19
Nitrogen wt. in Fume (g)	0.000243	0.000239	0.000177	0.000179	0.000059
2. Char wt. (g)	4.0334	3.3161	3.5597	4.3071	4.2375
Nitrogen wt. % in Char (%)	0.055	0.055	0.055	0.06	0.06
Nitrogen wt. in Char (g)	0.002218	0.001824	0.001958	0.002584	0.002543
Nitrogen Yield in Fume (%)	6.45	7.75	5.60	4.51	1.52
Nitrogen Yield in Char (%)	58.86	59.10	62.12	64.97	65.83
Estimate Nitrogen Yield in Gas(%)	34.70	33.15	32.27	30.52	32.65

Nitrogen Yield in Fume, and Char at 600 °C					
DATA ACQUISITION FILE	FVJL606	FVJL607	FVJL608	FVJL609	FVJL610
Date	7/7/96	7/8/96	7/8/96	7/8/96	7/8/96
Raw Material	Valdosta	Valdosta	Valdosta	Valdosta	Valdosta
Particle Size (micron)	90-125	90-125	90-125	90-125	90-125
Reactor Path Length (inch)	28.75	28.75	28.75	28.75	28.75
Residence Time (sec)	1.5	1.3	1.3	1.1	1.1
Temperature (c)	600	600	600	600	600
Nitrogen wt. % in Fume :					
1. Fume Filter Before (g)	0.0861	0.0869	0.0871	0.0868	0.0879
Fume Filter After (g)	0.0918	0.0907	0.0921	0.0899	0.0908
Collected Fume wt. (g)	0.0057	0.0038	0.0050	0.0031	0.0029
2. Fume Filter Before (gas outlet) (g)	0.4637	0.4696	0.4677	0.4705	0.4658
Fume Filter After (gas outlet) (g)	0.4906	0.4882	0.4835	0.4874	0.4818
Fume wt. (gas outlet) (g)	0.0269	0.0186	0.0158	0.0169	0.0160
Total Fume wt. in system (g)	0.0326	0.0224	0.0208	0.0200	0.0189
Total Paper weight (g)	0.5498	0.5565	0.5548	0.5573	0.5537
Percentage of Nitrogen (P+F) (%)	0.01	0.01	0.01	0.01	0.01
Percentage of Nitrogen in Paper(%)	0.00	0.00	0.00	0.00	0.00
Nitrogen wt. in Paper+fume (g)	0.0001	0.0001	0.0001	0.0001	0.0001
Nitrogen wt. in Paper (g)	0.00000	0.00000	0.00000	0.00000	0.00000
Nitrogen wt. in Fume (g)	0.0001	0.0001	0.0001	0.0001	0.0001
Nitrogen wt. % in Fume	0.18	0.26	0.28	0.29	0.30
Nitrogen Balance :					
Input :					
Total Input Black Liquor wt. (g)	5.8924	4.8849	4.5211	4.9114	4.7345
Nitrogen wt. % in Black Liquor (%)	0.07	0.07	0.07	0.07	0.07
Nitrogen wt. in Black Liquor (g)	0.004125	0.003419	0.003165	0.003438	0.003314
Output :					
1. Total Fume wt. (g)	0.0326	0.0224	0.0208	0.0200	0.0189
Nitrogen wt. % in Fume (%)	0.18	0.26	0.28	0.29	0.30
Nitrogen wt. in Fume (g)	0.000058	0.000058	0.000058	0.000058	0.000057
2. Char wt. (g)	4.5689	3.8534	3.5371	3.9616	3.8025
Nitrogen wt. % in Char (%)	0.06	0.06	0.06	0.06	0.06
Nitrogen wt. in Char (g)	0.002741	0.002312	0.002122	0.002377	0.002282
Nitrogen Yield in Fume (%)	1.41	1.69	1.82	1.68	1.73
Nitrogen Yield in Char (%)	66.46	67.61	67.06	69.14	68.84
Estimate Nitrogen Yield in Gas(%)	32.13	30.69	31.12	29.18	29.43

Nitrogen Yield in Fume, and Char at 600 °C					
DATA ACQUISITION FILE	FVJL611	FVJL612	FVJL613	FVJL614	FVJL615
Date	7/8/96	7/8/96	7/9/96	7/9/96	7/9/96
Raw Material	Valdosta	Valdosta	Valdosta	Valdosta	Valdosta
Particle Size (micron)	90-125	90-125	90-125	90-125	90-125
Reactor Path Length (inch)	25.75	25.75	19.75	19.75	13.75
Residence Time (sec)	0.9	0.9	0.7	0.7	0.5
Temperature (c)	600	600	600	600	600
Nitrogen wt.% in Fume :					
1. Fume Filter Before (g)	0.0861	0.0876	0.0876	0.0866	0.0868
Fume Filter After (g)	0.0901	0.0907	0.0913	0.0908	0.0905
Collected Fume wt. (g)	0.0040	0.0031	0.0037	0.0042	0.0037
2. Fume Filter Before (gas outlet) (g)	0.4656	0.4672	0.4791	0.4739	0.4731
Fume Filter After (gas outlet) (g)	0.4852	0.4851	0.4943	0.4906	0.4885
Fume wt. (gas outlet) (g)	0.0196	0.0179	0.0152	0.0167	0.0154
Total Fume wt. in system (g)	0.0236	0.0210	0.0189	0.0209	0.0191
Total Paper weight (g)	0.5517	0.5548	0.5667	0.5605	0.5599
Percentage of Nitrogen (P+F) (%)	0.01	0.01	0.01	0.01	0.005
Percentage of Nitrogen in Paper(%)	0.00	0.00	0.00	0.00	0.00
Nitrogen wt. in Paper+fume (g)	0.0001	0.0001	0.0001	0.0001	0.0000
Nitrogen wt. in Paper (g)	0.00000	0.00000	0.00000	0.00000	0.00000
Nitrogen wt. in Fume (g)	0.0001	0.0001	0.0001	0.0001	0.0000
Nitrogen wt.% in Fume	0.24	0.27	0.31	0.28	0.15
Nitrogen Balance :					
Input :					
Total Input Black Liquor wt. (g)	5.4536	4.5087	4.494	4.7983	4.4244
Nitrogen wt. % in Black Liquor (%)	0.07	0.07	0.07	0.07	0.07
Nitrogen wt. in Black Liquor (g)	0.003818	0.003156	0.003146	0.003359	0.003097
Output :					
1. Total Fume wt. (g)	0.0236	0.0210	0.0189	0.0209	0.0191
Nitrogen wt. % in Fume (%)	0.24	0.27	0.31	0.28	0.15
Nitrogen wt. in Fume (g)	0.000058	0.000058	0.000059	0.000058	0.000029
2. Char wt. (g)	4.2010	3.6627	3.6304	3.5083	3.7689
Nitrogen wt. % in Char (%)	0.065	0.06	0.065	0.07	0.065
Nitrogen wt. in Char (g)	0.002731	0.002198	0.002360	0.002456	0.002450
Nitrogen Yield in Fume (%)	1.51	1.82	1.86	1.73	0.93
Nitrogen Yield in Char (%)	71.53	69.63	75.01	73.12	79.10
Estimate Nitrogen Yield in Gas(%)	26.96	28.54	23.13	25.15	19.97

Nitrogen Yield in Fume, and Char at 600 °C			
DATA ACQUISITION FILE	FVJL616	FVJL617	FVJL618
Date	7/9/96	7/9/96	7/9/96
Raw Material	Valdosta	Valdosta	Valdosta
Particle Size (micron)	90-125	90-125	90-125
Reactor Path Length (inch)	13.75	9.75	9.75
Residence Time (sec)	0.5	0.3	0.3
Temperature (c)	600	600	600
Nitrogen wt.% in Fume :			
1. Fume Filter Before (g)	0.0864	0.0869	0.0861
Fume Filter After (g)	0.0904	0.0912	0.0914
Collected Fume wt. (g)	0.0040	0.0043	0.0053
2. Fume Filter Before (gas outlet) (g)	0.4796	0.4681	0.4697
Fume Filter After (gas outlet) (g)	0.5001	0.4909	0.4958
Fume wt. (gas outlet) (g)	0.0205	0.0228	0.0261
Total Fume wt. in system (g)	0.0245	0.0271	0.0314
Total Paper weight (g)	0.5660	0.5550	0.5558
Percentage of Nitrogen (P+F) (%)	0.005	0.005	0.005
Percentage of Nitrogen in Paper(%)	0.00	0.00	0.00
Nitrogen wt. in Paper+fume (g)	0.0000	0.0000	0.0000
Nitrogen wt. in Paper (g)	0.00000	0.00000	0.00000
Nitrogen wt. in Fume (g)	0.0000	0.0000	0.0000
Nitrogen wt.% in Fume	0.12	0.11	0.09
Nitrogen Balance :			
Input :			
Total Input Black Liquor wt. (g)	5.4212	4.5901	5.5056
Nitrogen wt. % in Black Liquor (%)	0.07	0.07	0.07
Nitrogen wt. in Black Liquor (g)	0.003795	0.003213	0.003854
Output :			
1. Total Fume wt. (g)	0.0245	0.0271	0.0314
Nitrogen wt. % in Fume (%)	0.12	0.11	0.09
Nitrogen wt. in Fume (g)	0.000029525	0.000029105	0.00002936
2. Char wt. (g)	4.5995	4.2696	5.0851
Nitrogen wt. % in Char (%)	0.065	0.065	0.065
Nitrogen wt. in Char (g)	0.002990	0.002775	0.003305
Nitrogen Yield in Fume (%)	0.78	0.91	0.76
Nitrogen Yield in Char (%)	78.78	86.37	85.77
Estimate Nitrogen Yield in Gas(%)	20.44	12.72	13.47

Nitrogen Yield in Fume, and Char at 500 °C					
DATA ACQUISITION FILE	FVAG601	FVAG602	FVAG603	FVAG604	FVAG605
Date	8/7/96	8/7/96	8/8/96	8/8/96	8/8/96
Raw Material	Valdosta	Valdosta	Valdosta	Valdosta	Valdosta
Particle Size (micron)	90-125	90-125	90-125	90-125	90-125
Reactor Path Length (inch)	28.75	28.75	28.75	28.75	28.75
Residence Time (sec)	2.0	2.0	1.7	1.7	1.5
Temperature (c)	500	500	500	500	500
Nitrogen wt.% in Fume :					
1. Fume Filter Before (g)	0.0874	0.0881	0.0876	0.0869	0.0878
Fume Filter After (g)	0.1003	0.0996	0.0961	0.0916	0.0926
Collected Fume wt. (g)	0.0129	0.0115	0.0085	0.0047	0.0048
2. Fume Filter Before (gas outlet) (g)	0.4709	0.4662	0.4685	0.4694	0.4745
Fume Filter After (gas outlet) (g)	0.4981	0.4923	0.4921	0.4856	0.4932
Fume wt. (gas outlet) (g)	0.0272	0.0261	0.0236	0.0162	0.0187
Total Fume wt. in system (g)	0.0401	0.0376	0.0321	0.0209	0.0235
Total Paper weight (g)	0.5583	0.5543	0.5561	0.5563	0.5623
Percentage of Nitrogen (P+F) (%)	0.04	0.04	0.03	0.03	0.01
Percentage of Nitrogen in Paper(%)	0.00	0.00	0.00	0.00	0.00
Nitrogen wt. in Paper+fume (g)	0.0002	0.0002	0.0002	0.0002	0.0001
Nitrogen wt. in Paper (g)	0.00000	0.00000	0.00000	0.00000	0.00000
Nitrogen wt. in Fume (g)	0.0002	0.0002	0.0002	0.0002	0.0001
Nitrogen wt.% in Fume	0.60	0.63	0.55	0.83	0.25
Nitrogen Balance :					
Input :					
Total Input Black Liquor wt. (g)	5.0837	4.5304	4.2378	3.1126	2.9778
Nitrogen wt. % in Black Liquor (%)	0.07	0.07	0.07	0.07	0.07
Nitrogen wt. in Black Liquor (g)	0.003559	0.003171	0.002966	0.002179	0.002084
Output :					
1. Total Fume wt. (g)	0.0401	0.0376	0.0321	0.0209	0.0235
Nitrogen wt. % in Fume (%)	0.60	0.63	0.55	0.83	0.25
Nitrogen wt. in Fume (g)	0.000239	0.000237	0.000176	0.000173	0.000059
2. Char wt. (g)	3.3487	2.8562	2.7995	1.9759	2.0084
Nitrogen wt. % in Char (%)	0.065	0.065	0.065	0.065	0.065
Nitrogen wt. in Char (g)	0.002177	0.001857	0.001820	0.001284	0.001305
Nitrogen Yield in Fume (%)	6.73	7.47	5.95	7.95	2.81
Nitrogen Yield in Char (%)	61.17	58.54	61.34	58.95	62.63
Estimate Nitrogen Yield in Gas(%)	32.11	33.99	32.71	33.11	34.56

Nitrogen Yield in Fume, and Char at 500 °C					
DATA ACQUISITION FILE	FVAG606	FVAG607	FVAG608	FVAG609	FVAG610
Date	8/8/96	8/8/96	8/8/96	8/13/96	8/13/96
Raw Material	Valdosta	Valdosta	Valdosta	Valdosta	Valdosta
Particle Size (micron)	90-125	90-125	90-125	90-125	90-125
Reactor Path Length (inch)	28.75	28.75	28.75	28.75	28.75
Residence Time (sec)	1.5	1.3	1.3	1.1	1.1
Temperature (c)	500	500	500	500	500
Nitrogen wt. % in Fume :					
1. Fume Filter Before (g)	0.0883	0.0881	0.0873	0.0857	0.0861
Fume Filter After (g)	0.0928	0.0906	0.0893	0.0882	0.0889
Collected Fume wt. (g)	0.0045	0.0025	0.002	0.0025	0.0028
2. Fume Filter Before (gas outlet) (g)	0.4687	0.4707	0.4727	0.4722	0.4663
Fume Filter After (gas outlet) (g)	0.4838	0.4816	0.4795	0.4882	0.4839
Fume wt. (gas outlet) (g)	0.0151	0.0109	0.0068	0.0160	0.0176
Total Fume wt. in system (g)	0.0196	0.0134	0.0088	0.0185	0.0204
Total Paper weight (g)	0.5570	0.5588	0.5600	0.5579	0.5524
Percentage of Nitrogen (P+F) (%)	0.01	0.01	0.01	0.01	0.01
Percentage of Nitrogen in Paper (%)	0.00	0.00	0.00	0.00	0.00
Nitrogen wt. in Paper+fume (g)	0.0001	0.0001	0.0001	0.0001	0.0001
Nitrogen wt. in Paper (g)	0.0000	0.00000	0.00000	0.00000	0.00000
Nitrogen wt. in Fume (g)	0.0001	0.0001	0.0001	0.0001	0.0001
Nitrogen wt. % in Fume	0.29	0.43	0.65	0.31	0.28
Nitrogen Balance :					
Input :					
Total Input Black Liquor wt. (g)	3.5777	2.1751	1.4012	4.2663	4.3929
Nitrogen wt. % in Black Liquor (%)	0.07	0.07	0.07	0.07	0.07
Nitrogen wt. in Black Liquor (g)	0.002504	0.001523	0.000981	0.002986	0.003075
Output :					
1. Total Fume wt. (g)	0.0196	0.0134	0.0088	0.0185	0.0204
Nitrogen wt. % in Fume (%)	0.29	0.43	0.65	0.31	0.28
Nitrogen wt. in Fume (g)	0.000058	0.000057	0.000057	0.000058	0.000057
2. Char wt. (g)	2.4421	1.5456	1.0306	3.3014	3.5031
Nitrogen wt. % in Char (%)	0.065	0.065	0.065	0.065	0.06
Nitrogen wt. in Char (g)	0.001587	0.001005	0.000670	0.002146	0.002102
Nitrogen Yield in Fume (%)	2.30	3.76	5.80	1.93	1.86
Nitrogen Yield in Char (%)	63.38	65.98	68.30	71.86	68.35
Estimate Nitrogen Yield in Gas(%)	34.31	30.26	25.90	26.21	29.78

Nitrogen Yield in Fume, and Char at 500 °C					
DATA ACQUISITION FILE	FVAG611	FVAG612	FVAG613	FVAG614	FVAG615
Date	8/13/96	8/13/96	8/14/96	8/14/96	8/14/96
Raw Material	Valdosta	Valdosta	Valdosta	Valdosta	Valdosta
Particle Size (micron)	90-125	90-125	90-125	90-125	90-125
Reactor Path Length (inch)	23.75	23.75	17.75	17.75	12.75
Residence Time (sec)	0.9	0.9	0.7	0.7	0.5
Temperature (c)	500	500	500	500	500
Nitrogen wt.% in Fume :					
1. Fume Filter Before (g)	0.0865	0.0872	0.0871	0.0867	0.0858
Fume Filter After (g)	0.0906	0.0901	0.0892	0.0904	0.0888
Collected Fume wt. (g)	0.0041	0.0029	0.0021	0.0037	0.003
2. Fume Filter Before (gas outlet) (g)	0.4702	0.4706	0.4693	0.4701	0.4711
Fume Filter After (gas outlet) (g)	0.4902	0.4909	0.4861	0.4909	0.4901
Fume wt. (gas outlet) (g)	0.0200	0.0203	0.0168	0.0208	0.0190
Total Fume wt. in system (g)	0.0241	0.0232	0.0189	0.0245	0.0220
Total Paper weight (g)	0.5567	0.5578	0.5564	0.5568	0.5569
Percentage of Nitrogen (P+F) (%)	0.01	0.01	0.01	0.01	0.005
Percentage of Nitrogen in Paper(%)	0.00	0.00	0.00	0.00	0.00
Nitrogen wt. in Paper+fume (g)	0.0001	0.0001	0.0001	0.0001	0.0000
Nitrogen wt. in Paper (g)	0.0000	0.00000	0.00000	0.00000	0.00000
Nitrogen wt. in Fume (g)	0.0001	0.0001	0.0001	0.0001	0.0000
Nitrogen wt.% in Fume	0.24	0.25	0.30	0.24	0.13
Nitrogen Balance :					
Input :					
Total Input Black Liquor wt. (g)	5.415	4.938	3.7626	5.4731	4.321
Nitrogen wt. % in Black Liquor (%)	0.07	0.07	0.07	0.07	0.07
Nitrogen wt. in Black Liquor (g)	0.003791	0.003457	0.002634	0.003831	0.003025
Output :					
1. Total Fume wt. (g)	0.0241	0.0232	0.0189	0.0245	0.0220
Nitrogen wt. % in Fume (%)	0.24	0.25	0.30	0.24	0.13
Nitrogen wt. in Fume (g)	0.000058	0.000058	0.000058	0.000058	0.000029
2. Char wt. (g)	4.3718	3.9025	3.0763	4.5202	3.6438
Nitrogen wt. % in Char (%)	0.065	0.065	0.065	0.065	0.065
Nitrogen wt. in Char (g)	0.002842	0.002537	0.002000	0.002938	0.002368
Nitrogen Yield in Fume (%)	1.53	1.68	2.18	1.52	0.96
Nitrogen Yield in Char (%)	74.97	73.38	75.92	76.69	78.30
Estimate Nitrogen Yield in Gas(%)	23.50	24.93	21.90	21.79	20.74

Nitrogen Yield in Fume, and Char at 500 °C			
DATA ACQUISITION FILE	FVAG616	FVAG617	FVAG618
Date	8/14/96	8/14/96	8/14/96
Raw Material	Valdosta	Valdosta	Valdosta
Particle Size (micron)	90-125	90-125	90-125
Reactor Path Length (inch)	12.75	9.75	9.75
Residence Time (sec)	0.5	0.3	0.3
Temperature (c)	500	500	500
Nitrogen wt.% in Fume :			
1. Fume Filter Before (g)	0.0869	0.0867	0.0864
Fume Filter After (g)	0.0898	0.0884	0.0881
Collected Fume wt. (g)	0.0029	0.0017	0.0017
2. Fume Filter Before (gas outlet) (g)	0.4716	0.4663	0.4733
Fume Filter After (gas outlet) (g)	0.4911	0.4811	0.4841
Fume wt. (gas outlet) (g)	0.0195	0.0148	0.0108
Total Fume wt. in system (g)	0.0224	0.0165	0.0125
Total Paper weight (g)	0.5585	0.5530	0.5597
Percentage of Nitrogen (P+F) (%)	0.005	0.005	0.005
Percentage of Nitrogen in Paper(%)	0.00	0.00	0.00
Nitrogen wt. in Paper+fume (g)	0.0000	0.0000	0.0000
Nitrogen wt. in Paper (g)	0.0000	0.00000	0.00000
Nitrogen wt. in Fume (g)	0.0000	0.0000	0.0000
Nitrogen wt.% in Fume	0.13	0.17	0.23
Nitrogen Balance :			
Input :			
Total Input Black Liquor wt. (g)	5.5464	5.4361	4.4073
Nitrogen wt. % in Black Liquor (%)	0.07	0.07	0.07
Nitrogen wt. in Black Liquor (g)	0.003882	0.003805	0.003085
Output :			
1. Total Fume wt. (g)	0.0224	0.0165	0.0125
Nitrogen wt. % in Fume (%)	0.13	0.17	0.23
Nitrogen wt. in Fume (g)	0.000029	0.000028	0.000029
2. Char wt. (g)	4.7505	4.8722	4.0662
Nitrogen wt. % in Char (%)	0.065	0.07	0.07
Nitrogen wt. in Char (g)	0.003088	0.003411	0.002846
Nitrogen Yield in Fume (%)	0.75	0.75	0.93
Nitrogen Yield in Char (%)	79.53	89.63	92.26
Estimate Nitrogen Yield in Gas(%)	19.72	9.62	6.81

Nitrogen Yield in Fume, and Char at 400 °C					
DATA ACQUISITION FILE	FVAG619	FVAG620	FVAG621	FVAG622	FVAG623
Date	8/15/96	8/15/96	8/15/96	8/15/96	8/15/96
Raw Material	Valdosta	Valdosta	Valdosta	Valdosta	Valdosta
Particle Size (micron)	90-125	90-125	90-125	90-125	90-125
Reactor Path Length (inch)	28.75	28.75	28.75	28.75	28.75
Residence Time (sec)	2.0	2.0	1.7	1.7	1.5
Temperature (c)	400	400	400	400	400
Nitrogen wt.% in Fume :					
1. Fume Filter Before (g)	0.0866	0.0872	0.0854	0.0854	0.0864
Fume Filter After (g)	0.0883	0.0902	0.0874	0.0876	0.0878
Collected Fume wt. (g)	0.0017	0.0030	0.0020	0.0022	0.0014
2. Fume Filter Before (gas outlet) (g)	0.4703	0.4713	0.4702	0.4656	0.4732
Fume Filter After (gas outlet) (g)	0.4765	0.4808	0.4798	0.4761	0.4821
Fume wt. (gas outlet) (g)	0.0062	0.0095	0.0096	0.0105	0.0089
Total Fume wt. in system (g)	0.0079	0.0125	0.0116	0.0127	0.0103
Total Paper weight (g)	0.5569	0.5585	0.5556	0.5510	0.5596
Percentage of Nitrogen (P+F) (%)	0.04	0.04	0.03	0.03	0.01
Percentage of Nitrogen in Paper(%)	0.00	0.00	0.00	0.00	0.00
Nitrogen wt. in Paper+fume (g)	0.0002	0.0002	0.0002	0.0002	0.0001
Nitrogen wt. in Paper (g)	0.0000	0.0000	0.0000	0.0000	0.0000
Nitrogen wt. in Fume (g)	0.0002	0.0002	0.0002	0.0002	0.0001
Nitrogen wt.% in Fume	2.86	1.83	1.47	1.33	0.55
Nitrogen Balance :					
Input :					
Total Input Black Liquor wt. (g)	1.9351	2.8298	4.1128	4.0197	4.6955
Nitrogen wt. % in Black Liquor (%)	0.07	0.07	0.07	0.07	0.07
Nitrogen wt. in Black Liquor (g)	0.001355	0.001981	0.002879	0.002814	0.003287
Output :					
1. Total Fume wt. (g)	0.0079	0.0125	0.0116	0.0127	0.0103
Nitrogen wt. % in Fume (%)	2.86	1.83	1.47	1.33	0.55
Nitrogen wt. in Fume (g)	0.000226	0.000228	0.000170	0.000169	0.000057
2. Char wt. (g)	1.5201	2.1397	3.1248	3.2285	3.7358
Nitrogen wt. % in Char (%)	0.06	0.06	0.06	0.06	0.06
Nitrogen wt. in Char (g)	0.000912	0.001284	0.001875	0.001937	0.002241
Nitrogen Yield in Fume (%)	16.68	11.53	5.91	6.01	1.73
Nitrogen Yield in Char (%)	67.33	64.81	65.12	68.84	68.20
Estimate Nitrogen Yield in Gas(%)	15.99	23.66	28.97	25.15	30.07

Nitrogen Yield in Fume, and Char at 400 °C					
DATA ACQUISITION FILE	FVAG624	FVAG625	FVAG626	FVAG627	FVAG628
Date	8/15/96	8/16/96	8/16/96	8/16/96	8/16/96
Raw Material	Valdosta	Valdosta	Valdosta	Valdosta	Valdosta
Particle Size (micron)	90-125	90-125	90-125	90-125	90-125
Reactor Path Length (inch)	28.75	28.75	28.75	28.75	28.75
Residence Time (sec)	1.5	1.3	1.3	1.1	1.1
Temperature (c)	400	400	400	400	400
Nitrogen wt.% in Fume :					
1. Fume Filter Before (g)	0.0878	0.0861	0.0861	0.0862	0.0867
Fume Filter After (g)	0.0891	0.0871	0.0877	0.0885	0.0884
Collected Fume wt. (g)	0.0013	0.0010	0.0016	0.0023	0.0017
2. Fume Filter Before (gas outlet) (g)	0.4709	0.4692	0.4711	0.4706	0.4741
Fume Filter After (gas outlet) (g)	0.4784	0.4751	0.4813	0.4834	0.4841
Fume wt. (gas outlet) (g)	0.0075	0.0059	0.0102	0.0128	0.0100
Total Fume wt. in system (g)	0.0088	0.0069	0.0118	0.0151	0.0117
Total Paper weight (g)	0.5587	0.5553	0.5572	0.5568	0.5608
Percentage of Nitrogen (P+F) (%)	0.01	0.01	0.01	0.01	0.01
Percentage of Nitrogen in Paper(%)	0.00	0.00	0.00	0.00	0.00
Nitrogen wt. in Paper+fume (g)	0.0001	0.0001	0.0001	0.0001	0.0001
Nitrogen wt. in Paper (g)	0.0000	0.0000	0.0000	0.0000	0.0000
Nitrogen wt. in Fume (g)	0.0001	0.0001	0.0001	0.0001	0.0001
Nitrogen wt.% in Fume	0.64	0.81	0.48	0.38	0.49
Nitrogen Balance :					
Input :					
Total Input Black Liquor wt. (g)	3.771	2.3171	4.5125	4.9372	4.1369
Nitrogen wt. % in Black Liquor (%)	0.07	0.07	0.07	0.07	0.07
Nitrogen wt. in Black Liquor (g)	0.002640	0.001622	0.003159	0.003456	0.002896
Output :					
1. Total Fume wt. (g)	0.0088	0.0069	0.0118	0.0151	0.0117
Nitrogen wt. % in Fume (%)	0.64	0.81	0.48	0.38	0.49
Nitrogen wt. in Fume (g)	0.000057	0.000056	0.000057	0.000057	0.000057
2. Char wt. (g)	3.1228	1.9236	3.8421	4.2969	3.6589
Nitrogen wt. % in Char (%)	0.06	0.06	0.06	0.06	0.06
Nitrogen wt. in Char (g)	0.001874	0.001154	0.002305	0.002578	0.002195
Nitrogen Yield in Fume (%)	2.15	3.47	1.80	1.65	1.98
Nitrogen Yield in Char (%)	70.98	71.16	72.98	74.60	75.81
Estimate Nitrogen Yield in Gas(%)	26.87	25.38	25.22	23.75	22.21

Nitrogen Yield in Fume, and Char at 400 °C					
DATA ACQUISITION FILE	FVAG629	FVAG630	FVAG631	FVAG632	FVAG633
Date	8/16/96	8/16/96	8/18/96	8/18/96	8/18/96
Raw Material	Valdosta	Valdosta	Valdosta	Valdosta	Valdosta
Particle Size (micron)	90-125	90-125	90-125	90-125	90-125
Reactor Path Length (inch)	23.75	23.75	17.75	17.75	12.75
Residence Time (sec)	0.9	0.9	0.7	0.7	0.5
Temperature (c)	400	400	400	400	400
Nitrogen wt.% in Fume :					
1. Fume Filter Before (g)	0.0859	0.0862	0.0879	0.0852	0.0867
Fume Filter After (g)	0.0874	0.0872	0.0881	0.0871	0.0889
Collected Fume wt. (g)	0.0015	0.0010	0.0002	0.0019	0.0022
2. Fume Filter Before (gas outlet) (g)	0.4751	0.4721	0.4709	0.4724	0.4731
Fume Filter After (gas outlet) (g)	0.4864	0.4789	0.4733	0.4789	0.4858
Fume wt. (gas outlet) (g)	0.0113	0.0068	0.0024	0.0065	0.0127
Total Fume wt. in system (g)	0.0128	0.0078	0.0026	0.0084	0.0149
Total Paper weight (g)	0.5610	0.5583	0.5588	0.5576	0.5598
Percentage of Nitrogen (P+F) (%)	0.01	0.01	0.01	0.01	0.005
Percentage of Nitrogen in Paper(%)	0.00	0.00	0.00	0.00	0.00
Nitrogen wt. in Paper+fume (g)	0.0001	0.0001	0.0001	0.0001	0.0000
Nitrogen wt. in Paper (g)	0.0000	0.00000	0.00000	0.00000	0.00000
Nitrogen wt. in Fume (g)	0.0001	0.0001	0.0001	0.0001	0.0000
Nitrogen wt.% in Fume	0.45	0.73	2.16	0.67	0.19
Nitrogen Balance :					
Input :					
Total Input Black Liquor wt. (g)	3.9668	3.0851	3.5493	4.3890	4.6073
Nitrogen wt. % in Black Liquor (%)	0.07	0.07	0.07	0.07	0.07
Nitrogen wt. in Black Liquor (g)	0.002777	0.002160	0.002485	0.003072	0.003225
Output :					
1. Total Fume wt. (g)	0.0128	0.0078	0.0026	0.0084	0.0149
Nitrogen wt. % in Fume (%)	0.45	0.73	2.16	0.67	0.19
Nitrogen wt. in Fume (g)	0.000057	0.000057	0.000056	0.000057	0.000029
2. Char wt. (g)	3.6146	2.8285	3.4712	4.1884	4.5907
Nitrogen wt. % in Char (%)	0.06	0.06	0.06	0.06	0.06
Nitrogen wt. in Char (g)	0.002169	0.001697	0.002083	0.002513	0.002754
Nitrogen Yield in Fume (%)	2.07	2.62	2.26	1.84	0.89
Nitrogen Yield in Char (%)	78.10	78.59	83.83	81.80	85.41
Estimate Nitrogen Yield in Gas(%)	19.83	18.79	13.91	16.36	13.70

Nitrogen Yield in Fume, and Char at 400 °C		
DATA ACQUISITION FILE	FVAG634	FVAG635
Date	8/18/96	8/18/96
Raw Material	Valdosta	Valdosta
Particle Size (micron)	90-125	90-125
Reactor Path Length (inch)	12.75	9.75
Residence Time (sec)	0.5	0.3
Temperature (c)	400	400
Nitrogen wt. % in Fume :		
1. Fume Filter Before (g)	0.0852	0.0865
Fume Filter After (g)	0.0872	0.0889
Collected Fume wt. (g)	0.002	0.0024
2. Fume Filter Before (gas outlet) (g)	0.4766	0.4762
Fume Filter After (gas outlet) (g)	0.4889	0.4908
Fume wt. (gas outlet) (g)	0.0123	0.0146
Total Fume wt. in system (g)	0.0143	0.0170
Total Paper weight (g)	0.5618	0.5627
Percentage of Nitrogen (P+F) (%)	0.005	0.005
Percentage of Nitrogen in Paper(%)	0.00	0.00
Nitrogen wt. in Paper+fume (g)	0.000029	0.000029
Nitrogen wt. in Paper (g)	0.0000	0.0000
Nitrogen wt. in Fume (g)	0.000029	0.000029
Nitrogen wt. % in Fume	0.20	0.17
Nitrogen Balance :		
Input :		
Total Input Black Liquor wt. (g)	4.0943	4.938
Nitrogen wt. % in Black Liquor (%)	0.07	0.07
Nitrogen wt. in Black Liquor (g)	0.002866	0.003457
Output :		
1. Total Fume wt. (g)	0.0143	0.0170
Nitrogen wt. % in Fume (%)	0.20	0.17
Nitrogen wt. in Fume (g)	0.000029	0.000029
2. Char wt. (g)	4.0140	4.9162
Nitrogen wt. % in Char (%)	0.06	0.069
Nitrogen wt. in Char (g)	0.002408	0.003392
Nitrogen Yield in Fume (%)	1.01	0.84
Nitrogen Yield in Char (%)	84.03	98.14
Estimate Nitrogen Yield in Gas(%)	14.96	1.03

Sulfur Yield in Fume, and Char at 600 °C					
DATA ACQUISITION FILE	FVJL601	FVJL602	FVJL603	FVJL604	FVJL605
Date	7/6/96	7/6/96	7/7/96	7/7/96	7/7/96
Raw Material	Valdosta	Valdosta	Valdosta	Valdosta	Valdosta
Particle Size (micron)	90-125	90-125	90-125	90-125	90-125
Reactor Path Length (inch)	28.75	28.75	28.75	28.75	28.75
Residence Time (sec)	2.0	2.0	1.7	1.7	1.5
Temperature (c)	600	600	600	600	600
Sulfur wt.% in Fume					
1. Fume Filter Before (g)	0.0874	0.0869	0.0868	0.0861	0.0865
Fume Filter After (g)	0.1023	0.0996	0.0954	0.0952	0.0925
Collected Fume wt. (g)	0.0149	0.0127	0.0086	0.0091	0.006
2. Fume Filter Before (gas outlet) (g)	0.4661	0.4666	0.4685	0.4687	0.4672
Fume Filter After (gas outlet) (g)	0.5053	0.4985	0.4931	0.5028	0.4928
Fume wt. (gas outlet) (g)	0.0392	0.0319	0.0246	0.0341	0.0256
Total Fume wt. in system (g)	0.0541	0.0446	0.0332	0.0432	0.0316
Total Paper weight (g)	0.5535	0.5535	0.5553	0.5548	0.5537
Percentage of Sulfur (P+F) (%)	0.24	0.24	0.16	0.16	0.06
Percentage of Sulfur in Paper (%)	0.00	0.00	0.00	0.00	0.00
Sulfur wt. in Paper+fume (g)	0.0015	0.0014	0.0009	0.0010	0.0004
Sulfur wt. in Paper (g)	0.00000	0.00000	0.00000	0.00000	0.00000
Sulfur wt. in Fume (g)	0.0015	0.0014	0.0009	0.0010	0.0004
Sulfur wt.% in Fume	2.70	3.22	2.84	2.21	1.11
Sulfur Balance :					
Input :					
Total Input Black Liquor wt. (g)	5.3845	4.4088	4.5022	5.6822	5.5174
Sulfur wt. % in Black Liquor (%)	2.44	2.44	2.44	2.44	2.44
Sulfur wt. in Black Liquor (g)	0.1314	0.1076	0.1099	0.1386	0.1346
Output :					
1. Total Fume wt. (g)	0.0541	0.0446	0.0332	0.0432	0.0316
Sulfur wt. % in Fume (%)	2.70	3.22	2.84	2.21	1.11
Sulfur wt. in Fume (g)	0.001458	0.001435	0.000942	0.000957	0.000351
2. Char wt. (g)	4.0334	3.3161	3.5597	4.3071	4.2375
Sulfur wt. % in Char (%)	1.28	1.20	1.32	1.22	1.28
Sulfur wt. in Char (g)	0.0516	0.0398	0.0470	0.0525	0.0542
Sulfur Yield in Fume (%)	1.11	1.33	0.86	0.69	0.26
Sulfur Yield in Char (%)	39.30	36.99	42.77	37.90	40.29
Estimate Sulfur Yield in Gas (%)	59.59	61.67	56.37	61.41	59.45

Sulfur Yield in Fume, and Char at 600 °C					
DATA ACQUISITION FILE	FVJL606	FVJL607	FVJL608	FVJL609	FVJL610
Date	7/7/96	7/8/96	7/8/96	7/8/96	7/8/96
Raw Material	Valdosta	Valdosta	Valdosta	Valdosta	Valdosta
Particle Size (micron)	90-125	90-125	90-125	90-125	90-125
Reactor Path Length (inch)	28.75	28.75	28.75	28.75	28.75
Residence Time (sec)	1.5	1.3	1.3	1.1	1.1
Temperature (c)	600	600	600	600	600
Sulfur wt. % in Fume :					
1. Fume Filter Before (g)	0.0861	0.0869	0.0871	0.0868	0.0879
Fume Filter After (g)	0.0918	0.0907	0.0921	0.0899	0.0908
Collected Fume wt. (g)	0.0057	0.0038	0.0050	0.0031	0.0029
2. Fume Filter Before (gas outlet) (g)	0.4637	0.4696	0.4677	0.4705	0.4658
Fume Filter After (gas outlet) (g)	0.4906	0.4882	0.4835	0.4874	0.4818
Fume wt. (gas outlet) (g)	0.0269	0.0186	0.0158	0.0169	0.0160
Total Fume wt. in system (g)	0.0326	0.0224	0.0208	0.0200	0.0189
Total Paper weight (g)	0.5498	0.5565	0.5548	0.5573	0.5537
Percentage of Sulfur (P+F) (%)	0.06	0.04	0.04	0.02	0.02
Percentage of Sulfur in Paper (%)	0.00	0.00	0.00	0.00	0.00
Sulfur wt. in Paper+fume (g)	0.0003	0.0002	0.0002	0.0001	0.0001
Sulfur wt. in Paper (g)	0.00000	0.00000	0.00000	0.00000	0.00000
Sulfur wt. in Fume (g)	0.0003	0.0002	0.0002	0.0001	0.0001
Sulfur wt. % in Fume	1.07	1.03	1.11	0.58	0.61
Sulfur Balance :					
Input :					
Total Input Black Liquor wt. (g)	5.8924	4.8849	4.5211	4.9114	4.7345
Sulfur wt. % in Black Liquor (%)	2.44	2.44	2.44	2.44	2.44
Sulfur wt. in Black Liquor (g)	0.1438	0.1192	0.1103	0.1198	0.1155
Output :					
1. Total Fume wt. (g)	0.0326	0.0224	0.0208	0.0200	0.0189
Sulfur wt. % in Fume (%)	1.07	1.03	1.11	0.58	0.61
Sulfur wt. in Fume (g)	0.000349	0.000232	0.000230	0.000115	0.000115
2. Char wt. (g)	4.5689	3.8534	3.5371	3.9616	3.8025
Sulfur wt. % in Char (%)	1.27	1.38	1.45	1.55	1.44
Sulfur wt. in Char (g)	0.0580	0.0532	0.0513	0.0614	0.0548
Sulfur Yield in Fume (%)	0.24	0.19	0.21	0.10	0.10
Sulfur Yield in Char (%)	40.36	44.61	46.49	51.24	47.40
Estimate Sulfur Yield in Gas (%)	59.40	55.19	53.30	48.66	52.50

Sulfur Yield in Fume, and Char at 600 °C					
DATA ACQUISITION FILE	FVJL611	FVJL612	FVJL613	FVJL614	FVJL615
Date	7/8/96	7/8/96	7/9/96	7/9/96	7/9/96
Raw Material	Valdosta	Valdosta	Valdosta	Valdosta	Valdosta
Particle Size (micron)	90-125	90-125	90-125	90-125	90-125
Reactor Path Length (inch)	25.75	25.75	19.75	19.75	13.75
Residence Time (sec)	0.9	0.9	0.7	0.7	0.5
Temperature (c)	600	600	600	600	600
Sulfur wt.% in Fume :					
1. Fume Filter Before (g)	0.0861	0.0876	0.0876	0.0866	0.0868
Fume Filter After (g)	0.0901	0.0907	0.0913	0.0908	0.0905
Collected Fume wt. (g)	0.0040	0.0031	0.0037	0.0042	0.0037
2. Fume Filter Before (gas outlet) (g)	0.4656	0.4672	0.4791	0.4739	0.4731
Fume Filter After (gas outlet) (g)	0.4852	0.4851	0.4943	0.4906	0.4885
Fume wt. (gas outlet) (g)	0.0196	0.0179	0.0152	0.0167	0.0154
Total Fume wt. in system (g)	0.0236	0.0210	0.0189	0.0209	0.0191
Total Paper weight (g)	0.5517	0.5548	0.5667	0.5605	0.5599
Percentage of Sulfur (P+F) (%)	0.02	0.02	0.03	0.03	0.02
Percentage of Sulfur in Paper (%)	0.00	0.00	0.00	0.00	0.00
Sulfur wt. in Paper+fume (g)	0.0001	0.0001	0.0002	0.0002	0.0001
Sulfur wt. in Paper (g)	0.00000	0.00000	0.00000	0.00000	0.00000
Sulfur wt. in Fume (g)	0.0001	0.0001	0.0002	0.0002	0.0001
Sulfur wt.% in Fume	0.49	0.55	0.93	0.83	0.61
Sulfur Balance :					
Input :					
Total Input Black Liquor wt. (g)	5.4536	4.5087	4.494	4.7983	4.4244
Sulfur wt. % in Black Liquor (%)	2.44	2.44	2.44	2.44	2.44
Sulfur wt. in Black Liquor (g)	0.1331	0.1100	0.1097	0.1171	0.1080
Output :					
1. Total Fume wt. (g)	0.0236	0.0210	0.0189	0.0209	0.0191
Sulfur wt. % in Fume (%)	0.49	0.55	0.93	0.83	0.61
Sulfur wt. in Fume (g)	0.000115	0.000115	0.000176	0.000174	0.000116
2. Char wt. (g)	4.2010	3.6627	3.6304	3.5083	3.7689
Sulfur wt. % in Char (%)	1.75	1.76	1.92	1.97	1.97
Sulfur wt. in Char (g)	0.0735	0.0645	0.0697	0.0691	0.0742
Sulfur Yield in Fume (%)	0.09	0.10	0.16	0.15	0.11
Sulfur Yield in Char (%)	55.25	58.60	63.57	59.03	68.78
Estimate Sulfur Yield in Gas (%)	44.67	41.30	36.27	40.82	31.12

Sulfur Yield in Fume, and Char at 600 °C			
DATA ACQUISITION FILE	FVJL616	FVJL617	FVJL618
Date	7/9/96	7/9/96	7/9/96
Raw Material	Valdosta	Valdosta	Valdosta
Particle Size (micron)	90-125	90-125	90-125
Reactor Path Length (inch)	13.75	9.75	9.75
Residence Time (sec)	0.5	0.3	0.3
Temperature (c)	600	600	600
Sulfur wt.% in Fume :			
1. Fume Filter Before (g)	0.0864	0.0869	0.0861
Fume Filter After (g)	0.0904	0.0912	0.0914
Collected Fume wt. (g)	0.0040	0.0043	0.0053
2. Fume Filter Before (gas outlet) (g)	0.4796	0.4681	0.4697
Fume Filter After (gas outlet) (g)	0.5001	0.4909	0.4958
Fume wt. (gas outlet) (g)	0.0205	0.0228	0.0261
Total Fume wt. in system (g)	0.0245	0.0271	0.0314
Total Paper weight (g)	0.5660	0.5550	0.5558
Percentage of Sulfur (P+F) (%)	0.02	0.03	0.03
Percentage of Sulfur in Paper(%)	0.00	0.00	0.00
Sulfur wt. in Paper+fume (g)	0.0001	0.0002	0.0002
Sulfur wt. in Paper (g)	0.00000	0.00000	0.00000
Sulfur wt. in Fume (g)	0.0001	0.0002	0.0002
Sulfur wt.% in Fume	0.48	0.64	0.56
Sulfur Balance :			
Input :			
Total Input Black Liquor wt. (g)	5.4212	4.5901	5.5056
Sulfur wt. % in Black Liquor (%)	2.44	2.44	2.44
Sulfur wt. in Black Liquor (g)	0.1323	0.1120	0.1343
Output :			
1. Total Fume wt. (g)	0.0245	0.0271	0.0314
Sulfur wt. % in Fume (%)	0.48	0.64	0.56
Sulfur wt. in Fume (g)	0.000118	0.000175	0.000176
2. Char wt. (g)	4.5995	4.2696	5.0851
Sulfur wt. % in Char (%)	2.00	2.26	2.37
Sulfur wt. in Char (g)	0.0920	0.0965	0.1205
Sulfur Yield in Fume (%)	0.09	0.16	0.13
Sulfur Yield in Char (%)	69.54	86.16	89.71
Estimate Sulfur Yield in Gas (%)	30.37	13.69	10.16

Sulfur Yield in Fume, and Char at 500 °C					
DATA ACQUISITION FILE	FVAG601	FVAG602	FVAG603	FVAG604	FVAG605
Date	8/7/96	8/7/96	8/8/96	8/8/96	8/8/96
Raw Material	Valdosta	Valdosta	Valdosta	Valdosta	Valdosta
Particle Size (micron)	90-125	90-125	90-125	90-125	90-125
Reactor Path Length (inch)	28.75	28.75	28.75	28.75	28.75
Residence Time (sec)	2.0	2.0	1.7	1.7	1.5
Temperature (c)	500	500	500	500	500
Sulfur wt. % in Fume :					
1. Fume Filter Before (g)	0.0874	0.0881	0.0876	0.0869	0.0878
Fume Filter After (g)	0.1003	0.0996	0.0961	0.0916	0.0926
Collected Fume wt. (g)	0.0129	0.0115	0.0085	0.0047	0.0048
2. Fume Filter Before (gas outlet) (g)	0.4709	0.4662	0.4685	0.4694	0.4745
Fume Filter After (gas outlet) (g)	0.4981	0.4923	0.4921	0.4856	0.4932
Fume wt. (gas outlet) (g)	0.0272	0.0261	0.0236	0.0162	0.0187
Total Fume wt. in system (g)	0.0401	0.0376	0.0321	0.0209	0.0235
Total Paper weight (g)	0.5583	0.5543	0.5561	0.5563	0.5623
Percentage of Sulfur (P+F) (%)	0.24	0.24	0.16	0.16	0.06
Percentage of Sulfur in Paper (%)	0.00	0.00	0.00	0.00	0.00
Sulfur wt. in Paper+fume (g)	0.0014	0.0014	0.0009	0.0009	0.0004
Sulfur wt. in Paper (g)	0.0000	0.00000	0.00000	0.00000	0.00000
Sulfur wt. in Fume (g)	0.0014	0.0014	0.0009	0.0009	0.0004
Sulfur wt.% in Fume	3.58	3.78	2.93	4.42	1.50
Sulfur Balance :					
Input :					
Total Input Black Liquor wt. (g)	5.0837	4.5304	4.2378	3.1126	2.9778
Sulfur wt. % in Black Liquor (%)	2.44	2.44	2.44	2.44	2.44
Sulfur wt. in Black Liquor (g)	0.1240	0.1105	0.1034	0.0759	0.0727
Output :					
1. Total Fume wt. (g)	0.0401	0.0376	0.0321	0.0209	0.0235
Sulfur wt. % in Fume (%)	3.58	3.78	2.93	4.42	1.50
Sulfur wt. in Fume (g)	0.001436	0.001421	0.000941	0.000924	0.000351
2. Char wt. (g)	3.3487	2.8562	2.7995	1.9759	2.0084
Sulfur wt. % in Char (%)	1.55	1.55	1.6	1.6	1.65
Sulfur wt. in Char (g)	0.0519	0.0443	0.0448	0.0316	0.0331
Sulfur Yield in Fume (%)	1.16	1.29	0.91	1.22	0.48
Sulfur Yield in Char (%)	41.84	40.05	43.32	41.63	45.61
Estimate Sulfur Yield in Gas (%)	57.00	58.67	55.77	57.16	53.91

Sulfur Yield in Fume, and Char at 500 °C					
DATA ACQUISITION FILE	FVAG606	FVAG607	FVAG608	FVAG609	FVAG610
Date	8/8/96	8/8/96	8/8/96	8/13/96	8/13/96
Raw Material	Valdosta	Valdosta	Valdosta	Valdosta	Valdosta
Particle Size (micron)	90-125	90-125	90-125	90-125	90-125
Reactor Path Length (inch)	28.75	28.75	28.75	28.75	28.75
Residence Time (sec)	1.5	1.3	1.3	1.1	1.1
Temperature (c)	500	500	500	500	500
Sulfur wt.% in Fume :					
1. Fume Filter Before (g)	0.0883	0.0881	0.0873	0.0857	0.0861
Fume Filter After (g)	0.0928	0.0906	0.0893	0.0882	0.0889
Collected Fume wt. (g)	0.0045	0.0025	0.002	0.0025	0.0028
2. Fume Filter Before (gas outlet) (g)	0.4687	0.4707	0.4727	0.4722	0.4663
Fume Filter After (gas outlet) (g)	0.4838	0.4816	0.4795	0.4882	0.4839
Fume wt. (gas outlet) (g)	0.0151	0.0109	0.0068	0.0160	0.0176
Total Fume wt. in system (g)	0.0196	0.0134	0.0088	0.0185	0.0204
Total Paper weight (g)	0.5570	0.5588	0.5600	0.5579	0.5524
Percentage of Sulfur (P+F) (%)	0.06	0.04	0.04	0.02	0.02
Percentage of Sulfur in Paper (%)	0.00	0.00	0.00	0.00	0.00
Sulfur wt. in Paper+fume (g)	0.0003	0.0002	0.0002	0.0001	0.0001
Sulfur wt. in Paper (g)	0.0000	0.00000	0.00000	0.00000	0.00000
Sulfur wt. in Fume (g)	0.0003	0.0002	0.0002	0.0001	0.0001
Sulfur wt.% in Fume	1.77	1.71	2.59	0.62	0.56
Sulfur Balance :					
Input :					
Total Input Black Liquor wt. (g)	3.5777	2.1751	1.4012	4.2663	4.3929
Sulfur wt. % in Black Liquor (%)	2.44	2.44	2.44	2.44	2.44
Sulfur wt. in Black Liquor (g)	0.0873	0.0531	0.0342	0.1041	0.1072
Output :					
1. Total Fume wt. (g)	0.0196	0.0134	0.0088	0.0185	0.0204
Sulfur wt. % in Fume (%)	1.77	1.71	2.59	0.62	0.56
Sulfur wt. in Fume (g)	0.0003	0.0002	0.0002	0.0001	0.0001
2. Char wt. (g)	2.4421	1.5456	1.0306	3.3014	3.5031
Sulfur wt. % in Char (%)	1.65	1.71	1.71	1.75	1.75
Sulfur wt. in Char (g)	0.0403	0.0264	0.0176	0.0578	0.0613
Sulfur Yield in Fume (%)	0.40	0.43	0.67	0.11	0.11
Sulfur Yield in Char (%)	46.16	49.80	51.55	55.50	57.19
Estimate Sulfur Yield in Gas (%)	53.44	49.77	47.79	44.39	42.70

Sulfur Yield in Fume, and Char at 500 ° C					
DATA ACQUISITION FILE	FVAG611	FVAG612	FVAG613	FVAG614	FVAG615
Date	8/13/96	8/13/96	8/14/96	8/14/96	8/14/96
Raw Material	Valdosta	Valdosta	Valdosta	Valdosta	Valdosta
Particle Size (micron)	90-125	90-125	90-125	90-125	90-125
Reactor Path Length (inch)	23.75	23.75	17.75	17.75	12.75
Residence Time (sec)	0.9	0.9	0.7	0.7	0.5
Temperature (c)	500	500	500	500	500
Sulfur wt. % in Fume :					
1. Fume Filter Before (g)	0.0865	0.0872	0.0871	0.0867	0.0858
Fume Filter After (g)	0.0906	0.0901	0.0892	0.0904	0.0888
Collected Fume wt. (g)	0.0041	0.0029	0.0021	0.0037	0.003
2. Fume Filter Before (gas outlet) (g)	0.4702	0.4706	0.4693	0.4701	0.4711
Fume Filter After (gas outlet) (g)	0.4902	0.4909	0.4861	0.4909	0.4901
Fume wt. (gas outlet) (g)	0.0200	0.0203	0.0168	0.0208	0.0190
Total Fume wt. in system (g)	0.0241	0.0232	0.0189	0.0245	0.0220
Total Paper weight (g)	0.5567	0.5578	0.5564	0.5568	0.5569
Percentage of Sulfur (P+F) (%)	0.02	0.02	0.03	0.03	0.02
Percentage of Sulfur in Paper (%)	0.00	0.00	0.00	0.00	0.00
Sulfur wt. in Paper+fume (g)	0.0001	0.0001	0.0002	0.0002	0.0001
Sulfur wt. in Paper (g)	0.0000	0.00000	0.00000	0.00000	0.00000
Sulfur wt. in Fume (g)	0.0001	0.0001	0.0002	0.0002	0.0001
Sulfur wt. % in Fume	0.48	0.50	0.91	0.71	0.53
Sulfur Balance :					
Input :					
Total Input Black Liquor wt. (g)	5.4150	4.9380	3.7626	5.4731	4.3210
Sulfur wt. % in Black Liquor (%)	2.44	2.44	2.44	2.44	2.44
Sulfur wt. in Black Liquor (g)	0.1321	0.1205	0.0918	0.1335	0.1054
Output :					
1. Total Fume wt. (g)	0.0241	0.0232	0.0189	0.0245	0.0220
Sulfur wt. % in Fume (%)	0.48	0.50	0.91	0.71	0.53
Sulfur wt. in Fume (g)	0.0001	0.0001	0.0002	0.0002	0.0001
2. Char wt. (g)	4.3718	3.9025	3.0763	4.5202	3.6438
Sulfur wt. % in Char (%)	1.90	1.90	2.11	2.11	2.33
Sulfur wt. in Char (g)	0.0831	0.0741	0.0649	0.0954	0.0849
Sulfur Yield in Fume (%)	0.09	0.10	0.19	0.13	0.11
Sulfur Yield in Char (%)	62.87	61.54	70.70	71.42	80.53
Estimate Sulfur Yield in Gas (%)	37.04	38.36	29.11	28.45	19.36

Sulfur Yield in Fume, and Char at 500 °C			
DATA ACQUISITION FILE	FVAG616	FVAG617	FVAG618
Date	8/14/96	8/14/96	8/14/96
Raw Material	Valdosta	Valdosta	Valdosta
Particle Size (micron)	90-125	90-125	90-125
Reactor Path Length (inch)	12.75	9.75	9.75
Residence Time (sec)	0.5	0.3	0.3
Temperature (c)	500	500	500
Sulfur wt.% in Fume :			
1. Fume Filter Before (g)	0.0869	0.0867	0.0864
Fume Filter After (g)	0.0898	0.0884	0.0881
Collected Fume wt. (g)	0.0029	0.0017	0.0017
2. Fume Filter Before (gas outlet) (g)	0.4716	0.4663	0.4733
Fume Filter After (gas outlet) (g)	0.4911	0.4811	0.4841
Fume wt. (gas outlet) (g)	0.0195	0.0148	0.0108
Total Fume wt. in system (g)	0.0224	0.0165	0.0125
Total Paper weight (g)	0.5585	0.5530	0.5597
Percentage of Sulfur (P+F) (%)	0.02	0.03	0.03
Percentage of Sulfur in Paper (%)	0.00	0.00	0.00
Sulfur wt. in Paper+fume (g)	0.0001	0.0002	0.0002
Sulfur wt. in Paper (g)	0.0000	0.00000	0.00000
Sulfur wt. in Fume (g)	0.0001	0.0002	0.0002
Sulfur wt.% in Fume	0.52	1.04	1.37
Sulfur Balance :			
Input :			
Total Input Black Liquor wt. (g)	5.5464	5.4361	4.4073
Sulfur wt. % in Black Liquor (%)	2.44	2.44	2.44
Sulfur wt. in Black Liquor (g)	0.1353	0.1326	0.1075
Output :			
1. Total Fume wt. (g)	0.0224	0.0165	0.0125
Sulfur wt. % in Fume (%)	0.52	1.04	1.37
Sulfur wt. in Fume (g)	0.0001	0.0002	0.0002
2. Char wt. (g)	4.7505	4.8722	4.0662
Sulfur wt. % in Char (%)	2.33	2.42	2.42
Sulfur wt. in Char (g)	0.1107	0.1179	0.0984
Sulfur Yield in Fume (%)	0.09	0.13	0.16
Sulfur Yield in Char (%)	81.79	88.89	91.50
Estimate Sulfur Yield in Gas (%)	18.13	10.98	8.34

Sulfur Yield in Fume, and Char at 400 °C					
DATA ACQUISITION FILE	FVAG619	FVAG620	FVAG621	FVAG622	FVAG623
Date	8/15/96	8/15/96	8/15/96	8/15/96	8/15/96
Raw Material	Valdosta	Valdosta	Valdosta	Valdosta	Valdosta
Particle Size (micron)	90-125	90-125	90-125	90-125	90-125
Reactor Path Length (inch)	28.75	28.75	28.75	28.75	28.75
Residence Time (sec)	2.0	2.0	1.7	1.7	1.5
Temperature (c)	400	400	400	400	400
Sulfur wt. % in Fume :					
1. Fume Filter Before (g)	0.0866	0.0872	0.0854	0.0854	0.0864
Fume Filter After (g)	0.0883	0.0902	0.0874	0.0876	0.0878
Collected Fume wt. (g)	0.0017	0.0030	0.0020	0.0022	0.0014
2. Fume Filter Before (gas outlet) (g)	0.4703	0.4713	0.4702	0.4656	0.4732
Fume Filter After (gas outlet) (g)	0.4765	0.4808	0.4798	0.4761	0.4821
Fume wt. (gas outlet) (g)	0.0062	0.0095	0.0096	0.0105	0.0089
Total Fume wt. in system (g)	0.0079	0.0125	0.0116	0.0127	0.0103
Total Paper weight (g)	0.5569	0.5585	0.5556	0.5510	0.5596
Percentage of Sulfur (P+F) (%)	0.24	0.24	0.16	0.16	0.06
Percentage of Sulfur in Paper (%)	0.00	0.00	0.00	0.00	0.00
Sulfur wt. in Paper+fume (g)	0.0014	0.0014	0.0009	0.0009	0.0003
Sulfur wt. in Paper (g)	0.0000	0.0000	0.0000	0.0000	0.0000
Sulfur wt. in Fume (g)	0.0014	0.0014	0.0009	0.0009	0.0003
Sulfur wt. % in Fume	17.16	10.96	7.82	7.10	3.32
Sulfur Balance :					
Input :					
Total Input Black Liquor wt. (g)	1.9351	2.8298	4.1128	4.0197	4.6955
Sulfur wt. % in Black Liquor (%)	2.44	2.44	2.44	2.44	2.44
Sulfur wt. in Black Liquor (g)	0.0472	0.0690	0.1004	0.0981	0.1146
Output :					
1. Total Fume wt. (g)	0.0079	0.0125	0.0116	0.0127	0.0103
Sulfur wt. % in Fume (%)	17.16	10.96	7.82	7.10	3.32
Sulfur wt. in Fume (g)	0.0014	0.0014	0.0009	0.0009	0.0003
2. Char wt. (g)	1.5201	2.1397	3.1248	3.2285	3.7358
Sulfur wt. % in Char (%)	1.80	1.80	1.89	1.89	1.97
Sulfur wt. in Char (g)	0.0274	0.0385	0.0591	0.0610	0.0736
Sulfur Yield in Fume (%)	2.87	1.98	0.90	0.92	0.30
Sulfur Yield in Char (%)	57.95	55.78	58.85	62.21	64.24
Estimate Sulfur Yield in Gas (%)	39.18	42.24	40.24	36.87	35.47

Sulfur Yield in Fume, and Char at 400 °C					
DATA ACQUISITION FILE	FVAG624	FVAG625	FVAG626	FVAG627	FVAG628
Date	8/15/96	8/16/96	8/16/96	8/16/96	8/16/96
Raw Material	Valdosta	Valdosta	Valdosta	Valdosta	Valdosta
Particle Size (micron)	90-125	90-125	90-125	90-125	90-125
Reactor Path Length (inch)	28.75	28.75	28.75	28.75	28.75
Residence Time (sec)	1.5	1.3	1.3	1.1	1.1
Temperature (c)	400	400	400	400	400
Sulfur wt. % in Fume :					
1. Fume Filter Before (g)	0.0878	0.0861	0.0861	0.0862	0.0867
Fume Filter After (g)	0.0891	0.0871	0.0877	0.0885	0.0884
Collected Fume wt. (g)	0.0013	0.0010	0.0016	0.0023	0.0017
2. Fume Filter Before (gas outlet) (g)	0.4709	0.4692	0.4711	0.4706	0.4741
Fume Filter After (gas outlet) (g)	0.4784	0.4751	0.4813	0.4834	0.4841
Fume wt. (gas outlet) (g)	0.0075	0.0059	0.0102	0.0128	0.0100
Total Fume wt. in system (g)	0.0088	0.0069	0.0118	0.0151	0.0117
Total Paper weight (g)	0.5587	0.5553	0.5572	0.5568	0.5608
Percentage of Sulfur (P+F) (%)	0.06	0.04	0.04	0.02	0.02
Percentage of Sulfur in Paper (%)	0.00	0.00	0.00	0.00	0.00
Sulfur wt. in Paper+fume (g)	0.0003	0.0002	0.0002	0.0001	0.0001
Sulfur wt. in Paper (g)	0.0000	0.0000	0.0000	0.0000	0.0000
Sulfur wt. in Fume (g)	0.0003	0.0002	0.0002	0.0001	0.0001
Sulfur wt. % in Fume	3.87	3.26	1.93	0.76	0.98
Sulfur Balance :					
Input :					
Total Input Black Liquor wt. (g)	3.7710	2.3171	4.5125	4.9372	4.1369
Sulfur wt. % in Black Liquor (%)	2.44	2.44	2.44	2.44	2.44
Sulfur wt. in Black Liquor (g)	0.0920	0.0565	0.1101	0.1205	0.1009
Output :					
1. Total Fume wt. (g)	0.0088	0.0069	0.0118	0.0151	0.0117
Sulfur wt. % in Fume (%)	3.87	3.26	1.93	0.76	0.98
Sulfur wt. in Fume (g)	0.0003	0.0002	0.0002	0.0001	0.0001
2. Char wt. (g)	3.1228	1.9236	3.8421	4.2969	3.6589
Sulfur wt. % in Char (%)	1.97	2.04	2.04	2.11	2.11
Sulfur wt. in Char (g)	0.0615	0.0392	0.0784	0.0907	0.0772
Sulfur Yield in Fume (%)	0.37	0.40	0.21	0.09	0.11
Sulfur Yield in Char (%)	66.86	69.41	71.19	75.26	76.48
Estimate Sulfur Yield in Gas (%)	32.77	30.19	28.61	24.64	23.40

Sulfur Yield in Fume, and Char at 400 °C					
DATA ACQUISITION FILE	FVAG629	FVAG630	FVAG631	FVAG632	FVAG633
Date	8/16/96	8/16/96	8/18/96	8/18/96	8/18/96
Raw Material	Valdosta	Valdosta	Valdosta	Valdosta	Valdosta
Particle Size (micron)	90-125	90-125	90-125	90-125	90-125
Reactor Path Length (inch)	23.75	23.75	17.75	17.75	12.75
Residence Time (sec)	0.9	0.9	0.7	0.7	0.5
Temperature (c)	400	400	400	400	400
Sulfur wt.% in Fume :					
1. Fume Filter Before (g)	0.0859	0.0862	0.0879	0.0852	0.0867
Fume Filter After (g)	0.0874	0.0872	0.0881	0.0871	0.0889
Collected Fume wt. (g)	0.0015	0.0010	0.0002	0.0019	0.0022
2. Fume Filter Before (gas outlet) (g)	0.4751	0.4721	0.4709	0.4724	0.4731
Fume Filter After (gas outlet) (g)	0.4864	0.4789	0.4733	0.4789	0.4858
Fume wt. (gas outlet) (g)	0.0113	0.0068	0.0024	0.0065	0.0127
Total Fume wt. in system (g)	0.0128	0.0078	0.0026	0.0084	0.0149
Total Paper weight (g)	0.5610	0.5583	0.5588	0.5576	0.5598
Percentage of Sulfur (P+F) (%)	0.02	0.02	0.03	0.03	0.02
Percentage of Sulfur in Paper (%)	0.00	0.00	0.00	0.00	0.00
Sulfur wt. in Paper+fume (g)	0.0001	0.0001	0.0002	0.0002	0.0001
Sulfur wt. in Paper (g)	0.0000	0.00000	0.00000	0.00000	0.00000
Sulfur wt. in Fume (g)	0.0001	0.0001	0.0002	0.0002	0.0001
Sulfur wt.% in Fume	0.90	1.45	6.48	2.02	0.77
Sulfur Balance :					
Input :					
Total Input Black Liquor wt. (g)	3.9668	3.0851	3.5493	4.3890	4.6073
Sulfur wt. % in Black Liquor (%)	2.44	2.44	2.44	2.44	2.44
Sulfur wt. in Black Liquor (g)	0.0968	0.0753	0.0866	0.1071	0.1124
Output :					
1. Total Fume wt. (g)	0.0128	0.0078	0.0026	0.0084	0.0149
Sulfur wt. % in Fume (%)	0.90	1.45	6.48	2.02	0.77
Sulfur wt. in Fume (g)	0.0001	0.0001	0.0002	0.0002	0.0001
2. Char wt. (g)	3.6146	2.8285	3.4712	4.1884	4.5907
Sulfur wt. % in Char (%)	2.16	2.16	2.21	2.21	2.33
Sulfur wt. in Char (g)	0.0781	0.0611	0.0767	0.0926	0.1070
Sulfur Yield in Fume (%)	0.12	0.15	0.19	0.16	0.10
Sulfur Yield in Char (%)	80.66	81.16	88.58	86.43	95.15
Estimate Sulfur Yield in Gas (%)	19.22	18.69	11.22	13.41	4.75

Sulfur Yield in Fume, and Char at 400 °C		
DATA ACQUISITION FILE	FVAG634	FVAG635
Date	8/18/96	8/18/96
Raw Material	Valdosta	Valdosta
Particle Size (micron)	90-125	90-125
Reactor Path Length (inch)	12.75	9.75
Residence Time (sec)	0.5	0.3
Temperature (c)	400	400
Sulfur wt.% in Fume :		
1. Fume Filter Before (g)	0.0852	0.0865
Fume Filter After (g)	0.0872	0.0889
Collected Fume wt. (g)	0.0020	0.0024
2. Fume Filter Before (gas outlet) (g)	0.4766	0.4762
Fume Filter After (gas outlet) (g)	0.4889	0.4908
Fume wt. (gas outlet) (g)	0.0123	0.0146
Total Fume wt. in system (g)	0.0143	0.0170
Total Paper weight (g)	0.5618	0.5627
Percentage of Sulfur (P+F) (%)	0.02	0.03
Percentage of Sulfur in Paper (%)	0.00	0.00
Sulfur wt. in Paper+fume (g)	0.0001	0.0002
Sulfur wt. in Paper (g)	0.0000	0.0000
Sulfur wt. in Fume (g)	0.0001	0.0002
Sulfur wt.% in Fume	0.81	1.02
Sulfur Balance :		
Input :		
Total Input Black Liquor wt. (g)	4.0943	4.938
Sulfur wt. % in Black Liquor (%)	2.44	2.44
Sulfur wt. in Black Liquor (g)	0.0999	0.1205
Output :		
1. Total Fume wt. (g)	0.0143	0.0170
Sulfur wt. % in Fume (%)	0.81	1.02
Sulfur wt. in Fume (g)	0.0001	0.0002
2. Char wt. (g)	4.0140	4.9162
Sulfur wt. % in Char (%)	2.33	2.39
Sulfur wt. in Char (g)	0.0935	0.1175
Sulfur Yield in Fume (%)	0.12	0.14
Sulfur Yield in Char (%)	93.62	97.52
Estimate Sulfur Yield in Gas (%)	6.27	2.34

Adjusted Carbon Yield in Char of Pyrolysis of Black Liquor							
Residence Time (sec)	Temperature (°C)			C% in gas	% in Fine Pr	Correction Fc	Adj. Char 500C
	600	500	400				
2.0	71.86	61.76	75.89	23.43	1.79	1.15	70.78
2.0	67.15	59.11	73.05	23.52	1.88	1.19	70.60
1.7	72.79	61.59	74.44	20.98	1.49	1.19	73.53
1.7	69.43	59.18	78.69	22.85	1.32	1.21	71.83
1.5	69.68	61.96	76.68	17.31	1.26	1.25	77.43
1.5	72.40	62.70	79.81	17.29	0.88	1.24	77.83
1.3	74.95	64.66	79.81	16.57	1.01	1.21	78.42
1.3	72.82	66.93	81.86	17.14	1.03	1.16	77.83
1.1	77.31	71.77	82.35	16.26	0.63	1.10	79.11
1.1	75.85	73.96	83.69	15.79	0.68	1.08	79.53
0.9	75.13	77.62	86.36	14.81	0.63	1.04	80.56
0.9	80.03	75.98	86.89	12.99	0.67	1.08	82.34
0.7	80.06	78.29	91.93	11.62	0.67	1.07	83.71
0.7	73.51	79.08	89.70	10.65	0.59	1.07	84.76
0.5	84.17	81.4	96.53	10.18	0.65	1.05	85.17
0.5	84.84	82.67	94.98	11.16	0.52	1.02	84.32
0.3	89.26	85.63	94.65	6.69	0.28	1.04	89.03
0.3	91.48	88.15		7.07	0.26	1.01	88.67

Adjusted Char Yield in Pyrolysis of Black Liquor					
Residence Time	Temperature (°C)				
(sec)	600	500	400	Con. Fac.	500 Adj
2.0	74.91	65.87	78.55	1.15	75.75
2.0	75.22	63.05	75.61	1.19	75.03
1.7	79.07	66.06	75.98	1.19	78.61
1.7	75.80	63.48	80.32	1.21	76.81
1.5	76.80	67.45	79.56	1.25	84.31
1.5	77.53	68.26	82.81	1.24	84.64
1.3	78.88	71.06	83.02	1.21	85.98
1.3	78.24	73.55	85.14	1.16	85.32
1.1	80.66	77.38	87.03	1.10	85.12
1.1	80.31	79.74	88.45	1.08	86.12
0.9	77.03	80.73	91.12	1.04	83.96
0.9	81.24	79.03	91.68	1.08	85.35
0.7	80.78	81.76	97.8	1.07	87.48
0.7	73.12	82.59	95.43	1.07	88.37
0.5	85.18	84.33	99.64	1.05	88.55
0.5	84.84	85.65	98.04	1.02	87.36
0.3	93.02	89.63	99.56	1.04	93.22
0.3	92.36	92.26		1.01	93.18

Adjusted Sulfur Yield in Pyrolysis of Black Liquor					
Residence Time	Temperature (°C)				
(sec)	600	500	400	Con. Fac.	500 Adj
2.0	39.30	41.84	57.95	1.15	48.12
2.0	36.99	40.05	55.78	1.19	47.66
1.7	42.77	43.32	58.85	1.19	51.55
1.7	37.90	41.63	62.21	1.21	50.37
1.5	40.29	45.61	64.24	1.25	57.01
1.5	40.36	46.16	66.86	1.24	57.24
1.3	44.61	49.80	69.41	1.21	60.26
1.3	46.49	51.55	71.19	1.16	59.80
1.1	51.24	55.50	75.26	1.10	61.05
1.1	47.40	57.19	76.48	1.08	61.77
0.9	55.25	62.87	80.66	1.04	65.38
0.9	58.60	61.54	81.16	1.08	66.46
0.7	63.57	70.70	88.58	1.07	75.65
0.7	59.03	71.42	86.43	1.07	76.42
0.5	68.78	80.53	95.15	1.05	84.56
0.5	69.54	81.79	93.62	1.02	83.43
0.3	86.16	88.89	97.52	1.04	92.45
0.3	89.71	91.50		1.01	92.42

Adjusted Nitrogen Yield in Pyrolysis of Black Liquor					
Residence Time	Temperature (°C)				
(sec)	600	500	400	Con. Fac.	500 Adj
2.0	58.86	61.17	67.33	1.15	70.35
2.0	59.10	58.54	64.81	1.19	69.66
1.7	62.12	61.34	65.12	1.19	72.99
1.7	64.97	58.95	68.84	1.21	71.33
1.5	65.83	62.63	68.20	1.25	78.29
1.5	66.46	63.38	70.98	1.24	78.59
1.3	67.61	65.98	71.16	1.21	79.84
1.3	67.06	68.30	72.98	1.16	79.23
1.1	69.14	71.86	74.60	1.10	79.05
1.1	68.84	68.35	75.81	1.08	73.82
0.9	71.53	74.97	78.10	1.04	77.97
0.9	69.63	73.38	78.59	1.08	79.25
0.7	75.01	75.92	83.83	1.07	81.23
0.7	73.12	76.69	81.80	1.07	82.06
0.5	79.10	78.3	85.41	1.05	82.22
0.5	78.78	79.53	84.03	1.02	81.12
0.3	86.37	89.63	98.14	1.04	93.22
0.3	85.77	92.26		1.01	93.18